UNIVERSITÀ
DEGLI STUDI
DI PADOVA

Università degli Studi di Padova

DIPARTIMENTO DI GEOSCIENZE

SCUOLA DI DOTTORATO DI RICERCA IN:

SCIENZE DELLA TERRA

CICLO XVIII

DIFFUSION OF ALPINE COPPER IN FRIULI VENEZIA GIULIA IN THE MIDDLE-LATE BRONZE AGE

Direttore della Scuola: Ch.mo Prof. Fabrizio Nestola

Supervisore: Ch.mo Prof. Gilberto Artioli

Co-supervisore : Dott.ssa Ivana Angelini

Dottorando : Caterina Canovaro

CONTENTS

Abstract

Since the early stages in the study of ancient metals, one important goal was to establish the geological origin of the metal employed to produce artefacts, with the intent to deduce the issues of trade, the commercial relationships and the movements of objects. Recently, a number of studies carried out by different research groups have expanded the traditional/conventional chemical and metallographic analyses by including the measurement of lead isotopic ratios, in order to determine the metal provenance. Although a deep interest for Friuli Venezia Giulia has been shown since the beginning of 19th century, a systematic research program that could define the metal circulation routes of Alpine copper in North-Eastern Italy has never been carried out. Actually, only sporadic chemical analyses on ingots found in Friuli have been performed and, until now, the interpretation of their provenance is not supported by isotopic data.

In this frame, the archaeometric study of copper and bronze artifacts from several well-dated protohistoric hoards in Friuli Venezia Giulia has allowed for the investigation of the origin of the metal, by identifying the ores exploitation areas and, therefore, has permitted to reconstruct its circulation paths in North-Eastern Italy in the Late Bronze Age. The choice of Friuli as investigation area was due to its key role as economic and commercial hub between the Adriatic area and Central Europe; therefore, in order to outline the role of this region, the study of sealed complexes embracing the time period from the Recent Bronze Age (RBA) to the Final Bronze Age (FBA) was needed. In this regard, the hoards of Cervignano, Muscoli, Castions di Strada, Celò, Verzegnis, Galleriano and Porpetto, all of them including both raw ingots and manufactured objects, were identified and selected in collaboration with the *Soprintendenza per i Beni Archeologici del Friuli Venezia Giulia*. There are no known hoards from the MBA and, therefore, two sporadic finds – one sword from Belvedere and one from Canale Anfora – have been properly selected in order to increase the number of samples representative of this period.

In the present work, a multi-analytical approach was applied. Particular relevance was given to the study of chemical composition (major, minor and trace elements) and to the observation of any residual phases due to an incomplete refinement of the raw material, since these information may shed light on the employed Cu-ore charge and on their smelting process, but are often insufficient to surely identify the exploitation area of the

metal. For this reason, such investigation methods were coupled with lead isotopes analysis carried out on selected samples. Therefore, the set of mineralogical, metallurgical, chemical and isotopic analyses, through a comparison with existing Pb-isotope databases, published data and the Alpine Archaeocopper Project database (AAcP) allowed for the identification of the provenance of the metal.

The results showed that ingots are basically made of almost copper and, only in few cases, of bronze, containing impurities whose concentrations depend on the mineral charge and on the employed extraction/refinement process. Moreover, weapons were found to be subject to a deliberate alloying process with the intent to obtain a malleable bronze. The large set of analyses collected in this study has led to the distinction of two mineral charges, used in well defined metallurgical circles, indeed, chalcopyrite-based deposits were exclusively exploited during Recent/Final Bronze Age (RBA/FBA) for the manufacturing of the ingots and objects of the Cervignano and Muscoli deposits, although few evidences are also documented in the later periods. In this scenario, a change in the mineral charge was revealed in Castions di Strada (FBA), attesting the restart of fahlerz-ores smelting, also confirmed by the findings belonging to the Porpetto hoard that, moreover, exhibited a chemical affinity to Slovenian cast ingots.

The provenance studies have highlighted that, from the MBA to the whole FBA, the Eastern South Alps were known and constantly exploited for smelting chalcopyrite in order to obtain pure copper ingots and, subsequently, prestige objects as weapons and tools. Only in the FBA, the copper from new ore sources (Austria, Central Europe and Bulgaria) was employed and its flow has been proven in Friuli Venezia Giulia. Concerning the metal trade, the bronze circulation in RBA was testified by the little bar-ingots that, in FBA2, assumed the well-known shape of pick-ingots as evidenced in Galleriano. However, the peculiar composition of the Porpetto pick-ingots has demonstrated that such standardized ingot was circulating independently from the alloy composition, but probably in well-distinguished commercial spheres.

Riassunto

Fin dalle prime fasi della ricerca archeometallurgica, un obiettivo importante è stato quello di determinare l'origine geologica del metallo impiegato per la produzione di manufatti, con l'intento di ricostruire i rapporti commerciali e il circuito di circolazione degli oggetti. Recentemente, diversi gruppi di ricerca hanno fatto ricorso, oltre alle tradizionali analisi chimiche e metallografiche, anche alle analisi dei rapporti isotopici del piombo per determinare il più accuratamente possibile la provenienza del metallo. Fin dall'inizio del 19° secolo il Friuli Venezia Giulia ha suscitato un profondo interesse, ma non è mai stato intrapreso un programma di ricerca sistematico in grado di definire i percorsi di circolazione del rame alpino nell'Italia Nord-Orientale. Infatti, solo sporadiche analisi chimiche sono state eseguite su alcuni lingotti ritrovati in Friuli e, fino ad ora, la loro interpretazione in termini di provenienza del metallo non è supportata da alcun dato isotopico.

In questa cornice, lo studio archeometrico di manufatti di rame e bronzo provenienti da vari rispostigli protostorici ben datati del Friuli Venezia Giulia ha permesso di indagare l'origine del metallo utilizzato, individuando le aree sfruttamento dei minerali e, di conseguenza, di ricostruirne la circolazione nell'Italia Nord-orientale nella tarda Età del Bronzo. La scelta del Friuli come regione di interesse è dovuta al suo ruolo chiave come centro economico e commerciale tra l'area adriatica e l'Europa Centrale; pertanto, per delineare il ruolo di questa regione si è reso necessario lo studio di complessi ben sigillati che abbracciassero un *range* cronologico dal Bronzo Recente (BR) al Bronzo Finale (BF). A questo proposito, i depositi di Cervignano, Muscoli, Castions di Strada, Celò, Verzegnis, Galleriano e Porpetto, in cui sono contenuti sia lingotti che manufatti, sono stati individuati e selezionati in collaborazione con la Soprintendenza per i Beni Archeologici del Friuli Venezia Giulia. Non ci sono ripostigli noti per il Bronzo Medio (BM) e, quindi, due ritrovamenti sporadici - una spada da Belvedere e una da Canale Anfora - sono stati selezionati con l'intento di aumentare il numero di campioni rappresentativi di questo periodo.

Nel presente lavoro è stato applicato un approccio multianalitico. Particolare rilevanza è stata attribuita allo studio della composizione chimica (elementi maggiori, minori e in traccia) e all'osservazione di eventuali fasi residue dovute a un raffinamento incompleto della materia prima; tali informazioni possono far luce sul tipo di carica minerale impiegata

e sulla tecnologia del processo di fusione, tuttavia sono insufficienti per identificare sicuramente l'area sfruttamento del metallo. Per questo motivo, tali metodi di indagine sono stati accoppiati con l'analisi degli isotopi del piombo ed effettuati su una selezione di campioni considerati rappresentativi. Pertanto, l'insieme delle analisi mineralogiche, metallurgiche, chimiche e isotopiche, attraverso il confronto con i database esistenti per gli isotopi del piombo, i dati pubblicati in letteratura e il database sviluppato all'interno dell' Alpine Archaeocopper Project (AAcP) ha consentito l'identificazione della provenienza del metallo.

I risultati hanno mostrato che i lingotti sono fondamentalmente costituiti da rame e, solo in pochi casi, da bronzo; le concentrazioni degli elementi minori e in traccia dipendono dalla carica minerale e dal processo impiegato per l'estrazione e il raffinamento. Inoltre, le analisi hanno rivelato che le armi sono state alligate intenzionalmente con lo scopo di ottenere un bronzo malleabile. La grande quantità di dati raccolti in questo studio ha portato alla distinzione di due cariche minerali utilizzate in ambienti metallurgici ben definite; infatti, i depositi caratterizzati da calcopirite sono stati sfruttati in maniera esclusiva durante Bronzo Recente-Finale per la produzione dei lingotti e degli oggetti dei depositi di Cervignano e Muscoli, mentre sporadiche testimonianze sono documentate nei periodi successivi. In questo scenario, in Castions di Strada (BF) si riscontra un cambiamento nella carica minerale e, conseguentemente, viene attestata la ripresa nell'uso di minerali *fahlerz*; inoltre, questa inversione di tendenza è stata confermata anche dai risultati riguardanti i materiali scoperti a Porpetto che hanno mostrato una spiccata affinità chimica con i lingotti sloveni.

Gli studi di provenienza hanno evidenziato che dal Bronzo Medio al Bronzo Finale evoluto le Alpi Sud-orientali erano costantemente sfruttate per l'estrazione di rame da calcopirite, con l'intento di ottenere lingotti di rame puro e, successivamente, oggetti di prestigio come armi e strumenti. Solo nel Bronzo Finale, si assiste all'impiego di il rame estratto da nuovi depositi minerali (Austria, Europa centrale e Bulgaria), la cui circolazione è stata dimostrata in Friuli Venezia Giulia. Inoltre, nel Bronzo Recente la circolazione del bronzo è testimoniata dal ritrovamento di piccoli lingotti a barra che, nel Bronzo Finale hanno assunto la forma ben nota dei pani a piccone, come evidenziato in Galleriano. Tuttavia, la particolare composizione dei pani a piccone di Porpetto ha dimostrato che tale lingotto circolava con forma standard indipendentemente dalla composizione della lega, probabilmente in sfere commerciali ben distinte.

Introduction

1.1 Chemical classification and provenance studies: The project origins

The application of scientific methods to the analysis of ancient metals is rooted in the beginnings of the analytical chemistry, in 19th century, when researchers started to concentrate their attention to the question of provenance. It was proposed that minor elements could be useful in determining the nature of the ore from which the metal came from and, perhaps, its geographical origin (Von Fellenberg 1860-1867; Von Bibra 1869). During the 20th century, the further progresses of analytical techniques and the even lower amount of sampling material required led to the development of different projects based on this topic.

A short history of the progress in the archaeometric investigations in Central Europe from the origins to today's issues has been outlined by Pernicka (2014 and 2011). In this section, the main themes of the present scientific debate about possibilities and limitations of the archaeometallurgical analyses and about different methodologies are reported, with the aim to delineate a brief summary focused on the main theme of this research.

Otto and Witter (Halle)

In 1932, W. Witter in collaboration with H. Otto started chemical and metallurgical investigations in order to solve the disputed problems of prehistoric extractive metallurgy in Central Europe. They pursued two principal aims: to identify copper mining in Central Germany and to determine which ore had been exploited (Otto and Witter 1952). The main assumption was that chemical impurities in copper directly reflect the ores from which they are smelted (Witter 1953). In few years, 1300 objects were investigated by atomic emission spectrometry and a classification based on technological and mineralogical aspects was proposed. These groups were identified as: 1. Very pure copper (Rohkupfer); 2. Unalloyed copper with minor impurities; 3. Copper-arsenic alloys; 4. Fahlore[1] (or fahlerz) metals with/without silver; 5. Copper-tin alloys. This is the beginning of the concept of “Leitlegierungen”, major alloy type.

[1] The term derives from the German “pale ore”, strictly any grey coloured ore mineral mainly composed by tetrahedrite-tennantite minerals.

Nevertheless, the lack of an equal number of analyses of copper ores from deposits considered as likely sources for the analysed objects raised several criticisms. Moreover, Otto and Witter implicitly considered ore deposits to be homogeneous, differentiated in their compositions, and they did not consider the changes in chemical composition during smelting. Taking into account the chemical elements for the development of this classification, they also included tin, which is an alloying element and rarely occurs in association with copper in natural deposits.

Their pioneering study led to the suggestion that 97% of all prehistoric metals objects found in Germany were produced in Saxony. This conclusion cannot be accepted today but, from a methodological and archaeological point of view, Otto and Witter opened the door to new approaches to the *vexata questio* of metal origin and diffusion.

Neuninger, Pittioni and Preuschen (Vienna)

At the same time of the investigation of Otto and Witter, another group of researchers in Vienna composed by R. Pittioni, E. Preuschen and H. Neuninger tried to link finished objects to ore deposits. They supposed that the impurity patterns in metals are similar to those in the related ores and included more than 2000 ore analyses in their research, one-step ahead respect to the Halle group. Moreover, the Vienna group was aware of the inhomogeneity of ores and of fractionation in element concentrations due to the smelting process. Since smelting causes changes in the raw material composition, the good intuition was to extend the analysis to slags.

However, the main problem of the work of the Vienna group resides in the technology available at that time. In fact, they realized that the presence/absence of certain elements could be used to determine the trace element pattern useful for the classification, but they carried out semi-quantitative analyses without any absolute numerical value for concentrations. In conclusion of this work, five copper classes related to copper deposits were defined, but the obtained analytical data are not comparable with other investigations. There were many disputes between Halle and Vienna group about the correct methodological approach, which continued until a larger project was started in Stuttgart, following that of Otto and Witter.

Stuttgart team (SAM)

In 1950s, a group in Stuttgart and Freiburg directed by S. Junghans and E. Sangmeister began a new project with the aim to establish in which region copper was

mined and worked, and in which direction and age the technology has diffused. However, the material sources were not actually determined. In fact, for the SAM group it was not a priority to answer the provenance question. Rather, the chemical analyses of metal objects were used for clustering, in combination to conventional archaeological typologies. For this purpose, about 22'000 analyses of objects from all over Europe were performed (Junghans *et al.* 1960, 1968, 1974), using the same analytical methods employed in Halle.

In order to identify the smelting technologies, the results were grouped based on arsenic, antimony, nickel, silver and bismuth concentration. Tin and lead were not considered for the classification, since they could be added to copper in a second moment. The proposed statistical arrangement (Fig. 1.1), based on a "decision tree", first gave rise to 12 metal classes (Junghans *et al.* 1960), later expanded into 29 (Junghans *et al.* 1968). However, this method manifested some problems related both to the use of fixed concentration ranges and to the fact that some of them were close to the detection limits. In this developed classification, the metal groups are not very clear and difficult to use.

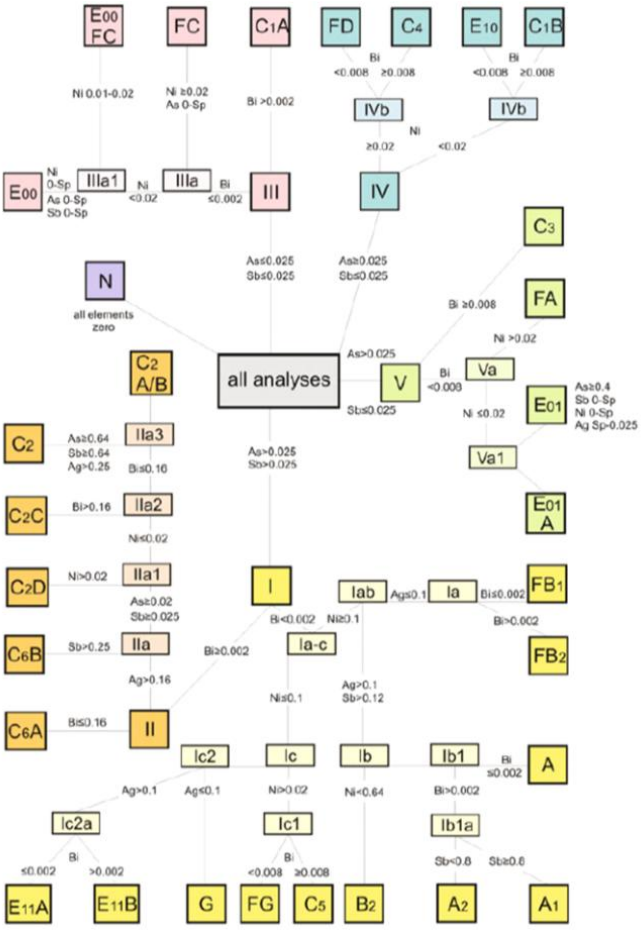

Fig.1.1 – Classification scheme developed and used by the Stuttgart team apt to find chemical similarities among prehistoric copper objects.

Nevertheless, thanks to the results of this large analytical program, it has been established that metallurgy began with the use of native copper and that the extractive metallurgy did not appear to be significant before the 5th millennium B.C.; even then, copper remained rather pure. In the 4th millennium, arsenical copper dominated over a large area of Eurasia, but only at the beginning of the Bronze Age the composition of metal objects changed because of tin, both in major and minor elements.

Disregarding the much discussed problems of representativeness and accuracy, at that time justified by the scarce need of an inter-laboratory comparison, different criticisms arose: 1. the employed statistical methods for data interpretation; 2. the possible changes during the metal production and 3. the chronological framework used for the evaluation of the analyses (Pernicka 2014).

In 1990s, a re-evaluation of the Stuttgart's data started. First, Eckel (1992) reinterpreted the results and set-up material classes based on analysis of variance; the relation of As/Sb, Ag/Ni and Sb/Bi was investigated, but the main disadvantage was that the analysis was based on bivariate plots. Later, the collaboration between E. Pernicka and R. Krause led to the integration of the available analyses of Neolithic and Early Bronze Age metal objects in Central Europe (Krause and Pernicka 1996) with additional regional studies in order to determine significant copper-ore types. Thus, the metal compositional groups individuated by the Stuttgart team were divided in (1) ultrapure and pure copper, (2-3) arsenical and antimonial copper, and (4-5) fahlore metal with/without nickel (Pernicka 1990). These five groups represent different ores, while the sub-groups presumably identify different ore deposits or metal circles.

The advent of lead Isotope analyses

The isotopic ratios of several elements are currently used in geology both for dating purposes and to trace the history and mode of formation of rocks and minerals (Faure 1986). The introduction of lead isotope analyses first applied to lead and silver and later extended to copper and copper-based alloys, marked a turning point in provenance studies (Gale and Stos-Gale 1981; Pernicka *et al.* 1984). The validity of Pb-isotopes methods for metal provenance was widely discussed for many years (Tite 1996; Pollard 2009; Gale 2009).

Lead has four stable isotopes, from which ^{206}Pb, ^{207}Pb and ^{208}Pb are the stable end-members of three long-term natural radioactive decay chains starting with Uranium and Thorium. The fourth isotope (^{204}Pb) is not radiogenic, even though it is very weakly radioactive and decays to stable ^{200}Hg by α-emission with a long half-life (1.4 x 10^{17}

years). Because of its very long half-life, ^{204}Pb is treated as a stable reference isotope. In Tab.1.1 the parameters of U-Th-Pb system are reported (Faure and Mensing 2005).

Tab.1.1 – Parameters of the U-Th-Pb system

Isotope	Decay mode	Half-life (years)	Daughter
^{232}Th	α,β	14.010×10^9	^{208}Pb
^{235}U	α,β	0.7038×10^9	^{207}Pb
^{238}U	α,β	4.468×10^9	^{206}Pb

The relative natural abundances of these four isotopes are 1.4% (^{204}Pb), 24.1% (^{206}Pb), 22.1% (^{207}Pb) and 52.4% (^{208}Pb), but the absolute abundances in any particular mineral or geological deposit depend on the geological age of the deposit and on the initial concentration of U and Th, which are related to the nature of the deposit. These four isotopes can be combined into several ratios, but only three of them are independent (Villa 2009). The interpretation of data for provenance studies is based on the simultaneous interpretation of at least two bidimensional plots. The most commonly diagrams used in geology are $^{206}Pb/^{204}Pb$ vs $^{207}Pb/^{204}Pb$ and $^{206}Pb/^{204}Pb$ vs $^{208}Pb/^{204}Pb$, whereas $^{206}Pb/^{204}Pb$ vs $^{207}Pb/^{206}Pb$ and $^{206}Pb/^{204}Pb$ vs $^{208}Pb/^{206}Pb$ are more frequent in archaeology; for the purpose of the present study, the first method of representation is preferred. An exhaustive explanation of the reasons behind the two options is described by Nimis (2010) and Artioli *et. al*. (2015).

The application of this method implies that the isotopic composition of the raw material of the artefact is not influenced by the change in chemical/physical state occurring during the metallurgical process. Indeed, all the experimental tests showed that the reduction and refinement stages do not change the isotopic signal, and no fractionation occurs (Pernicka 2014); therefore, the Pb-isotope ratios measured on metal and slags can be reasonably assumed to be the same of those in smelted minerals, within the experimental error (Addis 2013).

The major problems involved in the lead isotope method are the following (Artioli 2010):

1. Lead isotopes alone cannot allow for a distinction between different ore bodies formed at the same geological time in similar type of hosting rocks;
2. The ore sampling is a crucial step in order to obtain reliable signals. In fact, an ore deposit is a very complex reality that comprises different “generations” of ores

(primary sulphides, remobilized sulphides, secondary high temperature minerals, secondary low temperature minerals and, sometimes, native metal). Knowing that, a proper sampling of the deposit and the application of the isochronal line model commonly permits to overcome this problem;

3. The melting/mixing of recycled metal scraps and/or the addition of lead may influence or erase the signal of the ores originally employed for each component. Thus, the resulting signal depends on the Pb content and on the extent of alloying/mixing.

In order to increase the discriminant power of the lead isotope ratios, it is common sense to combine these data with trace element analysis in order to have a comprehensive metallurgical fingerprints and additional indications of the deposits such as age and mineralogical assemblage (Artioli 2010). Although metallurgical processes affected the trace elements concentration (Tylecote *et al.* 1977; Pernicka 1987, 1999), their investigation may be very helpful in the discrimination of different sources (Pernicka *et al*. 1993; Artioli *et al.* 2008).

Alpine Archaeocopper Project (AAcP)

In the last decade, a substantial work involving sampling and analysis of copper mines was conducted within the Alpine Archaeocopper project (AAcP). The aims of the AAcP are to define the mineralogical, petrological and geochemical features of the Alpine copper deposits and to develop a go-forward database of elemental and isotopic tracers for the provenance of ancient copper metals and smelting slags. The AAcP research group[2], led by Professor Artioli, collaborates with several academic and non-academic Institutions, such as the Institut für Geologie, Universität Bern (in the person of the Professor Igor M. Villa), the Gruppo Archeologico Agordino (ARCA), the Museo di Scienze Naturali dell'Alto Adige, and many others. The copper mines so far taken into consideration are located across the entire Italian Alps from Liguria to Friuli, in the northern Apennines and in the Queyras Region (France). Several copper districts have almost completely been characterised, such as those in the Trentino-Alto Adige region (*i.e.* Valsugana, Valle dei Mocheni, Valle Isarco, Val Venosta and others); whereas others have been at least partially covered and are the subject of the on-going research. To date, the only Italian Alpine area that has not been systematically investigated is the Central Alps of Lombardy. Currently, the AAcP database consists of more than 400 Pb-isotopic

[2]Web site: http://www.geoscienze.unipd.it/aacp/welcome.html

analyses performed on metallurgical artefacts, mine ore samples and copper smelting slags.

Although a significant number of investigations conducted in the last decades has resulted in the publication of lead isotope data for many deposits in Europe and around the Mediterranean region (OXALID database at the Oxalid Isotrace Laboratoy[3]; Brettscaife Mediterranean database[4]; Ling *et al.* 2014 and references within cited), only few studies have been focused on the Italian Alps. This lack of data represents a serious gap, since the Western Alps, and especially the Italian Eastern Alps, are well-known sources of prehistoric metal, testified by the presence of vast amounts of smelting slags (Weisgerber and Goldenberg 2004). Nevertheless, a re-visitation of copper metallogeny in central-eastern South alpine region (Nimis *et al.* 2012) and a further investigation of the deposits in the Western Alps (Artioli *et al*. 2009) started to fill this deficiency. The potential of the AAcP database was widely remarked by Artioli *et al.* (2008, 2010 and 2014) and confirmed by its preliminary application to archaeological slags (Addis *et al.* 2012; Artioli *et al*. 2015). The analyses of trace elements and Rare Earth Elements (REE) of the samples included in the database have been partially performed and are still in progress, in order to provide an additional comprehensive geochemistry database. This combination of geochemical and isotopic parameters is considered to be useful to resolve ambiguities for mines having similar isotopic signal (Baron *et al*. 2013).

Considering that there are only few isotopic works on the Bronze Age in Northern Italy, one should cite the isotopic analyses in the paper of Jung *et al.* (2011), in which 35 total objects of the Middle and Final Bronze Age were analysed (22 from Veneto and Lombardy and 6 from Apulia and Calabria). Unfortunately, it is not possible to compare such data with those from other experiments, since the isotopic ratios and chemical data are not reported. On the other hand, some compositional/isotopic data are available for Early Bronze Age materials found in the North Alpine area (Hoppner *et al*. 2005; Duberow *et al*. 2009; Cattin *et al.* 2009, 2011a, 2011b) and belonging to the Unetice Culture in Central Europe (Niederschlag *et al.* 2003). It should be also mentioned the project "I Bronzi del Garda", in which 176 objects found in several site in the Verona province were analysed by XRF, and a selection of 18 samples were subjected to lead isotope analysis (Pernicka and Salzani 2011); in this case-study, the time span goes from the Copper Age to the Entire Bronze Age.

[3]Web site: http://oxalid.arch.ox.ac.uk
[4] Web site: http://www.brettscaife.net

1.2 Historical contest of the Late Bronze Age in *Caput Adriae* region

The Italian Bronze Age can be approximately divided into four periods: the Early Bronze Age (EBA: 2300 – 1700 B.C.), the Middle Bronze Age (MBA: 1700 – 1300 B.C.), the Recent Bronze Age (RBA: 1300 – 1200 B.C.), and the Final Bronze Age (FBA: 1200 – 950/900 B.C.) (Pearce 2004; Peroni 2004; De Marinis 1999; Bietti Sestieri 1996). Contrary to the English academics, who refer to the RBA as the *Late*-BA, the Italian academics use the term Late in order to describe the RBA and the FBA (Pearce 2004). In this dissertation, the Italian convention will be used, *i.e*. the Late Bronze Age will indicate both Recent and Final Bronze Ages.

As it happened throughout Central Europe, the last part of MBA in Friuli Venezia Giulia was characterized by a consolidation of the territorial organization of the settlements and deep socio-economic changes; entire villages were abandoned and scattered settlements have arisen as fortified hill-top sites (the so-called *Castellieri*). These settlements were part of a structured and organized exchange system that linked the Terramare area, located approximately in the northern Italy south of the Po River, to the Alpine and Danubian regions (Cassola and Vitri 1997). New classes of objects, as spears and swords, appeared in the metallurgical production while EBA models were still circulating and a typological development of other classes of objects models is attested. In fact, during the Bronze Age the winged flanged axes undergo an evolution of the wings shape (Carancini and Peroni 1999) and this chronological transformation will be useful for the purposes of this thesis. Despite the widespread diffusion of metallurgy, the phenomenon of metal hoarding was not more frequent than earlier periods. In parallel, weapons were deliberately thrown in rivers or placed on the top of mountains as tributes to gods or spirits. This type of ceremonial deposition is widely attested in Friuli Venezia Giulia, especially in the Southern Plain, and the discovery of such swords having technical features and decorative style consistent with European models (De Marinis 2011) demonstrated the role of this area as a hinge between Po-Valley and the Danube areas.

In the RBA, the technological and industrial progress perceived in the MBA were further developed and the circulation of techniques, ideas, models and types across Europe encouraged the production of standardised objects and to the formation of a common language*,* defined as metallurgical *Koiné* (Peroni and Carancini 1997). For archaeologists, the main consequence standing behind this increase in demand of the metallurgical production was the growth of the exploitation of the Carpathian area and Alps. Moreover, another connected effect is the explosion in the number of metal hoards, usually hidden outside settlements.

At around 1200 B.C., an unstable situation occurred, leading to the collapse of the Palafitticolo-Terramaricola culture. The so-called Proto-Villanovian culture was the new cultural phase that began in the FBA in the area of the central Po plain and influenced the adjacent areas in the Apenninic and Alpine margins. With the collapse of Terramare culture, the Friuli Venezia Giulia plain acquired a strategic importance as the connection area for commercial traffics between the Alps (Slovenia and Urnfield spheres) and the Po Valley (Simeoni and Corazza 2011). In this regard, strong contacts with Frattesina were attested by funerary assemblages (Borgna 2006). Frattesina was the most important LBA site for the craftsmanship activity and it was certainly a centre for bronze metallurgy (about 70 moulds, numerous metallic objects and several pick-ingots were found), glass production, and ivory and amber working (Angelini *et al.* 2010; Bellintani and Stefan 2009; Angelini *et al.* 2004; Towle *et al*. 2001).

In general, the FBA was characterised by a change in the settlement strategy, in the production technology of different materials (*i.e.* metals, glasses,..), in the economy of sustenance and in the food procurement (Bagolan and Leonardi 2000; Harari and Pearce 2000; Leonardi 1979), possibly related to the recession period due to conflicts, migrations and demographic depopulation. Under these circumstances, the number of metal deposits increased. These hoards consisted of large amounts of raw metal fragments and ingots, predominantly associated with very few objects, which were also mostly drastically fragmented. Pick-ingots and shovels, together with other objects such as winged-axes (Ponte San Giovanni type), constitute a very important signature of the last part of FBA (FBA2). Moreover, basing on their distribution maps, they seem to be a strong indication of a directional exchange between the Slovenian hinterland and the South-Eastern Alps, the Friuli Plain and the site of Frattesina (Borgna and Turk 1996).

1.3 Research aims

As discussed by Cierny (1992, 1995, 1997, 2001) and Zucchini (1998), in the southern part of the Alps there are only modest copper ore deposits, with the notable exceptions of the Trentino and the South Tyrol regions. In particular, copper ore deposits are almost non-existent in Friuli Venezia Giulia. One single deposit with mixed ores such as tetrahedrite is attested on Mount Avanza, apparently firstly exploited in the Middle Age (Giumlia-Mair 2005 and 2009). This fact poses the question on the origin of the copper circulating in Friuli Venezia Giulia, contributing to the hypothesis that it had to be imported from outside the region.

Therefore, the principal aims of the present research are to investigate the origin of the metal, identify the ores exploitation areas and try to reconstruct the circulation paths in the North-Eastern Italy in the Late Bronze Age (LBA). Thus, in order to face these crucial points, the research focused on the archaeometric study of copper and bronze artefacts from well-dated protohistoric "stock-in-trade" hoards in Friuli Venezia Giulia (Fig. 1.2), with the aim to establish possible correlations between composition and typology of the objects, and to investigate the skills involved in the object creation, such as the consciousness of the alloying process.

Fig. 1.2 – Map of Italy in which the Friuli Venezia Giulia region is highlighted in black**.**

Although a deep interest for this region has been shown since the beginning of 1900 (Pellegrini 1911), a systematic research program that could define the circulation routes of Alpine Copper in North-Eastern Italy has never been carried out. Actually, only sporadic chemical analyses have been performed (Pigorini 1985; Tuniz *et al*. 1986; Casagrande *et al.* 1994, Giumlia-Mair 2000, 2003, 2005, 2009) and, until now, the interpretation of their provenance is not supported by isotopic data. In this regard,an extensive study of copper ingots, weapons and tools found in Friuli's metal hoards is considered interesting for the definition of a more detailed picture that, besides clarifying the mineral charge used, should confirm the hypothesis of a change in the copper supply between the MBA and the RBA/FBA, possibly shifting from the Balkans to the Eastern Alps source areas (Giumlia-Mair 2009).

As mentioned in Section 1.2, the choice of Friuli Venezia Giulia is due to its geographical key role as an economic and commercial hub between the Adriatic area and Central Europe and, therefore, the study of sealed complexes embracing the time period from the MBA to the FBA is needed. In this regard, the hoards of Cervignano (RBA), Muscoli (RBA-FBA1), Castions di Strada (FBA1), Celò (FBA1/2), Verzegnis (FBA1/2), Galleriano and Porpetto (FBA2) were identified and selected, all of them including both raw ingots and manufactured objects. Unfortunately, there are no known hoards from the MBA; therefore, only sporadic finds dated to this period have been selected (further details in Chapter 2).

The composition and microstructure of the selected objects were fully investigated in order to shed light on the different Cu-ore charge used and on their alloying and manufacturing process; moreover, another goal was to compare the results with the available data, especially those of coeval materials found in Veneto and in the Slovenian area (Chapters 4-5). Among the selected ingots, pick-ingots show a characteristic shape that allows tracking a well-defined distribution area, which extends from Balkans to France (Pellegrini 1992; Bietti Sestieri 1997; Borgna and Turk 1998; Bellintani and Stefan 2008) and in Italy such ingots do not turn up in contexts earlier than FBA2 (Carancini and Peroni 1999). For these reason they were frequently discussed in terms of FBA metal trade (Borgna 1992, Borgna and Turk 1996). Particularly interesting are the pick-ingots appearing in Slovenia, as well as in several sites of Friuli Venezia Giulia, Veneto and Tuscany. The present work is also extended to the chemical and metallographic analysis of weapons (in particular swords and axes), since these artifacts possess distinctive typologies that can be related to specific chronological and geographical distributions. Furthermore, since weapons possess very stringent and controlled compositional/physical

properties, they are assumed to be less prone to metal recycling and more suitable for provenance studies.

Finally, based on chemical results, lead isotopes analysis was carried out on selected samples, both objects and ingots. The set of mineralogical, metallurgical, chemical and isotopic analyses, through a comparison with existing Pb-isotope databases (OXALID; BRETTSCAIFE; Ling *et al.* 2014), published data (Nimis *et al.* 2012) and the Alpine Archaeocopper Project database (AAcP, Artioli *et al*. 2008) allowed should indicate a pattern for the provenance and diffusion of the metal (Chapter 6).

Archaeological Contexts and Materials

Metal deposition in hoards is known to be a common phenomenon during the entire Bronze Age, whose distribution covered a wide area from Europe to Eurasia (Harding 2000). The term “hoard” indicates the collection of entire or fragmented artefacts, usually of fine quality or high value, which has been well-sealed and hidden in the ground. In general, the main hoard components are tools and weapons as well as metal ingots, but pendants and ornaments can be often found in association (Gori 2014). Thus, the discovery in hoard of personal equipment can be useful in order to distinguish between the male or female nature of the hoard itself, allowing for the attribution of roles, tasks and the social *status* that prevailed in the deposition activity. These accumulations are known to be mostly located outside of settlements, forming isolated contexts; therefore,their chronology can be deduced from their components and in part from the context, which could provide useful information. Moreover, it should be remarked that there are hoards in which metal objects lie in association to other materials, such as glass beads and amber, in this regard, Mount Cavanero hoard (Chiusa di Pesio) could be an example of these depositions (Venturino Gambari 2009). However, in this work the attention will be only focused on metal deposition.

In these metal hoards, copper and bronze objects were purposely buried for reasons that are difficult to fathom. Earlier generations of archaeologists thought that hoards were caches of itinerant metalsmiths, who buried their wares either for safekeeping or to avoid carrying them over long distances, and never returned to dig them up (Bogucki 2008). Although this is a possible explanation, especially when there is evidence of metalworking tools, in many cases this represents a romantic interpretation that can actually assume different meanings. In a first instance, the principal approach concerns the distinction between ritual hoards, characterized by permanent depositions perhaps involving votive offerings or ritual practises, and non-ritual hoards buried with the idea of a later retrieval which are composed predominantly by functional objects (Coles and Harding 1979, Levy 1982; Gori 2014). In addition, recent studies (Bradley 2005) highlighted two interesting aspects which are helpful for the interpretation of the hoards, both ritual that utilitarian ones. First, it should be stressed the difficulty of discriminating between the ritual and the

profane purpose and, therefore, the inability to distinguish the evidences of utilitarian activities (*e.g.* burial of foundry materials in a smelting site) from ritual ones (*e.g.* foundry materials buried following the rules of a ritual deposition). In fact, in some contexts, the same class of objects might be used as grave goods or as votive offerings, whilst, , they appear to have been accumulated as re-casting metal in others. Thus, far from representing opposite poles in the study of prehistoric metalworking, the 'votive' and 'utilitarian' models overlap, also because metalworking is a ritual practice itself (Bradley 1988 and 2005). On the other hand, it should be admitted the possibility that the hoards, considered well-sealed and containing materials removed together out of the circulation, does not always represent a unitary chronological phase but, actually, they could be subject to continuous re-openings and mixings before the definitive closure. This could partly explain the constant inability to reconstruct the fragmented objects present in the hoard (Bradley 2005).

The complex nature of a hoard can be described by several parameters, such the number of objects, the typology of the artefacts and their association in the deposit, as well as by their conservation state and the place where they are buried. Following these principles, several interpretations have been developed in order to categorize this phenomenon (Knapp 1988; Harding 2000; Gori 2014). In the following, the major functional classes are reported:

- A founder's hoard contains scraps of metal objects, ingots, casting waste and, often, complete objects in the finished state, usually fragmented or with signs indicating a deliberate breakage. These objects were probably buried with the intention to be recovered in a later time for re-casting purposes (Levy 1982).
- A merchant's hoard is a collection of new of half-finished functional items, generally of the same type, originated from different "metallurgical circles", whose assemblage has been explained as the result of a long-distance commerce (Gori 2014).The main conjecture is that the travelling merchant buried them for safety, with the intention of a later retrieval.
- A personal hoard is a collection of personal objects referring to clothing and the personal equipment, linked to the funerary sphere or buried for safety in times of unrest.
- A votive hoard, differently from the above mentioned, represents a permanent abandonment, buried in places where the objects cannot be recovered, typically out of settlement in watery places or boundaries. Votive hoards are often distinguished from functional deposits by the presence of other elements that can be interpreted as the material remains of ritual practises (animal bones, rest of fires, *etc*..), and the

presence of functional objects broken or intentionally deformed could be indicative of a ritual practise (Harding 2000; Dietrich 2014; Gori 2014).

Thus it is important to point out that the objects recovered from the previously listed deposits are indicative of commodities transactions of both raw metal and prestige goods, and they can be exploited as an excellent opportunity to investigate the potential copper sources and the flow of the metal during the Bronze Age.

In Friuli Venezia Giulia, numerous metal deposits embracing a chronological period between the Recent and Final Bronze Age were discovered (Fig. 2.1). To date, the known Friulian metal hoards are those of Castions di Strada, Belgrado di Varmo, sited on the right bank of the Tagliamento River, and those of Muscoli and Cervignano, located in the in the lower part of the Udine Plain; to these, it must be added the discoveries of Porpetto, near the Corno River (Borgna 2001). Moreover, besides the not well studied hoard of Carlino (Marano Lagunare), others deposits were discovered in the upper Plain and in the hills: Madriolol (near Cividale, Gargaro and San Pietro in the Gorizia province, Galleriano di Lestizza in the centre of the Friuli region, Verzegnis in the Carnia area, and Celò in the Eastern part on the Natisone River (Borgna 2001). For the main purposes of this research, seven metal hoards were selected from the above listed in collaboration with Prof. Elisabetta Borgna (University of Udine).

Fig. 2.1 – Distribution map of the metal hoard located in Friuli Venezia Giulia: ▲hoards, ■stray finds. After (Borgna 2000).

As mentioned before, the items were not always buried intact and is not possible to exclude that their breakage could be accidental or, in other cases, that they could be broken for ritual purposes or in order to make them useless; however, in most cases, the typological features of the selected artefacts were preserved, allowing for their chrono-typological connotation. Regarding the voluntary destruction or fragmentation of objects in LBA hoards, this practice is extensively discussed in literature through different theories (Sommerfeld 1994; Chapman 2000; Bradley 2005) and it will not be treated here in detail, except to describe the features of particular samples.

For the purpose of the present work, the study of ingots may be considered of fundamental importance, since they possess a composition very close to the ore-charge used in the smelting process. Their selection has been conducted in order to be representative of the various morphologies occurring in each hoard, considering macroscopic characteristics such as the type of alterations, the state of corrosion and the possible presence of concretions on the surface. Moreover, whenever possible, the selection was extended to weapons, with the aim to better outline the commercial trade patterns and improve the knowledge about the following steps of the copper-working. In this regard, the classes considered in this study are axes, swords, spearheads and socketed-shovels. In Appendix 1 the main features of each investigated sample and the related archaeological references are reported.

2.1: MBA: Canale Anfora and Belvedere (stray finds)

Up to now, MBA hoards in Friuli Venezia Giulia are not known and, in order to increase the number of samples dated to this period, some stray finds belonging to this period was chosen for the analysis. The absence of associated material or structures makes their interpretation difficult, but swords can be generally well dated according to their typology. Therefore, two swords discovered in watery contexts, one from Canale Anfora and the other from Belvedere, were taken into account for this research (Fig. 2.1).

According to Harding (2000), river finds may have interpreted as funeral gifts, but also as offerings to the supernatural or as a means for deceased to fix their *status* and claim their prestige. It should be stressed that it is not possible to firmly exclude the occurrence of the metal recycling, since evidences of this practice has been attested at least from the Early Bronze Age (Barzero *et al.* 1991); therefore, there is no guarantee that the present day composition of ancient artefacts accurately reflects that of the mineral sites exploited (Pearce 1992). However, besides the actual weapons, the prestige bronzes from rivers

and bogs can be considered bronzes of high quality and seldom subject to such practice because of their votive meaning.

The sword of Canale Anfora

In 1980, during the excavations of Canale Anfora settlement, a fragmented sword (Can-S) was recovered out of an archaeological context as results of a superficial survey (Gnesotto 1980 and 1981). Looking at its conservation state, it should be considered that the fragment is difficult to interpret owing to its surface highly corroded and the presence of thick alteration patina (Fig. 2.2a); moreover, owing to the absence of the hilt it is not possible to attribute it with confidence to any group. Nevertheless, on the basis of the blade typology, its section and the presence of two grooves at the edge (Fig. 2.2b), this sword could be cautiously compared with the MBAIII-RBA types, very common in the *Caput Adriae* area (Gnesotto 1980: 393, 1981: 6-36; Tasca 2011).

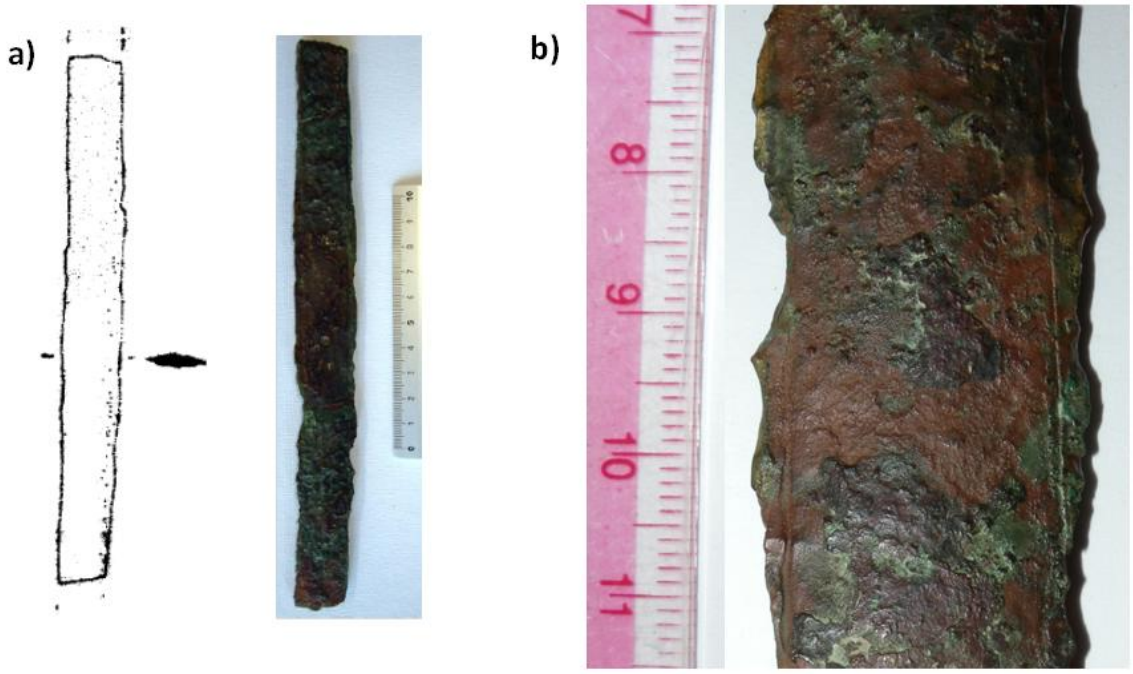

Fig. 2.2 – a) Photo and archaeological drawing of the Canale Anfora sword and b) a detail in which the blade grooves and the alteration patina are evident.

The sword of Belvedere

In 1914, a sword (Bel-S) was accidentally found 5 km far from Aquileia, more precisely at S. Marco di Belvedere, in Udine province. It is a 55 cm long sword whose hilt-plates were secured by five rivets, four in the handguard and one in the handgrip (Fig. 2.3). It shows wide round shoulders and distinctive midribs that allow for its attribution to the transitional phase between the types *Sprockhoff Ia* and *Sprockhoff IIa* (Foltiny 1964). The pattern of the rivet holes is characteristic of the type *Sprockhoff Ia* (Cupitò 2006: 86), but the blade is broader. This sword was associated to the Montegiorgio-type by Bianco Peroni (1970) and dated to the last phase of the MBA by Schauer (1971), and could be connected to two similar weapons, discovered in Zlebić toward the Slovenian hinterland and near Gradisca, close to the Adriatic Sea (Cowen 1956).

Fig. 2.3 – Photo and archaeological drawing of the Belvedere sword, Bel-S.

2.2 RBA: Cervignano

Accidentally discovered in 1984, the Cervignano hoard encloses 29 metal objects laid with numerous pottery remains, which allow for a RBA dating of the deposit (Vitri 1984, 1991; Borgna 2001; Tasca 2011). Moreover, the archaeological investigations performed by the Soprintendenza enabled to suppose that this hoard had been hidden on the border of a settlement that has been dated to the MBA/RBA on the basis of pottery remains (Borgna 2001).

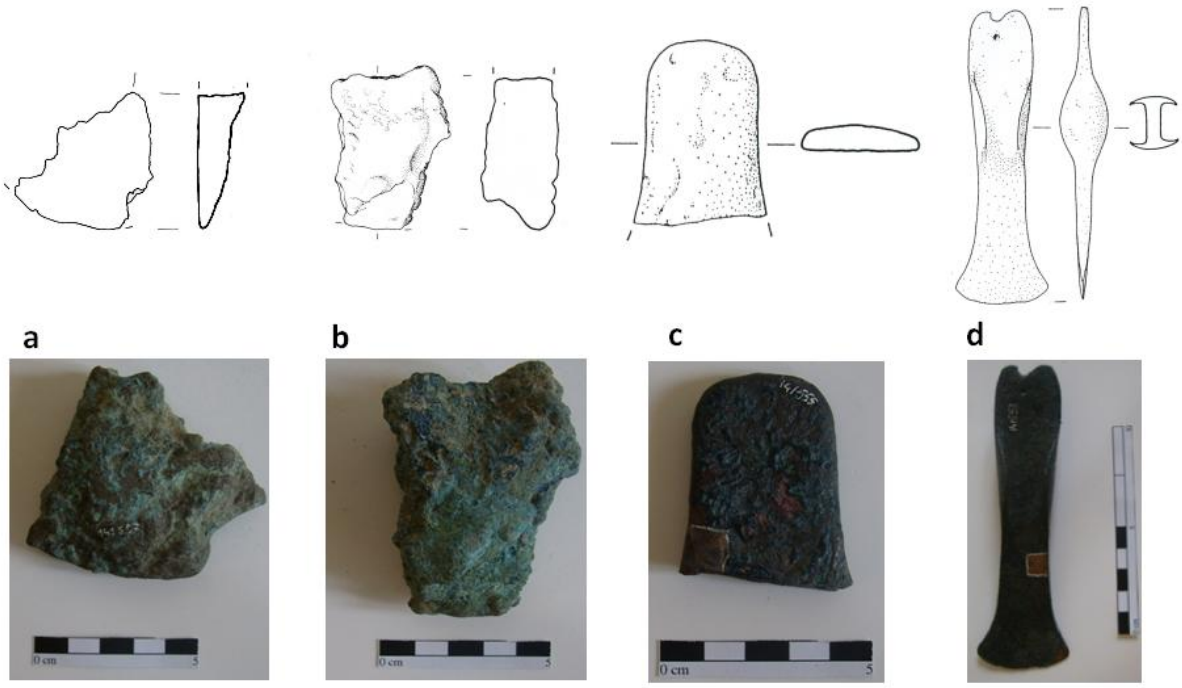

Fig. 2.4 – Photos and archaeological drawings of the different types of copper ingots belonging to the Cervignano hoard. a) Plano-convex ingot (Cer-PC-56); b) Parallel-surface ingot (Cer-PS-62); c) Tongue-shaped ingot (Cer-TS) and d) bronze winged-axe (Cer-Ax). Archaeological drawings from Borgna (2001).

The deposit was interpreted as a founder's storage because of the exclusive presence of many fragmented ingots and some tools, such as a winged axe, a chisel and a sickle blade (Vitri 1984; Vitri 1991;Borgna 2001). For the analyses, six Plano-Convex ingots (PC), five Parallel-Surfaces ingots (PS) and one Tongue-Shaped ingot (TS) were taken into account. PC-ingots are sub-triangular or rectangular fragments, in which the flat section on top and the underneath curved surface are preserved (Fig. 2.4a); in most cases, the ingots fractures are net at the top and irregular at the bottom, reflecting a dividing action. The weight of each PC-ingot is fairly typical for European LBA plano-convex melting products deriving from small furnaces, and estimated 2–to–4 kg (Tylecote

1992).On the other side, the PS-ingots differs from the PC ones for the flat surfaces and the constant section, as depicted in Fig. 2.4b. Finally, a fragment having flat ends and exhibiting rounded margins on the tapering sides represents the unique evidence of TS-ingot; as can be seen from Fig. 2.4c, the fracture highlights the convex section.

Among the objects found in Cervignano, the attention was focused on the axe (Cer-Ax, Fig. 2.4d), having a curved blade edge and large wings like flanges. In antiquity, a wooden pole would have inserted under the winged flanges and held in place by a thick rope, tied through the loop. Basing on Alpine comparisons, the winged-axe, as the chisel, may be referred to a non-advanced stage of the RBA (Vitri 1984; Borgna 2001).

Thus, the Cervignano hoard can be compared to the Slovenian metal deposits belonging to the Phase I, characterized by reduced amount of metal, almost exclusively in combinations with entire tools, such as axes, chisels and sickles (Turk 1996).

2.3 RBA-FBA1: Muscoli

The deposit of Muscoli was found outside a settlement and it contains tools (10 sickles and 2 socketed-axes), weapons (2 swords deliberately broken) and fragmented PC-ingots (Marchesetti 1903: 135; Pigorini 1904: 138; Anelli 1949: 7-15; Vitri 1990: 170). Due to typological evidences, it could be dated to a later period than Cervignano and definitively sealed at the beginning of FBA (Borgna 2001).

The set of findings could be interpreted as a generic form of hoarding containing materials removed from the circulation for safekeeping, perhaps in times of unrest; this hypothesis is supported by the presence of prestige goods as swords and axes in the collection. In addition, the preservation study of these artefacts reveals clear traces of use/wear that suggest a prolonged circulation and use (Borgna 2001).

Besides the six PC-ingots (Fig. 2.5a), comparable in weight and shape to those of Cervignano, two swords and two axes were selected for this study. The swords, both fragmented, reflect an ancient chronological placement; in fact, one is associable to the Sacile-type (Bianco Peroni 1970: 55, fig 16, 113; Cupitò 2006: 203) and it refers to the end of MBA (Fig. 2.5c, Mus-S-3), whereas the other, a Cetona-type (Bianco Peroni 1970: 63, Fig.16, 140), can be dated to the RBA (Fig. 2.5b, Mus-S-2). As suggested by Rezi (2010), the fragmentation or defunctionalisation could be addressed to avoid any further use of the weapon, possibly for votive reasons, as also attested in Central Europe and in the Carpathian basin, although it is not possible to exclude that the storage of fragments could be due to a metal recycling practice.

The socketed-axes have different decorations. One axe (Mus-Ax-6, in Fig. 2.5d) shows an evident V-shaped decoration that commonly appears in weapons dated to the RBA and found in the eastern part of the Central Europe, in Austria, in Hungary and in the Northern Croatia (Turk 1996). Differently, the sample Mus-Ax-7 (Fig. 2.5e) shows "pseudo-wings" decoration embossed on each sides of the body and obtained with ribs arranged in concentric circles. From a chrono-typological point of view, such axe should be dated to a later period, probably to the FBA (Borgna 2001).

Fig. 2.5 – Photos and archaeological drawings of the artifacts belonging to the Muscoli hoard. a) Plano-convex ingot (Mus-PC-1); Muscoli swords; b) Mus-S-2; and c) Mus-S-3; bronze socketed-axes: d) Mus-Ax-6; and e) Mus-Ax-7. Archaeological drawings from Borgna (2001).

2.4 FBA1: Castions di Strada

As described by Pellegrini (1911), in the early 19th century two distinct metal hoards were discovered by chance near Castions di Strada. The deposits, 450m far from each other, are centrally located into the ancient commercial road system, close to the fortified settlement of Castions, which is dated to MBA/RBA and which was still active in the FBA and in the early Iron Age (Cassola Guida and Vitri 1997).

The first hoard, called Castions A, is composed by several fragments of axes, sickles, spearheads, and encloses a broken knife, a sword's blade, a decorated metal sheet, a

single bar-ingot, nine intact PC-ingots and some Truncated plano-Convex ingots (TC). Conversely, Castions B contains ingot fragments and undamaged tools and weapons; overall, two winged axes, an axe's blade, three sickles, a blade, a socketed-hammer, a chisel, several spearheads and a three-rings chain are ascertained (Borgna 2001). The complementary nature of the two hoards can be compared with the Slovenian deposits of Dragomelj (FBA), which exhibits the same "complete-fragmented" *chiasmus* structure (Turk 1997). As suggested by Borgna (2001), the presence of such different typologies of metal artefacts could be explained by the hypothesis of a tools and ingots storage, thesis that is reinforced by the absence of known in-situ metallurgical activity.

The depositions chronology assigns Castions A and B to the early FBA (FBA1), but ancient objects dated to the RBA were found in both of them (Borgna 2001). Since there are not significant differences in the hoard compositions, Castions A and B will be considered as a single context. Specifically, the examined samples are:

- twelve ingot fragments representative of the different shapes included in the hoard, such as PC-ingots, TC-ingots and the bar-ingot (Fig. 2.6a-c). Some of them are characterized by deep tracks, in order to remark the division and to facilitate the subsequent breakage;

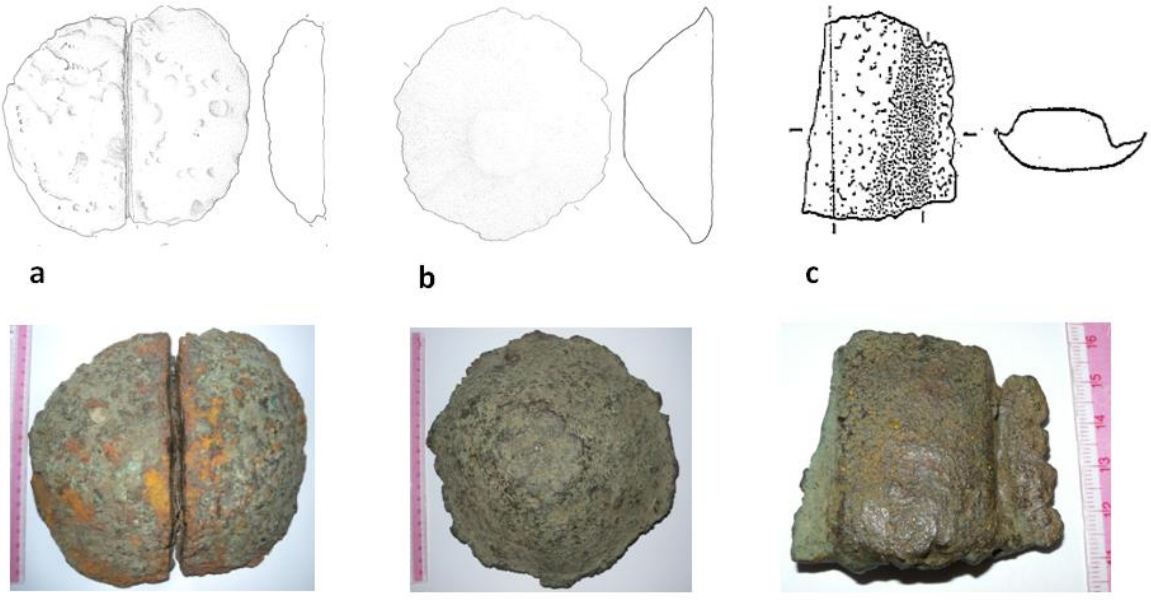

Fig. 2.6 – Examples of the different ingot typologies found in the Castions di Strada hoard: a) plano-convex ingot (CdSA-P-20); b) truncated plano-convex ingot (CdSA-P-18); and c) bar-ingot (CdSA-PnB).

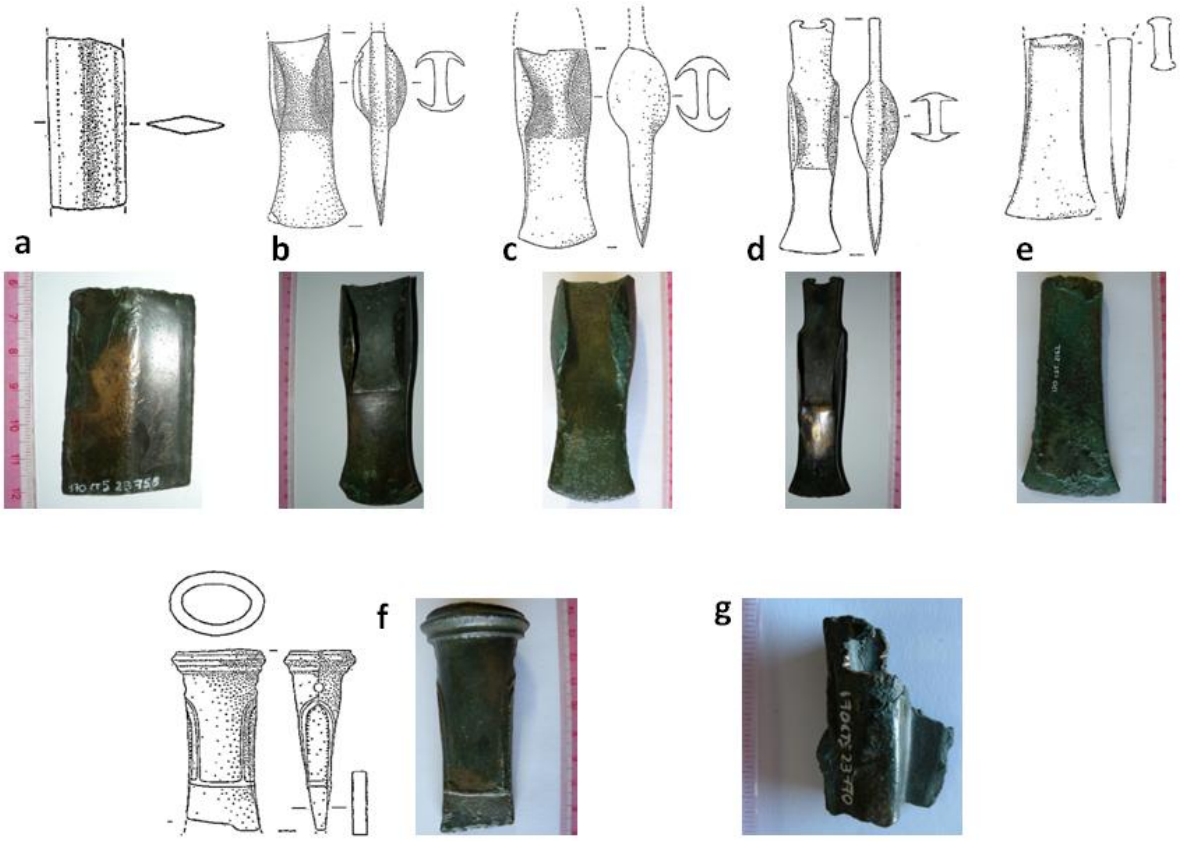

Fig. 2.6 – Photos and archaeological drawings of the weapons and tools belonging to the Castions hoard. a) sword's blade (CdSA-S); b-e) winged-axes: b) CdSA-Ax-59, c) CdSB-AxA-9; d) CdSB-AxA-1; e) CdSB-AxA-2; f) socketed-axe (CdSA-AxC-4); and g) spearhead fragment (CdSB-Cp). Archaeological drawings from Borgna (2001).

- a sword's blade (Fig. 2.6a, CdSA-S) dated to the MBA (Pellegrini 1911: 32; Foltiny 1964: 249; Bianco Peroni 1970: 39-40; Carancini and Peroni 1999: fig. 16, 3; Cupitò 2006: 79);
- two winged-axes (CdSA-Ax-59 and CdSB-AxA-9, Fig. 2.6b-c), broken on the top and exhibiting signs of wear on the cutting edge; in Fig.2.7a a detail of the blade of the sample CdSB-AxA-9 is reported;
- one winged-axe (CdSB-AxA-1) intact and well preserved (Fig. 2.6d);
- a further specimen of axe was taken into account; it has been always referred to the winged typology, but it is only characterized by the blade and, recently, it was reconsidered as doubtful (CdSB-AxA-2 in Fig. 2.6e);
- one socketed-axe without the blade (CdSA-AxC-4,Fig. 2.6f), broken in antiquity, on whose body the three-rib decorations are well-preserved on one side and altered by corrosion on the other; the two symmetrical holes were probably used to attach the handle. In Fig.2.7b a detail of the decoration is reported;
- a spearhead (CdSB-Cp) having signs of wear on the handle-hole (Fig. 2.6g).

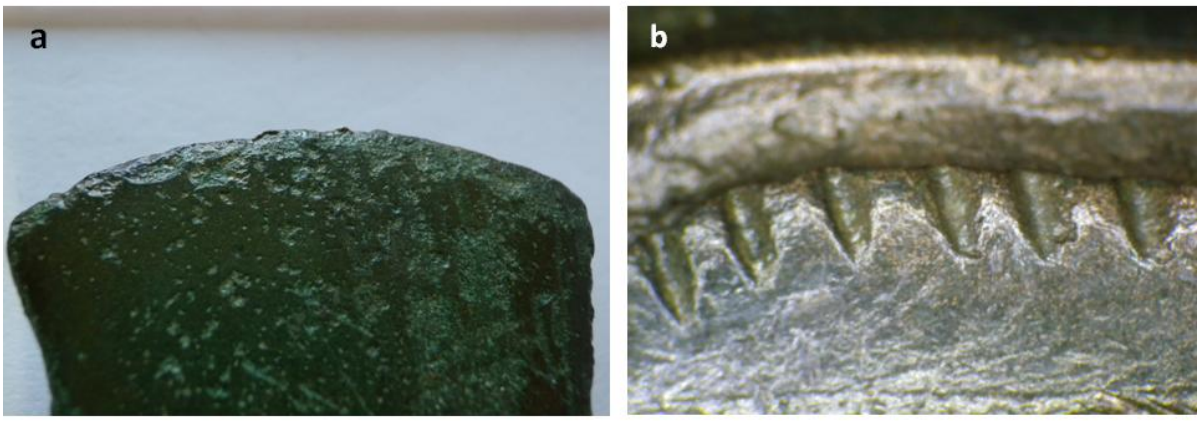

Fig. 2.7 – a) Detail of the Castions di Strada winged-axe's blade (CdSB-AxA9) exhibiting evident use-wear traces; and b) Particular of the body decoration of the sample CdSB-AxC-4.

2.5 FBA 1/2: Celò-Cicigolis and Verzegnis

Celò-Cicigolis[5]

In 1997, the National Archaeological Museum of Cividale has carried on an emergency excavation in Celò, in the municipality of Pulfero. In this occasion, it was brought to light an important protohistorical hoard, located on a hillin an isolated area on the right side of the Natisone River. The objects were arranged in a pit surrounded by large stones, perhaps in a container of perishable material (Concina 1997).This deposit encloses well-preserved items, among which four socketed-axes, eight winged-axes, eight sickles, a knife, a sword's blade, a socketed-shovel, several fragments of tools and weapons, and thirteen ingots are present. Observing the artefacts, two groups are recognizable. The first is composed by objects that were clearly subjected to a concrete use and whose deposition have taken place after an intense circulation, while the second group is characterized by objects possessing fusion defects, due to the mould casting, and unfinished artefacts, such as axes without a cutting edge or having a smoothed blade (Borgna 2001 and 2007).

Chronologically, Borgna (2006) attributed the Celò deposit to the FBA1/2 and, because of the presence of weapons, tools, ornaments and ingots, it can be comparable with *Phase II* of the Slovenian deposits, defined by Turk (1996, p. 110) as *large hoards of mixed compositions*. The possible interpretations are different: utilitarian deposit, "stock-in-trade" or reserve workshop. Furthermore, since its location along the Natisone

[5] The archaeological detailed study of this hoard is now the topic of a master thesis (Anna Nardini, tutored by prof. E. Borgna, Department of History and Preservation of the Cultural Heritage, University of Udine).

waterway, this deposit can be interpreted as a metal collection for distribution in a long-distance range, from the Alpine sources to the centres of the Friulan Plain (Borgna 2007; Concina 1997).

For this research, the selected samples are:

- Two PC-ingots and two TC-ingots (Fig. 2.8a-b), intact and exhibiting evident signs of extraction from the pit, probably done when the metal was not solidified at all (Fig. 2.8c). The weight varies from 2-to-6 kg.

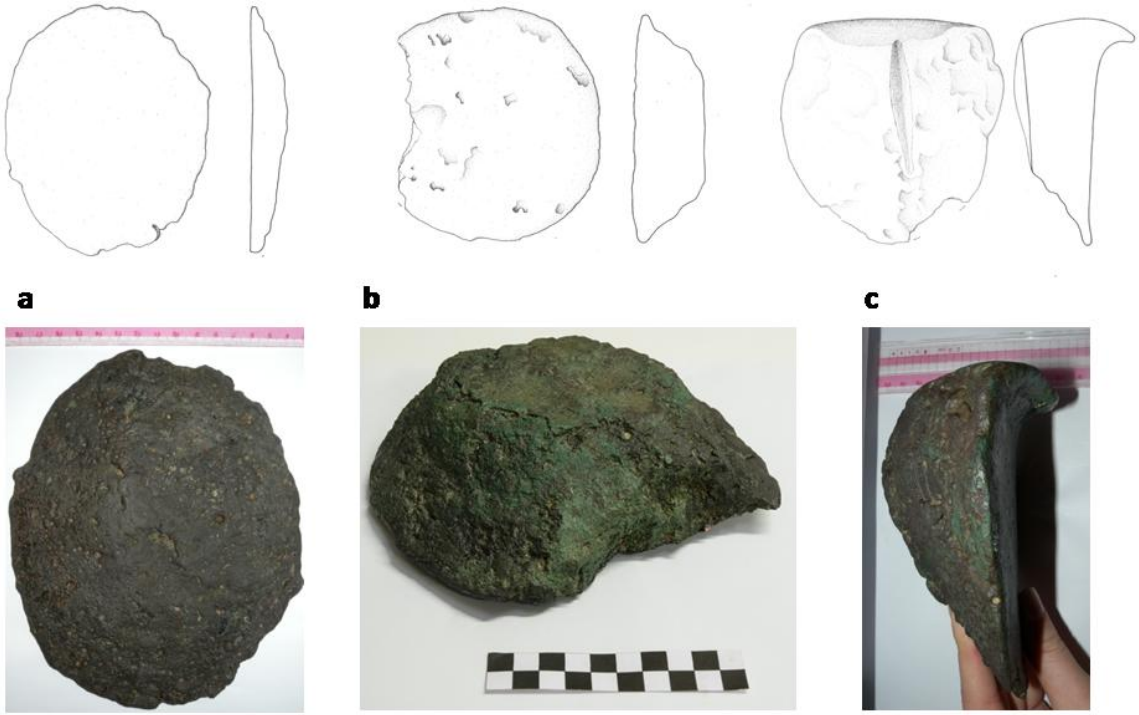

Fig. 2.8 – Examples of the ingot typologies found in the Celò hoard. a) PC-ingot (Cel-P-37); b) of TC-ingot (Cel-P-38); and c) PC-Ingot (Cel-P-39) showing an evident deformation of the edge due to the extraction from the pit. Archaeological drawings by Giuliano Merlatti, Archive of the Proto-historic Laboratory of the University of Udine.

- The fragment of a socketed-shovel (Cel-Pal, in Fig. 2.9a) characterized by tight shoulders. As stated by Bellintani and Stefan (2008), this typology is characteristic of FBA contexts of Northern and North-Eastern Italy and it can be interpreted as a commercial/economic indicator since this typology counts few specimens widespread between Lake Garda's area and Hungary; moreover, they associated this particular find to the *Fondo Paviani*-type. Specifically, Borgna (2007) compares this particular specimen to the socketed-shovel of Torretta di Legnago e Sabbionara di Veronella (Verona) on the basis of the handle shape and the blade length, dating this find to the beginning of the FBA; even if, as reported in Angelini

(2009), in the past the dating of the Fondo Paviani-type was attributed to the Recent-Final Bronze Age (Fasani and Salzani 1975), and most recently in the late XIII- early XII century B.C. (RBA 2) by the Santi and Leonardi (2007). For what concerns the distribution of socketed-shovels characterized by tight shoulders, see Figure 3 in Bellintani and Stefan (2008).

- The fragment of the sword's blade (Cel-S). At the top, the hilt has been broken in antiquity, as well as the blade. It still shows ending-pointed shoulders, the edges are sharpened and the blade is in good conditions; along the blade, a V-shaped incision is well-preserved (Fig. 2.9b). According to (Borgna 2001), this tang-sword should be referred to an early RBA production, probably MBA, and a properly comparison is proposed in *Le Terramare* (1997, p.726, Fig. 428, 2).

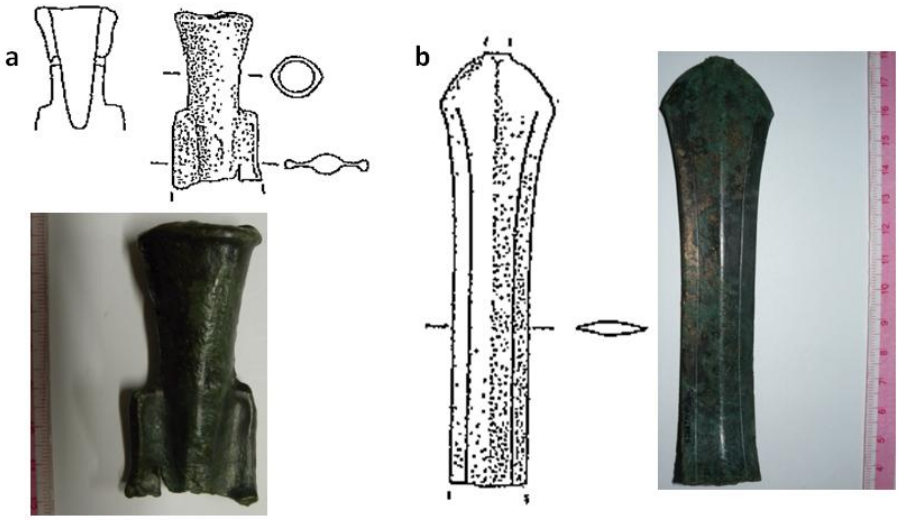

Fig. 2.9 – Photos of the a) socketed-shovel and b) the sword belonging to the Celò hoard. Archaeological drawings from Borgna 2007.

- Three winged-axes (Fig. 2.10a-c). Cel-AxA-2 and Cel-AxA-3 are complete samples, characterized by evidences of working and refining on the body and on the wings. Conversely, only the blade identifies the third axe (Cel-AxA-8), broken in correspondence of the handle location; its blade is asymmetrical, probably for the use.
- Two socketed-axes. The first possesses the V-shaped decoration (Cel-AxC-8, in Fig. 2.10d); the deburring on the cutting edge and the typical signs of the merge-moulds suggest that this model has not been treated after the moulding; its blade tip is massive and not sharpened, moreover, it shows one-side wear that can lead to suppose its employment only as stroke tools. The other sample, Cel-AxC-1, has

no decoration and, on one side, the merge of the two-moulds is clearly evident, as it has not been completely smoothed (Fig. 2.10e).

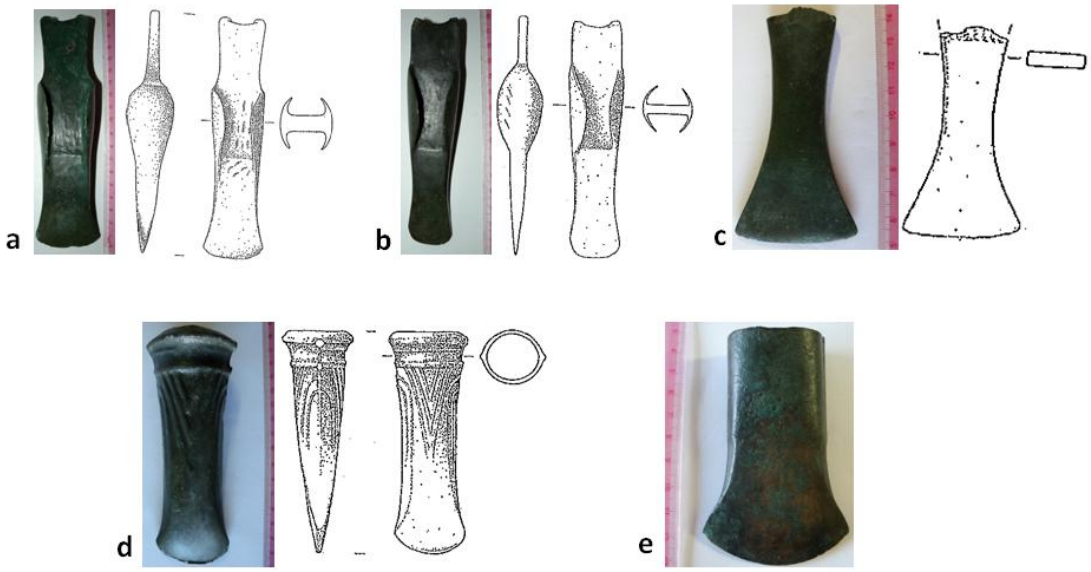

Fig. 2.10 – Photos and archaeological drawings of the axes belonging to the Celò hoard: Winged-axes a) Cel-AxA-2; b) Cel-AxA-3; c) Cel-AxA-8; and socketed-axes: d) Cel-AxC-8; e) Cel-AxC-1. Archaeological drawings from Borgna 2001.

Verzegnis

Among the selected hoards, that of Verzegnis is located further toward the North, in the Upper Tagliamento Basin (Carnia). The objects of ornamental/personal use and the ingots were contained in a vessel buried in a circular pit. Its interpretation is still doubtful and, if there are elements that could be related the deposit to the votive sphere, it is not possible to exclude that it could be simply destined to the recycle (Vitri, 1999; Borgna 2001). According to archaeologists (Borgna 2001), Verzegnis can be interpreted as contemporary of the Celò hoard, or possibly slight more recent. In this case, only two PC-ingots were made available for the sampling (Fig. 2.11).

Fig. 2.11 – Photo of one PC-ingot belonging to the Verzegnis hoard, sample Ver-P-0.

2.6 FBA 2: Galleriano and Porpetto

Galleriano di Lestizza

In March 1999, close to the hill-fort of Galleriano, a small hoard was unearthed (Vitri 1999). In the deposit, artefacts of practical use, such as a winged axe, a sickle, a socketed-chisel, a knife and a decorated bangle, laid in association with two pick-ingots and a fragment, interpreted as a possible axe blade by Borgna (2001).All these evidences support the interpretation of the Galleriano hoard as a storage, placed in a convenient area for the control of metal circulation in a long-distance commerce. Furthermore, the presence of pottery-remains and, in particular, that of pick-ingots has permitted to identify Galleriano as a FBA2 hoard, having evident correlations with Slovenian deposits belonging to the Phase III (Turk 1996). In addition, before the discovery of Galleriano hoard, the presence of pick-ingots has never been attested in this Central part of Friuli region, representing the first witness of such ingot type outside of their traditional distribution area. Therefore, the Galleriano pick-ingots must be added to those already discovered in Friuli in the hoards of Nimis, Purgessimo, Porpetto, Revidischia, Redipuglia and Madriolo (Borgna and Girelli 2011). In this study, the pick ingots, the winged-axe and the blade's fragment were selected for the analyses (Fig. 2.12).

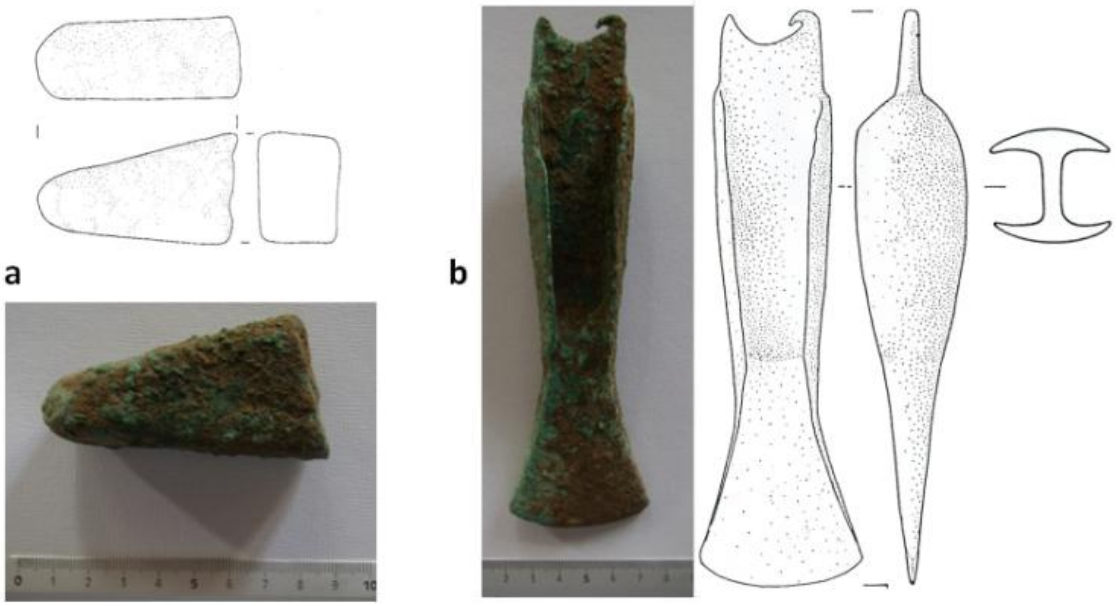

Fig. 2.12 – Photos and archaeological drawings of a) one pick-ingot (Gal-PI-4) and the Galleriano winged-axe. (Gal-Ax). Archaeological drawingsby Giuliano Merlatti, Archive of the Proto-historic Laboratory of the University of Udine.

Porpetto

Between 1996 and 1999, a deposit was discovered inside the Porpetto settlement (FBA), in the Isonzo region (Borgna 1996-1997, Borgna Turk 1998; Vitri 1999). Actually, the hoard is composed of two units in nearby locations that for the purpose of this study, will be treated as one. The deposit, located along the main communication routes, consists of huge amounts of raw metal and ingots mostly associated with very few objects that were sometimes drastically fragmented. Pick-ingots and socketed-shovels are in association with pottery that constitute an important evidence for a FBA2 chronology. As mentioned before, these types of ingots and shovels are interpreted as exclusive metal exchange indicators, testifying a strong hint for a highly directional commerce between the Slovenian hinterland and the Po Valley through the Friuli Plain; this combination is even attested in Frattesina and Montagnana sites (Borgna and Turk 1998; Bietti Sestieri 1997; Bellintani and Stefan 2008). Nearby the hoard, smelting evidences were found, such as metal wastes, lumps and ferrous encrustations, indicating a permanent activity near the settlement (Borgna 2000).

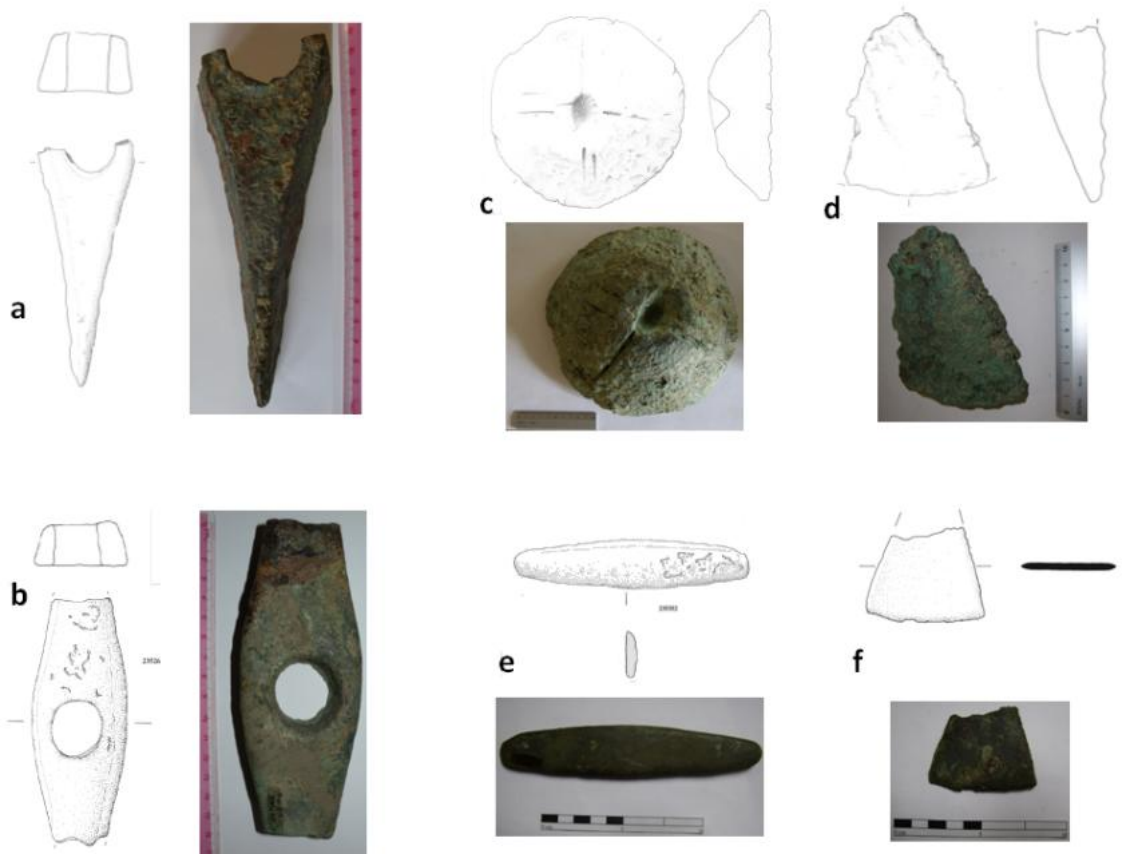

Fig. 2.13 – Examples of the ingot typologies belonging to the Porpetto hoard. a-b) pick-ingots: a) Por6-PI9 and b) Por9-PI-60; c) TC-ingot (Por6-TC-8); d) PC-ingot (Por6-PC-6); e) bar-ingot (Por9-Bar-5) and f) a flat/blade's axe-ingot (Por9-SN-1). Archaeological drawings by Giuliano Merlatti, Archive of the Proto-historic Laboratory of the University of Udine.

From this site, seven pick-ingots (Fig. 2.13a-b), nineteen ingots of different shapes (Fig. 2.13c-f), two socketed-shovels and one spearhead have been considered. The socketed-shovels are damaged and one of them only possesses the handle-hole (Fig. 2.14a), whereas the other is a fragment that does not show signs of actual use on the shoulder and on the blade (Fig. 2.14b); however, in the work of Bellintani and Stefan (2008), these findings are treated as a doubtful case, proposing a possible relation with the *tra Manciano e Semprugnano*-type. Therefore, the socketed-shovels from Porpetto should be dated later than the socketed-shovel from the Celò hoard, probably in the full FBA (Bellintani and Stefan 2008). For what concerns the distribution of socketed-shovels characterized by tight shoulders, see Figure 4 in Bellintani and Stefan (2008).

Even the spearhead appears fragmented, without the tip and without evidences of the handle-hole; however, it is only possible to distinguish the thick central rib and the sub-circular section (Fig. 2.14c).

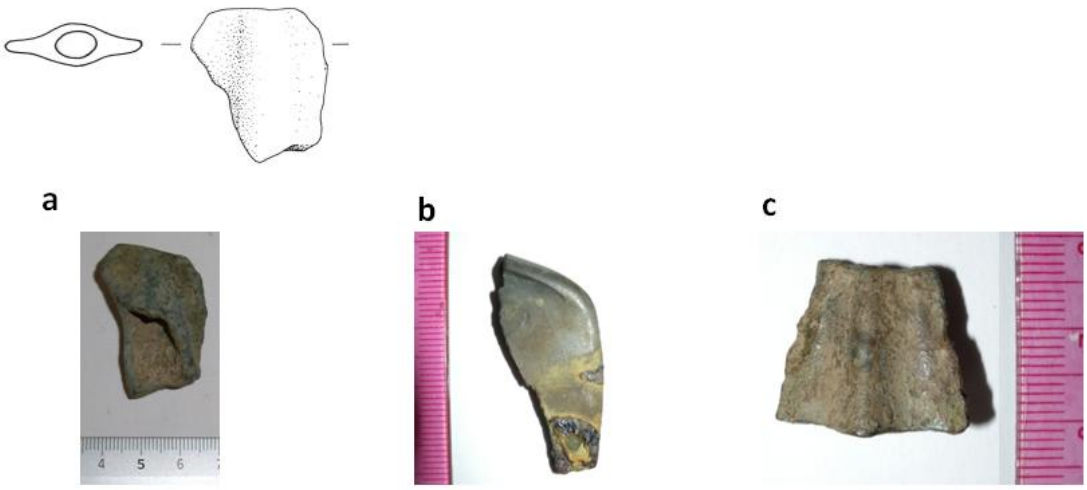

Fig. 2.14 – Photos of the different artifacts belonging to the Porpetto hoard. a) - b) The socketed-shovels and c) the spearhead. Archaeological drawings by Giuliano Merlatti, Archive of the Proto-historic Laboratory of the University of Udine.

Analytical Techniques

The archaeometric study of the selected samples involved the employment of several characterization techniques, and the related analytical protocol was divided into different steps. All the items were *in primis* macroscopically observed in order to study their weathering conditions, morphologic characteristics and, especially for objects, traces of manufacturing; moreover, weight and dimensions were recorded and photographic images of the samples were collected. At the time of the sampling, each specimen was analysed under the Stereo Microscope (SM) to observe the alteration state of the metal and choose the more representative sample from the examined object. The sampling was performed using a fine steel blade. Initially, all the obtained microsamples (0.5–1 mg of fresh metal) were embedded in epoxy resin and manually ground using 800, 1200, 2400 and 4000 grit SiC papers. Subsequently, the samples were properly smoothed and polished. The polishing was achieved using first 3 and then 1 micron-size diamond suspension (Dpsuspension-Struers) on a silk cloth at 250 RPM, in order to obtain scratch-free sections.

The samples prepared as indicated above were firstly examined in reflected light by an optical microscope(RL-OM) and then analysed by Scanning Electron Microscopy (SEM) coupled with an X-ray energy dispersive spectrometer (EDS) and an Electron Probe MicroAnalysis (EPMA). Subsequently, all sections were re-polished and chemically etched in order to perform the metallographic observations.

Finally, all the finished objects and the most significant ingots were subjected to lead-isotope analysis; this choice was carried out on the basis of the chemical results and on the archaeological relevance of the findings. The protocol step involving acid digestion and chromatography of specimens was realized in an ultra-clean laboratory of the Department of Geosciences (University of Padova), tested in order to produce reliable isotopic samples (Villa 2009), whereas the mass spectrometry analysis (MC-ICP-MS) was performed in part at the University of Bern (Institut für Geologie) and in part at the Gent University (Department of Analytical Chemistry).

3.1 Reflected-Light Optical Microscopy (RL-OM)

The optical microscopy observations were carried out on all samples, with the purpose of gaining information concerning the microstructures (*i.e.* grains morphology, phases typology and distribution of the different components), and how such features affected the casting and working properties of the metals themselves. The employed optical microscope is a Nikon Eclipse ME600 equipped with a Canon EOS 600D Digital single-lens reflex camera, operating in reflected light (RL-OM).

Generally, a metal or alloy possessing a cubic crystalline structure is viewed uniformly dark when observed in cross-polarized light; however, such view-mode is a fundamental tool that allows for the observation of certain microstructural details, such as Cu_2O inclusions, which appear as bright ruby-red particles in polarized light. In fact, other inclusions that have a similar morphology and colour to Cu_2Oinclusions do not respond to polarized light when viewed under bright-field illumination(Vander Voort 1984).

Furthermore, according to Scott (2012) in matter of copper and bronze metal objects, the application of acid aqueous ferric chloride ($FeCl_3$) for few seconds is sufficient to reveal grain boundary contrast. Indeed, the etching is basically a controlled corrosion process which produces grooves at grain boundaries and reflectivity differences.

3.2 Scanning Electron Microscopy (SEM-EDS)

Scanning Electron Microscopy (SEM) enables the study of the morphological and textural characteristics of the metal matrix. In particular, backscattered electrons (BSE) images are used to detect the contrast between areas having different chemical compositions and to evaluate the weathering conditions of the samples. The investigation was performed at the Department of Geosciences of the University of Padua using a CamScan MX 3000 SEM equipped with a LaB6 cathode, coupled with an energy dispersive spectrometer (EDS) for chemical analyses working in high vacuum mode. The back-scattered electrons images and the micro-chemical analyses were acquired using the CamScan Helios 5.2.22 software and the SEM Quant PhiZAF software, respectively. The bulk compositions were acquired analysing 3÷5 dimensionally similar areas, whereas the inclusions dispersed within the α-phase were characterized using the spot-mode analysis. All the observations were performed at 25 kV, with a working distance of 25 mm and the count time applied for the EDS analysis was 180 s. The analyses were performed on the polished sections samples, coated with a thin carbon layer as conductive material. The detection limits in the SEM-EDS analysis are about 0.1–0.3 wt% for the most part of

the elements and, for this reason, reliable quantitative analyses for trace and minor elements were obtained from Electron Probe MicroAnalysis.

3.3 Electron Probe MicroAnalysis (EPMA)

Quantitative chemical analyses of trace and minor elements in the metal matrix, inclusions and segregations were performed at the CNR-IGG laboratory in Padova (Department of Geosciences), using a CAMECA SX50 electron microprobe fitted with four vertical wavelength-dispersive spectrometers (WDS) and one energy dispersive spectrometer (EDS). In this instrument, SEM and BSE imaging plus sophisticated visible light optics provide very flexible sample inspection with image magnification ranging from 40 to 400'000 X.

The adopted working conditions for the selected suite of elements (S, Cl, Mn, Fe, Co, Ni, Cu, Zn, As, Ag, Sn, Sb, Pb and Bi) were accelerating voltage of 20 kV, beam current intensity of 20nA and counting times of 5-10-5 s on background-peak-background, respectively. The spot size of the beam was about 2 μm^3. Synthetic metallic oxides were used as standards for most of elements, whereas, in some cases minerals were employed – such as blenda for S and Zn, vanadinite for Cl, cassiterite for Sn, galena for Pb, gallium arsenide for As – and pure elements for Fe, Co, Ni, Cu, Ag and Bi. The analyser crystals were: LIF (LiF) for Mn, Fe, Co, Ni, Cu, Zn and Bi; TAP (C8H5O4Tl) for As; PET (C5H12O4) for S, Cl, Sn, Sb, Ag and Pb. The results were processed using the PAP (CAMECA) software for the ZAF corrections. Measurement precision was within 1% for major elements, about 3–4% for minor elements and about 8% for trace elements.

The lowest detection limits of EPMA with these analytical conditions were approximately 0.1 wt% for the major and minor elements and varied from 250-to-300 ppm for Co. For Pb and Bi the detection limits rise to 0.25 and 0.9%, respectively. The results of the EPMA chemical analyses are expressed as weight percent (wt%) of element, calculated as a mean of 7÷10 point analysis with the relative standard deviations (SD).The analyses were performed on the polished sectioned samples coated with a thin carbon layer.

3.4 Multi-Collector Inductively Coupled Plasma Mass Spectrometry (MC-ICP-MS)

Lead Isotope Analyses (LIA) are largely used in archaeometry for provenance studies (see Chapter 6). In this work were applied to the study of metal ingots and artifacts. These isotopic analyses require a preliminary chemical Pb-separation that was performed in an ultra-clean laboratory of the CNR-IGG unit, hosted in the Department of Geosciences, as described below. An amount of 2–3 mg of fresh metal was dissolved in 1000 µl of *Aqua Regia*[6] at 120°C for at least 12 h and left to evaporate. The formed chlorides were converted to nitrates using 100 µl of 14.4 M nitric acid and evaporated. The nitrates were then dissolved in 500 µl of 1M nitric acid at 90°C for five minutes. In order to separate the lead from all the other elements, a cation exchange resin was employed (SrSpec™, EIChroM Industries; Horwitz *et al.* 1992), as also reported by Gale (1996). The resin, loaded into 3–mm diameter hand-made PTFE columns, was conditioned with 500 µl of 0.01 M nitric acid (the eluting solution) and then 500 µl of 1 M nitric acid (the washing solution). Subsequently, the sample solution was loaded in 500 µl of 1 M nitric acid and filled into the columns; 1500 µl of 1 M nitric acid were also used for removing all the elements, while Pb was strongly retained on the resin. At this point, the lead was eluted from the matrix metals using 3000 µl of 0.01 M nitric acid and collected in miniature glass beakers (Villa 2009).

The mass spectrometer used for the analysis is a Nu Instruments™ multicollector plasma-source (MC-ICP-MS) located at the Institut für Geologie of the University of Bern (Switzerland). The Pb setup uses eight Faraday collectors to measure all masses between ^{202}Hg and ^{209}PbH+.The sample solution was ionized by introducing it into a 9000 K plasma allowing for the simultaneous ionization of all elements.

Mass fractionation was monitored by adding few nanograms of natural thallium, which possesses a known ^{203}Tl/^{205}Tl ratio, fractionated by the same mechanism as Pb and not interfering with Pb isotope measurements (White *et al.* 2000). Every five measured sample solutions, a calibration was carried out using the NIST SRM 981 international standard. The measured values of NIST SRM 981 matched favourably with those reported in literature, as shown in Table 3.1, assuring the reliability of the performed isotopic analyses.

The determinations of lead isotope ratios carried out at the Gent University was performed using a Thermo Scientific Neptune Multi-collector ICP–MS instrument. This instrument is a dedicated tool for highly precise determination of lead isotope ratios,

[6]Nitro-hydrochloric acid.

equipped with a double-focusing mass spectrometer of Nier-Johnson geometry and an array of 9 Faraday collector and 3 ion counting devices. The sample introduction system consisted of an auto-aspirating low-flow (50 ml min–1) PFA nebulizer (ESI Scientific, Omaha, NE, USA) mounted on to a combined cyclonic/double-pass spray chamber made of quartz glass. Potential isobaric interference of ^{204}Hg on ^{204}Pb was controlled and, if necessary, corrected for by monitoring the ^{202}Hg signal.

Tab. 3.1 – Measured values of NIST SRM 981 from different literature sources compared with those obtained in this study. Analytical error (2 σ) refers to the least significant digits and results shown in italic font were calculated from the data given in the original publication.

Reference	Year	^{208}Pb/^{206}Pb	^{207}Pb/^{206}Pb	^{206}Pb/^{204}Pb	^{207}Pb/^{204}Pb	^{208}Pb/^{204}Pb
Hirata (Plasma 54)[1]	1996	2.16636 ±82	0.914623 ±37	16.9311 ±90	*15.4856*	36.6800 ±210
Rehkamper *et al*. (Plasma 54)[2]	1998	2.1667 ±14	0.91469 ±5	16.9364 ±55	15.4912 ±51	36.6969 ±128
Belshaw *et al*. (Nu Plasma)[3]	1998	2.1665 ±2	0.91463 ±6	16.932 ±7	*15.487*	*36.683*
White *et al*. (Plasma 54)[4]	2000	2.1646 ±8	*0.91404*	16.9467 ±67	15.4899 ±39	36.6825 ±78
Rehkamper *et al*.	2000	2.16691 ±29	0.91459 ±13	16.9366 ±29	15.4900 ±17	36.7000 ±23
This study (Bern)	**2015**	**2.1671 ±10**	**0.9146 ±4**	**16.9415 ±1**	**15.4947 ±1**	**36.6977 ±9**
This study (Gent)	**2015**	**2.1661 ±10**	**0.9145 ±5**	**16.9345 ±6**	**15.4865 ±5**	**36.6823 ±20**

[1] Modified power law normalization relative to ^{205}Tl/^{203}Tl=2.3871
[2] Exponential law normalization relative to ^{205}Tl/^{203}Tl=2.388808
[3]Exponential law normalization relative to ^{205}Tl/^{203}Tl=2.3875
[4]Empirical external normalization technique relative to ^{205}Tl/^{203}Tl=2.3871

3.5 Statistical treatments

The multivariate statistical methods are commonly employed to analyze the relations among more than one random variable. There are a wide range of multivariate techniques available and, among these, the Principal Component Analysis (PCA) is the statistical technique that enables for identifying patterns and correlations in dataset of high dimension, permitting to express the data by highlighting their similarities and differences. The other main advantage of PCA is that, once data relations were found, it is possible to reduce the number of dimensions, without much loss of information.

Basically, the Principal Components (PC) is defined as the set of orthogonal linear combinations of the data that have the greatest variance. When the variables are highly correlated, the first few principal components may be sufficient to describe most of the

variability present. In many cases, a small number of components may explain a large percentage of the overall variability. Moreover, a proper interpretation of the factors could provide important insights into the mechanisms that rule the reality and that are not easily perceived by simple data observation. In this study, the PCA treatment was performed on the statistical software STATGRAPHICS® Centurion XVI; however, for consistency in graphics rendering, the PC values for each sample available in the "Data Table" were visualized using SigmaPlot™ software (version 11).

The comparison with literature data, collected using analytical technologies that differ from the one adopted in the present study, revealed either the occurrence of missing values for certain elements or the presence below the detection limit. In this latter case, the compositional value taken into account for the comparison was the detection limit itself reported in each of the respective publication. In the case of few missing values (*e.g.* not analysed element), the STATGRAPHICS software is able to reconstruct these lacks by using proper algorithms, in order to evenly perform the statistical analysis of the dataset. However, it must be noticed that too many missing values could negatively affect the yield of the performed investigation.

Moreover, the comparison of SEM-EDS and EPMA analyses with literature bulk chemical data, such as ICP-MS, was allowed by a simple *éscamotage*: the substitution in the EPMA point analysis with the SEM-EDS values for the elements that segregate in the matrix and that cannot be revealed by means the punctual probe. Indeed, when in the α-phase were present segregations – possibly enriched in Sn, As, Sb and Ni –, sulphides – typically containing S, Fe, and Zn – and lead particles, the EPMA point analysis of such elements were consciously substituted with the SEM-EDS values obtained by the average of 3-5 areal analyses.

Chemical and Metallographic Results

In this chapter, the results of the chemical, textural and metallographic analysis of the samples are presented. The data are grouped by following the chronological order of the metal hoards attributed by archaeologists and they will be thoroughly discussed in Chapter 5. The results of SEM-EDS and EPMA chemical analyses are reported in Appendix 2 (Table 1 for SEM-EDS analyses and the main observed features; Table 2 for EPMA analyses), together with the main metallographic features of each sample. Concerning the metallographic analysis, since the observations are strictly related to the sampled area, each RL-OM micrography is accompanied by the object drawing in which the red point indicate the sampled area in order to facilitate the discussion.

4.1 MBA: Canale Anfora and Belvedere swords

From Canale Anfora and Belvedere, two stray swords dated to MBA III were analyzed (see Chapter 2). The results of SEM-EDS and EPMA (Appendix 2) show that both samples are composed by bronze containing a Sn amount in the range 11–12.3%, classified as tin bronzes. Such tin concentrations are very close to what one would expect from a LBA copper–tin alloy; in fact, as stated by Coghlan (1975) "the prehistoric metallurgist eventually appeared to aim to this optimum tin content", since a bronze alloy with 10%-12% of tin presents good thermo-mechanical properties (*i.e.* hard but not brittle). Moreover, Bel-S is characterized by the presence of 1.3% Ni and 0.23% As, whereas no traces of such elements were detected in Can-S. In both cases, the Pb content is lower than 1% and, therefore, its presence could be attributed to the extractive charge excluding a deliberate addition. Although a Pb limit value above which the voluntary addition can be surely recognized does not exist, Liversage (2000) defines it to be approximately 1% for the refined objects.

The microstructural observation revealed diffuse interdendritic segregations of the (α+δ)-eutectoid phase (Fig. 4.1a-b), owing to the extended *liquidus-solidus* gap that characterize tin-bronze castings. The δ-phase ($Cu_{31}Sn_8$) was detected in the matrix, showing its typical eutectoid morphology. This intermetallic compound tends to behave as

a crystalline solid without ductility and, since it is brittle, the alloys containing δ-phase generally do not exhibit good workability performances (Scott 2012). Moreover, a phenomenon of microsegregation is observed in both samples; indeed, the inner areas of the dendrite arms are less enriched in Sn (dark gray) than the alloy in the external regions (light gray), resulting in local compositional difference ranging from 6.9% to 13.5% in the Belvedere sword, and from 13.6% to 7.3% in the sample from Canale Anfora. In addition, the presence of Cu-Fe sulphides dispersed in the α-phase further negatively affects the alloy properties (Fig. 4.1a-b).

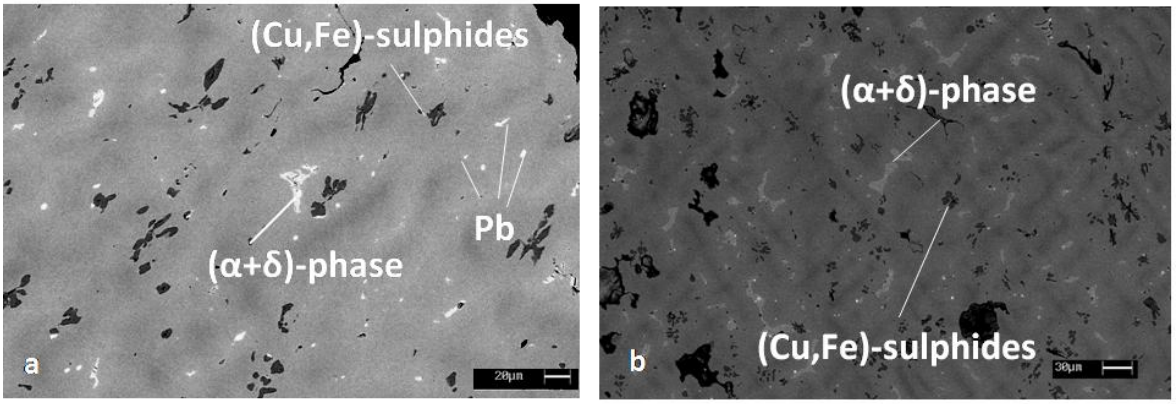

Fig.4.1 – SEM-BSE images of (a) Bel-S and (b) Can-S cross-sections, showing a dendritic structure of as-cast Sn bronze and exhibiting in (Cu,Fe)-sulphides and eutectoid (α+δ)-phase.

The Can-S sample differs from Bel-S both in chemical composition and for some significant microstructural characteristics. Indeed, the dendritic microstructure of Can-S, combined with solidification porosities and globular sulphides dispersed within the matrix (Fig. 4.1a-d), attests a rather poor casting quality and suggests a raw nature of the artefact, inconsistent with a sword manufacture. Furthermore, in Fig. 4.2a it is evident that the δ-phase increases from the outside towards the inside of the blade section, as well as porosities and sulphides (from left to right in Fig. 2.4a); these latter features also increase in number and in dimensions. This phenomenon can be attributed to the solidification process, which implies a differentiate metal cooling owing to the onset of a thermal gradient, and to the lack of any further working and annealing cycle. Thus, these attributes rise some doubts about the actual function of this artefact, evidently not suitable for the use as a sword.

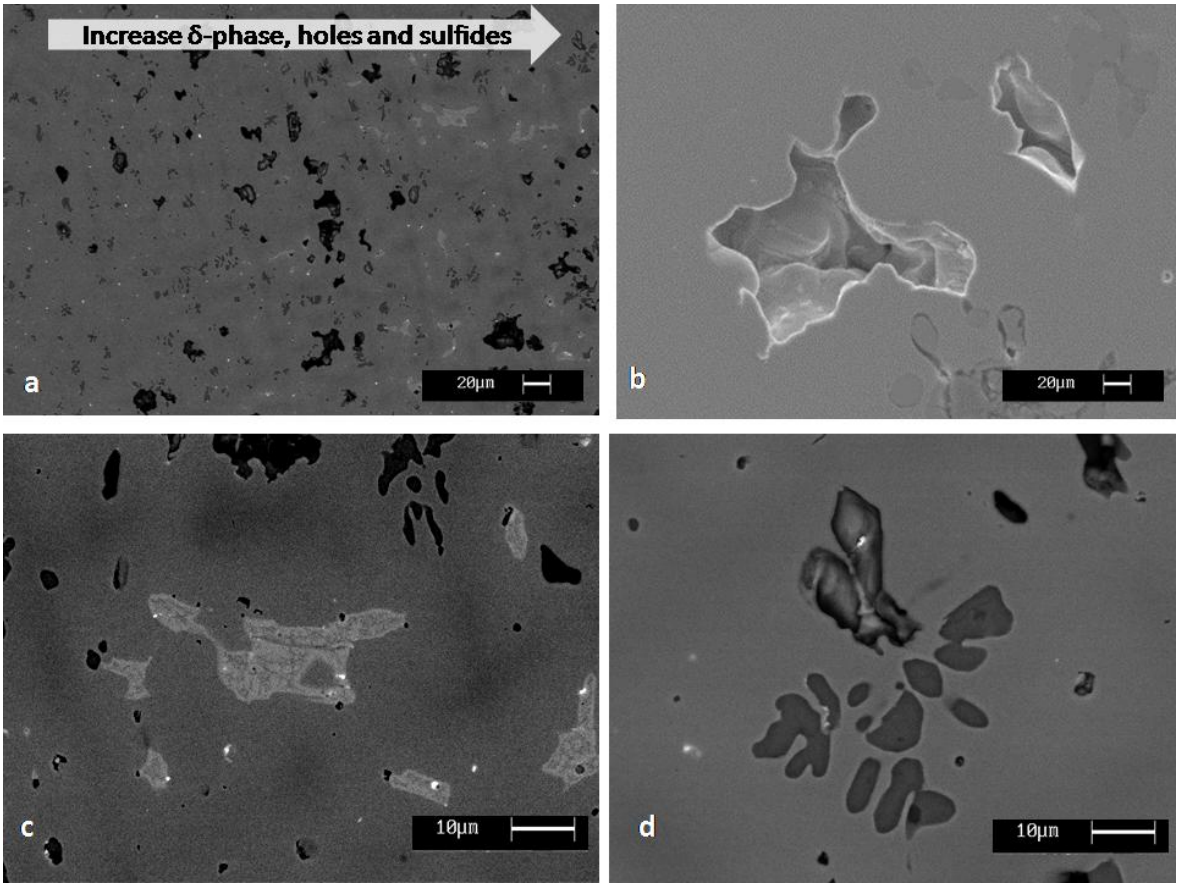

Fig. 4.2 – Canale Anfora sword, Can-S: SEM-BSE (a, c, d) and SEM-SE images (b). In a) it is evident the increase in number and dimension towards the inner part of the section of the solidification porosities, of the light gray (α+δ)-eutectoid phase and the dark gray round sulphides; in b) detail of a hole due to the solidification process; in c) detail of the (α+δ)-eutectoid phase, associated to small particles of lead (white); an d) detail of a dark gray round sulphide.

The metallographic observations on Can-S cross-section (after etching) confirm the cored dendritic structure and reveal the presence of distorted dendrites and slip-lines (Fig. 4.3b), testifying only a slight cold-working after the casting. These evidences, together with the presence solidification porosities, sulphides observed in the matrix are unusual for the external part of an actual sword's blade, area from which the cross-section was taken. Thus, the doubts about the function of this object are reinforced and the structure of this sample can be interpreted as more close to a cast ingot. On the other hand, the Bel-S cross-section shows distorted dendrites, flattened sulphides and many slip-line patterns consistent with a casting and a subsequent hammering (Fig. 4.3a). Therefore, the absence of a grain structure testifies that in the central part of the blade (sampled area) the annealing was not performed or reached. However, this aspect should not be in

contradiction with the production technology of swords suitable for the combat, because, as suggested by Moedingler (2011), only the outer part of the blade of the most of the analyzed swords was intensively hammered as last step.

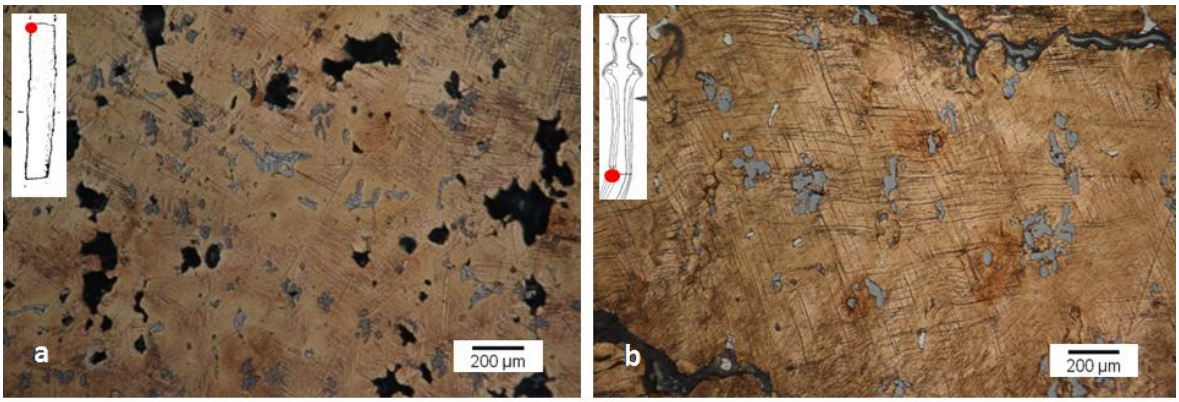

Fig. 4.3 – Polished and etched micrographs of a) the Canale Anfora sword (Can-S) and b) the Belvedere sword (Bel-S) cross-sections.

4.2 RBA-FBA1: The Cervignano and Muscoli hoards

From the Cervignano hoard, twelve ingots and a winged-axe were taken into account, while six ingots, two socketed-axes and two swords were chosen as representative of the Muscoli hoard (see Chapter 2).

Ingots

According to the chemical analyses, all the ingots belonging to Cervignano and Muscoli hoards are made of pure or almost pure copper (92–98%), primarily associated to Fe, Zn S and Pb as impurities (Fe=0.01÷3.5%, Zn=0.01÷0.6%, S=0.5÷1.9% and Pb=0.5÷2.6%). In only one case (Cer-PS-64), traces of Zn (0.4%) and a remarkable content of Sb (1.9%) were detected, leading to the development of Sb-rich phases.

In general, the detection of such high Fe concentrations in smelted copper could be related either to the presence of (Cu,Fe)-sulphides in the metal, to the use of an iron ore flux in the smelting process or, even, to the smelting technology, which was not efficient enough to remove all the impurities (Maddin *et al.* 1980; Craddock and Meeks 1987; Tylecote *et al.* 1977). In this regard, further information are achieved by the microstructural observations, which reveal the presence of chalcocite (Cu_2S) and bornite (Cu_5FeS_4), principally interpreted as copper sulphide residues not completely roasted and trapped in the intergranular or interdendritic spaces (Fig. 4.4a and c), owing to their relatively low solidification temperature range (<250° C, Ribbe 1974). The composition of

the sulphides mostly ranges from chalcocite and bornite, with many particles showing an intermediate *non-equilibrium* composition. Further, in addition to the common Fe-zoning, the SEM observations revealed several Zn-zonings in sulphides (Fig. 4.4b); Fe- and Zn-zonings were even observed in PC-ingots, but of sub-micrometric size and considerably smaller than in PS-ingots (Fig. 4.4d). Such evidences testify that for all these samples the original ore-charge was a (Cu-Fe) sulphide, probably chalcopyrite associated to sphalerite and possibly galena if lead is present. Differently, owing to the simultaneous presence of sulphides and Zn and Sb concentrations, Cer-PS-64 could be interpreted as a mixing between chalcopyrite, sphalerite, galena and tetrahedrite $(Cu,Fe)_{12}Sb_4S_{13}$. Moreover, the mean value of Fe detected in the α-matrix of the Cervignano and Muscoli ingots is very variable in the range 0.01–2.5% (EPMA, Appendix 2, Table 2); this evidences could be firstly related to the amount of Fe present in the extractive charge, but it is also indicative of the smelting technology.

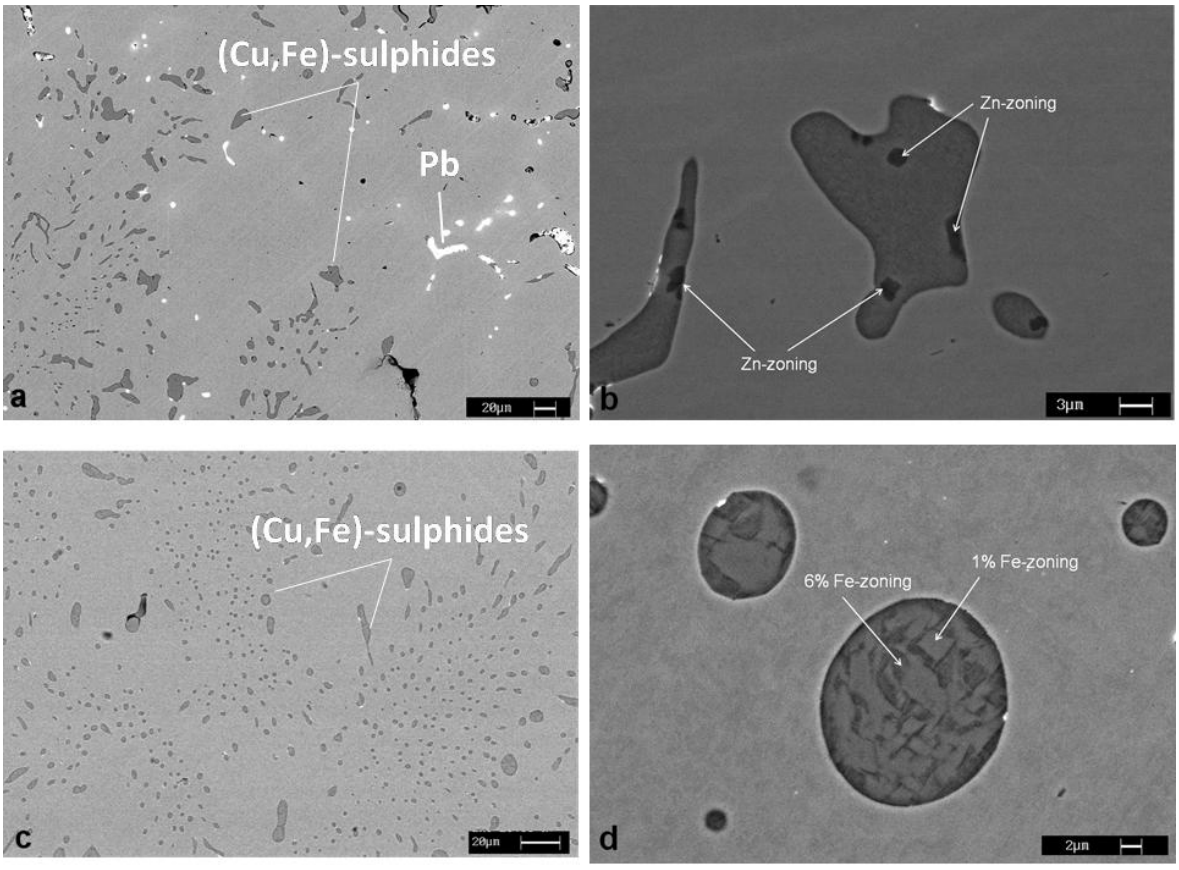

Fig. 4.4 – a) SEM-BSE image of one PS-ingot (Cer-PS-61); b) detail of Cer-PS-61, showing Zn-zoned sulphide (30% Zn in dark areas); c) SEM-BSE image of one PC-ingot (Mus-PC-1); d) detail of Mus-PC-1 showing Fe-zoned sulphide (light gray area 1 % Fe, dark gray area 6% Fe).

In all ingots, lead is always segregated and mixed with small amounts of other elements such as Bi, As, Sb and Ag, and its content is extremely variable. In PS-ingots, the Pb content was found to vary from 1.0% to 3.5%, whereas it ranges from 0.2% to 1.0% in PC-ingots. In general, for the ingots, the lead amount depends on the galena present in the extractive charge and, therefore, percentages up to 2.0–2.5% can be interpreted as deriving from the ores, permitting to consider the sample proper for the lead isotope analysis. Consistently, in most of the PS-ingots, lead-based segregations can be seen in large quantities, mainly arranged at the grain boundaries (white areas in Fig. 4.4a). On the other hand (Fig. 4.4c), lead in PC-ingots was detected in minor concentrations or as trace element, and the cross-sections only exhibit very small Pb and/or Pb-Bi segregations that, in two samples, are even almost absent (Mus-PC-6 and Mus-PC-7). Furthermore, in some PS-ingots, the presence of sporadic flower-shaped or butterfly-shaped inclusions is detected, such as reported in Fig. 4.5. These phases are Fe-Co oxide dendrites, characterized by variable concentrations of Cu and Ni.

Therefore, considering the high amounts of Zn, the Pb-segregations and the Fe(Co)-inclusions, PS-ingots can be interpreted as less refined than PC ones, probably because either the lack of the last refining step or the use of a less evolved process (Craddock and Meeks 1987; Hauptmann *et al.* 2002; Mangou and Ioannou 2000). This consideration is also supported by the levels of Fe and Zn detected in the α-phase (EPMA data, Appendix 2, Table 2) and that will be discussed in detail in Chapter 5.

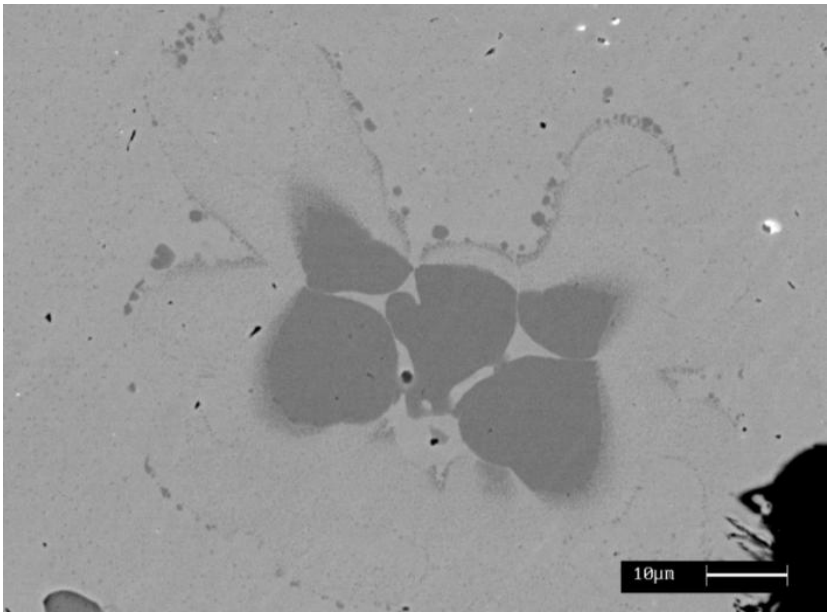

Fig. 4.5 – SEM-BSE image of the butterfly-shaped phase detected in a PS-ingot sample (Cer-PS-82).

Metallographic examinations show that all ingots possess a dendritic structure, as expected in as-cast objects (Fig. 4.6a). Cuprite inclusions (Cu_2O) were detected in almost every specimen, except in Cer-PC-72, Mus-PC-2 and Mus-PC-8, resulting from the nearly complete immiscibility of oxygen in copper, both in liquid and solid states. Cuprite occurs as spherical droplets showing eutectic intergrowth (Fig. 4.6) and, according to Hauptmann *et al.* (2002), this is an evidence for a re-melting of the copper, since Cu_2O cannot be directly present in smelted copper. These oxide particles, along with sulphides, affect the malleability of the copper making it brittle and facilitating the breaking of ingots, useful feature for the commerce. In this regard, before casting alloying or metallurgical working, these copper ingots should be subjected to a further purification in order to reduce or eliminate cuprite inclusions and (Cu,Fe)- sulphides for improving the metal quality.

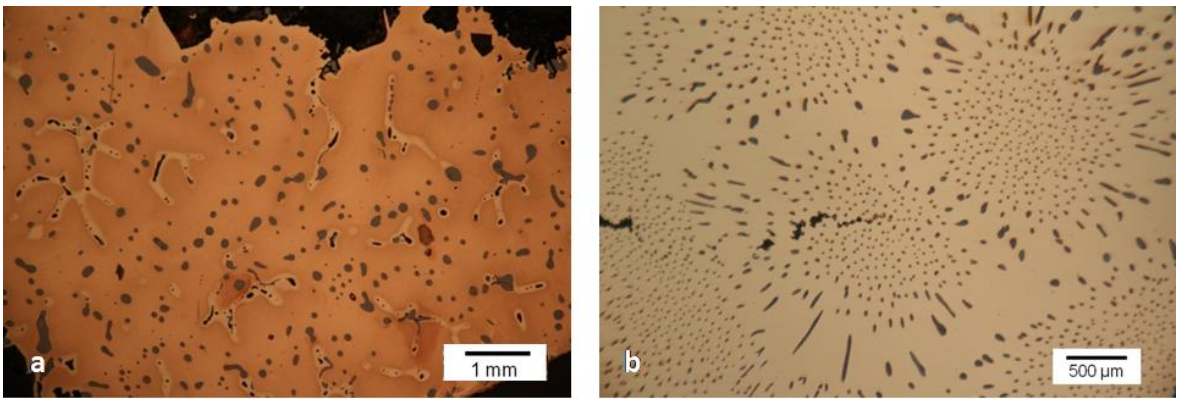

Fig. 4.6 – a) Polished and etched micrograph shoving the dendritic microstructure of the Cer-PC-56 ingot; b) Equiaxed grain of copper and cuprite intergrowth formed by a surplus of oxygen in the liquid copper during casting (sample Cer- PC-79).

Tongue-shaped ingot

Among all ingots, the TS-ingot does not show much similarity with the others, since it is a bronze ingot with a high tin content (20.2%), low level of nickel (1.2%) and traces of arsenic (0.3 %); thus, it represents the most ancient occurrence of Sn-alloyed ingot analyzed in this study. The optical analyses reveal the presence of coarse dendrites (Fig. 4.7a), testifying a slow ingot cooling (Scott, 2012). This bronze consists of α-dendrites with an infill of (α+δ)-eutectoid phase containing a considerable quantity of Sn in proportion to copper (29.5% Sn and 69.4% Cu); moreover, EPMA analysis also reveals small amounts of Ni (0.8%) in δ-phase. As mentioned before, this latter compound is a hard and brittle constituent that reduces the alloy ductility, making the alloy easy to break consistently with its ingot function. Moreover, since this alloy is not suitable to be hammered, this ingot cannot be interpreted as a ready-to-use ingot for tools or weapon making.

Therefore, there are two possible explanations for the employment of such alloy. On one side, a high-tin bronze ensures a bright silver-like appearance which could be visually attractive and simulate silver in the creation of pin or ornaments that require only casting, whereas the second hypothesis implies the obtainment of a more workable alloy by adding nearly-pure copper in the 1:1 proportion. In this case, a proper alloy for sword and axes (~10%-Sn bronze) can be produced. Moreover, the microstructural observations reveal the presence of numerous Cu- and (Cu,Fe)-sulphides dispersed in the matrix (Fig. 4.7b), confirming that it is a raw ingot not obtained by recycle of already refined bronzes. Then, consistently with the above said, this metal should be necessarily further refined before being used by the craftsman.

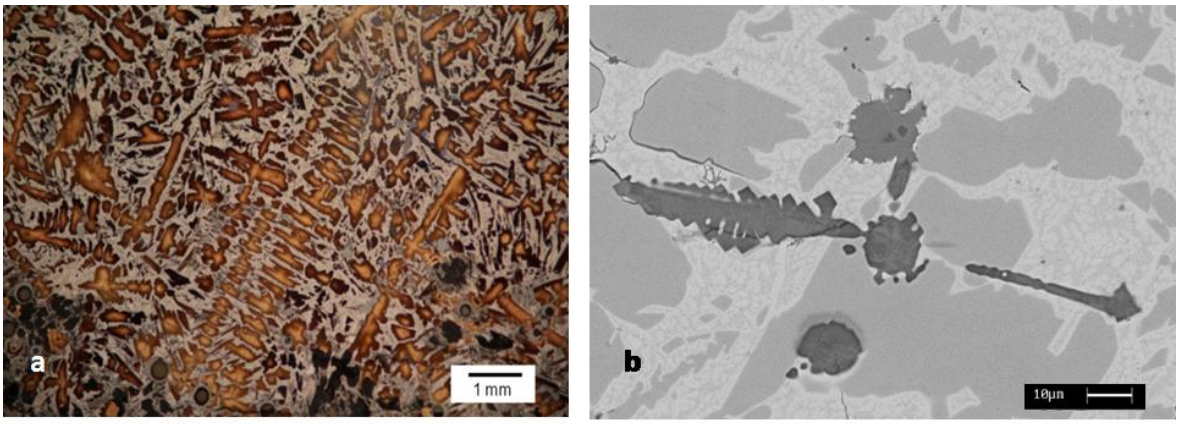

Fig. 4.7 – a) Optical image of the tongue-shaped ingot cross-section (TS-ingot). The image shows the (α+δ)-eutectoid phase in copper matrix (in light gray). Etched in alcoholic ferric chloride. b) Detail of the TS-ingot metal matrix showing in dark gray the Fe-zoned sulphides.

Objects

The structural and chemical results of objects disclose that swords and axes are bronzes having 8-to-12% of Sn; such compositional range guarantees a proper castability and a good workability of the alloy. In all samples, lead is detected in minor concentrations (Pb<1.0%). Focusing on trace elements (EPMA analyses, Appendix 2, Table 2), all the objects manifest very low amount of Fe and Zn, indicating a further purification of the metal (Craddock 2000). In addition, the chemical results clearly show that objects and the TS-ingot are characterized by the presence of As and Ni in the α-phase, not detected in ingots. Arsenic is a volatile element and the smelting process leads to its reduction or elimination (Tylecote *et al.* 1977); therefore, its presence in objects is justified if the raw copper ingots were characterized by relatively high As amounts. Contrariwise, As in the objects is recorded in different concentrations (0.1–0.4%) that are systematically comparable to that in ingots and not higher as expected (Fig. 4.8, in the dashed circle).

For this reason, it is possible that this element was added in a following step with the purpose of metal hardening, but its concentration is too low to support this hypothesis. It is also possible that the creation of these weapons could have involved the addition of further As-rich ingots. On the other hand, Ni is also found as a distinguishing element of objects (0.3–0.6%), exhibiting a good correlation with As (Fig. 4.8). Therefore, since they do not possess any chemical affinity with tin, they cannot be interpreted as tin impurities and the most plausible hypothesis is that As and Ni have been introduced during the alloying step for technological reasons or as involuntary additions, but at the moment *how* and *why* are still open questions.

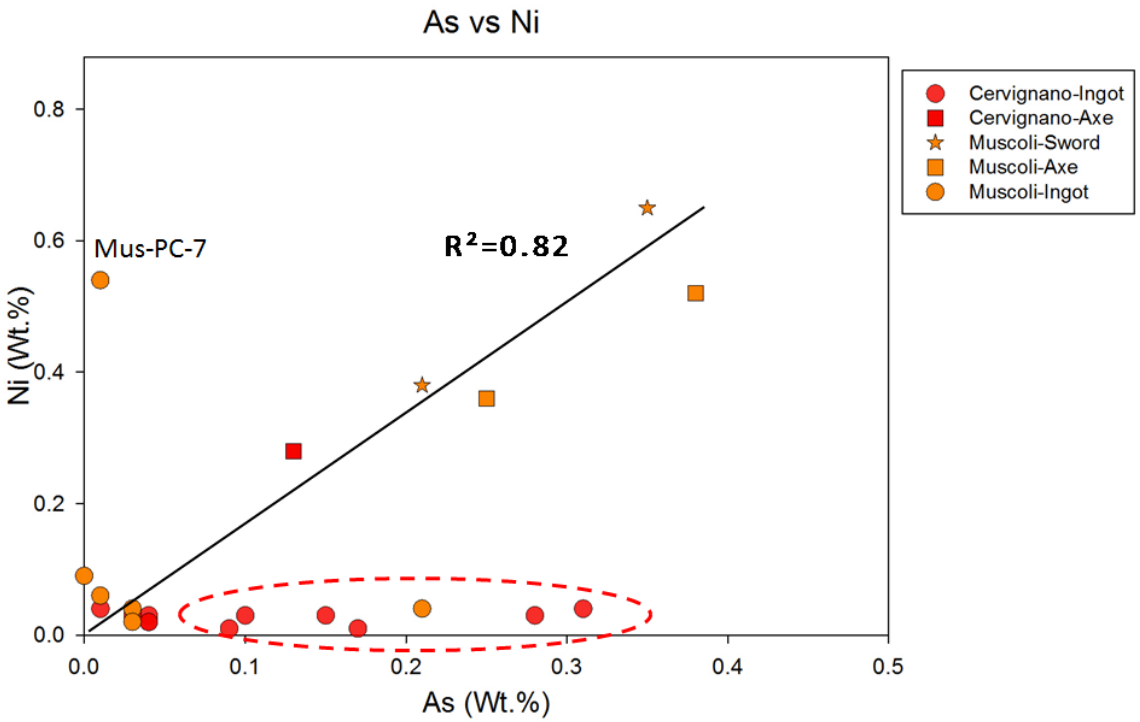

Fig. 4.8 – Scatter plot of As and Ni showing the regression line calculated for the objects. The dashed circle enclose the ingots exhibiting As in the copper matrix. The ingot Mus-PC-7 is the only sample in which appreciable levels of nickel were detected.

The examination of the microstructure of each sample provides information about the degree of working, annealing and homogenisation. The cross-section of the sword Mus-S3, representative of the handle area, exhibits a microstructure that is consistent with a plastic deformation followed by annealing cycles, since recrystallized and twinned grains are observed (Fig. 4.9a). Moreover, numerous slip-lines across the α-phase crystals are evident, testifying a strain-hardened state due to a plastic deformation as last step of the refining process. These evidences lead to suppose that also the handle of the sword has been subjected to a plastic deformation after the casting. A meaningful difference is

instead remarked in Mus-S2 cross-section (Fig. 4.9b), which is characterized by exclusively large twinned crystals, attesting the complete annealing and the absence of further deformations in this area. However, although slip-lines are not observed, it is not possible to exclude that the external part of the blade has undergone a final hammering in order to harden it.

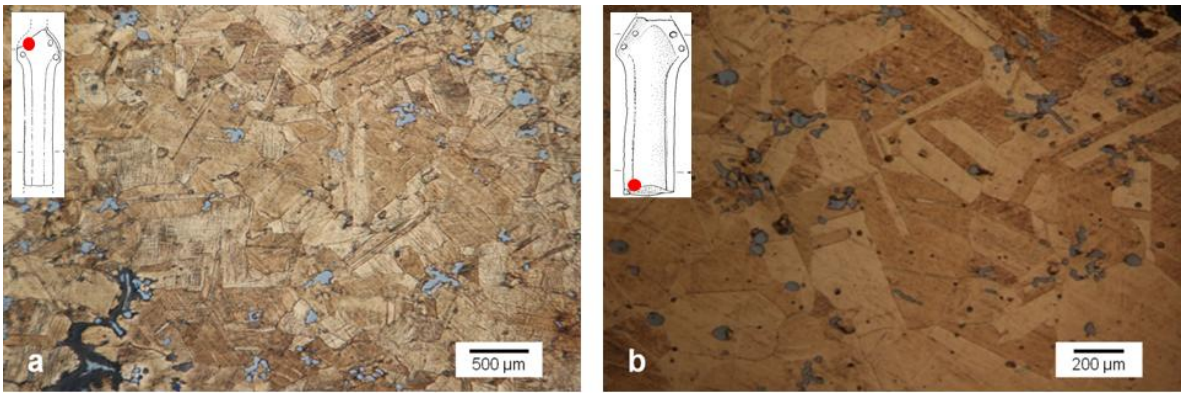

Fig. 4.9 – RL-OM micrographs after etching. a) Bronze sword Mus-S3 sampled on the handle area. Note the slip lines and the twin bands. b) Bronze sword Mus-S2 sampled on the central part of the blade. Note the equiaxial grains with twins, testifying the last annealing process. In both cases, the round gray inclusions are sulphides.

Differently, the socketed axes were sampled near the handle-hole and their microstructure suggests a weak plastic deformation after casting, probably carried out to remove the slight imperfections that may result from the casting in two-part mould. As reported in Fig. 4.10, the presence of distorted dendrites, slip-lines and only few polygonal grains supports this interpretation and, moreover, the incomplete absorption of δ-phase by the α-phase is a further indication that the annealing was not fully reached.

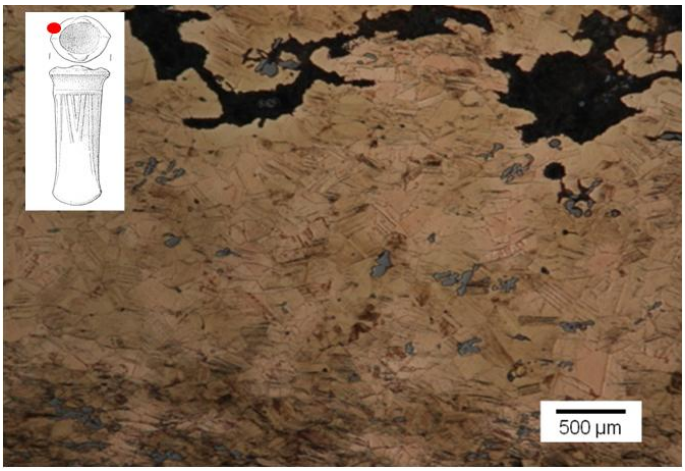

Fig. 4.10 – RL-OM image of Mus-Ax6 after etching by $FeCl_3$. Note the clearly visible residual coring that persists despite the twinned grains.

4.3 FBA1: The Castions di Strada hoard

In the Castions di Strada hoard, the selected finds for the analyses are twelve ingots, a sword, four winged-axes, one socketed-axe and a spearhead (see Chapter 2).

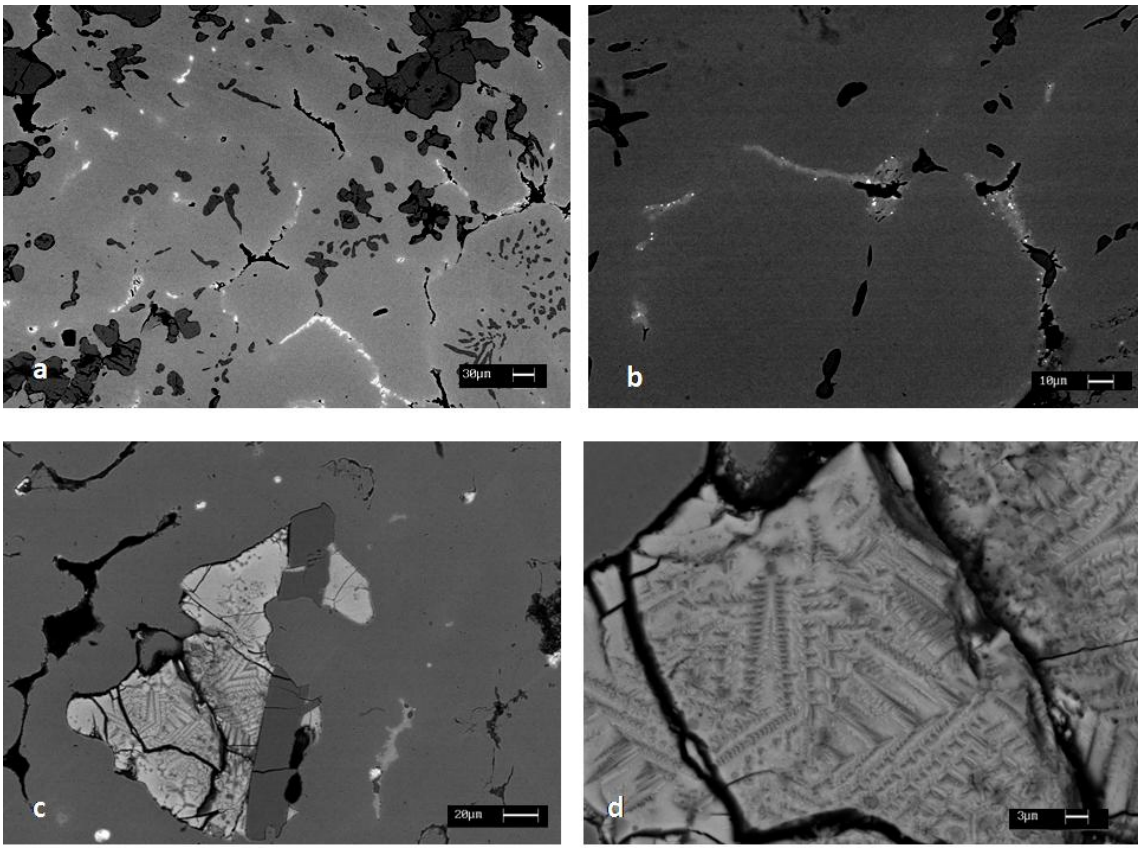

Fig. 4.11 – SEM-BSE image of the a) plano-convex ingot CdSA-P-20, exhibiting a coarse dendritic structure; b) microstructure of plano-convex ingot CdSA-P-17 showing As- and Sb-rich segregations (pale gray) into interdendritic spaces; c)-d) mineral remain trapped in the melt, ingot CdSA-P-22.

Ingots

The results obtained by the elemental analyses clearly show the presence of two compositional groups. The first is constituted by three ingots, chemically and microstructurally similar to those of Muscoli and Cervignano, that exhibit a mean Fe contents varying from 0.7% to 2.3%. Nevertheless, in all of these samples no traces of Zn were detected, except in CdSB-P-81. The microstructural observations reveal a dendritic structure, as expected in as-cast manufacts and exactly comparable to that of the ingots from Muscoli e Cervignano. Conversely, the second group of ingots is characterized by different amounts of As (1–3.5%), Sb (1–3.3%), Ni (1–1.8%) and traces of Co. These samples are characterized by a coarse dendritic structure (Fig. 4.11a), indicating relatively low cooling rates after the casting process; moreover, in the interdendritic spaces, As- and Sb-rich segregations are more or less evident (Fig. 4.11b), depending on the amount of

such alloying constituents. Besides these fluid segregations, the presence of a possible mineral remain, not completely melted, is observed in one case (CdSA-P-22, in Fig. 4.11c-d). EPMA and SEM-EDS analyses of this finely dendritic residue revealed that it is an oxide phase of Cu (23%), As (18%), Sb (24%) and Pb (15%), with traces of Fe, Co and Sn, not referable to a precise mineral, owing to its non-stoichiometric composition.

It is important to stress that As and Sb partly volatilize during the smelting, but they are not completely eliminated. During the roasting, As and Sb volatilize as arsenic- and antimony-trioxide (As_2O_3 and Sb_2O_3, respectively), but they are partially re-converted to arsenic- and antimony-pentoxide (As_2O_5 and Sb_2O_5, respectively), which are less volatile and form with copper non-volatile arsenate and antimonite (Newton and Wilson 1942). Thus, in the alternate oxidizing and deoxidizing operations of roasting and fusions, a consistent part of these elements pass alternately from the state of sulphide to the non-volatile completely oxidized condition and back again; in each passage, a portion is expelled in the intermediate volatile state of As_2O_3 and Sb_2O_3 (Howe, 1885). Therefore, the reduction of As and Sb mainly depends on the atmosphere used in each roasting step and how many refinement cycles have been made. For these reasons, it is impossible to clearly identify the amount of As and Sb present in the starting-ores and quantify their loss during the process; however, the correlation coefficient between As and Sb is statistically significant (R^2=0.86) and, therefore, one may assume the same origin of these two elements (Fig. 4.12); as can be seen from the diagram, no significant relationship between the ingots shape and their composition has been observed.

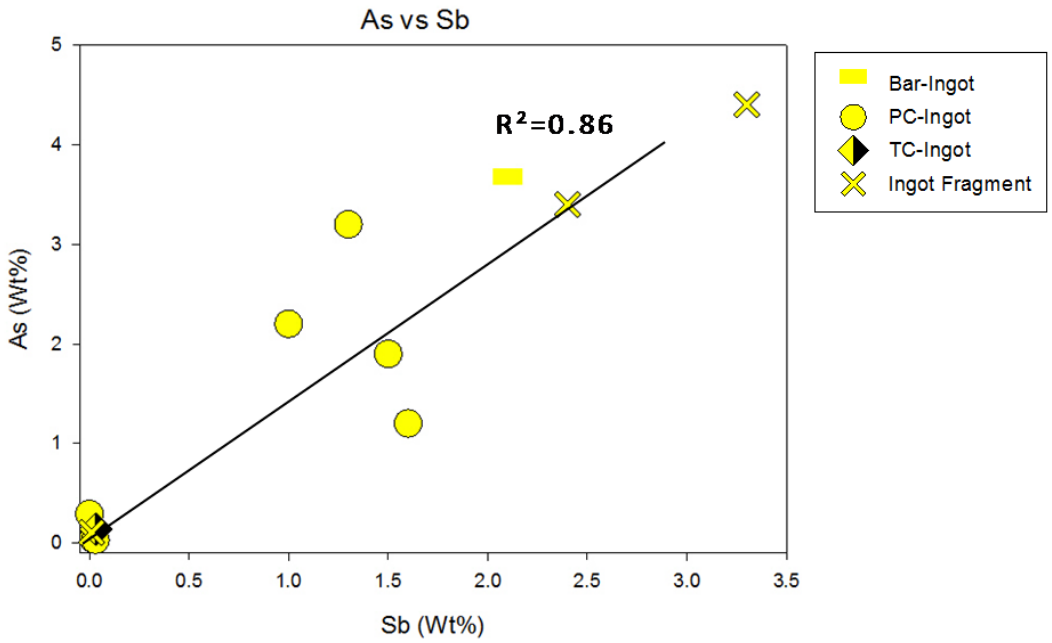

Fig. 4.12 – Scatter plot of As and Sb content in the different typologies of ingots found in Castions di Strada (SEM-EDS bulk analysis).

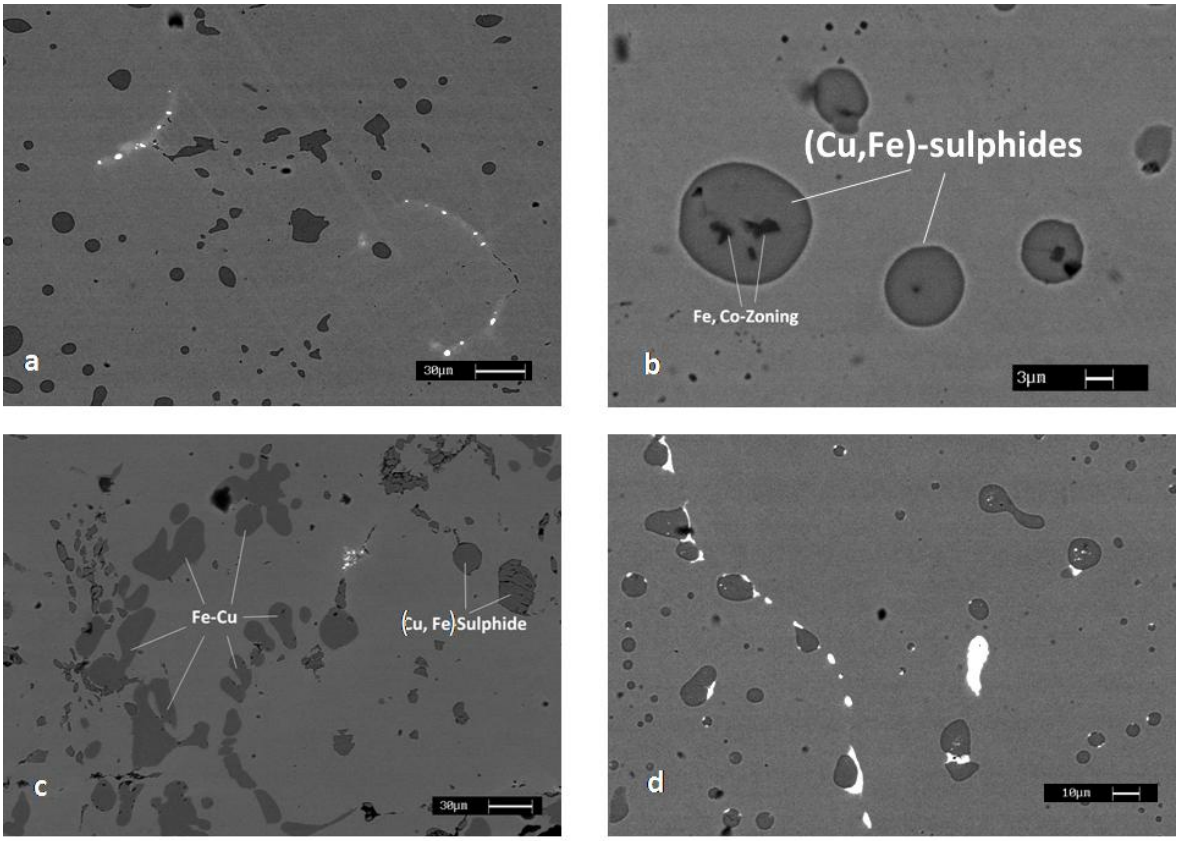

Fig. 4.13 – SEM-BSE image of the a) CdSB-P-50 ingot, showing Cu- and (Cu,Fe)-sulphides dispersed in the matrix (dark gray); b) (Fe-Co)-zoned sulphide in sample CdSB-P-61; c) Coexistence in CdSB-P-60 of Cu-Fe sulphides and Fe-Cu segregations (Fe=89% and Cu=11%); and d) Pb-Bi segregations (in white) along grain boundaries in CdSB-P-81.

As mentioned for the Cervignano and Muscoli ingots, even the observation of sulphides inclusions and their quantity in the matrix can yield information on the extractive charge and on the efficiency of the employed smelting/refining process. In all the analysed ingots, significant amounts of copper and copper-iron sulphides are dispersed in the α-phase (Fig. 4.13a), suggesting the use of sulphide-ores for producing the metal. Moreover, considering the chemical composition, if the extractive charge for the first group of samples might be associated to chalcopyrite/sphalerite and small contents of galena (as for the Cervignano and Muscoli ingots), for the second one the charge could be identified as a fahlerz-ore type because of its distinctive chemical pattern (Craddock, 1995). In this latter case, the original ores must also contain Co as impurity, since EPMA analyses has revealed in some samples traces of such element in the α-phase (0.1–0.37%) and (Fe,Co)-oxides were recognized as sulphides-zoning (Fig. 4.13b). Since a large number of these sulphides are still present in the matrix, it possible that their incomplete elimination might be attributed to a relatively short processing time or a not evolved smelting process.

Therefore, the observation of sulphides, together with the high percentages of As, Sb, S and Fe, can lead to suppose that for these ingots the maximum efficiency in the refining step has not been achieved. A clear example of a quite scarce, or missing, refining step can be given by the sample CdSB-P-60, which contains As (3.2%), Sb (1.3%) and high Fe concentrations (9.5%); in this sample, Fe-rich dendritic and rounded inclusions are precipitated out of α-copper solid solution on cooling, owing to the low solubility of iron in copper (Fig. 4.13c). As reported in literature (Tylecote and Boydell, 1978), some of the iron content could be simply eliminated by melting the copper in a crucible and skimming off the oxidized dross, taking most of the iron with it; obviously, this operation has not been accomplished for this ingot.

Although in some cases the metal has not been thoroughly refined and As and Sb are still present, an intentional use of such alloy in the object-manufacture cannot be excluded for technological reasons. In fact, when the sum of As and Sb reaches 4–5%, the tensile strength of copper is improved and the alloy is within the optimal compositional range that guarantees a good compromise between workability and hardening (Junk 2003).

The lead content of the ingots must be also considered. Among the Castions di Strada ingots, seven samples do not contain lead, except as traces or impurity levels, whereas in the other ingots its content ranges from 1% to 2.5%; lead occurs either within the copper grains as small spherules (Fig. 4.13d), generally in association with bismuth and occasionally silver, or in solid solution with As and Sb. It should be noted that such concentrations are strictly related to the presence of variable amount of galena in the copper mineralization employed as ore-charge and, for this reason, even the samples characterized by several percentages of lead can be safely selected for the Pb isotope analysis.

Further microstructural considerations can be stated after the chemical etching of the Castions di Strada ingots cross-sections and, in accordance with the previous observations, it must be noted that in a cast copper microstructure the etching effects depend on the local chemical composition. In those samples having Fe as major impurity, grains with very different sizes are evident and, as shown in Fig. 4.14a, they are more large in the inner part, owing to the higher cooling rate on the surface. Conversely, in the samples characterized by As and Sb, the as-cast structure, only perceived in BSE-images, is highly emphasized by the chemical etching (Fig. 4.14b). The darker regions are copper-rich alpha grains and the infill corresponds to an arsenic/antimony-rich phase. In both cases, copper sulphides, copper-iron sulphides and inclusions are trapped along the grain boundaries. Moreover, in Fig. 4.14a, the considerable oxygen absorption into the copper during the ingot melting is testified by the copper oxide globules arranged in a

eutectic structure. As suggested by Maddin *et al.* (1980), an ingot with one surface in contact with air may absorb only a small amount of oxygen on the exposed surface, creating a narrow zone in which copper oxides occurs; conversely, the interior does not show any copper oxidation, and this could be the reason of the microstructure dichotomy prevailing in Fig. 4.14a.

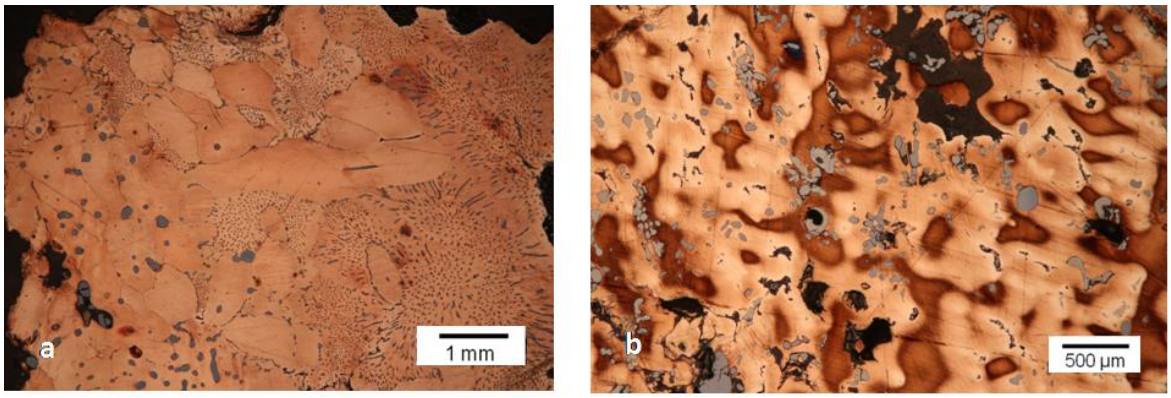

Fig. 4.14 – RL-OM image of a) grain structure of CdSB-P-19 cross-section, after etching $FeCl_3$; b) dendritic structure in Cu-As-Sb alloyed ingot (CdSB-P-74).

Objects

The chemical analyses reveal that all the objects belonging to Castions di Strada hoard are bronzes characterized by a Sn content that averagely lies at 10.5%, ensuring a good workability of the alloy. Regarding the trace elements, Ni is always present in the amount of ~1%, while As varies from 0.2% to 2.0%. The only exception is a winged-axe (CdSB-AxA-1), which is As- and Ni-free. Interestingly, three out five axes exhibit a dendritic structure (Fig. 4.15a), while the other weapons show a homogeneous α-phase free from δ-phase (Fig. 4.15b). In these latter cases, given the significant amounts of Sn (8.3–13.1%), the eutectoid phase has been absorbed by the α-phase owing to a full annealing. On the other hand, little amounts of δ-phase were noticed in the objects characterized by a cored structure, evidence of the lack of homogenization. In particular, in CdSA-Ax59 the Sn content varies from 11.5% in the centre of the primary dendrite arm up to 13.3% in the outer part of the dendrite; likewise, in CdSA-AxC-4 it varies from 7.2% to 12.0% and in CdSB-AxA-9 from 6.8% to 10.1%. Moreover, by observing the microstructure it is possible to note that the number of sulphides is much lower in the artefacts than in ingots and, when present, generally exhibit smaller dimensions (max. 10–15 µm), as expected. This evidence, together with the occurrence of very finely dispersed Pb-inclusions, confirms that the ingot metal employed for the creation of weapons has been subjected to a further refining.

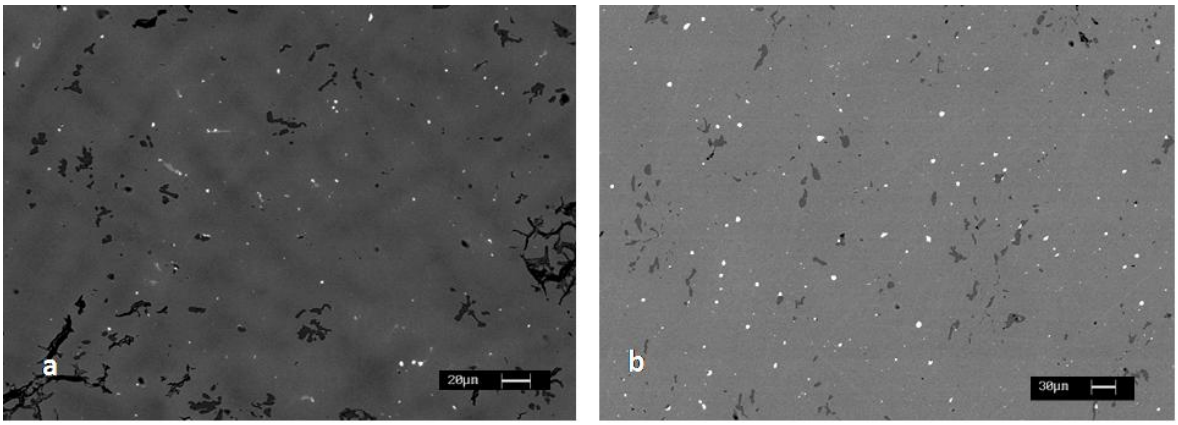

Fig. 4.15 – SEM-BSE image of a) the dendritic structure in the socketed-axe of Castions di Strada (CdSA-AxC4) and b) the homogeneous structure in the alloy of the winged-axe sample (CdSA-AxA2).

The chemical etching better highlights the thermo-mechanical history of these objects, allowing for further interesting observations about their production. In the three axes on which the BSE-images revealed a cored structure, the presence of twinned and recrystallized grain testifies a heat treatment after a heavy plastic deformation (Fig. 4.16a-b). However, despite this Sn-bronze alloy was subject to several working and annealing cycles, remnants of the original melt are still persistent in the microstructure (Fig. 4.16b); moreover, the intensive hammering step after the casting in the CdS-AxA-59 sample is attested by the strongly oriented-distribution of the elongated sulphides (Fig. 4.16a), thus suggesting that the blade of this sample has been heavily worked.

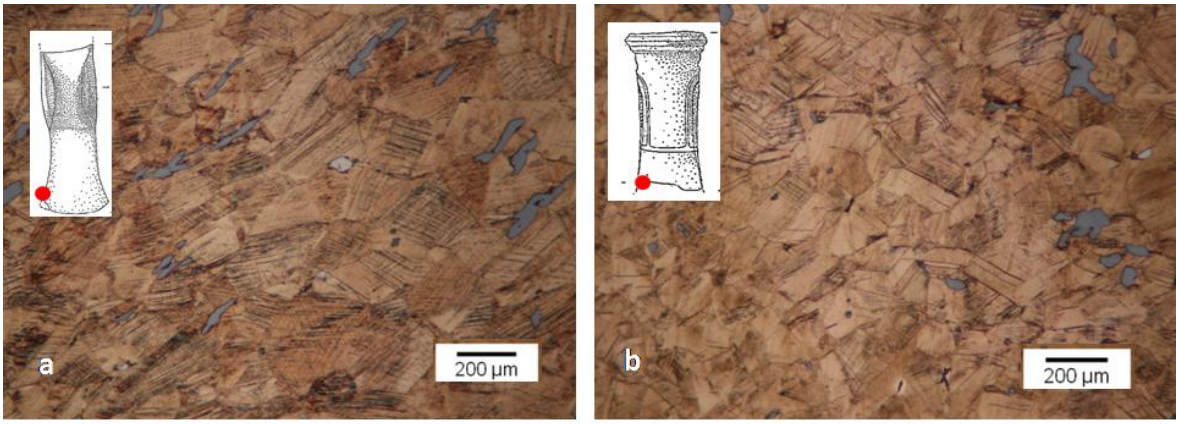

Fig. 4.16 – a) RL-OM image of the grains and slip-lines visible in the sample CdSA-AxA-59; note the sulphides oriented (gray elongated particles) for the hammering strokes. b) RL-OM image of the dendrite remnants (lighter areas) persisting in the socketed-axe microstructure, CdSA-AxC-4 sample.

Differently, those samples exhibiting a homogeneous microstructure in the SEM-BSE image in Fig. 4.15b show large twinned grains (300-400 µm), equally distributed throughout the matrix. In these cases, a complete recrystallization occurred and the annealing has been the final working operation, since no slip-line systems are observed.

The hypothesis of an extended plastic deformation is also supported by the flattened shape of sulphides (Fig. 4.17a).

Conversely, the microstructure of the CdSA-S sword the observations highlight twinned grains that could suggest the reiteration of cycles of hardening and annealing; moreover, since the sample was taken in the central part of the blade, the presence of several slip-lines inside the grain cannot be surely attributed to a slight cold working as final step. In fact, in this case it is possible that the slip lines could be interpreted as a residue of the hardening not completely eliminated during the last annealing process, which was not fully reached in this inner area (Fig. 4.17b).

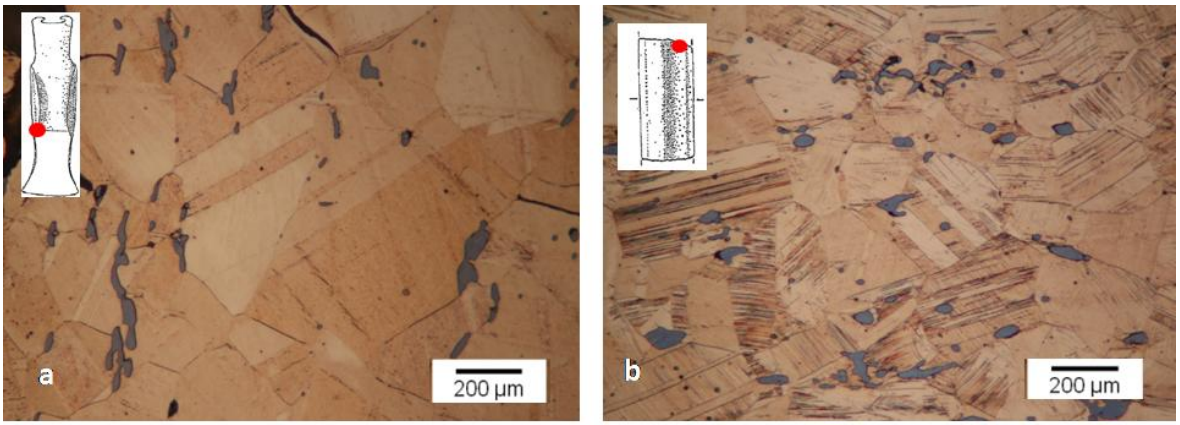

Fig. 4.17 – RL-OM images of a) the twinned grains in the winged-axe sample (CdSA-AxA-1); and b) the recrystallized grains and slip-lines in the sword's blade cross-section (CdSA-S).

4.4 FBA 1/2: The Celò-Cicigolis and Verzegnis hoards

From the Celò-Cicigolis hoard, four ingots, three winged-axes, two socketed-axes, a sword and a socketed-shovel were investigated, whereas from the Verzegnis hoard only two ingots were available for sampling.

Ingots

The results of the ingots chemical composition are summarized in Appendix 2, together with the main microstructural observations. A first compositional evaluation has allowed for a distinction in two copper groups having different chemical patterns related to the corresponding finding place (Celò and Verzegnis). In the case of the Celò deposit, ingots are uniformly copper-based (97–98%) and are characterized by a low impurity level, mostly associated to As (0.3–0.5%), Ni (0.1–0.2%) and Co (0.2–0.3%); even Fe is present in amounts that do not exceed 1%. The only exception among these samples is represented by Cel-P-38, in which the EPMA analysis recorded traces of silver dissolved in the matrix (0.1%). In the Verzegnis hoard, the scenario is different, aware of the fact

that only two samples were considered. Actually, in Ver-P-0 and Ver-P-9 noticeable amounts of Fe (3.2% and 1.8%, respectively), As (0.2% and 2.4%), Sb (0.6% and 0.4%) and Zn (0.4% and 1.7%) were detected and, in addition, traces of Co (0.1%), Ag (0.3%) and Sn (0.46%) were only recorded in Ver-P-9.

As mentioned for Castions di Strada samples, the presence of coring and segregation in the matrix depends on the concentration of the alloying elements and their relative solubility in copper, as well as on the cooling rates, which in ingots are considered to be slow. According to their low impurity composition, the specimens of Celò show a relatively homogeneous structure (Fig. 4.18a), whereas in Ver-P-0 and Ver-P-9the coring structure is characterized by interdendritic (As, Sb)-rich phases (Fig. 4.18b). Furthermore, in Verzegnis ingots, iron-based segregations were observed within the copper matrix, because of the Fe content involved during the smelting process; in Ver-P-0, dendritic Fe-Cu segregations (90% Fe and 10% Cu) very similar to those observed in Castions of Strada ingots are observed (Fig. 4.18 c-d), whereas small oxidized iron particles were found in Ver-P-9. In this regard, it is possible to assume that imperfectly controlled smelting conditions might be responsible for such variability in iron content.

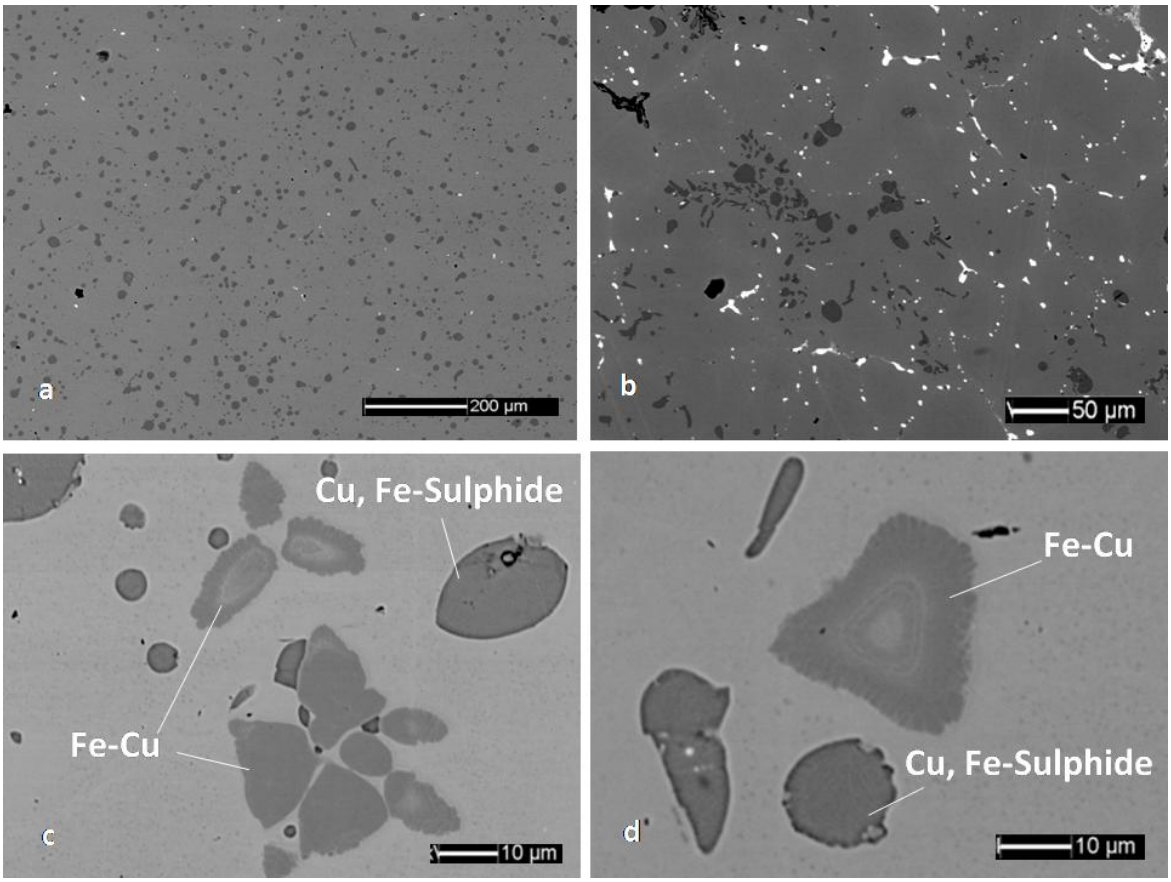

Fig. 4.18 – SEM-BSE image of a) the homogeneous alloy characterizing the Celò ingot Cel-P-37; b) the cored structure exhibited by the Verzegnis sample Ver-P-9; c) – d) Details of the Fe-rich segregations in the sample Ver-P-0 (Cu 10%-Fe 90%).

Microstructurally, all ingots belonging to Celò and Verzegnis hoards show rounded Cu- and (Cu, Fe)-sulphides dispersed in the metal; however, a slight difference lies in the recorded sulphide zoning-type (Fig. 4.19a-c). Indeed, the sulphides in Celò ingots are characterized from Fe and Fe-oxides (Fig. 4.19a), whereas those of Verzegnis only exhibited Zn-zoning (Fig. 4.19c) in which Zn rises up to 38% (as observed in the ingot sulphides of Cervignano and Muscoli). Moreover, all Celò ingots show a Cu_2O eutectic structure (Fig. 4.19d), totally absent in Verzegnis ones.

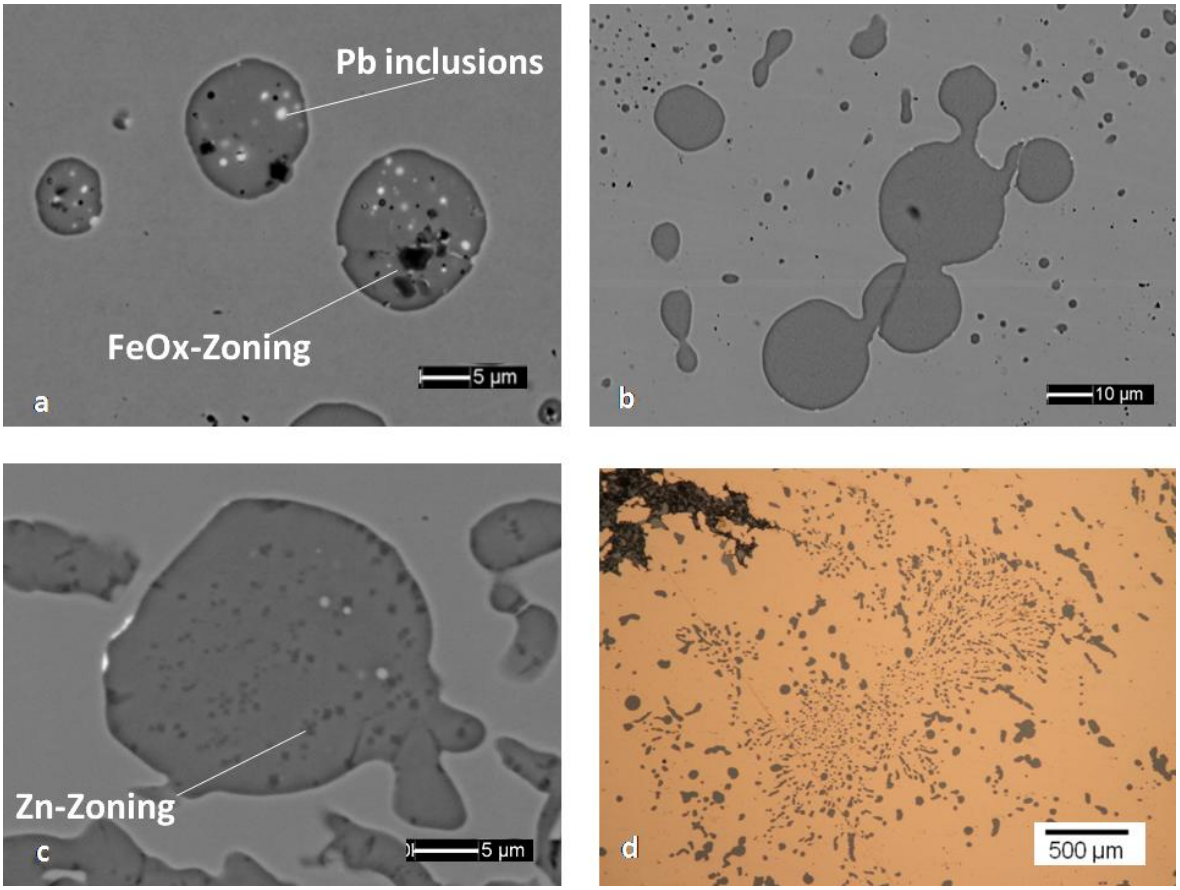

Fig. 4.19 – SEM-BSE images of a) the FeOx-zoned sulphides and lead particles within them in the sample Cel-P-38 ; b) the homogeneous structure and (Cu,Fe)-sulphide (dark gray) in the sample Cel-P-37; c) Zn-zoned sulphides in Ver-P-9; and d) Cu_2O eutectic structure in Cel-P-41.

For what concerns lead-based segregations, those in Celò ingots are mostly associated with As, Sb and Bi, while those of Verzegnis are mixed with Ag. In most cases, Pb segregations are found in sulphides (Fig. 4.19a-c) as fine segregations. Conversely, in Ver-P-9 high amount of Pb solidified along the grain boundaries because of the limited solubility of Pb in Cu (Scott 2012); even in this case, anything suggests that the lead does not derive from the ore-charge.

Basically, both Verzegnis ingots show the same microstructure and the same impurity pattern, which were of lower amount in Ver-P-0 than in Ver-P-9. Two explanations to these evidences are equally probable: the more intuitive hypothesis is a different extraction process of the same fahlore-charge; however, it is not possible to exclude that these ingots could be a mix of different copper types available at the same smelting site. Assuming that, it is clear that in Ver-P-0 such mixing should be intended as minimum, while in Ver-P-9 should be considered as more generous. Three out the four ingots from Celò are almost pure copper with traces of As, Ni and Co probably due to a mixing of chalcopyrite and small amount of fahlerz-type ores, in particular from the tennantite-tetrahedrite series. Nevertheless, it is not possible to identify the extent of the mixing, but the homogeneity of the α-phase allows to suppose that subsequent remelting steps have occurred, leading to the reduction of these elements, especially As. The compositional pattern of Cel-P-38 is characterized by small amounts of trace elements, and the presence of Zn-zoned copper sulphides argues in favour of chalcopyrite-sphalerite association.

The metallographic examination after etching on the Celò ingots confirms that they are constituted of a single-phase alloy, while a dendritic structure is strongly emphasized in Verzegnis ingots (Fig. 4.20).

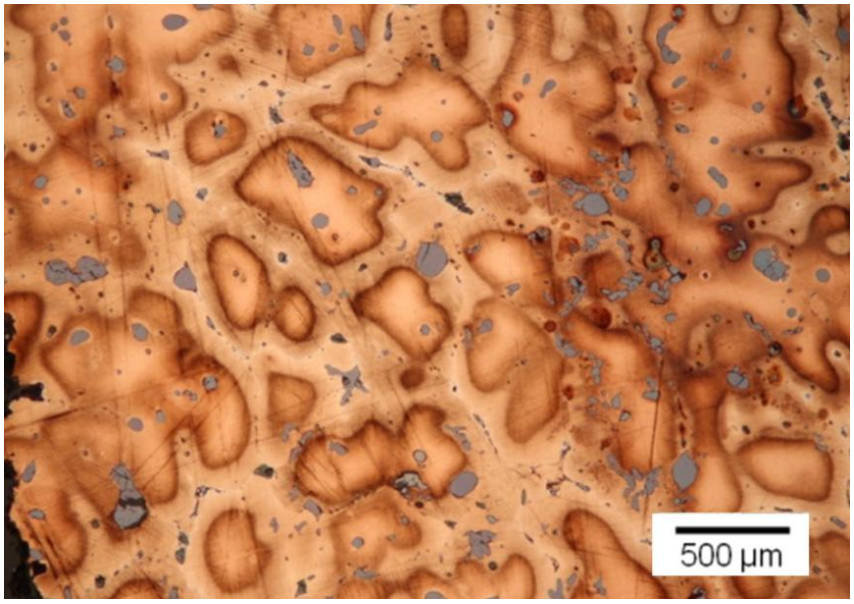

Fig. 4.20 – RL-OM image showing the cored structure of the Ver-P9 cross-section, after $FeCl_3$ etching.

Objects

The results of the chemical analyses show that all the objects are constituted by Sn-binary bronze alloys, with arsenic and nickel as major impurities. The winged-axes Cel-AxA2, Cel-AxA3, Cel-AxA8 are characterized by a Sn-content in the range 6.7%–8.1% and, on average, As and Ni were detected in amount of 0.6% and 0.4%, respectively. Moreover, the BSE images revealed similar homogenized microstructure (Fig. 4.21a), owing to a sequence of repeated cold-working and annealing operations; this is also testified by the presence of polygonal grains characterized by a large number of annealing twins and without any remains of solidification dendrites (Fig. 4.21b). These features permit to establish that these artefacts were extensively hammered and annealed, which is also corroborated by the observed grain size (50-100 μm). The presence of many slip-lines suggests that the cold-working has been performed as final step; however, this evidence could be also interpreted as a witness of the more probable actual use of these weapons. In fact, it is important to stress that both the hypotheses are compatible with the sampled areas, which is in the poll/butt of the axes in all the three cases, as exemplified in Fig. 4.21b. Furthermore, by observing the lead inclusions and the sulphides dispersed in the matrix, the hypothesis of a heavy work is reinforced. On one side, each annealing step leads to a reduction in size of the Pb inclusions, assuming micrometric dimensions (Fig 4.21a). On the other, the sulphide shapes provides information about the plastic deformation; in fact, depending on the intensity and strength of hammering, sulphides develop a more or less pronounced flattened orientation (Fig 4.21a) depending on the number of working/annealing cycles. According to these features, the (α+δ)-eutectoid phase is completely absent from this microstructure because it has been totally absorbed by the α-phase during the annealing.

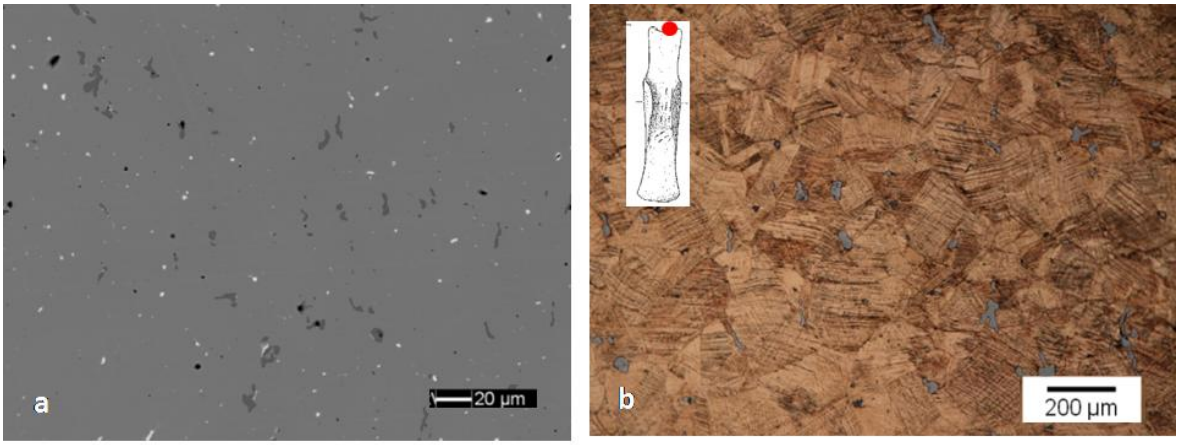

Fig. 4.21 – Sample Cel-AxA-2: a) SEM-BSE image of its homogenized bronze alloy in which FeOx-zoned sulphides and Pb-inclusions are finely dispersed; b) RL-OM image showing the polygonal structure, after etching.

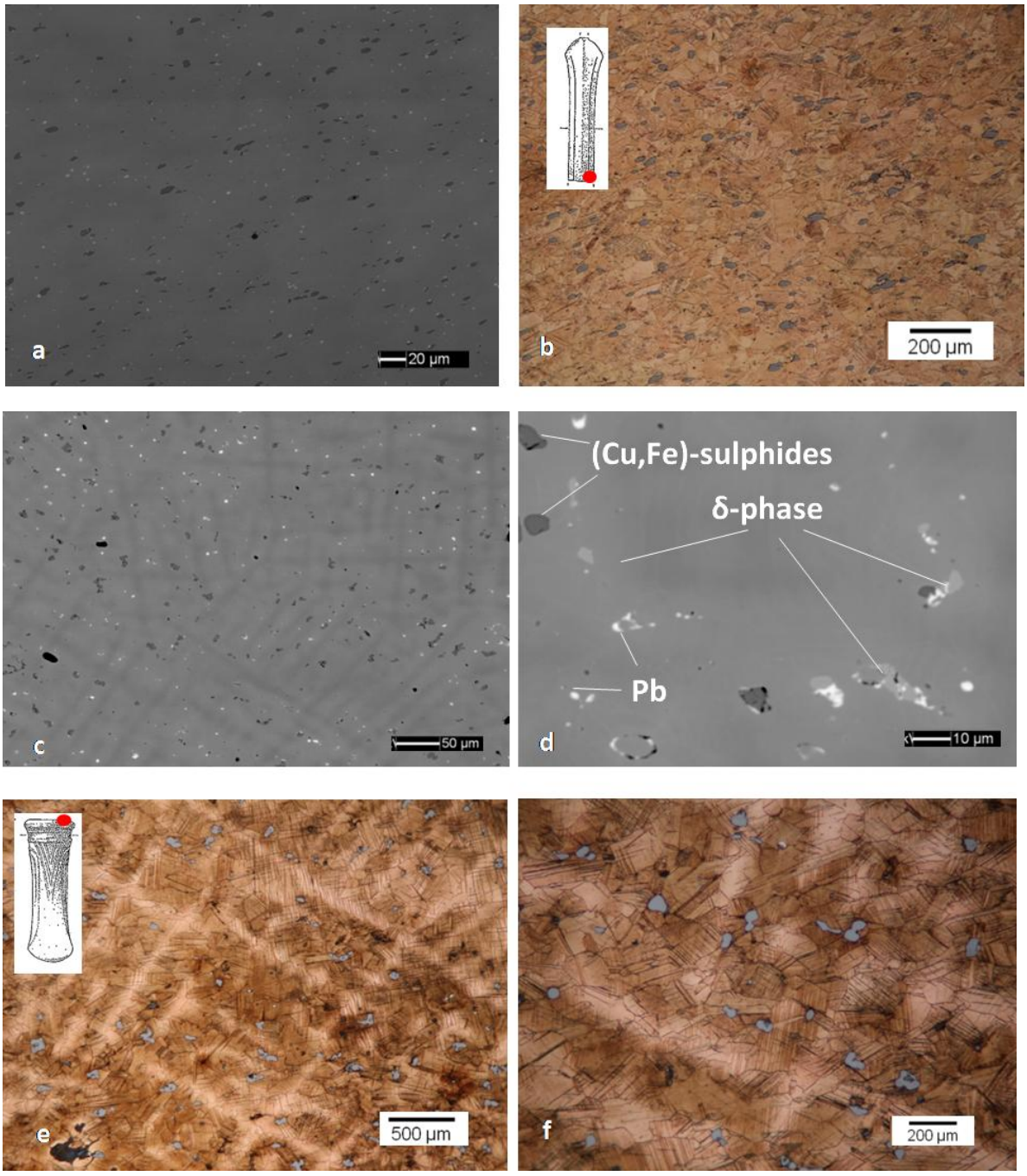

Fig. 4.22 – a)-b) The Celò sword cross-section: a) SEM-BSE image of the slight cored structure and the oriented sulphides within dispersed; b) RL-OM image showing simultaneously grains and dendrite remnants, after etching; c)-f) The socketed-axe cross-section (Cel-AxC-8): a) SEM-BSE image of the dendritic structure; d) the δ-phase not completely absorbed in by the α-phase; e)-f) RL-OM images of the dendrite structure still present in the cross-section, after etching.

In the Celo's sword and in the socketed-axe Cel-AxC-8, the metallographic examinations (Fig. 4.22) revealed the presence of weak dendritic coring, suggesting that the homogenization of the alloy was incomplete (*i.e.* the temperature was low or the soaking time was short). In the BSE-images, both of them exhibit a biphasic dendritic microstructure (Fig. 4.22a and c); in Cel-S this is just perceived, whereas in Cel-AxC-8 the dendritic growth is clearly visible. The SEM-EDS analyses reveal that the Sn average composition is about 8.8% in the sword alloy, whose dendrites are characterized by 7.2% of Sn in their centre and 11.0% in their outside areas. On the other hand, the segregation in the axe is much more predominant, with a variation of Sn across the dendrites from 8.8% to 3.2%. In this latter case, chemical analyses on different areas reveal that the Sn average composition is about 8.0%, more than the simple mathematical mean because of several remnant of δ-phase dispersed in the matrix.

In both cases, the chemical etching reveals the presence of annealing twins inside the primary α-Cu dendritic structures (Fig. 4.22b), but for Cel-AxC-8 the situation is more extreme (Fig. 4.22e-f). In fact, the few twins can be associated to a heat treatment made after a medium-scale plastic deformation that was not sufficient to achieve the complete recrystallization of the metal. Therefore, it is probable that the thermo-mechanical operations were performed just to give to the socketed-hole its final smoothed shape; even the rounded shape of the sulphides argues in favour of a quite weak plastic deformation. Consequently, its microstructure seems to be more related with the "as cast" type, but compatible with the sampled area on the handle-hole. After the chemical etching, small grains characterize the sword microstructure, representative of an area close to the cutting edge. These evidences lead to suppose that the blade undergone extensive cycles of hammering and annealing, even if the achieved temperatures allow for a recrystallization but not for the homogenization of the alloy. Consistently, flattened and oriented sulphides were observed in the sword cross section and the presence of numerous slip-line systems inside the grains testifies for a work-hardening state of the sword's blade.

The other two objects, specifically the socketed-shovel (Cel-Pal) and the socketed-axe (Cel-AxC-1), show an evident dendritic coring typical of a slow cooling after a casting process (Scott 2012). In both cases, the structure appears rather inhomogeneous and the dendritic arms are well visible in the BSE-images (Fig 4.23a and c). The two phases can be identified as follows: the dark regions represent the area of the dendrite in which Sn is present in lower amount, while Sn-rich phase are identified in light grey (Fig 4.23a-c) In the socketed-axe, the tin variation between the inner and the outer part of the dendrites was recorded between 2.1% and 9.6%, respectively, while in the socketed-shovel Sn

ranges between 1.2% and 10.5%. The dendrites are not bent and there is no sign of a recrystallization. In both cases, the microstructural observations suggest a rough casting without any other evidences of cold working (Fig. 4.23b-d), such as dendrite distortions or slip lines, in accordance with the sampled area on the margin of handle-hole. Probably, only a finishing treatment of the surface has been made to hide the marks of the two-part mould and to get a shiny surface.

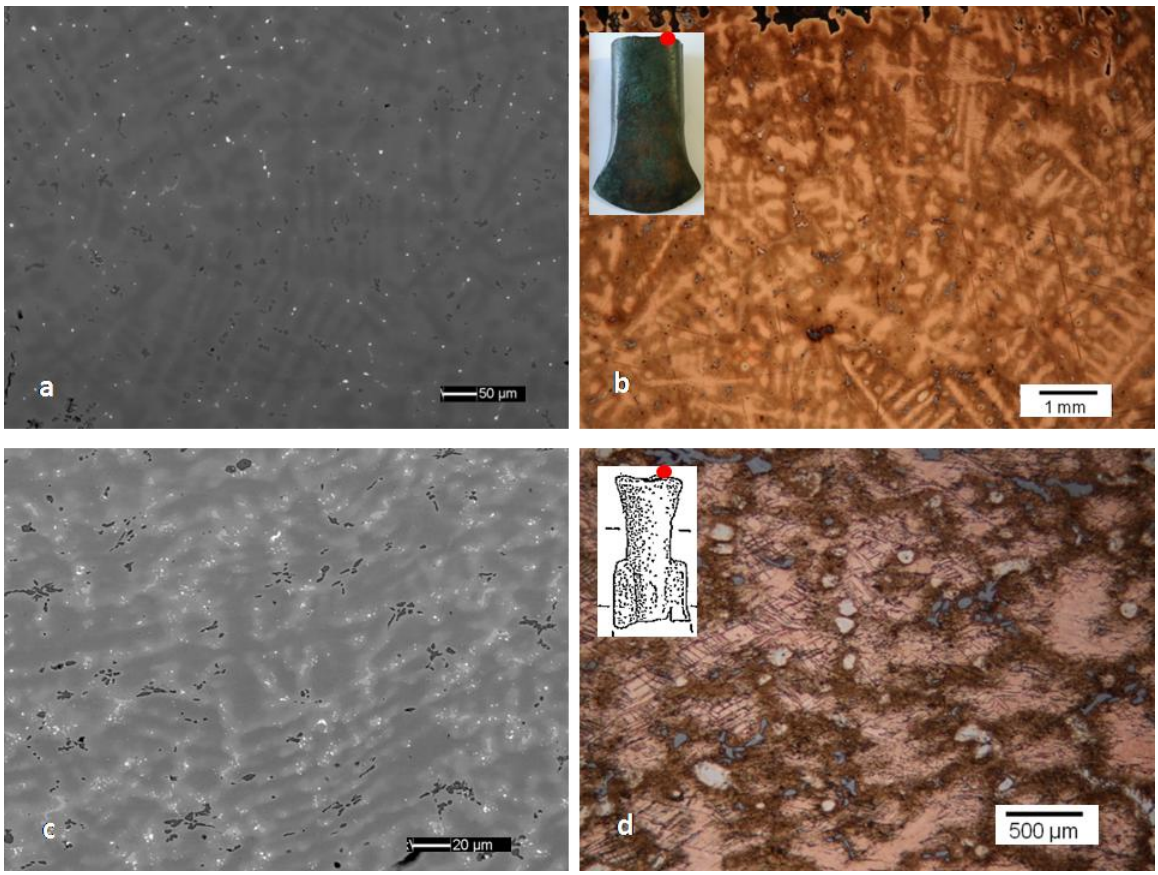

Fig. 4.23 – a)-b) Cross-section of the socketed-axe Cel-AxC-1: a) SEM-BSE image of as-cast dendritic structure; b) RL-OM image showing the dendrites, after etching; c)-d) Cross-section of the socket-shovel Cel-Pal: c) SEM-BSE image of as-cast dendritic structure; d) RL-OM image clearly showing the dendrites, after etching.

4.5 FBA2: The Galleriano and Porpetto hoards

Among the artefacts discovered in the Galleriano hoard, a winged-axe, two pick-ingots and an ingot (possible axe blade, see Chapter 2) were taken into account for the analyses. From the Porpetto hoard, the number of samples is significantly higher in order to reflect the wide heterogeneous composition of the deposit; a spearhead, two socketed-shovels, seven pick-ingots and nineteen ingots were selected. Even if the hoards belong to the same chronological phase, the results will be discussed separately to make more comprehensible the presentation.

Galleriano

Ingots

The chemical analyses and the microstructural observations performed on the three ingots confirm a substantial compositional difference between the two ingot shapes. On one side, the pick-ingots can be defined as tin-bronze, containing high percentages of Sn (12% in Gal-PI-4 and 15% in Gal-PI-5), while the third ingot is made of copper (93.4%) containing Fe (1.5%) and Zn (1.3%) as major impurities and low amounts of Sb (0.7%).

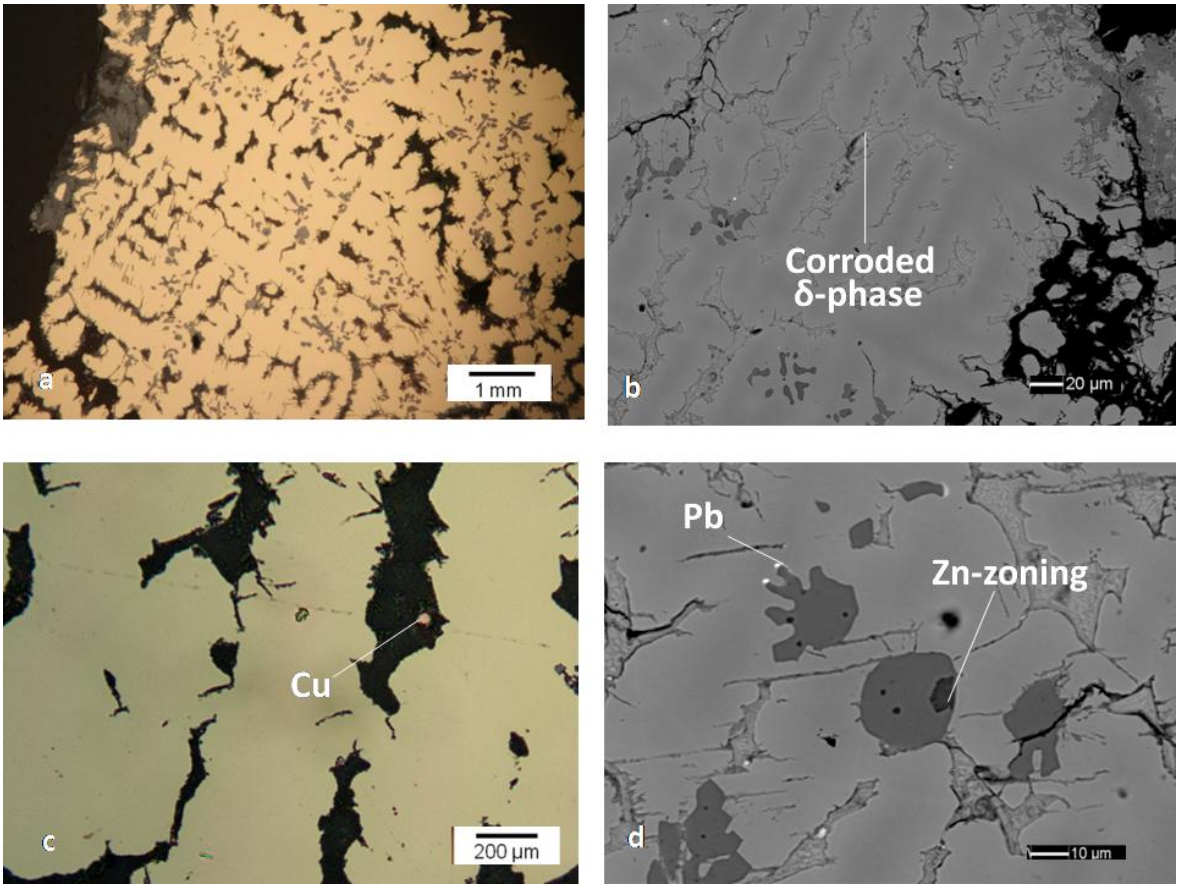

Fig. 4.24 – a) RL-OM image of dendritic structure in the Gal-PI-4 cross-section; b) SEM-BSE image showing the interdendritic corrosion in the Gal-PI-5 cross-section; c) RL-OM image of unalloyed "Cu" replacing the corroded (α+δ)-phase, sample Gal-PI-5; and d) SEM-BSE image of the sulphides observed in the Gal-PI-5 matrix.

The dendritic microstructure of Gal-PI-4 and Gal-PI-5 is clearly visible by optical microscopy without any chemical etching (Fig. 4.24a), since an extended interdendritic corrosion has been developed during the burial; in Fig. 4.24b, the BSE-image allows to better appreciate the degree of extension of such degradation. Moreover, according to Scott (2012), the preferential corrosion of the tin-rich phase leads to the reduction of the metal and, therefore, to an underestimation of the tin concentration. Besides this

phenomenon called *destannification*[7] (Leoni *et al.* 1991; Bosi *et al*. 2002), a contemporary re-deposition of little copper prills takes place as result of localised electrolytic processes (Fig. 4.24c). In both samples, a large number of copper-sulphide inclusions dispersed in the copper rich α-phase matrix were observed, which are mostly Zn-zoned and exhibit a Zn content that reaches 45–55% (Fig. 4.24d). Lead particles are almost absent and only recorded in small traces, mostly associated to the δ-phase survived to the burial environment.

On the other side, premised the different chemical composition, Gal-PI-3 exhibits a microstructure constituted of coarse dendrites. (Fig. 4.25a). In this case, the chemical analyses reveal that interdendritic segregations consist in Sb-rich segregations with traces of Ag and As. Moreover, globular Cu- and (Cu,Fe)-sulphides of large dimensions (averagely 30-40 μm) containing lead particles are observed (Fig. 4.25b). Lead is not recorded only inside the sulphides, but also in solid solution with As and Sb in their rich segregations, reaching a content of 2.4%. As reported in Chapter 2, this sample is a doubtful fragment interpreted by Borgna (2001) as a possible axe blade, but the quality of the metal, its raw nature and the comparison of its feature with those observed in the axes up to here discussed lead to exclude this hypothesis in favour of a ingot interpretation.

Considering all the features above described, and in the first place the presence of sulphides, it is possible to attribute the origin of the three Galleriano ingots to the smelting of chalcopyrite, possibly in association with sphalerite. In Gal-PI-3, the presence of antimony and traces of arsenic and silver could be attributed to a possible mixing of low amount of tetrahedrite present in the ore-charge during the smelting process.

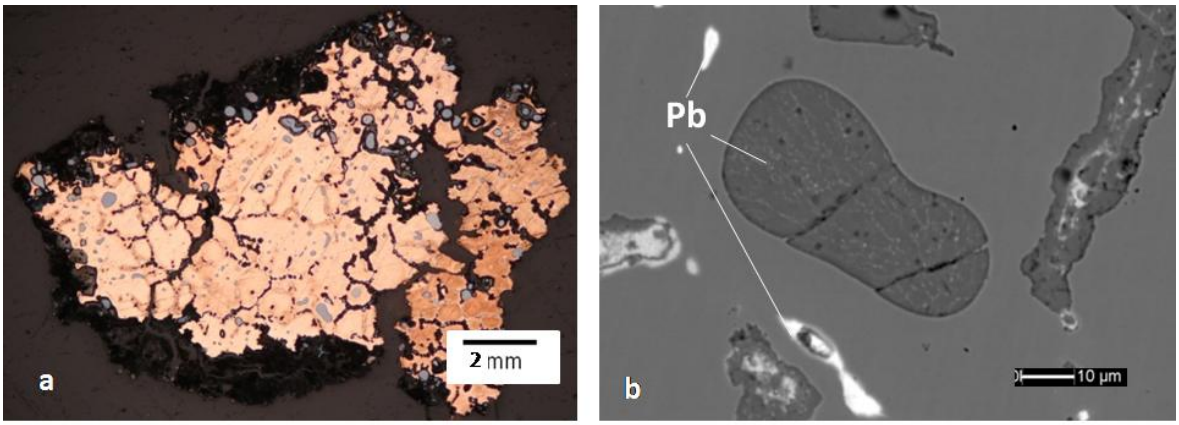

Fig. 4.25 – The Gal-PI-3 sample: a) RL-OM image of the coarse dendritic structure; b) SEM-BSE image showing the Pb particles (in white) inside the sulphides and dispersed in the copper matrix.

[7]Destannification is defined as selective removal of tin leaving residual copper (Wang and Merkel 2001)

Object

The Galleriano winged-axe is a homogeneous tin-bronze alloy (Sn 9.9%), and the (α+δ)-phase was only occasionally observed in the α-matrix. In Fig. 4.26, flattened (Cu,Fe)-sulphides and lead globules can be appreciated. From a microstructural point of view, equiaxed grains with twins and slip lines were clearly marked out by the chemical etching (Fig. 4.26c-d) testifying a plastic deformation followed by annealing cycles that, in this specific case, were not long or strong enough to provide for the full δ-phase dissolution. Therefore, these evidences suggest that even the poll/butt area from which the sample was taken has been strongly worked after the casting process; moreover, the presence of many slip-lines in this area can be attributed not only to the last hardening phase, but also to the actual use of this axe.

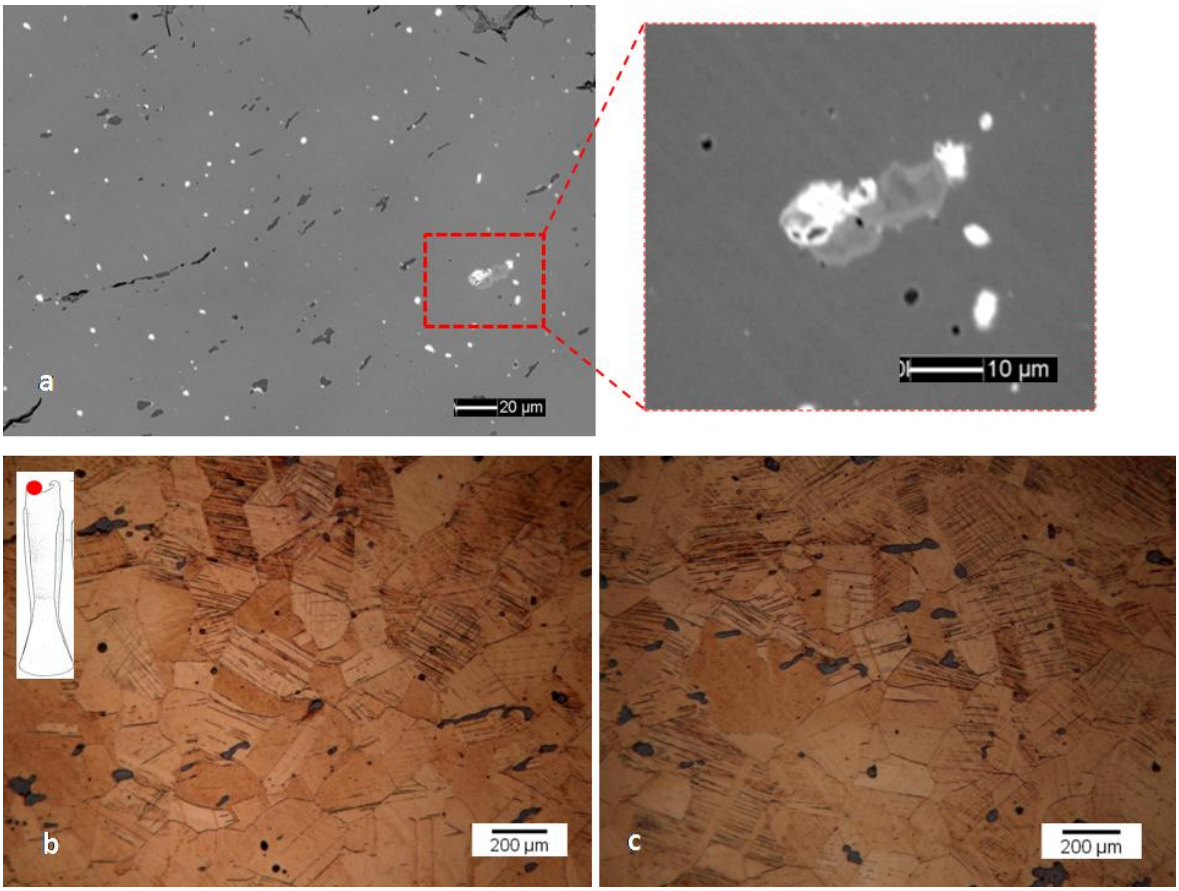

Fig. 4.26 – The winged-axe from Galleriano: a) SEM-BSE image of the homogeneous microstructure exhibiting traces of (α+δ)-phase (in light gray) associated to lead segregations (in white); b)-c) RL-OM image showing the twinned grains with many slip lines within.

Porpetto

Ingots

As seen in Chapter 2, the pick-ingots in the Porpetto hoard were found in association to many others ingot shapes. Chemical analyses revealed that all these samples are made of copper, ranging from 73.7% to 94.3%, with high contents of other elements, mainly As and Sb. Moreover, by comparing the plots in Figs. 4.27 and 4.28, two groups are clearly evident, although not correlated to the shape. All the ingots are characterized by the presence of As and Sb, in different percentages; As varies from 0.7% to 7.0%, whereas Sb from 0.9% to 9.5% (Fig. 4.27). On the other hand, the main difference in the two compositional groups is the presence/absence of Ni and Co in the alloy; in fact, as reported in Fig. 4.28, the content of such elements in twelve of the analysed samples reached noticeable amounts, very variable also in this case (Ni 0.5–7% and Co 0.5–3%). In some ingots, Ag was also recorded (0.7–1.6%), mostly in association with As and Sb, whereas Fe (max. 3.0%) was occasionally detected and does not seem to be correlated with the presence or absence of any other element.

From a metallurgical point of view, the presence of Ni in the alloy tends to stabilize Sb- and As-rich phases, and inhibits their loss during smelting (Sabatini 2015). In fact, Sb and As generally would be considered as desirable elements when added in few percentages, since they harden copper, but an alloy containing the detected amounts is not workable and very brittle. Therefore, this metal should be considered not technologically apt to tools and weapons making, but only for a casting process. However, if for the first group these element patterns are referable to a fahlerz-type charge (tetrahedrite-tennantite series), for the second, with Ni and Co, the interpretation is less intuitive and it could be traced to a mixing between fahlerz-ores and minerals belonging to the skutterudite series[8] $(Co,Ni,Fe)As_3$. Moreover, as demonstrated in the graph (Fig. 4.28) Co and Ni show a good correlation that could suggest the same origin of the two elements, reinforced by their non-volatile nature. For these reasons, they should be indicative tracers and their distinctive amounts could be useful for chemical comparisons and, especially, for supporting the isotopic interpretation (Chapter 6).

[8] Group of closely related arsenide minerals with varying rates of cobalt, nickel, and sometimes iron.

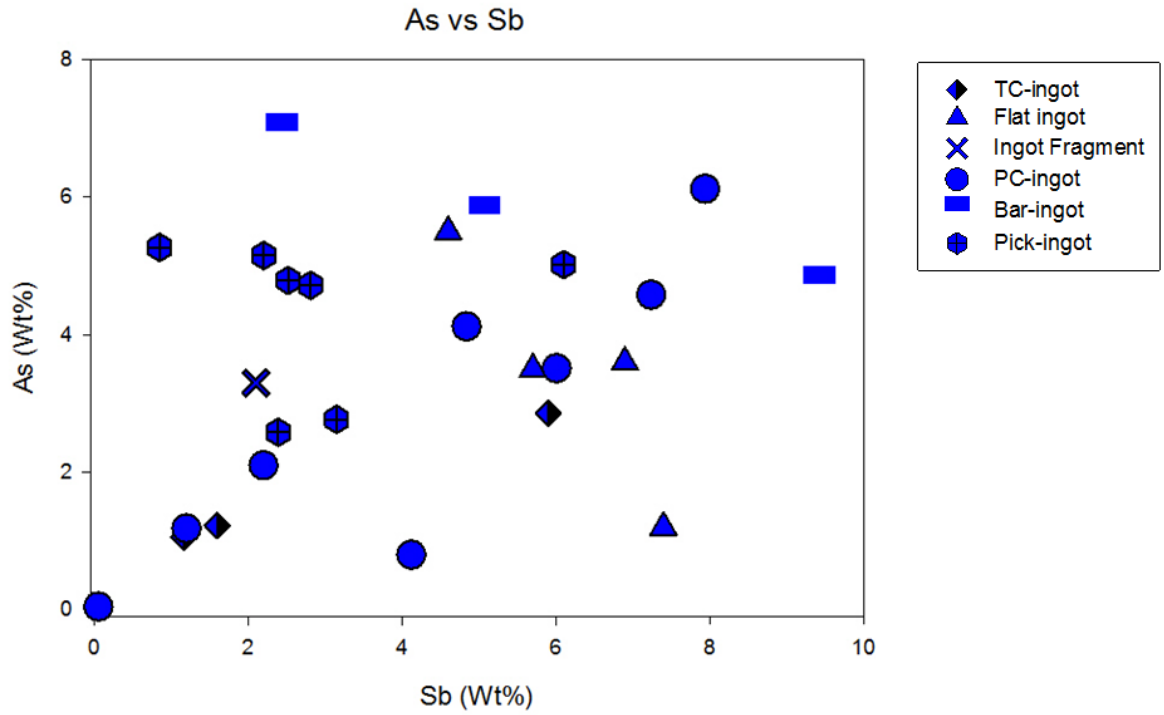

Fig. 4.27 – Scatter plot of the contents of As and Sb detected in ingots found in Porpetto (SEM-EDS bulk analysis). In the diagram, the different typologies are remarked by the symbols.

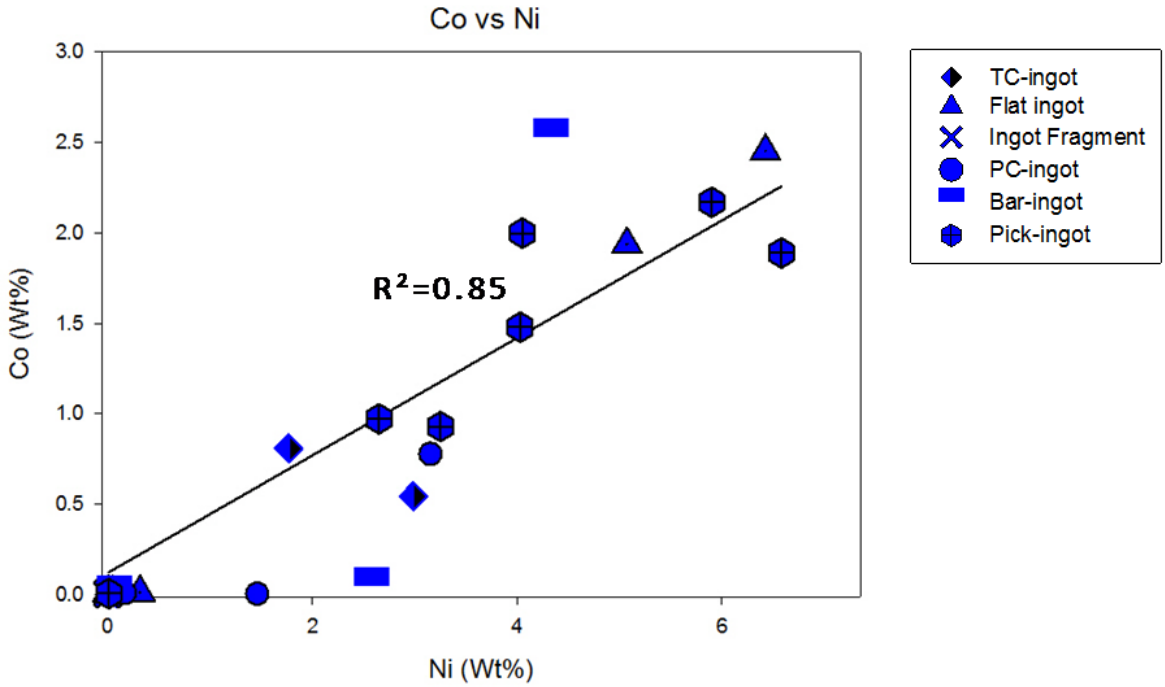

Fig. 4.28 – Scatter plot of the contents of Co and Ni detected in ingots found in Porpetto (SEM-EDS bulk analysis). In the diagram, the different typologies are remarked by the symbols

From a microstructural point of view, different features were detected in the cross-sections of these ingots, mainly due to their compositional pattern and in part to the smelting process, which in all cases seems quite rudimentary and not controlled. In first instance, for high amount of As, Sb, Ni and Co and when their sum reaches or exceeds 10%, a remarked coring structure is expected (Fig. 4.29a). This situation is clearly exemplified by the samples Por6-SN1 and Por6-SN2: besides the same composition, they exhibit almost the same dendritic microstructure, which is finer in Por6-SN2. The Cu-rich dendrites (in pink in the RL-OM images) are averagely characterized by few percentages of Sb (1.0–2.0%), As (1.8–2.5%), Fe (1.5–2.0%), Co (2.0–2.5%) and Ni (5.0–7.0%), whereas the interdendritic spaces (in light grey in the RL-OM images) are considerably enriched by these same elements, showing Sb up to 30%, As to 19%, Ni to 22%, Co to 8% and Fe to 7%. In *non-equilibrium* conditions, the cooling rate plays an enormous role in the alloying elements redistribution and in the dendritic growth dynamics; for these reasons, starting from the same composition, different segregation morphologies could occur (Davis 2001). Therefore, in the light of what was said, it is not possible to exclude that these two ingots could have been created from the same casting, although (Fe,Co,Ni)-rich precipitates are observed in the Por6-Sn2 cross section and not in Por6-SN1 (Fig.4.29b).

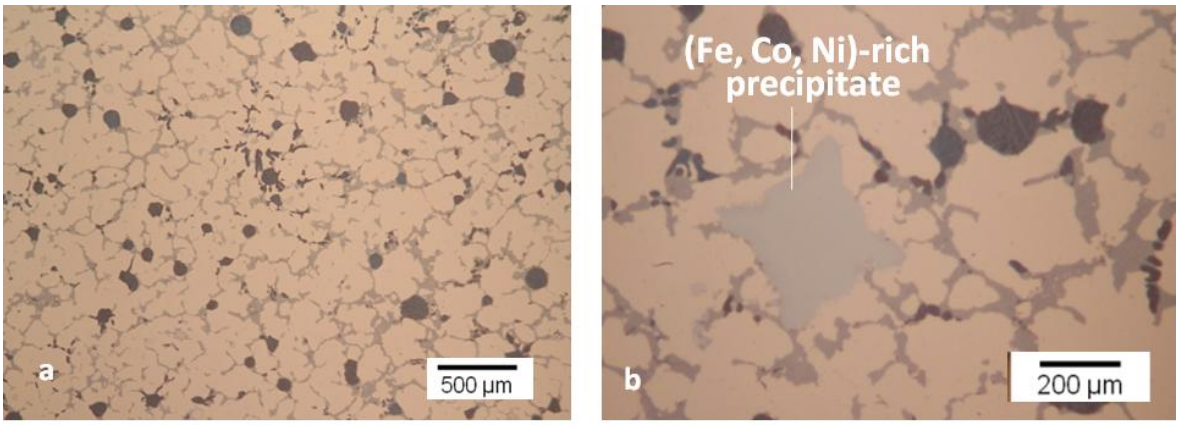

Fig. 4.29 – Sample Por6-SN-2: a) RL-OM image showing the dendritic microstructure and b) detail of the the (Fe,Co,Ni)-precipitate.

On the other hand, when the composition is characterized by minor amounts of As, Sb, Co and Ni (overall 2–4%) it must be noticed that the microstructural evidences primarily depend on the smelting process efficiency. Actually, if the alloy has been subjected to a fairly long process that reached proper temperatures, “fluid” segregations would appear along the grain boundaries (Fig. 4.30a); contrariwise, if the smelting process is poorly efficient, mineral remains not completely roasted are trapped in the alloy (Fig. 4.30b-d). Unfortunately, the solidification course of complex Cu-based alloys with such variable

amounts of Ni, Co, As and Sb cannot be careful studied because multi-component diagrams are not available; hence, at the moment, it is not possible to make precise considerations on the melting temperatures.

Moreover, the investigation showed that Cu- and (Cu, Fe)-sulphides are always present in the microstructure, mostly exhibiting Fe-zoning (Fig. 4.30e) or lead inclusions (Fig. 4.30f). Their occurrence reinforces the hypothesis of (Cu,Fe)-sulphide ores as the initial charge for the smelt.

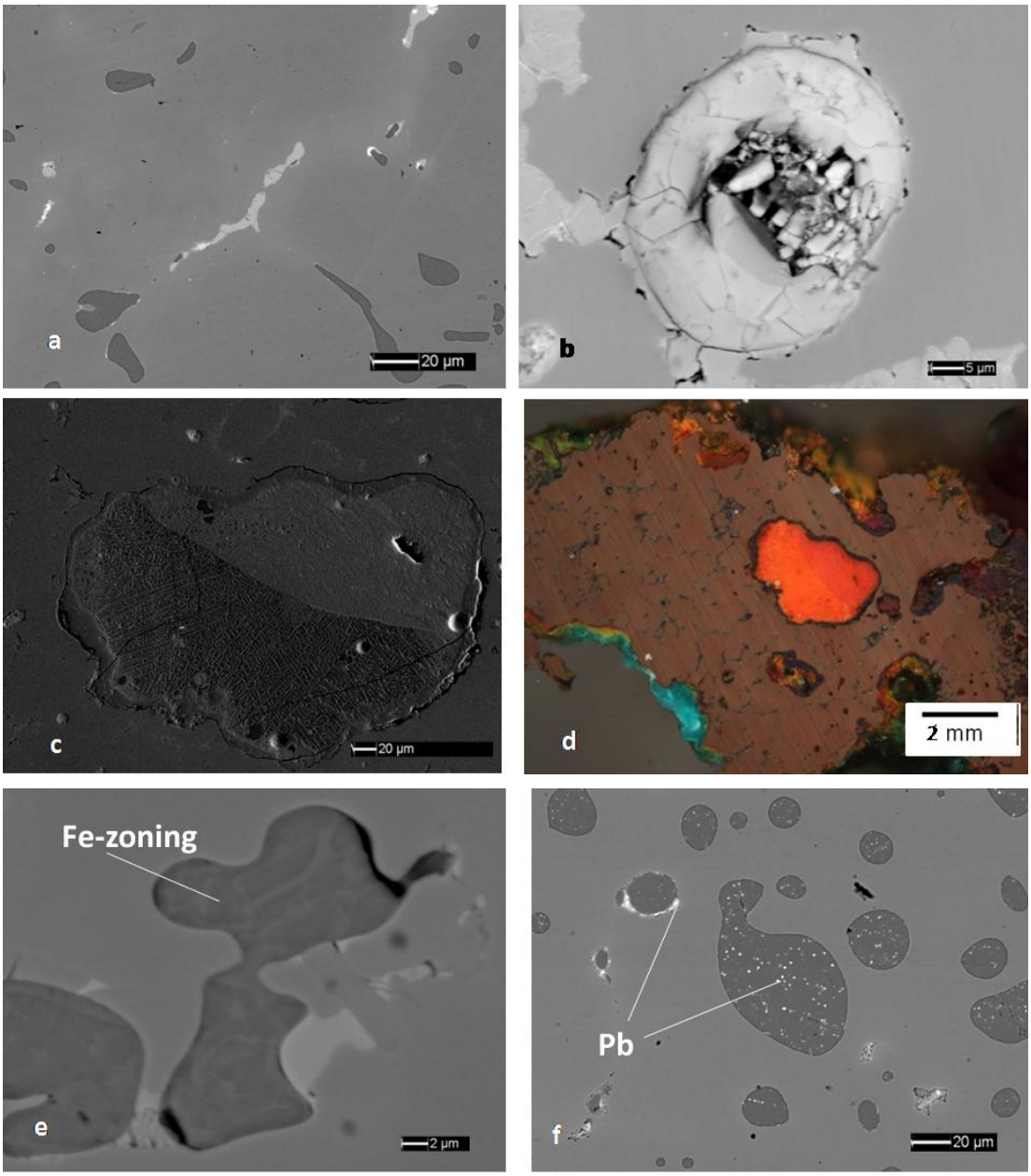

Fig. 4.30 – a) SEM-BSE image of the "fluid" segregations in the ingot microstructure of Por6-PC-6, in light gray; b) SEM-BSE image of the mineral residue (Cuprite) in the Por9-PC-30 sample; c) SEM-SE image of the mineral residue partially melted (copper rich in As and Sb) in Por6-PP-7 and d) RL-OM of the same residue (polarised light); e)-f) SEM-BSE images of the different sulphide morphologies observed in the metal matrix in Por9-Bar-5 and Por9-TC-29.

Consistently with chemical and microstructural observations, these ingots could be cautiously compared to those belonging to Kanalski Vrh (Slovenia) and studied by Paulin *et al*. (1999). In this case-study, the authors suggested the employment of *speiss* in order to explain the composition of the Slovenian ingots rich in As, Sb, Co and Ni. *Speiss* is a metallurgical term that describes a complex solution of heavy-metal arsenides – compounds of As, with Co, Ni, Co and Fe which can form alongside matte – and interpreted as intermediate products in the extractive metallurgy. It is obtained from the smelting of sulphidic copper ores containing fahlerz, and sometimes nickel and cobalt arsenides, next to chalcopyrite, chalcocite and other copper and copper-iron sulphides. Moreover, the great variety in the extractive charge composition results in *speisses* with differing chemical contents. Moreover, since matte has been never observed in Friulan ingots, it must be noted that the two cases cannot be directly compared, even if it could be safely said that a similar complex mineral charge has been involved for the Friulan ingot making and that they were subjected to further refinement respect to the Slovenian ones.

Interestingly, the plano-convex ingot Por9-Pn-25 represents an exception in this scenario, containing high percentages of Fe (13%), traces of Zn (0.25%) – never found in any other ingots from Porpetto – and no traces of As, Sb, Co or Ni. These features, associated with the presence of copper sulphide containing Zn traces, relate this sample to the smelting of chalcopyrite, probably in association with sphalerite. It must be stressed the point that such high percentages of Fe denote a refining level not accurate or not controlled, as proposed for the other ingots. Indeed, several globular Fe-Cu segregations are distributed in the matrix, together with (Cu,Fe)-sulphides (Fig. 4.31).

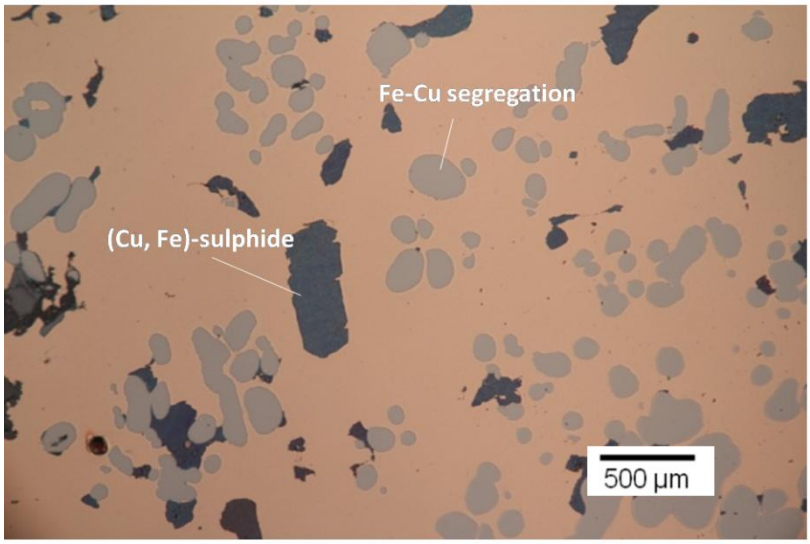

Fig. 4.31 – Sample Por9-Pn-25: RL-OM image showing the Fe-rich segregations (92%Fe–8%Cu) and the sulphides present in the copper matrix.

Objects

The chemical analysis performed on the objects discovered in the Porpetto hoard revealed a startling similarity to the chemical composition of the ingots from the same deposit. For one socketed-shovel and the spearhead (Por9-Pal and Por9-Cus46) the amount of As, Sb, Co and Ni are lower than in ingots, but the impurity suite is clearly the same, although in both cases tin has been also added to the alloy (7.2% and 6.0%, respectively). Conversely, the other socketed-shovel (Por6-Pal) exhibits higher values of As (10.5%), Sb (6.8%), Ni (3.4%), Co (0.7%) and none Sn as recorded for ingots but, in addition, an incredible percentage of Pb was recorded (23.0%).

In Por9-Pal and Por9-Cus46 cross-sections, the microstructures are characterized by a coarse dendritic solidification (Fig. 4.32), in which the interdendritic spaces are filled by a Sn-rich phase (23.0%) with high Sb (7.9%), Ni (7.4%), As (2.8%) and low amounts of Co (1.0%). It is difficult to think that such not-homogenized alloy could be hammered and, in fact, the chemical etching reveals that both of them have been subjected only to the casting process. However, it can be assumed that the addition of the other elements have been motivated by a Sn saving without losing its properties (*i.e.* hardness for the spearhead and the silver-colour for the socketed-shovel).

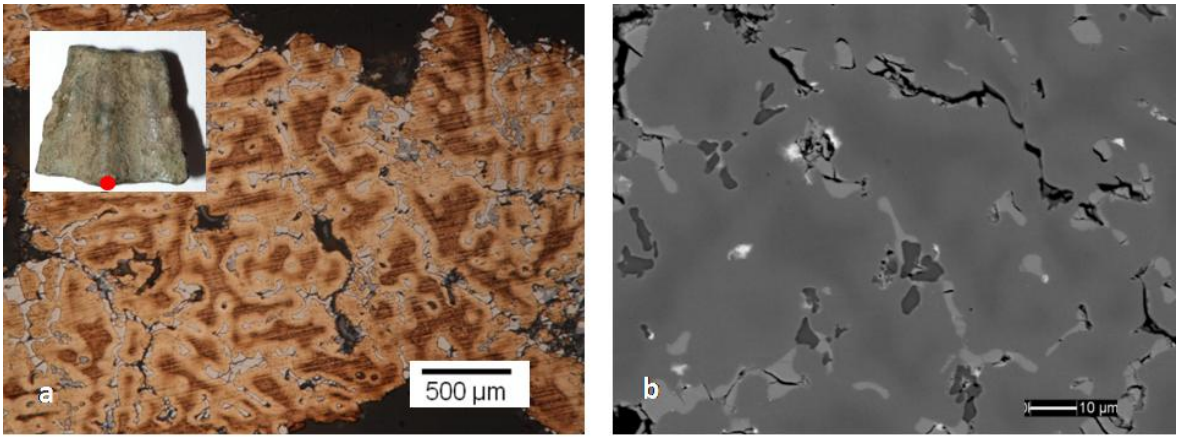

Fig. 4.32 – Cross-section of the spearhead, Por9-Cus-46: a) RL-OM image of the coarse dendritic structure, etched; and b) SEM-BSE image showing macrosegregation in the matrix.

In Fig. 4.33, the cross section of the socketed-shovel exhibits a coring microstructure characterized by Cu-rich dendrites (93-94%) and interdendritic spaces in which Cu falls to 44%, substituted by Sb (30.3%), Ni (14.7%), As (8.8%) and Co (2.2%), as presented for the samples Por-SN1 and Por-SN2 in the previous section. The large amount of lead, sometimes in association with silver, is clearly recognizable in the alloy as bright segregations. This chemical composition enhances the castability of the alloy, but makes it completely unsuitable for any working. These features are consistent with the

metallographic evidences, which testify a casting into the mould and, probably, the smoothing in order to remove the signs of casting. Undoubtedly, the lead addition in such high percentages makes this object not reliable for the lead isotope analysis.

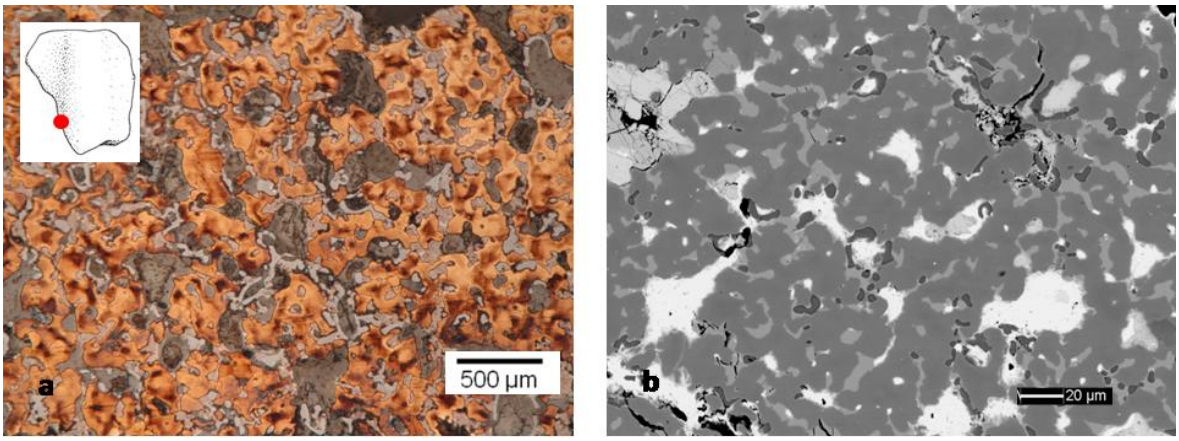

Fig. 4.33 – Cross-section of the socketed-shovel, Por6-Pal: a) RL-OM image of the coarse dendritic structure, etched; and b) SEM-BSE image showing lead inclusions (in white) and the interdendritic segregations (in light gray).

Chemical data: Discussion

The determination of the nature of the metal is fundamental for its metallurgical characterization and for the further investigation on its provenance by Lead Isotope Analysis (see Chapter 6). Hence, the discussion of the chemical data reported in this chapter could give useful indications about the attribution of the mineral charges used for the copper extraction. In this perspective, it must be kept in mind that a change in trace element concentrations does not automatically mean a change in ore source (Pollard *et al*. 1990) and that, contrariwise, the employed metallurgical processes might affect the in different ways the behaviour of trace elements (Tylecote 1970 and 1977). These element variations have led to numerous debates about the classification of copper objects and their attribution to particular ore deposits (Junghans *et al*. 1968; Pernicka 1990). Therefore, since the samples treated in this study are very heterogeneous (especially ingots) it was decided to globally assess the pattern of impurities without exceeding in an absolute and rigid clustering. In fact, as stated by Liversage (1994), the copper/bronze archaeometallurgy is much more than just seeking for compositional groups as a key to identify the sources from which the copper may have come. Thus, in order to characterize ingots belonging to different smelting stages, it seemed more useful to not exclusively consider the suite of elements and their concentrations, but also define the connections with the microstructural features, which can give useful information on the refining step. On these bases, it is possible to justify the presence of a volatile element (*e.g.* Zn, As, Sb) and discuss about its original quantity in the ore charge. For what concerns ingots, the classification is based on the concentrations of arsenic, antimony, silver, nickel, cobalt, lead and zinc, whereas tin enables the discrimination between unalloyed copper and bronze objects. Moreover, since these samples can not only be evaluated by a mathematical point of view, the presence of individual items in a borderline position in the reported diagrams requires that the interpretation must be left to a personal judgement, based on an overall view of the obtained data.

In the following sections, the results are presented and discussed maintaining the division between objects and ingots, since they represent two different steps of the metallurgical *chaîne opératoire* (Ottaway 1994). In the discussion, the provenance of the hoards, their ages and the typology of objects are considered.

5.1 Ingots

The ingots can be sorted into four main chemical groups by using the global amount of such elements that characterize a fahlerz-ore mineral assemblage (As, Sb, Co, Ni and Ag) against the quantity of Sn recorded in the alloy (Fig. 5.1). The groups are named as follows:

- "pure copper", which is made up of pure or almost pure copper ingots (28 samples)and is characterized by a low amount of impurity (<2%, in total), mainly Fe and Zn;
- "impure copper", whichexhibitsfew percentages of fahlerz elements in the range 2–8%(11 samples);
- "high-impurity copper", which consists of ingots having variable contents of As, Sb, Co and Ni,reaching a total amount of about15–20% (24 samples);
- "bronze ingots", which are represented by only four ingots deliberately alloyed with a tin content greater than 12% (4 samples).

As mentioned before, the dottedlinesin the plots are arbitrary boundaries, adopted to differentiate the different classes but without representing a defined limit; this situation is highlighted by the fact that some ingots lie on a borderline position between two compositional fields that does not allow for an univocal classification.

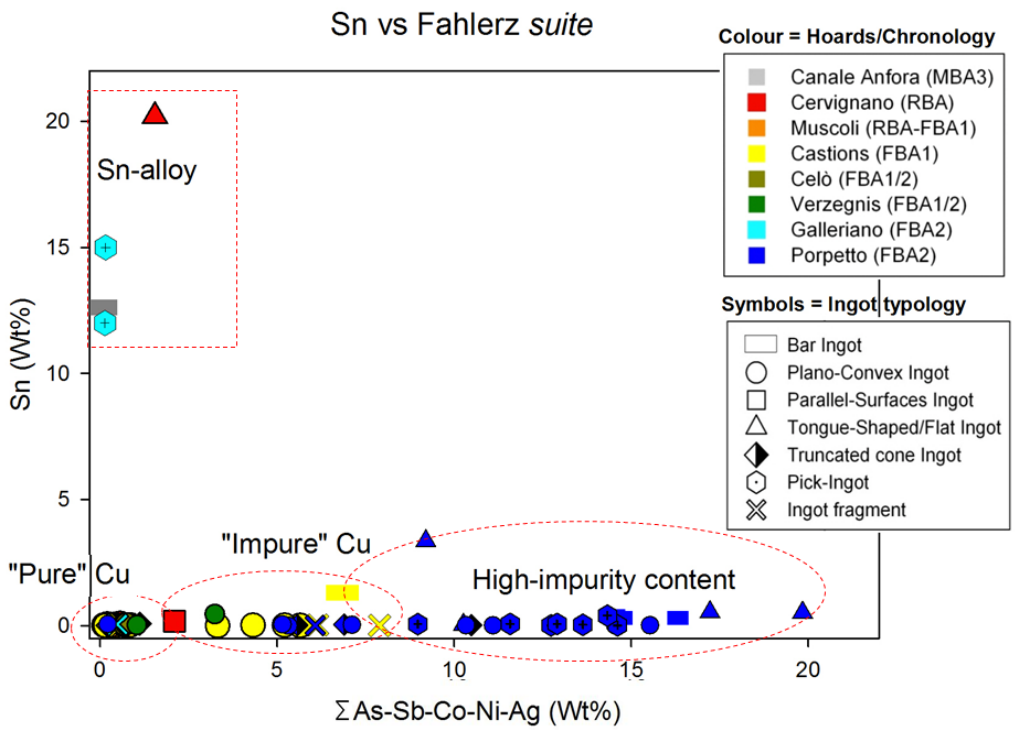

Fig. 5.1–Scatter plot of the overall content of As, Sb, Co, Ni and Ag (fahlerz-suite) against the amount of Sn; all percentages are expressed as wt%. The dotted lines identify the four major groups determined in this study.

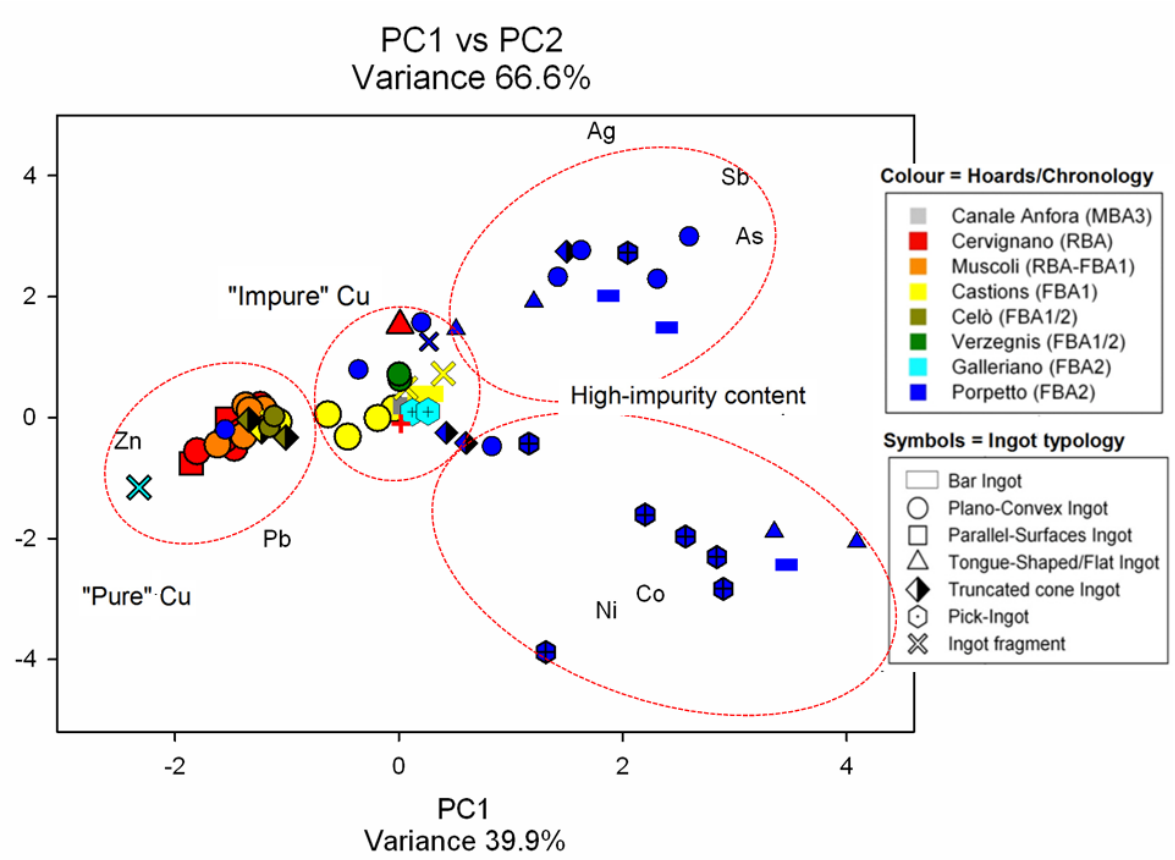

Fig. 5.2–PCA loading and scores plot of all the analyzed ingots (PC1 vs PC2) showing the defined compositional copper groups. The "bronze ingots" group does not appear in the diagram since tin is omitted from the analysis.

In order to present the chemical data without losing information, a multivariate data processing has been carried out by following the approach explained in Chapter 3. In this case, the Principal Component Analysis (PCA) has proved to be a powerful tool, since it allows for an immediate visual impression of the composition of any copper group by taking simultaneously into account all the elements that characterize the chemical pattern of ingots. However, since tin derives from the alloying step and not from the ore-charge, it has been voluntary omitted in the performed PCA statistical analysis, but bronze ingots were evenly included in order to give an overall chemical representation, avoiding a tin contribution that may distort the PCA results. In the diagram in Fig. 5.2, the first two principal components (PC1 and PC2) carry the 66.6% of the total information and, although a quite similar distinction to the above listed groups is remarked, a more detailed differentiation among ingots is noticed. On one hand, two sub-groups can be clearly identified in the "high-impurity content" area, both of them characterized by high levels of As and Sb, and one distinguished for the presence of high amounts of Co and Ni; in

particular, it can be noticed that these two groups are exclusively composed by the samples of the Porpetto hoard. Moreover, it is important to underline that the dotted-circles do not remark rigid groups, and that the partial overlaps must be intended as a compositional continuity toward an increased impurity content, very evident in the case of the "high impurity copper" groups.

On the opposite side, the "pure copper" group is sharply separated from the other fields, owing to the great impact of Zn, and it is mainly composed by all the ingots belonging to Cervignano, Muscoli and Celò; interestingly, all the other hoards possess at least one ingot belonging to this group. Moreover, it should be noted that Zn strongly influences the outcome PCA and the general distribution of ingots, playing an antithetical role respect the fahlerz-suite; for this reason, such element can be considered as a discriminating variable and its relationship with the other elements must be investigated. Finally, the “impure copper” group lies in the centre of the diagram, owing to the presence of moderate amounts of impurities, and embraces ingots belonging to different deposits. All the bronze ingots fall in the field of the “impure copper” for different reasons; for the tongue-shaped ingot (Cer-TS, marked as red triangle), this classification is correctly motivated by the presence of several percentages of Ni (1.2%) and traces of As (0.3%), whereas the pick-ingots from Galleriano (light blue hexagons) and the "sword" from Canale Anfora (gray bar) do not exhibit relevant amounts of trace elements (<0.2-0.3% in total). These latter three items lie near the centre of the PCA diagram and, therefore, they are not influenced by any element.

In Fig. 5.3, the fahlerz-suite (Sb, As, Ni, Co, Ag) is compared to the amount of Zn detected in the ingots, from which can be easily observed that, in general none of the samples characterized by such elements show any traces of Zn dissolved in the α-phase. However, an isolated case is represented by Por6-PI-9, which slightly deviates from this behaviour since it contains a Zn amount of 0.2%. Conversely, as mentioned before, variable amounts of Zn widely characterize the “pure copper” group and, even in this case, three exceptions can be recognized; in addition to Zn, Cer-PS-64 possesses 1.9% of Sb, whereas both the ingots form Verzegnis are characterized by different amount of arsenic, low in Ver-P0 (0.4%) and more significant in Ver-P9 (2.4%). This preliminary approach allows for the identification of two different chemical peculiarities that could lead to suppose the use of two distinct mineral charges. Indeed, for these four outliers (Por6-PI-9, Cer-PS-64, Ver-P0 and Ver-P9, which show features of both groups, even if slight), their borderline position can be explained by hypothesizing either a mix of the two charge-ore types or a partial metal recycling. All these groups are discussed in detail in the following sections.

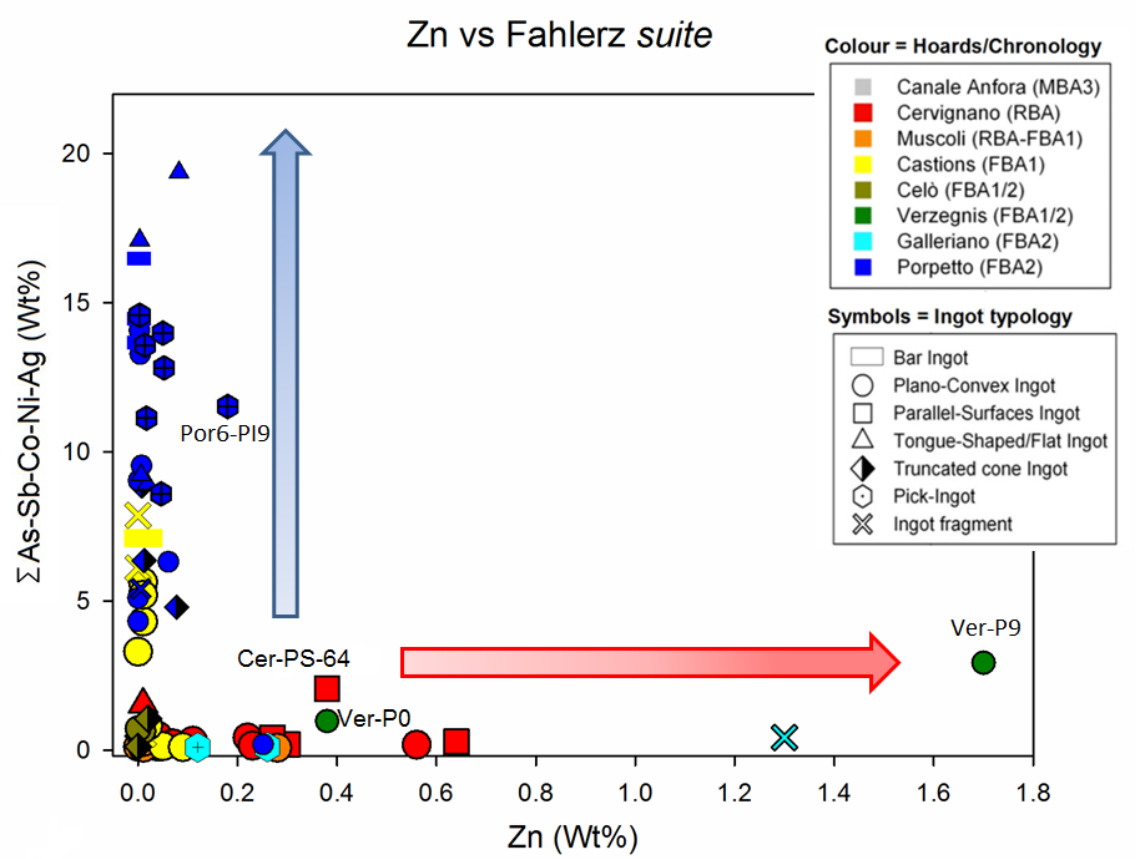

Fig. 5.3–Scatter plot of the mean overall content of As, Sb, Co, Ni and Ag (fahlerz-suite) against the amount of Zn recorded in the α-phase (EPMA analyses); all percentages are expressed as wt%. The diagram shows thealmost complete absence of Zn in the samples characterized by a fahlerz composition.

5.1.1 Pure copper

This group is composed by ingots possessing a minimal amount of trace elements and, for some of them, the purity of copper does not allow for a distinctive identification of the mineral source. As first hypothesis, the trace element scarcity could be attributed to the employment of pure copper exploited from one or more sources; however, it is not possible to exclude that the extreme purity of the copper could be explained by a sequence of several remelting and refining steps, which leaded to a consequent weakening of the chemical link respect to the original charge. Anyway, these considerations will be discussed in more detail in Chapter 6, in relation to the lead isotope analyses. Further, since sulphides were observed in the matrix of the “pure copper” ingots (Chapter 4), the hypothesis of a solely employment of either oxide minerals or native copper is not plausible (Mangou and Ioannou 2000). Moreover, even the chemical differences in terms of Zn and Fe content suggest that pure copper ingots may be mined from different sources, but it must be considered that the conditions achieved during the

smelting process or in a subsequent refining step could have led to losses in Fe and Zn amounts, as it will be discussed later in this chapter.

Conversely, in those samples exhibiting Fe (0.1–3.2%) and Zn (0.3–1%) in the α-phase, the metallographic observations revealed the presence of Cu- and (Cu,Fe)-sulphides, mostly Fe- and Zn-zoned and interpreted as relics of the smelted sulphidic ore (Hauptmann *et al.* 2002); these evidences allow for a sure identification of the extractive charge as chalcopyrite associated with sphalerite. This attribution is compatible with the unavailability of oxide ores during the Late Bronze Age in Europe and with the necessity of employing sulphide ores in order to answer to the more and more increasing demand for metal (Rapp 2013). The smelting of sulphide ores essentially required at least three stages and a strict control over the air supply. In the first stage, the ore is partially roasted to remove the sulphur as sulphur dioxide, producing what is called matte; in the second stage, similar to smelting oxide ores, the matte is reduced to form the so-called blister or black copper that would be later refined in the final stage (Craddock 1995). However, as reported by Addis et al. (2015) in a recent research on the LBA copper smelting slags from Luserna (Trentino, Italy), this process can be even more complex. In any case, during the process, the unwanted amounts of waste material – including iron oxides – are reduced or eliminated by slagging, whereas the volatile elements such as zinc or arsenic are lost in quantity depending on temperature and reducing conditions.

In this direction, the observation of Zn-Fe diagram (Fig. 5.4) provides useful information about the technology used for the smelting process of such ingots. As stated by Craddocks and Meeks (1987), the iron content can be explained by either the employed copper-ore or the smelting conditions (*i.e.* the reducing atmosphere and the use of an iron-oxide flux), whereas the presence of zinc primarily depends on the extractive charge. However, both elements decrease in quantity when they are subjected to subsequent stages of remelting (Tylecote *et al.*1977; Merkel 1983). Consistently with the above said, in the diagram in Fig. 5.4 only the samples surely smelted from chalcopyrite and sphalerite are reported, in order to discuss the possible correlations between Fe and Zn. In first instance, the attention should be focused on the oldest deposit of Cervignano, labelled in red; in this case, it is possible to note that Fe and Zn are basically lower and more correlated in the PC-ingots than in the PS-ones, evidence that is strongly supported by the microstructural observations performed in the previous chapter. All these considerations lead to suppose a correlation between chemical and microstructural features, and their typological distinction permits to consider PS-ingots as less refined than PCs. The Cervignano hoard contains both types of such ingots and this lead to the main idea that PS- and PC-ingots can be associated to two different stages of a multi

stage production process, probably similar to that proposed by Tylecote (1981). Indeed, since ancient smiths should have been aware of different properties resulting after the smelting and the refining process, the different shape of the ingots probably allowed for their proper handling in the workshop. Thus, the PC- ingots could be intended as raw metal (almost) ready for the objects production, whereas the PS-ingots, having also few percentages of Fe, are not appropriate for the creation of usable objects at this stage, since the high concentration of iron negatively affects casting and hammering steps (Craddock and Meeks 1987). However, it should be noted that a comparison between structure, composition and shape (*i.e.* between PS- and PC-ingots) is not possible for any other hoard except Cervignano, since PS-ingots were only found in Cervignano and a case of a clear coexistence between these two shapes in the same hoard is not attested elsewhere. The diagram in Fig. 5.4 shows that the some ingots fall in a well-defined region, or at least in its proximity, characterized by a strong Fe-Zn correlation, and this behaviour leads to suppose for the Cervignano hoard an apparent standardization of the smelting process, not recorded for the hoards dated to later periods.

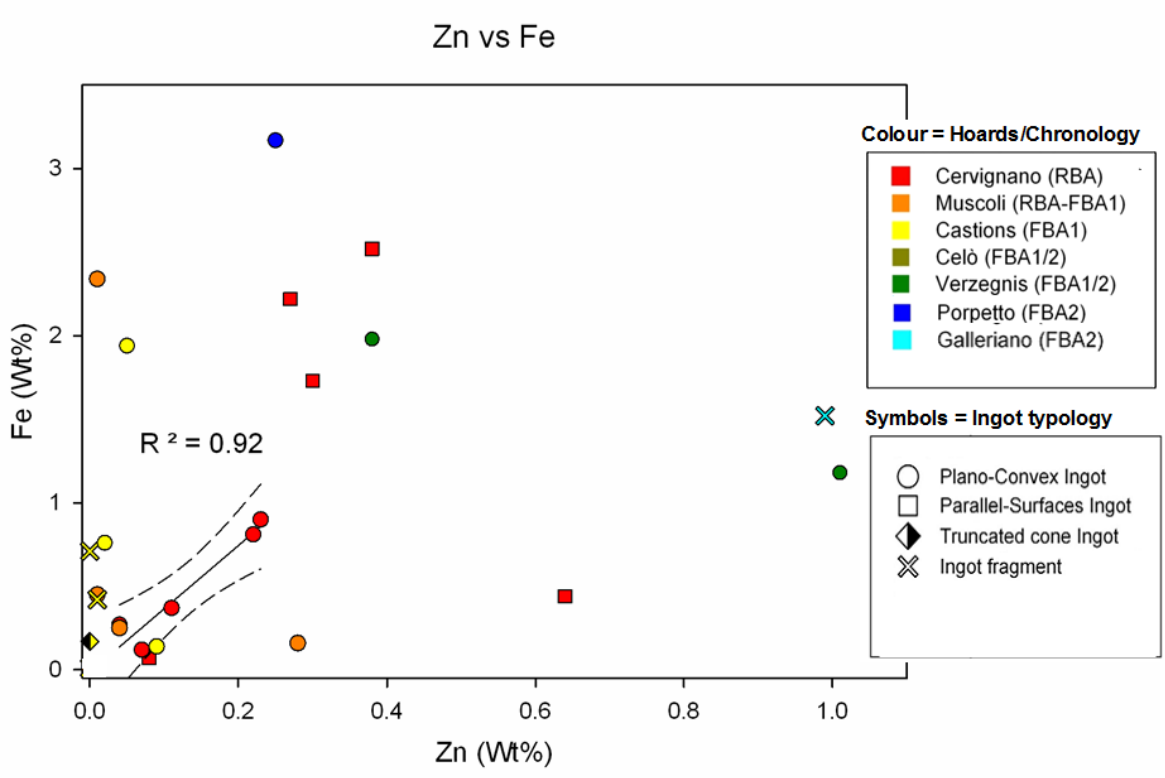

Fig. 5.4– Scatter plot of Fe and Zn concentrations detected in the α-phase of all the investigated "pure copper". In the diagram, the regression line calculated for PC-ingots from Cervignano and its coefficient of determination (R^2=0.92) is reported.

In literature, few comparisons for this type of ingots are available. In Central Europe, during the Late Bronze Age, the presence of pure copper-ingots is known to be scarce, whereas in Northern Italy only sporadic analyses attest the use of chalcopyrite (Pigorini 1985; Casagrande *et al.* 1993). Conversely, a significant parallelism is attested in the Western Transdanubia region (Hungary) where, similarly to Cervignano, the LBA Celldölmöllk-Ságheghy deposit only contained ingots deriving from chalcopyrite in order to obtain pure copper (Czajlik and Sólymos 2002); furthermore, the authors define this site as unique. Unfortunately, only a microstructural characterizations supported by punctual analyses is available, without any numerical bulk analysis or lead isotope analysis. On the other hand, many chemical data are accessible for the Slovenian deposits, thanks to the systematic research project carried out by Trampuž-Orel and her colleagues (1996; 1991; 1998). This latter study allowed for a comparison between the ingots from Friuli and the plano-convex ones belonging to Slovenian LBA deposits (Crmosnjice, Hocko Pohorje, Jurka Vas, Pekel and Silovec), from which the so-defined "cast ingots"[9] were not considered owing to their different chemical composition. In this work, all the ingots selected for the PCA can be considered in pure state, since the average concentrations of minor elements are below 2%, without counting the amounts of Fe. In Fig. 5.5, the first two principal components are plotted considering Co, Ni, Zn, As, Ag, Sb and Pb, whereas Fe was not taken into account for the statistical analysis, since it primarily depends on the process technology. Moreover, all the Slovenian hoards are considered together because, according to Klemenc *et al.* (1999), there are no significant differences among copper ingots from the different locations.

The statistical comparison shows a sufficiently clear distinction between the chemical trend exhibited by the Friulian ingots and the Slovenian ones; in fact, despite the high purity degree that characterize both ingot groups, a first discrimination can be performed by considering the type of raw material employed during the smelting process. In Fig. 5.5, the spatial differentiation between Italian and Slovenian ingots suggests that Slovenian samples are in most cases characterized by the presence of As, Co, Ni and Sb, even in low amounts. In this case, the use of fahlerz-ore as extractive charge is assumed, without any apparent similarities with the ores employed for the smelting of Friuli's ingots belonging to this group. In the PC1 negative area of the diagram, the overlap of some Slovenian and Friulian ingots has not to be considered as a connection among single deposits, since each ingot comes from different hoards, but must be interpreted as

[9] The term "cast ingot" refers to fragments of metal, and also alloys that were cast in univalve or bivalve moulds of various form. The most commonly published and analysed ingot shapes are bar ingots, loaf-shaped ingots, slab ingots and hammer-shaped ingots (Trampuž-Orel 1996).

isolated cases. Therefore, the main hypothesis is the employment of the same extractive charge and smelting technology for the creation of these ingots, but it is not possible to exclude a possible contact between these regions. However, this crucial issue could be resolved by coupling the lead-isotopic results to the chemical analyses but, at the moment, no isotopic data for the Slovenian items are available.

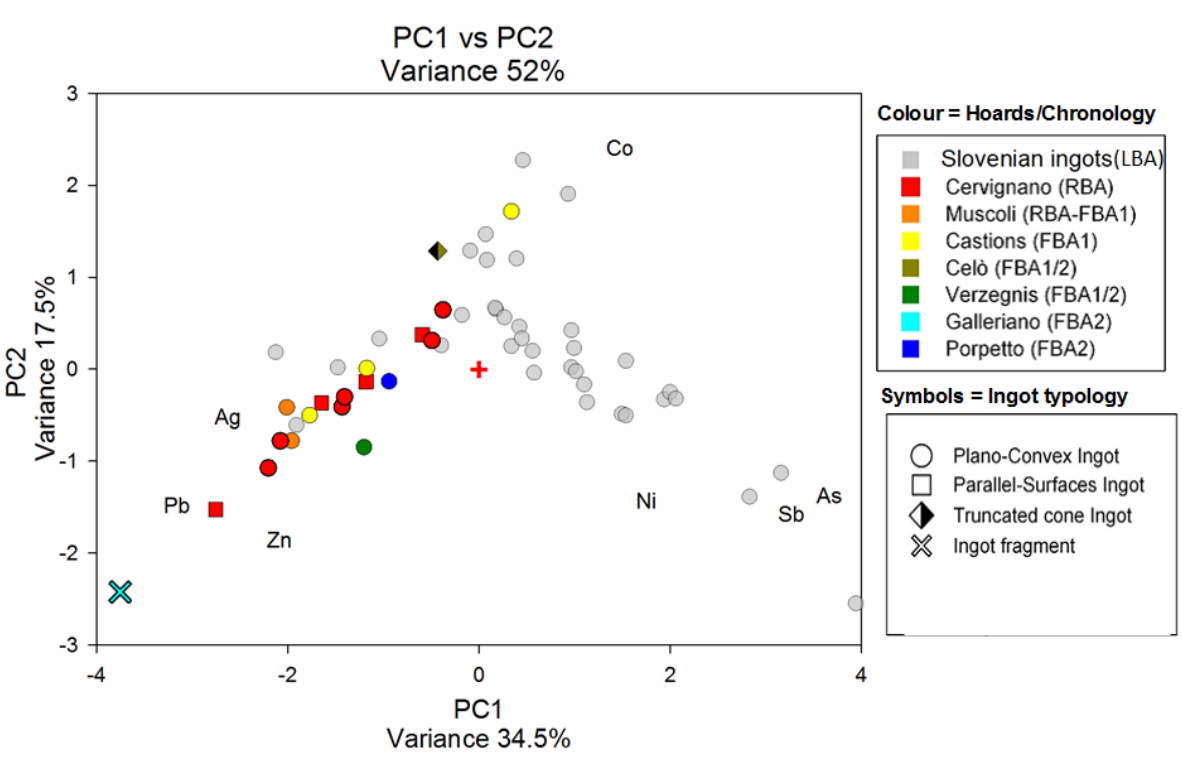

Fig. 5.5– PCA loading and scores plot of the Friulian "pure copper" ingots compared to the LBA Slovenian plano-convex ingots (PC1 vs PC2). The first two principal components (PC1 and PC2) carry the 52% of the total information.

5.1.2 Impure copper

This group is composed of copper containing different amount of As (2–4.5%), Sb (1–3.5%), Ni (0–1.8%) and traces of Co (<0.5%). The microstructure of these ingots is quite similar, since Cu- and (Cu,Fe)-sulphides are present as witness of the sulphidic ore used for smelting, together with As- and Sb-rich segregations and mineral remains not completely roasted during the smelting process (Chapter 4). Therefore, these evidences could suggest that this type of copper has been smelted from ores of the tennantite-tetrahedrite series, widespread and intensively employed during the European Early Bronze Age (Merkl2011). This group is represented by a part of the Castions di Strada ingots, an ingot from Verzegnis and few others from Porpetto; very interestingly, there are not ingots that belong to the oldest deposits of Cervignano and Muscoli.

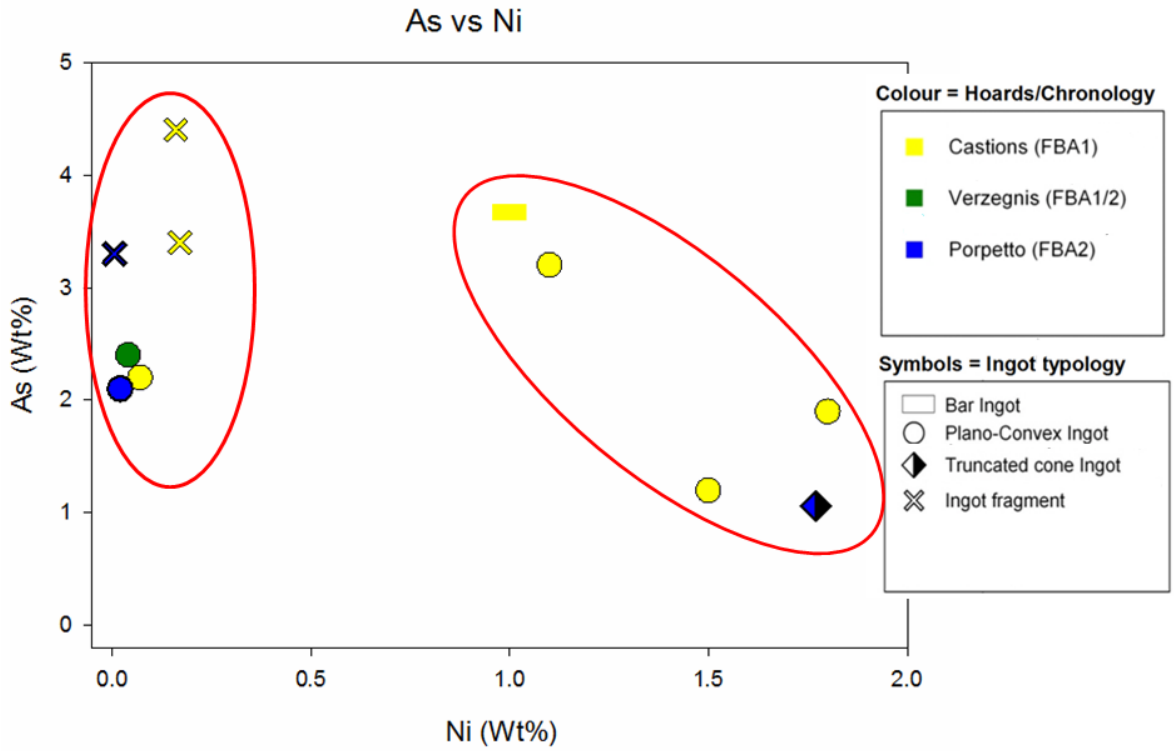

Fig. 5.6 – Scatter plot of the As and Ni bulk concentrations detected in the "impure copper" ingots. The resulting sub-groups are remarked by the red circles.

Depending on the levels of Ni, a further division in two sub-groupscan be made (Fig. 5.6); in the first, Ni is almost completely absent whereas, in the second, the Ni content ranges from 1.0 to 2.0%. A great deal of attention in archaeometallurgical research in copper and bronze has been paid to those elements that are considered to be important to distinguish ore sources (Pernicka 1990) and recent extensive researches have shown that arsenic and antimony, in combination with nickel, can be addressed as distinctive tracers. Indeed, focusing the attention on the metal finds from the cemetery in Hainburg/Teichtal, Duberow's analyses (2009) have pointed out that such artefacts could divided different metal clusters. The first group can be described as fahlore metal without nickel, which is characteristic for the *Osering* copper; conversely, the second group can be interpreted as originating from fahlore with nickel, characteristic for the so-called East Alpine Copper, which occurs mainly during the developed Early Bronze Age (Krause 2003). As shown in Fig 5.6, the coexistence of these two distinct metal groups seems to be present even in the Castions di Strada hoard and a comparison it is possible thanks to chemical data available in literature.

In the first case, among all available data for metals classified as *Osering*-type, it was considered appropriate to take into account only the copper-based smelting products; for this reason, in Table 5.1 the chemical data of *Osering* metal from ingot hoard in Bohemia, Austria and Germany are reported and compared to the Friulian ones (Liversage 1994). From the table, it is evident that the mathematical mean for the Friulian samples shows the characteristic pattern As=Sb>Ag, consistent with that exhibited by the *Osering* ingots, and that the value of Ni (0.01%) is just indicative, since this percentage is below the detection limit indicated for the EPMA analysis.

Tab 5.1 – Main values of the chemical analyses (wt%) referred to the *Osering* metal ingots discovered in several hoards in Bohemia, Austria and Germany (Liversage 1994) and compared to the average of the chemical composition of the Friulian "impure copper" ingots without Ni.
(SD=Standard Deviation)

Site	N. Samples	Co	Ni	As	Ag	Sn	Sb	Pb
Ceske Budejovice	45	0	0.001	1.56	0.65	0	1.56	0
SD			*0.001*	*0.31*	*0.19*		*0.31*	
Radostice	84	0	0.003	1.53	0.75	0	1.44	0
SD			*0.004*	*0.34*	*0.19*		*0.29*	
Suchorelly	16	0	0.001	1.54	0.9	0	1.77	0
SD			*0.001*	*0.45*	*0.3*		*0.45*	
Neuruppers dorf	67	0	0.002	1.38	0.59	0.006	1.34	0.003
SD			*0.003*	*0.32*	*0.15*	*0.004*	*0.35*	*0.002*
Waging	43	0.003	0.001	2.1	0.7	0.004	1.94	0.002
SD		*0.011*	*0.002*	*0.7*	*0.17*	*0.004*	*0.62*	*0.009*
Average		**0.002**	**0.006**	**1.023**	**0.459**	**0.010**	**1.007**	**0.005**
Friuli ingots Average	6	0.004	0.01	1.03	0.39	0.02	0.99	0.01
SD		*0.004*	*0.01*	*0.63*	*0.23*	*0.01*	*0.58*	*0.01*

On the other hand, the remaining samples of Castions di Strada and one of Porpetto match quite good with the *Singen* metal composition (Tab. 5.2), characterized by a multi-impurity pattern with high levels of Sb and Ni and moderate levels of As. In addition, Co is detected at constant levels (0.1–0.2%), leading to be sure of its presence in the ore-charge (Liversage 1994). However, it must be aware that the comparison is between ingots (Friulian samples) and finished objects (*Singen* metal objects); therefore, the content of As and Sb could be misrepresented, owing to the volatile nature of these elements. Nevertheless, in spite of the fact that the Friulian ingots show a greater amount

of As respect the *Singen* metal average, a resemblance in the suite of elements is recognizable. Indeed, one can notice that the sites of Tyrdosovce, Vel'kyGrob, Leithaprodersdorf, Gattendorf and the Neudorf hoard have on average much more As, which obviously increases the final average and can lead to inaccurate conclusions; conversely, the other sites taken one by one show a perfect affinity. This discrepancy can be explained by thinking that the alloy of the finished objects has been subjected to further refining steps, leading to the loss of this element.

Tab 5.2 – Main values of the chemical analyses (wt%) referred to the *Singen* metal objects discovered in several sites located in the Carpathian Basin (Liversage 1994) and compared to the average of the chemical composition of the Friulian "impure copper" ingots with Ni. (SD=Standard Deviation)

Site	N. Samples	Co	Ni	As	Ag	Sn	Sb	Pb
Vicapy-Opatovce	110	0.17	1.15	0.6	0.46	0.1	1.79	0.01
SD		*0.19*	*0.46*	*0.39*	*0.14*	*0.38*	*0.72*	*0.08*
Tyrdosovce	5	0.17	1.03	1.58	0.59	0.05	2.57	0.004
SD		*0.19*	*0.7*	*0.58*	*0.17*	*0.08*	*0.64*	*0.004*
Vel'kyGrob	9	0.07	1.16	0.83	0.61	0.24	2.16	0.02
SD		*0.07*	*0.5*	*0.49*	*0.18*	*0.66*	*0.93*	*0.03*
Rusovce	15	0.1	1.06	0.56	0.54	0.07	1.85	0.002
SD		*0.09*	*0.49*	*0.44*	*0.12*	*0.1*	*0.86*	*0.003*
Kisapostag	13	0.07	0.71	0.36	0.54	1.01	1.01	0.001
SD		*0.12*	*0.38*	*0.27*	*0.2*	*1.21*	*0.45*	*0.003*
Kules	10	0.17	0.86	0.77	0.55	0.05	1.75	0.02
SD		*0.17*	*0.42*	*0.49*	*0.16*	*0.05*	*0.8*	*0.04*
Gemeinlebarn	42	0.26	1.35	0.67	0.69	0.6	1.76	0.03
SD		*0.29*	*0.61*	*0.33*	*0.3*	*1.59*	*0.87*	*1.15*
Leithapodersdorf	9	0.1	1.85	0.8	0.89	0.09	3.49	0.02
SD		*0.03*	*0.71*	*0.23*	*0.2*	*0.004*	*0.64*	*0.03*
Gattendorf	10	0.16	0.92	0.73	0.58	0.004	2.4	0.22
SD		*0.19*	*0.39*	*0.43*	*0.21*	*0.006*	*0.7*	*0.066*
Neudorf hoard	5	0.12	1.29	0.82	0.81	0.06	2.38	0.009
SD		*0.08*	*0.55*	*0.3*	*0.24*	*0.08*	*1.01*	*0.011*
Singen	38	0.043	1.5	0.94	0.68	0.69	2	0.003
SD		*0.0064*	*0.71*	*0.46*	*0.2*	*1.69*	*0.67*	*0.05*
Average		**0.13**	**1.17**	**0.79**	**0.63**	**0.27**	**2.11**	**0.03**
Friuli ingots Average	*5*	0.19	1.43	2.19	0.17	0.21	1.53	0.65
SD		*0.35*	*0.37*	*1.16*	*0.34*	*0.44*	*0.36*	*0.85*

An additional similarity can even be found with the Velem and Nyergesujfalu-type ingots discovered in the Sághegy hoard, in Hungary (Czajlik and Sólymos 2002); in this study, only compositional indications are reported, making difficult a proper comparison which is in any case helpful to expand the picture frame on the spreading of this type of metal in Europe. As previously mentioned, this raw material is characterized by 1–3% of Ni, variable amounts of Sb and As, whereas Co is revealed only in few traces within the copper matrix. Moreover, all morphological characteristics (*i.e*. traces of sulphides, Sb-rich phases and mineral residues similar to those of Friulian samples) suggest that these ingots had gone through few phases of processing, and their element association reflects the composition of the original ore. Therefore, basing on these metallurgical observations and also considering geological and cultural data, the history of mining and the geographic conditions of transport and commercial traffic, the authors suggested that the possible raw copper sources with Ni could be those of the tetrahedrite-tennantite series located in Slovakia (Spania Dolina-Piesky-Lubietova) and Austria (Mitterberg-Kitzbuhel and Lienzn-Schladming). For these deposits, isotopic data are available and will be considered in the discussion presented in Chapter 6.

The proved diffusion of fahlore, with or without Ni, and the discovery of ingots showing a refined composition very similar to that of objects, as in Castions di Strada, leads to make conjectures on the knowledge of the use of this metal. As stated by Coghlan (1960), three factors were mainly important for the ancient metalworker: the suitability of the metal for casting, its behaviour under hot- and cold-forging and the hardness and strength of the metal in the finished product. In fact, the intentional smelting of ores aimed to obtain a high-impurity copper is something related to the intentional needs to provide, modify or improve the properties of the metal; in any case, the use of such metal is near to the alloying purpose. For this reason, it is possible to think that this type of alloy could be deliberately used to create ornaments characterized by a shiny-silvered colour and for which a good castability was mandatory; alternatively, it could be employed for objects in order to increase the mechanical properties of copper without sacrifice the ductility, especially in substitution of Sn. Indeed, most of scholars involved in Italian metallurgy agree that arsenical and antimonial copper alloys were intentionally sought through the selection of fahlores, naturally rich in these elements, rather than by adding such elements to the melt (Barker 1971 and 1981; De Marinis 2006; Northover 1989; Pare 2000).

5.1.3 High-impurity copper

As presented before in Figs. 5.1 and 5.2, the “high- impurity” copper group is populated exclusively by the samples belonging to the Porpetto hoard and two sub-groups can be clearly identified. The first is characterized by high levels of As and Sb – on average 4% and 5%, respectively – most of the times associated with Ag (>1%). Conversely, in addition to very high-levels of As and Sb, the second sub-group shows significant amounts of Co (~1.4%) and Ni (~4%), whereas silver was seldom detected in traces. It is interesting to note thatthis latter group is mainly populated by pick-ingots.

It is quite evident that the copper used for ingots in this hoard is totally different from that used in the other deposits and in the previous periods. In both cases, the difference is primarily due to the amounts of the impurity levels recorded in the bulk, since the suite of elements is typical of a not refined ore rich in tennantite-tetrahedrite minerals. Based on these evidences, a proper comparison can be performed between the chemical composition of Porpetto ingots and that of several Slovenian ingots (Trampuž-Orel 1996) identified as *speiss* by Paulin *et al.* (1999). Base-metal *speiss* is typically a complex mixture of copper, nickel, iron and/or silver as arsenides and antimonides, often with some sulphur and lead; *speiss* is a material similar in appearance to metal, although it is brittle and cannot be worked other than by casting. Thus, it is usually discarded as a waste product (Thornton *et al*. 2009). This type of metal is known from a number of prehistoric and historic metal smelting sites, forming especially when smelting complex arsenic- or antimony rich copper or lead ores (see Bachmann, 1982: 29–30; Keesmann, 1999; Rehren *et al*., 1999). In this purpose, it was supposed that not only deposits rich in tetrahedrite were working during the LBA, but also deposits with more complex ores containing other minerals rich in cobalt and nickel (Trampuž-Orel *et al.* 1991), which are similar to copper sulphides but are more difficult to reduce, and for this reason they can be used a tracers.

Concerning the comparison between the Porpetto ingots and the previously defined Slovenian “cast ingots”, the logarithmic presentation is particularly suitable for the large range of concentration values that characterize the samples, since the linear scaling results in a misleading illustration and in a compression of the compositional fields. Moreover, the logarithmic scaling corresponds to the natural distribution of trace elements and to the physical laws that govern the distribution of elements between slag and metal (Pernicka 1990). Fig 5.7 shows the relationship between nickel and cobalt for all the samples of this group compared with the “cast ingots” found in several Slovenian hoards (Hoko Pohorje, Veliki Otok and Kanalski Vrh I-II, Trampuž-Orel 1996), where it is clear that those samples characterized by exceptionally high levels of Ni and Co show a perfect

overlapping with the Slovenian cast ingots. Unfortunately, in the work of Trampuž-Orel (1996), the reported analyses have not been placed in connection with the different shapes and, therefore, the published data are referred to generic “cast ingots”. Thus, even if it is not possible to connect shape and chemical composition, the authors attested the presence of hammered-shaped ingots in Veliki Otok and Kanalski Vrh (Trampuž-Orel 1996), associable to pick-ingots. In the case under study, most of the investigated samples are pick-ingots that are similar to those found in Veliki Otok and Kanalski Vrh (Trampuž-Orel 1996), not only in shape but also in composition (Fig 5.7). In addition, even the ingots discovered in Dragomelj can be qualitatively associated to those of Porpetto, since they contain high quantities of arsenic, nickel, antimony and cobalt (Trampuž-Orel *et al.* 2001). This fact further reinforces the idea of a contact with the Slovenian trade circles.

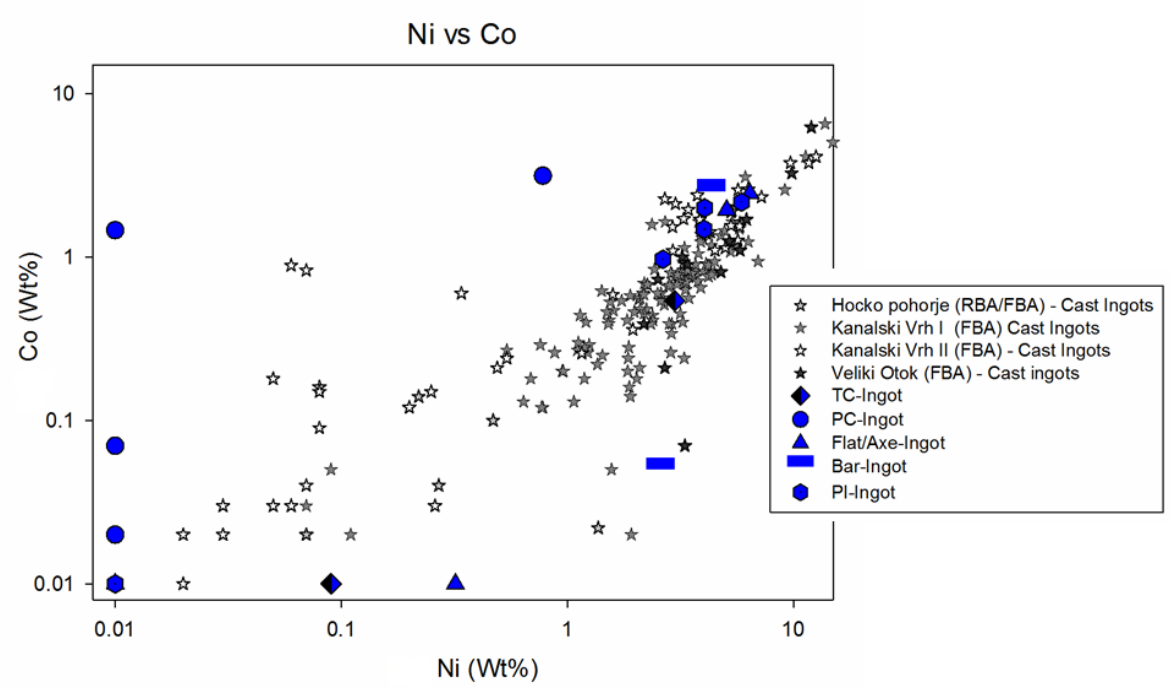

Fig. 5.7 –Scatter plot of the content of Ni and Co (wt%) detected in the bulk (SEM-EDS analyses) of the “high-impurity copper” ingots from Porpetto. The diagram shows the overlap between the Porpetto ingots exhibiting noticeable amount of Ni and Co and the Slovenian cast ingots.

Another interesting comparison is presented in the work of Giumlia-Mair (2003) on the metal findings discovered in Pozzuolo del Friuli (17 km far from Porpetto) and S. Lucia in Tolmino/Most na Soci, on the Slovenian border. Even in these ingots, relatively high concentrations of As, Ni, Ag and Sb have been detected and the presence of Co reinforces the similarity between these samples. Thus, all these sites, including Porpetto, could be interpreted as important centres on the routes, most probably beaten by metal

traders (Giumlia-Mair 1998). Furthermore, as reported by several authors (Trampuž-Orel *et al.* 2001; Borgna1992; Bulat 1967; Vinski Gasparini 1973; Smodic 1956), other pick-ingots were discovered in the hoards of Miljana, Ivanec Bistranski and Kapelna (Croatia), although no chemical analysis has been performed on these samples and, therefore, it is not possible to extend the discussion to the commercial networks in these regions. Even in this case, the coupling of lead-isotopic results to the chemical analyses might help for a proper comparison, but no isotopic data are available.

Considering the amount Sb, As, Ni and Co in the alloy, it is possible to observe that, on average, their sum is about 10% in ingots with only As and Sb, whereas goes up to 14% in those with Ni and Co. As suggested by Giumlia-Mair (2005) and Trampuž-Orel *et al.* (2001), and consistently with the absence of tin in the alloy, this fact could be related to the scarcity of tinthat occurred at some point in the LBA. Indeed, the employment of As, Ni, Co and Sb in these percentages ensured a low melting point and a good castability at the expense of workability; as mentioned before, such kind of alloy could not be worked by hammering since it was very brittle.

5.1.4 Bronze ingots

The tin-bronze group is the less numerous class. It counts four bronze ingots, alloyed with different amounts of Sn (Fig. 5.1). On one hand, the “sword” of Canale Anfora[10] and the two pick ingots from Galleriano show a tin content in the range 12–15%, whereas the Tongue-Shaped ingot (TS) from Cervignano exhibits a higher Sn amount (~20%), accompanied by 1.2% of Ni and traces of As (0.3%); up to now, samples with such composition have not been discovered or analysed.In these samples, the tin content itself is not comparable, but what is important is the idea of bronze stockpiling. Indeed, for lower concentrations (7–12%), it is not possible to exclude that these ingots could be interpreted as remelted scraps which were traded in form of small bars; conversely, for higher concentrations, such as in the TS-ingot, the production of ingots starting from tin and copper is more plausible, as previously discussed in Chapter 4. It is, of course, rather difficult to prove that there was an organized trade of recycled bronze; but it is possible that the main purpose of these ingots was to trade and convey tin across a commercial network.

In Friuli Venezia Giulia, the presence of bronze ingots is further attested by the discovery of three similar bar-ingots possessing 7% of Sn. Two samples come from the

[10]In Chapter 4, this sample was reinterpreted as an ingot rather than an object and, for this reason, it is considered in this section.

hillfort of Variano, in the Friuli Plain, not far from Udine, which had been inhabited from the Middle Bronze Age to the Early Iron Age, while the other was found during the excavation of the Iron Age workshop remains of the nearby site of Pozzuolo del Friuli (Giumlia-Mair 1998 and 2009). It is interesting to note that, in both these two cases, and in the Cervignano and Galleriano excavations as well, similar alloys are not found to be employed to produce finished objects or in association to bronze ingots. This fact reinforces the hypothesis of the employment of TS-ingot or pick-ingots as a raw material for trading.

The tin content in pick-ingots is illustrated in Fig.5.8 and, interestingly, the high amount detected in the Galleriano pick-ingots agrees with the few analytical data available for pick-ingots in literature. According to Pigorini (1895), the pick-ingots from the Madriolo hoard have a high percentage of tin (up to 12–14%), even though more recent analyses suggest quite a low tin content (qualitative data in Pellegrini 1992), while the four pick-ingots from the Redipuglia hoard (Borgna 1992) exhibit a lower tin concentration (3.2–4.8%) if compared to the Galleriano ones. Moreover, Pellegrini (1992) reported qualitative analytical data for one sample with a high tin content from a hoard discovered in an unknown locality in central Italy and conserved in the Pigorini Museum in Rome. Therefore, it is possible to suggest that the two analyzed pick-ingots reinforce the hypothesis that Galleriano, as well as Frattesina (Zaghis 2005), had been far away from the tin trade crisis recorded in the Slovenian area (Trampuž-Orel *et al.* 2001) and, possibly, in Porpetto. On the contrary, in Redipuglia, the situation is slightly different, since less amounts of tin have been employed. Moreover, it should be reported that recent studies carried out by Jung, Mehofer and Pernicka (2011) have increased the number of existing analyses on pick-ingots. Indeed, four pick ingots from Frattesina have been chemically identified as bronzes having a tin content in the range 10.2–14.7% (one sample with traces of Sb) and suggesting in this site a high quality production.

A problem that is still being defined is to understand from where tin was mined. Recently, Afghanistan emerged as the most promising eastern source of tin (Cierny and Weisgerber 2003), with western sources most likely located in southern England and Brittany; conversely, tin sources in Central Europe are not surely recognized and still provide serious problems regarding the Bronze Age mining technology used at that time (Muhly 1985). Concerning the tin supply in Friuli, several hypotheses may arise: one source could be identified in the mineral rich areas of southern Tuscany (Benvenuti *et al*. 2003), where cassiterite deposits were available. Otherwise, according to Giumlia-Mair (2000), another option is that tin could be easily been transported to the territory of the *Caput Adriae* from the deposits on the mountains of Bukulia and Cer (Western Serbia),

located along the important fluvial arteries Danube and Sava (Huska *et al.* 2014). However, at the moment, it is not possible to further argue this matter, although it should be noted that the Tuscanian cassiterite is a very limited occurrence and there is no evidence of exploitation before the Middle Age.

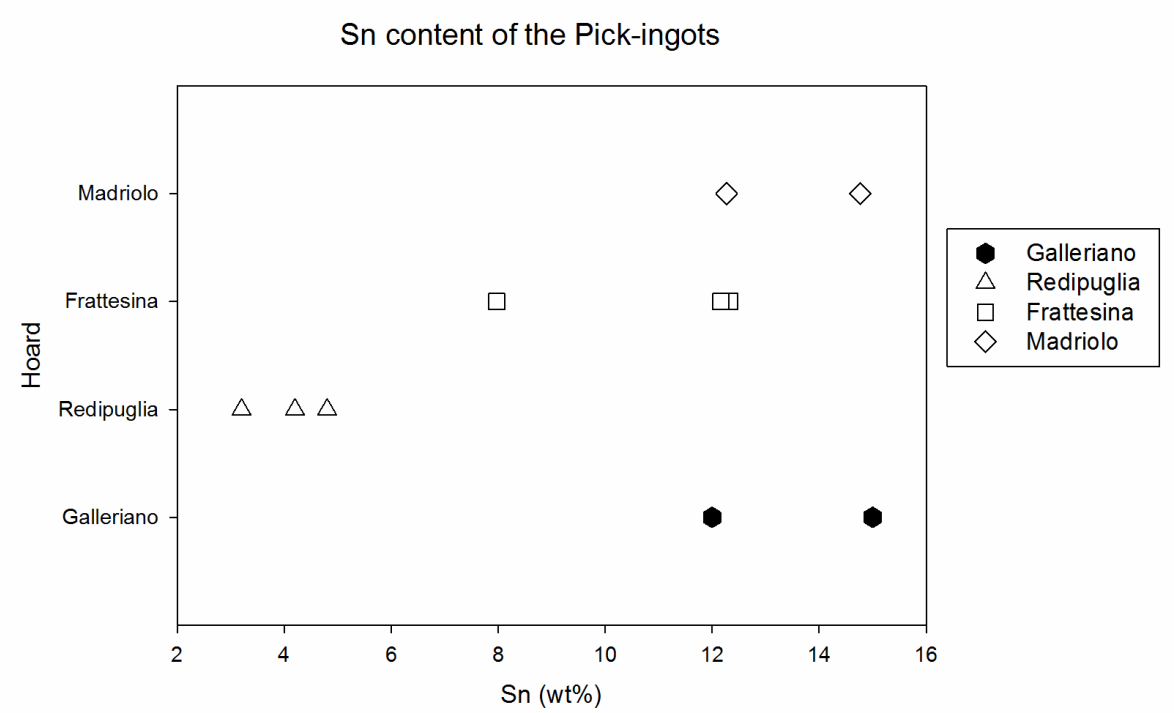

Fig. 5.8 – Scatter plot of the Sn content of the pick-ingots discovered in the Galleriano hoards and compared to those found in Frattesina (Zaghis 2005), Madriolo (Pigorini 1895) and Redipuglia (Borgna 1992). The samples from Galleriano are remarked in black.

5.1.5 Concluding remarks

The results of this investigation on different typology of ingots show that the composition of copper alloys in LBA hoards depended on the technological knowledge of ancient smiths as well as upon the various sources of raw material. It is very interesting to note that, in the ancient hoards of Cervignano and Muscoli (RBA/FBA), the chemical composition of ingots is quite homogeneous and almost exclusively characterized by the exploitation of chalcopyrite deposits. On the other side, during the passage through the FBA2, the hoards are more heterogeneous, and various type of copper coexisted, including fahlore with or without nickel *in primis*. Furthermore, according to the availability of raw materials, the fahlore composition of the ingots from Castions di Strada (*i.e*. with or without Ni) leads to suppose that the smiths carefully selected the alloy and processed it consciously of their technological properties. Contrariwise, different considerations must be made for Porpetto, whose composition is similar to the FBA Slovenian cast ingot and

can be associated to the smelting of complex ores containing not only tetrahedrite, but also rich in Co and Ni. All these sample, both Friulian and Slovenian, can be classified as *spiess*, apparently linked to the trade sphere of the Carpathian Basin. This aspect is also supported by the pick-ingots analysis, indicating that the bronze pick-ingots of Galleriano seem to be connected to a trade with Frattesina or to the employment of similar raw metal for their production, whereas those discovered in Porpetto show a particular composition that, up to now, was only attested in the Slovenian region (Fig. 5.9). It really looks that Friuli was the overlap of two independent West- and East-oriented metal circles.

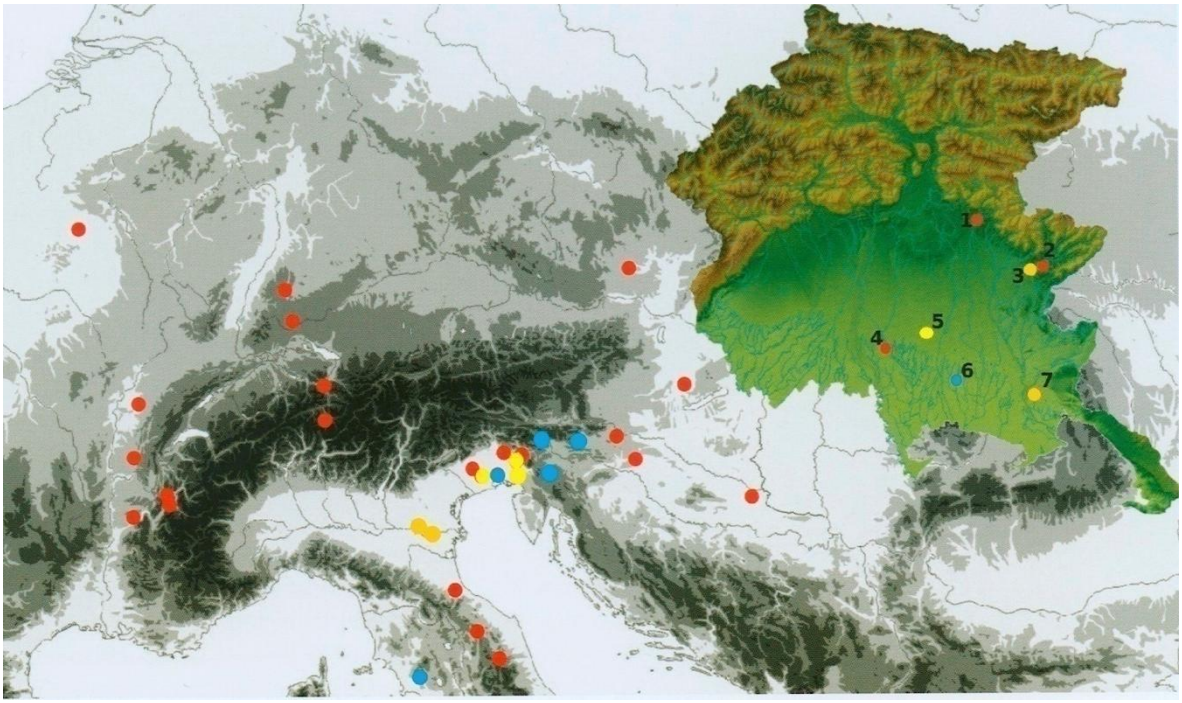

Fig. 5.9 – Distribution of the pick-ingots in Europe and in the Northern-Central Italy in the end of the II millennium B.C. (after Simeoni and Corazza 2011). In the picture, the deposits in which pick ingots had been found are numbered: 1. Nimis; 2. Purgessimo (Cividale); 3. Rividischia (Codroipo); 5. Galleriano (Lestizza); 6. Porpetto; 7. Redipuglia. The colours are indicative of the composition: yellow=Bronze; Blue=Fahlerz metal; red=unknown composition. The references of the analyses are reported in Fig. 5.7.

5.2 Weapons and tools

On the basis of the chemical analyses, it is possible to note that all but one artefacts (Por6-Pal) are bronzes characterized by a tin content in the range 4.7–14.3%. Furthermore, two groups exhibiting different trace patterns are recognized: the most populated shows As and Ni as principal impurities (0.8% and 0.4%, respectively, see the red circle in Fig.5.10), whereas the second, composed by the three objects from Porpetto, exhibits few level of Sn together with a pronounced fahlerz composition (see the blue

circle in Fig. 5.10). In this latter group, the total absence of tin in the Porpetto socketed-shovel (Por6-Pal) is counterbalanced by the large amount of fahlerz elements (>20%).

On the other hand, for the first group, it should be suggested a deliberate alloying, possibly for different purposes, *i.e.* for different type of weapons. In fact, variable amounts of tin are noticed in axes, whereas swords show a more defined alloying range (10–13%). However, further considerations about a conscious choice in the different Sn amount for the tools- and weapons-making, as noted by Trampuž-Orel et al. (1991), are not allowed, since only three socketed-shovels are take into account and their function, at the moment, is not certainly attributable (see Section 5.2.2 in this Chapter).

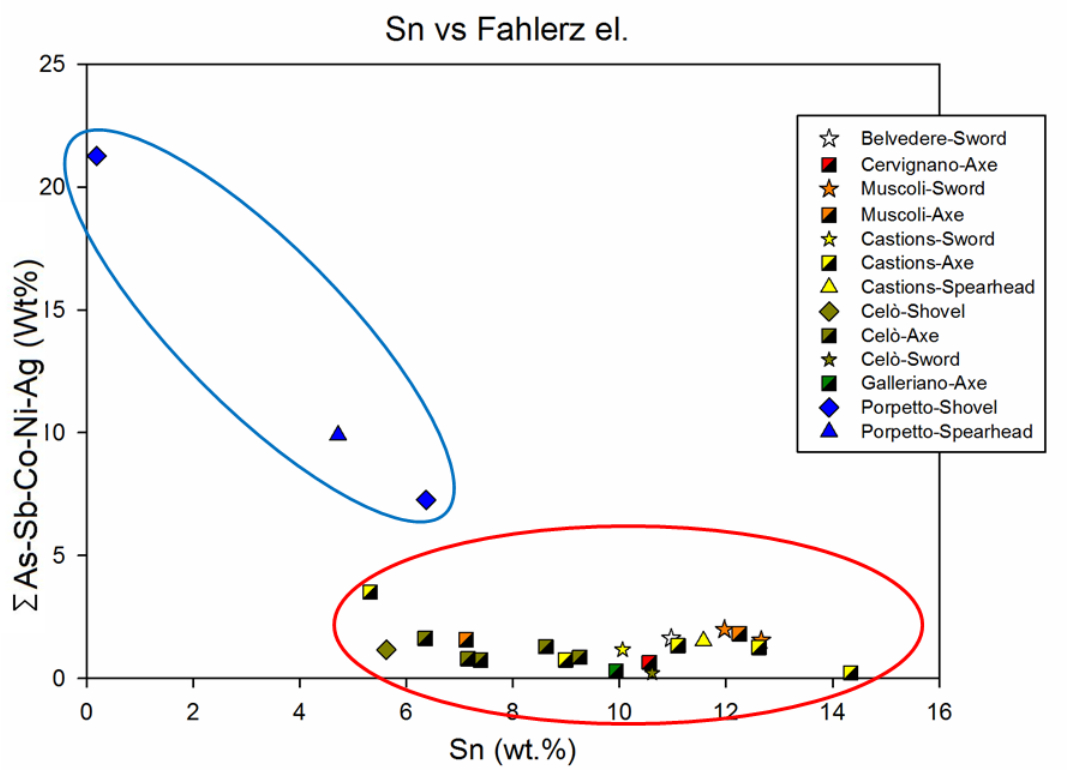

Fig. 5.10– Scatter plot of the overall mean content of the fahlerz-suite against the amount of Sn (SEM- EDS, bulk analyses) of the weapons and tools belonging to the Friulian hoards.

By comparing the chemical composition of ingots and objects using PCA, the situation is even more defined. In Fig. 5.11, the plot shows that the three objects characterized by a fahlerz composition – two socketed-shovels and one spearhead (see the arrows in the plot) – fit rather well with the chemical pattern described for the Porpetto ingots, whereas the other “pure bronze” objects coincide with the ingots compositional field indicating the employment of chalcopyrite as extractive charge.

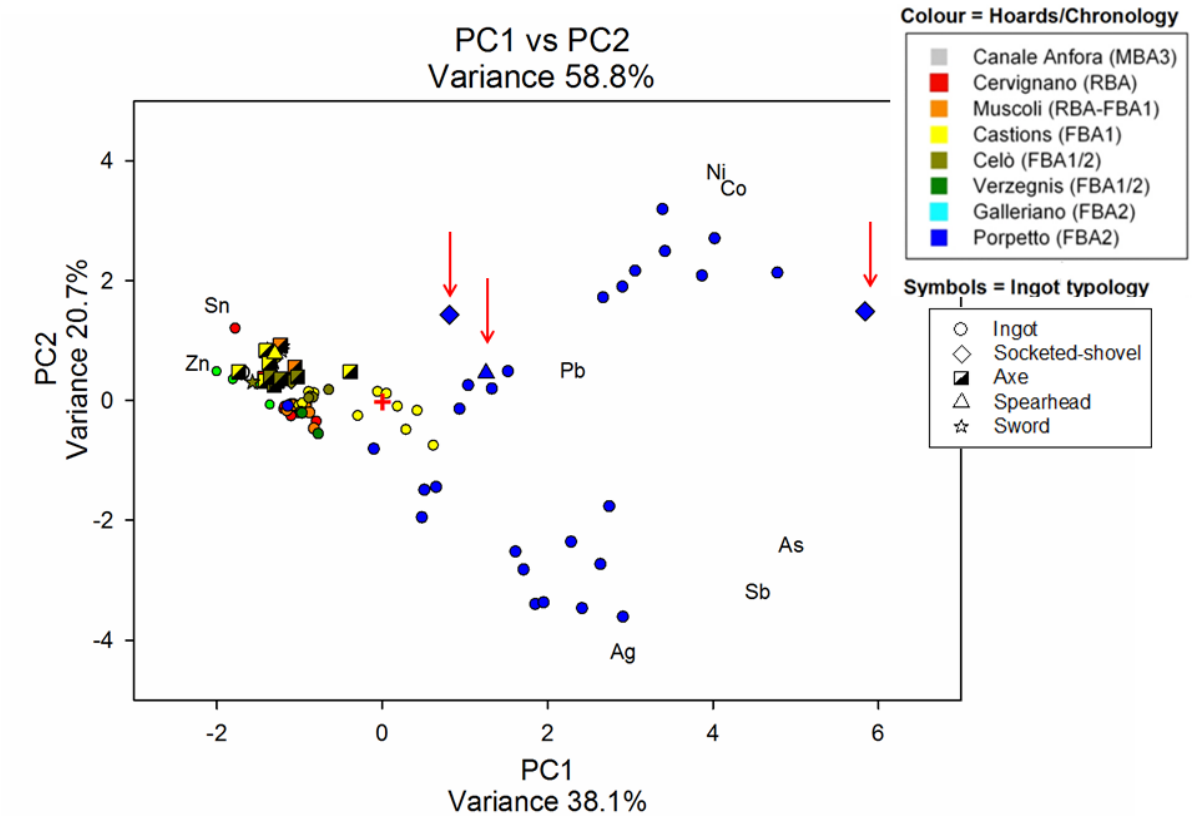

Fig. 5.11 – PCA loading and scores plot of the ingots and the objects analysed in this study (PC1 vs PC2). The position of the objects from Porpetto is remarked by the red arrows. The first two principal components (PC1 and PC2) carry the 58.8% of the total information.

5.2.1 Axes, swords and spearheads

The chemical analyses on these objects reveal the employment of a quite pure bronze alloy, characterized by As and Ni as major impurities. In Fig. 5.12, for the large part of the samples, a strong correlation between these elements is evident. Contrariwise, four axes from Celò are farther away from this trend, showing higher amounts of As in the α-phase rather than Ni; even two axes from Castions di Strada are also located in this field (see the red circle in Fig. 5.12). However, this "clustering" could not be a coincidence, since these same axes exhibit lower percentages of tin than the other samples (see Fig. 5.13). Therefore, the idea that nickel is linked in some way to the alloying step is becoming more strong, although it is not possible to further argue on this question.

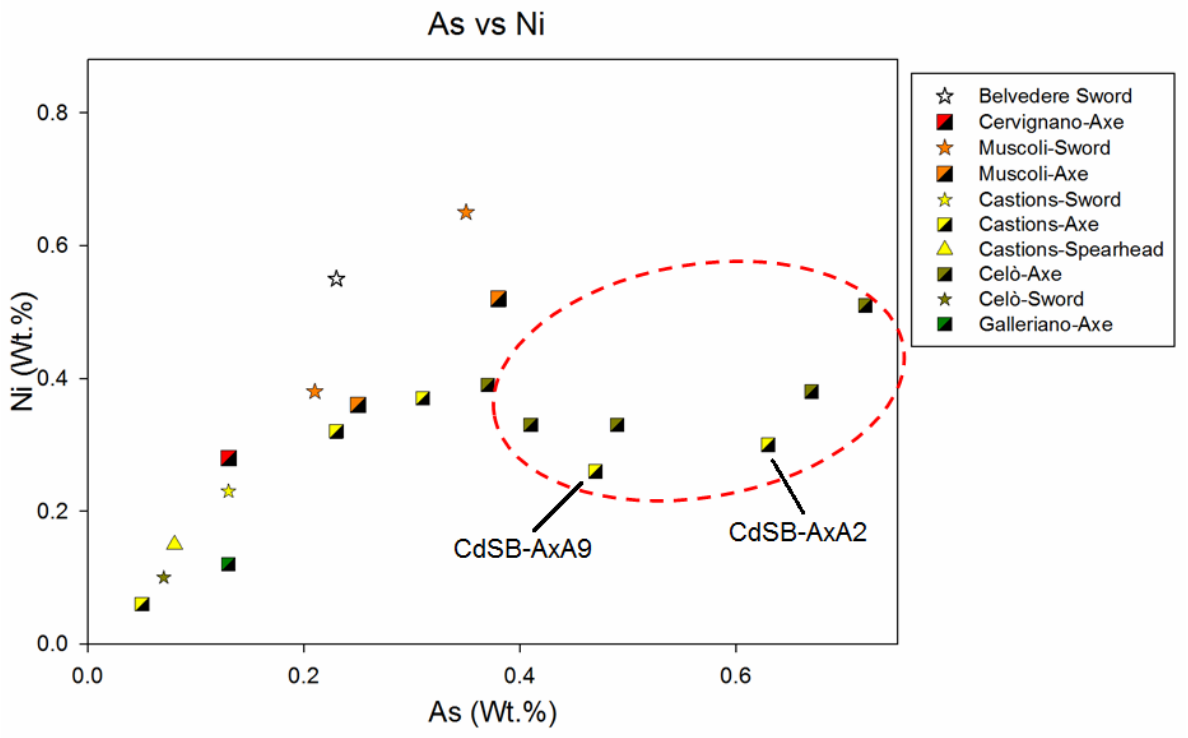

Fig. 5.12 – Scatter plot of the As and Ni values in the weapons (wt%). In the dashed-circle, the samples from Celò and Castions di Strada are characterized for the higher amount of As in the matrix.

In the Bronze Age, the presence of traces of Ni, sometimes associated to small amount of As, is very common in a number of European objects, but little can be said about the distribution of As-Ni in the metal (Liversage 1994). In fact, it is yet unknown if such elements were present in the extractive charge – and where the dominant metal was mined – or if there was a conscious mixing for technological reasons, as the addition of Ni in order to retain the As (as discussed in Chapter 4). However, the quantities of such elements are so low that this hypothesis seems to be excluded.

In the axes, the chemical analyses reveal that there are not noticeable differences in the Sn content depending on their typology, and winged- and socketed-axes show almost the same Sn variability (in the range 5.3–14.3% and 6.3–12.2%, respectively); therefore, they can be regarded as a single class. The data obtained from the examined axes can be compared with other archaeometric studies found in literature, concerning both the Slovenian area and the Veneto region (specifically Verona province); such comparison must be considered as fundamental, since the geographical position of Friuli leads it to be a connection region between East and West. The discussion involves axes typologies dated from MBA III and FBA in order to achieve a wider statistical representation, without deeply considering the distinguishing typological features pertaining to each item. Hence, by comparing the Sn content of the Friulian axes with that of Veneto (Pernicka and

Salzani, 2011) and Slovenian ones (Trampuž-Orel 1996), it is certain that the Sn percentage is averagely higher in Friulian weapons (~9%), even if two axes from Castions di Strada and one from Muscoli exhibit significant Sn concentrations peaks that raise the average. In fact, observing in detail the diagram (Fig. 5.13) and excluding such samples, two axes from Castions di Strada (CdSB-AxA2 and CdSB-AxA9) and those from Celò show a consistent tendency toward lower Sn amounts (~7.7%) that may be connected with the previously discussed lack of tin in that area. However, in any case, such alloys cannot be considered a bad metallurgical choice; rather, it seems that the smiths were aware that these amounts of tin are a good compromise in order to balance toughness and to obtain sharp cutting edges. In addition, owing to the variability of tin in the Castions di Strada hoard, it could be plausible that this deposit had represented a point of accumulation of different commercial circles, possibly characterised by a different know-how or by a different availability of tin. Nevertheless, these are just assumptions that could be solved by the lead isotope analyses, but there would be no opportunity to go further in this hypothesis in the case that the copper was exploited from the same deposits or if the bronze was subject to recycling.

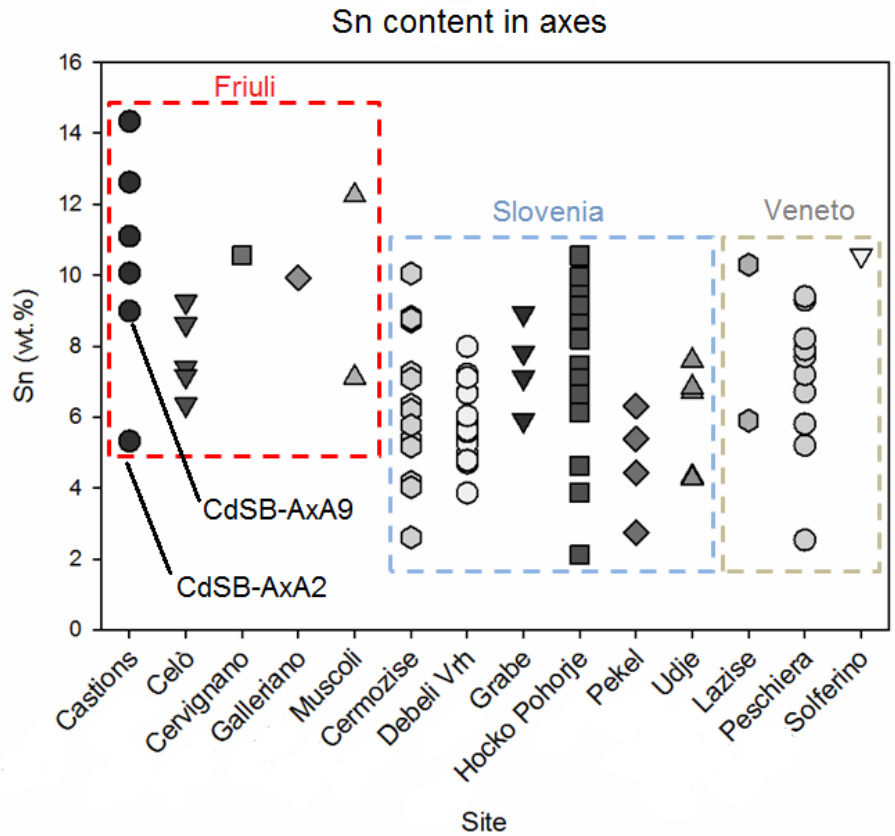

Fig. 5.13 – Tin content of the axes belonging to the Friulian hoards compared to those found in Slovenia (Trampuž-Orel 1996) and in the Veneto regions (Pernicka and Salzani 2011).

Concerning the swords, the observed tin range is more confined (10–12%), since the alloy had to be ductile during the weapon-making, resistant to breaking under the strokes of hammer, and it must also retain a sharp edge during the combat. Moreover, the metallographic observations confirm that only the outer parts of the blades were finished by hammering, in order to obtain cutting edges. In swords, the manufacturing process commonly involved a heating treatment performed to recover ductility through recrystallization, and a subsequent hammering in order to confer the desired bronze mechanical properties. All these features are in completely accordance with the metallographic studies carried out on swords from Olmo di Nogara (Verona province, Italy) in which the blades show signs of hammering and annealing cycles and a final cold-working, in order to improve the hardening of the alloy (Angelini 2005). In this regards, all the analysed swords have adequate properties for practical use proving that these swords could be not only used for ceremonial rituals or as *status*-display, but also as weapon in battle.

A more detailed discussion of the investigated Friulian swords can be performed by plotting Sn- against Ni-content (Fig. 5.14) and by considering the chemical analyses carried out by Bunnefeld and Schwenzer (2011) on German swords, Angelini (2005 and in press) on Olmo di Nogara swords, Trampuž-Orel (1996) on Slovenian weapons and (Pernicka and Salzani, 2011) on Garda Lake. Focusing the attention on the average tin content, the Friulian swords are generally in agreement with the MBA swords from Olmo di Nogara (Angelini in press), showing a higher tin content not frequently detected in the Italian metallurgical production (Garagnani *et al.* 1997). Moreover, the Friulian swords overlap with only a part of the swords from Low Saxony dated to MBA and LBA, owing to the wide range attested for the German weapons (5.5–16.8%, Bunnefeld and Schwenzer 2011). Conversely, the Slovenian swords (Trampuž-Orel 1996) and those discovered in the Verona province (Pernicka and Salzani 2011) basically exhibit a lower tin content that does not put them in relation with the Friulian swords. On the other hand, the main difference lies in the amount Ni recorded in the alloys investigated in the present work. In fact, their significant Ni contents place the Friulian weapons in the upper part of the diagram (Fig. 5.14), without no other comparison; only some Saxon swords exhibit values of Ni greater than 0.8-1.0%, but these percentages are too low for suggesting a connection. Only the Celò sword, possessing very low traces of Ni, shows a complete overlapping with some German swords and a partial contact with some others from Olmo di Nogara.

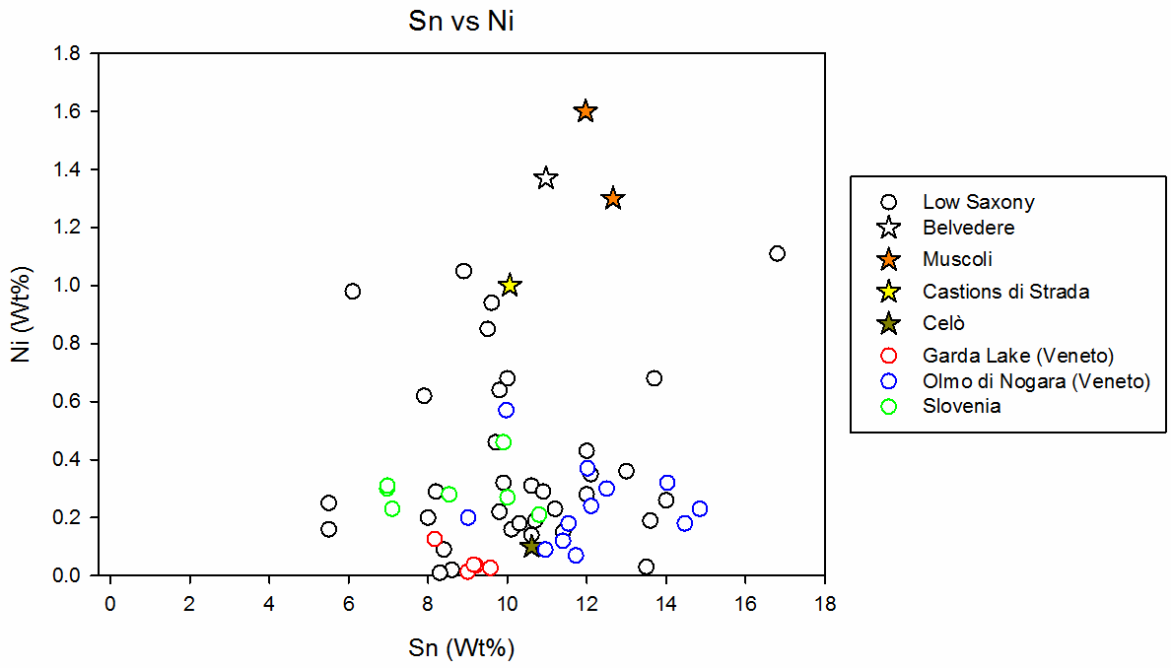

Fig. 5.14 – Tin distribution against the Ni content in the swords discovered in Friuli, Germany (Bunnefeld and Schwenzer 2011), Slovenia (Trampuž-Orel 1996) and Veneto region (Angelini in press; Pernicka and Salzani 2011).

In addition, it should be reported that a large archaeometric study has been conducted by Jung et al. (2011) on objects and weapons from Northern Italy (Veneto and Lombardy), covering an overall time span from MBA III to FBA 2; unfortunately, the results of the analyses are only plotted in logarithmic scale and any comparison would be extremely approximate. It is only possible to rely on the notes of the authors, which refer to a concentration of Ni that is less pronounced in the Northern artefacts if compared to the South ones and, although the "Ni issue" is for this work an interesting topic, it is not possible to go further.

Regarding the spearheads, the considerations are restricted on the basis of two samples, whose composition is very different. In fact, the Castions di Strada sample is a bronze characterized by high Sn content (11.6%) and low amount of Ni (1.4%), whereas the one from Porpetto shows a low Sn content (4.7%) and the typical fahlerz impurity pattern. The Castions spearhead underwent a hammering followed by a heat treatment, since it displays an annealed structure characterized by polygonal equiaxed grains and annealing twins (see Chapter 4). Conversely, the dendritic structure observed in the Porpetto spearhead allow for its definition as a cast object; in fact, knowing the quality of alloy employed, other operations such as the hammering would not have been possible since the metal was too brittle.

Nevertheless, considering only two samples, a comparison with literature data cannot be statistically significant. However, it is possible to affirm that the composition of the spearhead from Castions di Strada can be associated to that of two similar findings found in the Verona region, more precisely in Cisano and Bor di Pacengo, and dated to the RBA and to the MBA (Salzani and Pernicka 2011), although in this latter samples the bronze is characterized by a lower tin content (10.9% and 8.1%). Moreover, even the Slovenian spearheads analysed by Trampuž-Orel (1996) are bronzes showing Sn in the range 8–9%. Conversely, no comparisons are available for the Porpetto spearhead.

5.2.2 Socketed-shovels

The study of these materials and their specific archaeological issues are the subject of many publications from the 70s to today; in this work, only a brief overview in relation to the archaeometric studies is given. For further information about this matter, please refer to the most recent publications and literature cited, in particular Santi and Leonardi (2007) and Bellintani and Stefan (2008).

The three analysed shovels are considered as belonging to two different chronological phases. The sample discovered in Celò is associated to the *Fondo Paviani*-type socketed-shovel, characterized by tight shoulders and elongated blade (Borgna 2007), whereas a sure attribution is more complicate for the two Porpetto samples, since they are severely damaged. However, according to Bellintani and Stefan (2008), the sample Por9-Pal, could be referable to the *tra Manciano e Semprugnano*-type, owing to the shoulders slope. For what concerns the chronology, *Fondo Paviani*-type shovels are dated to FBA1 by Bellintani and Stefan (2008) although, as reported in Angelini (2009), the dating of the *Fondo Paviani*-type was attributed to the Recent-Final Bronze Age (Fasani and Salzani 1975), and most recently to the late XIII – early XII century B.C. (RBA 2) by Santi and Leonardi (2007); on the other side, the *tra Manciano e Semprugnano*-type are interpreted as successive and dated to the FBA2 (Bellintani and Stefan 2008).

From a chemical point of view, the composition denotes pronounced differences. The Celò sample is a bronze socketed-shovel alloyed with 5.7% Sn, whereas both the samples from Porpetto exhibit a complex impurity pattern suggesting the employment of a fahlerz-type metal. In particular, Por6-Pal is characterized by high contents of As (10.5%), Sb (6.8%), Ni (3.4%), traces of Co (0.6%) and the strong addition of Pb (23%). The other, Por9-Pal, shows the presence of 6.2% of Sn and lower percentages of the fahlerz-suite elements, without the addition of Pb.

To date, a few analyses are available for socketed-shovels only and the comparison with published data is very limited, since qualitative analyses have been generally performed on the fragmented socketed-shovels from the *tra Manciano e Semprugnano* hoard (Casagrande *et al*. 1993; Pellegrini 1995; Antonacci 1992), confirming that they are made of bronze with traces of Ni. Moreover, the metallographic observations deriving from this work reveal an as-cast structure. Fortunately, several chemical analyses have been performed on socketed-shovels by Dr. Federico Zaghis (2005) and Dr. Ivana Angelini (2009) in relation to their Ph.D. theses, not yet published. By comparing the compositions (Fig. 5.15), it is possible to note that in Frattesina (Zaghis 2005) the majority of the samples are alloyed with a Sn content ranging between 8–12%, but in one sample certain amounts of As, Ni and Sb have been also detected. On the other hand, the samples from Gazzo Veronese, Fondo Paviani and Sabbionara Veronella (Angelini 2009) are made of copper alloyed with a lower amount of tin (5.9–10.7%), and no other impurity has been detected. In this scenario, although partial, the socketed-shovel from Celò fits very well with the most ancient samples belonging to the same typology (Fondo Paviani and Sabbionara Veronella). Conversely, Por9-Pal is located in a borderline region characterized by the coexistence of low amount of Sn and impurities, but still in accordance with the composition of some Frattesina shovels, whereas Por6-Pal is distinguished and no similarities with other samples have been found so far.

At the moment, for both the typologies, it is quite difficult to evaluate if the manufacturing process has been suitable for use, since only few comparisons are available. However, the analysis of the blades belonging to the more ancient typology has testified a scarce ore inexistent actual employment of the Italian socketed-shovels (Santi and Leonardi 2007), while in Hungary samples, the entire blade is worn (Jankovits 1999; Santi and Leonardi 2007; Bellintani and Stefan 2008) and it has been suggested their use in relation to the metalworking process (Jankovits 1999). For the second type of socketed-shovels dated to a later period of the FBA, the assumptions are different: possible chisel; generic cutting tool, hoe for the ground, unidentified tools connected to the metalworking or ingot (see Bellintani and Stefan 2008 and literature there reported).The only certainty about this question is that the alloy of the two samples from Porpetto was not suitable to support a hammering process, not even weak.

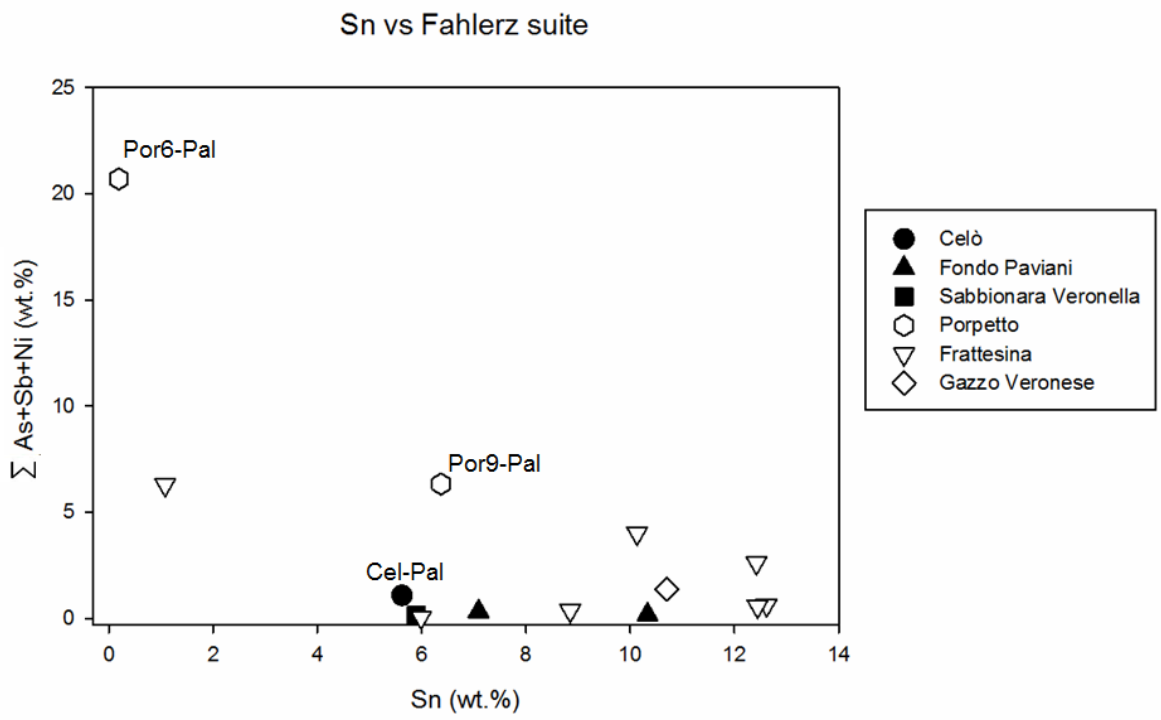

Fig. 5.15 – Scatter plot of the overall content of As, Sb and Ni against the amount of Sn (wt%) in the socketed-shovels found in Celò and Porpetto, in Frattesina (Zaghis 2005), in Gazzo Veronese, Sabbionara Veronella and Fondo Paviani (Angelini 2009). The black symbols identify the more ancient shovels, whereas the white remarks the second type of shovels dated to a later period.

From these results, at least three conclusionscan be deduced. Firstly, as in more ancient periods, although a mix of bronzes obtained from chalcopyrite cannot be excluded in advance, bronze and copper seem not to be mixed through recycling steps, and, despite the shovel has been created by casting alone, the alloy was found to bealmost well refined. Secondly, in later periods, if the smiths did not have enough tin for bronze production, they may have deliberately alloyed part of the copper with other elements such as Ni, Sb and As or, more simply, the raw material could come from other sources characterized by ores with high levels of As, Sb, Ni and Co. However, even in this case the "ghost-idea" of the recycling of copper that may have brought with it the characteristic elements of fahlerz is still valid. Finally, the Porpetto socketed shovels can be defined as a compositional *uniquum*, since it could be interpreted as witness of the circulation of this particular model even in a different composition respect to the bronze one attested for the other samples and here discussed.

5.2.3 Concluding remarks

The chemical analyses and the metallographic observations carried out on the objects suggest an organization of production in which alloying and the other stages of production take place under a strict control. Copper alloys with a larger amount of tin result in a hard bronze suitable for striking weapons, such as swords and axes. This bronze sustains whetting, although the high amounts of tin hamper high degree of mechanical working (Scott 2012). This technical/economical approach was hypothesized by Trampuž-Orel *et al*. (1991), and theoretically linked with products of the Carpathian craft circles, due to typological similarities; this connection has been also confirmed later by Liversage (1994).

In objects, the tin content decreases in some axes of the Castions di Strada and Celò hoards, and in the Porpetto samples, in which Sn is almost completely replaced by other alloying elements (As, Sb, Ni and Co). This could be related to the incipient technology change in the use of raw materials noticed by Trampuž-Orel et al. (1999) during the transition to the 1st millenniumin the Slovenian area. Further, the addition of Pb as a cheap alloying element, apparently observed in the Slovenian area, is not evident in the Friuli objects. Moreover, the coexistence of weapons (axes and spearhead) with a high Sn content, which have not found a comparison in Italy, Slovenia and Europe, and axes with significantly lower levels of tin, allow for the interpretation of the Castions di Strada hoard as a hub of different commercial networks, possibly characterised by a different know-how or a different availability of tin.

Finally, an overview of the composition of Italian, German and Slovenian swords shows that the alloy employed in Friuli exhibits a tin content very similar to those exceptionally recorded in the Olmo di Nogara swords (Angelini in press), but the trace element pattern are inconsistent, since all but one swords possess noticeable amounts of Ni, without any possibility to compare it to other items.

Provenance

In the archaeological research, the use of isotopic analysis is aimed to date the prehistoric artefacts, allowing to trace them back to their ore source. The lead isotopic tracing has originally been developed in the Physical and Earth Science fields for the study of rocks and minerals, but it can equally well be used for the analysis of silver, lead and copper-based materials found in archaeological contexts. Indeed, even if elemental concentrations change considerably during the smelting and the refining steps, the lead isotopic composition is not essentially affected by fractionation during these metallurgical processes. Therefore, all the components of the smelting *chaîne opératoire* (*i.e.* ores, slags and metals produced from a given ore deposit) will have the same, unchanged, lead isotope fingerprint (Gale and Stos-Gale 1982; Gale *et al.* 1999; Cui and Wu 2011). However, in order to have a comprehensive metallurgical fingerprint, it is necessary to couple this method with minor and trace elements analysis.

The availability of published lead isotope data on ore deposits and metal objects, mainly deriving from the systematic analysis started in the 70s (Stos-Gale and Gale 2009), ensures that such analyses are a key tool for the provenance studies of archaeological metal findings. With respect to the Bronze Age period, different research groups have published data on ores deposits, artefact and slags from the Mediterranean and Alpine areas. For provenance studies, the most valuable data are the archaeometallurgical surveys on ancient mining and metallurgy, many of them reported in the work of Ling *et al.* (2014) and the related references. Concerning the comparison and the identification of the ore sources exploited in the Bronze Age, it is necessary to have three kinds of information: the geochemical characterization of the ore deposit, the lead isotope analysis of the ore samples and the indication of the period of exploitation. Not every copper and lead deposit in Europe has been fully characterized in this way, although there is a reasonable amount of published data for the major copper-producing areas.

On the basis of these remarks, the employment of the Alpine Archaeocopper Project (AAcP) database has allowed for the comparison of the Friulian objects with the deposits of the Central-Eastern Southalpine area located in Trentino and Veneto regions, as studied by Nimis *et al.* (2012). The measured Alpine data have been simplified by Artioli *et*

al. (2014) into two major fields: (1) the pre-Variscan stratiform deposits (called "Valsugana VMS[11]" in the diagrams), whose most notable mining areas are those located along the Valsugana tectonic line (Calceranica, Vetriolo, Valle Imperina); and (2) the deposits related to post-Variscan volcanism in the Southalpine region (called "Southalpine AATV[12]" in the diagrams), which include a number of mining areas in the Trentino and Alto Adige regions (*e.g.* Pfundererberg, Val dei Mocheni). Although this is a schematic projection, these fields can be efficiently used as a start-point for the interpretation of the Alpine ore provenance. This schematized view, of course, does not give justice to the complex Alpine geology, whose details are to be found in the original papers (Artioli *et al.* 2009, Nimis *et al*. 2012). In addition, a further contribution in improving the Alpine picture is given by the lead isotopes analysis on slags found in Luserna, Transacqua and Segonzano from Late Bronze Age smelting sites (Addis 2013).

For the purposes of the research, a number of 42 ingots were analyzed by means of MC-ICP-MS, as well as twelve axes, five swords, three socketed-shovels and two spearheads. The lead isotope analyses performed on these samples are listed in the Appendix 3. The isotopic ratios of the artefacts are presented in $^{206}Pb/^{204}Pb$ vs $^{207}Pb/^{204}Pb$ and $^{206}Pb/^{204}Pb$ vs $^{208}Pb/^{204}Pb$ diagrams, since these ratios carry a more direct relationship to the geological and geochemical significance of the deposit, *i.e.* age isochrones and parent reservoir (Faure and Mensing 2005), and because they allow for a better discrimination between the deposits (Nimis *et al*. 2010; Baron *et al.* 2013).

As seen up to here, the provenance question often requires the comparison of data for a large numbers of ores, slags and artifacts, and a preliminary screening is needed in order to identify uncertain cases that could then subjected to more detailed graphical scrutiny, using point-by-point comparisons (Stos-Gale and Gale 2009). Thus, according to Baxter (2003), this initial screening was performed by calculating the Euclidean distance in three-dimensional space between the lead isotope data for the investigated artefact and the entire isotopic database for copper ores samples; for each sample, the top ten results are reported in Appendix 4. Subsequently, a second stage for data interpretation must include the comparison on two bi-dimensional plots of lead isotope ratios, in order to assess the pattern of distribution of all data point for each deposit field. Finally, the geochemistry and the exploitation history of those deposits identified as the possible ore sources have to be evaluated.

In the present chapter, the data are firstly presented according to the chronological division suggested by the hoards, focusing the attention on the ingots. As mentioned in

[11] The acronym VMS stands for Volcanogenic Massive Sulphide ore deposits.
[12] The acronym AATV stands for Alto Adige-Trentino-Veneto regions.

the previous chapters, these artefacts to the metallurgical category of the semi-products, strictly connected to the ores from which they have been smelted; thus, since the danger of an uncontrolled recycling process is limited, their analysis allows for relevant results, useful for the provenance question. However, except for the pick-ingots connected to the FBA2 production, it is not possible to date the shapes of the other ingots; in fact, their chronological range primarily depends on the dating attributed to the hoards by archaeologists. In a complementary manner, the weapons and tools contained in each hoard are more surely dated and their typology allows for a comparison with similar specimens. For this reason, the second step of the discussion foresees the analyses of objects, divided for typology and for period of circulation. Moreover, in the objects discussion, two key points should be kept in mind. On one side, as stated by Gale and Stos-Gale (1982), the addition of tin for the creation of bronze alloys does not involve the change of the Pb isotope signals, since Sn derives from cassiterite[13] SnO_2 and it is not associated to Pb. On the other hand, it is important to be conscious that, in general, one should not to rule out categorically the risk of recycling, even if the possibility that it could occur it is mitigated by the fact that for weapons creation the alloy proportions had to be closely controlled, especially for the swords. Therefore, the provenance discussion is based on the combination of the results of ingots and objects, and acquires strength by the consideration of chronological, geographical and typological aspects.

The artefacts analyzed in the present work belong to hoards and deposits sited in the North-East of Italy, specifically in Friuli Venezia Giulia (see Fig.2.1 in Chapter 2, for the specific hoard locations). Thus, in order to facilitate the comprehension of the discussion reported in the present chapter, the geographic displacement of the mining districts mentioned in the text are reported in Fig. 6.1, which underline the extent of the possible interactions between Friuli and the surrounding regions.

In all the diagrams presented in the following sections, unless otherwise specified by defined terms in the legend (*i.e.* ingot, axe, sword,..), the data refers to the ore deposits of the indicated geographical region, and in Tab. 6.1 the relative bibliography is reported. Moreover, in order to simplify the exposition, the references are not specified in each caption, and the reader is refered to the table.

[13] Cassiterite deposits in Precambrian rocks are chiefly in granite pegmatite and do not contain lead. Cassiterite deposits in rocks younger than Cambrian age display a wider range of genetic association, but of the five classes of deposits noted by Rapp (1978) only the subvolcanic and the pneumotolytic-hydrotermal deposits rarely contain small amount of Pb.

Tab. 6.1. References of the Lead isotope data of the ores deposits, sub-divided by country, that are directly involved in the comparison with the Friulan ingots and objects.

Country	Region/Area	References
Switzerland	Alps	Cattin *et al*. 2011, Guenette Beck *et al.* 2009
Austria	Schwaz, Brixlegg, Innsbruck, Styria, Carinthia, Eastern Taueren window	Höppner *et al.* 2005, Horner *et al.* 1997, Koppel *et al.* 1983, Schroll *et al.* 2006
Germany Rep. Czech	Erzerbirge Bohemia Slovakia	Niederschlag *et al.* 2003
Italy	North and Alps	Artioli *et al.* 2008, Artioli *et al.* 2009, Nimis *et al.* 2012, Curti 1997, Pettke *et al.* 1996, Brigo L. and Colbertaldo D. 1972, and AAcP unpublished data.
Italy	Tuscany	Stos-Gale *et al.* 1995, Lattanzi *et al.* 1992, Dayton *et al.* 1986
Serbia Bulgaria Romania	Balkans	Pernicka *et al.* 1993, Stos-Gale *et al.* 1998, Amov 1999, Amov *et al.* 1993, Gale *et al.* 2000, Pernicka *et al.* 1997.

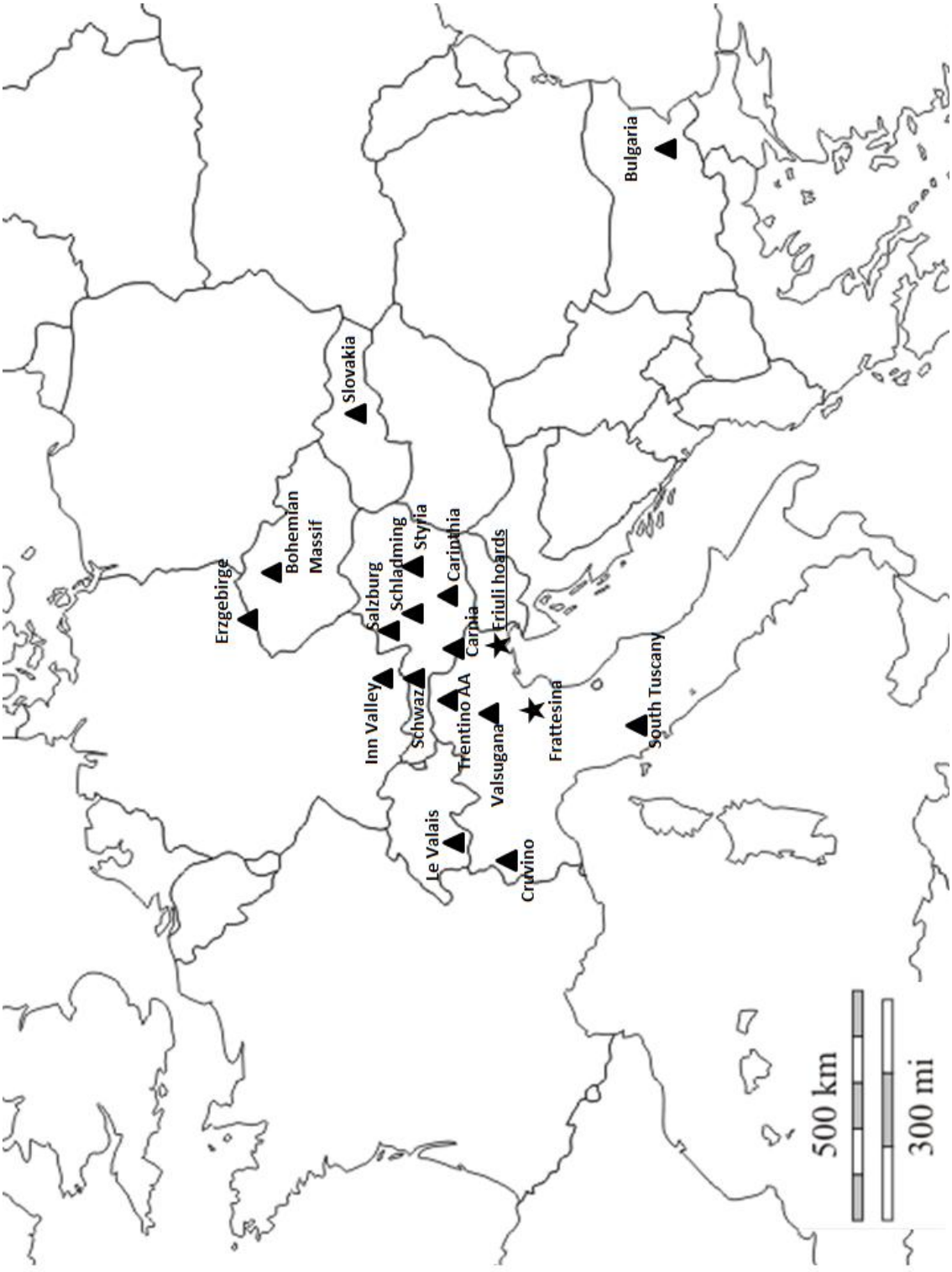

Fig. 6.1 – Map of the geographical areas involved in the provenance study; the black markers are placed in an approximate location. ▲Ore deposit area ★Archaeological site

6.1 RBA-FBA1: The Cervignano and Muscoli hoards

As suggested by the Euclidean test, the lead isotope ratios of the Cervignano and Muscoli samples are compared to those of the minerals that define the fields of the Eastern Alps (Italy and Austria), Southern Tuscany and Bulgaria (Fig. 6.2). All but one of the ingots and objects from Muscoli exhibit a lead isotope signal and a composition perfectly compatible with the Eastern Southalpine field (Veneto and Trentino-Alto-Adige), whereas three samples from Cervignano appear to cluster together (dotted circle in $^{206}Pb/^{204}Pb$ vs $^{207}Pb/^{204}Pb$ diagram), showing a less radiogenic signal that agrees rather well with pre-Variscan deposits studied by the AAcP such as Calceranica, Vetriolo and Valle Imperina. Differently, the other Cervignano ingots fall in a region between these two major fields, the Valsugana VMS and the Southalpine AATV fields, leading to two interpretations. On one side, the mismatch with a determined ore field could be associated to the existence of unexplored mines, even if this area has been extensively surveyed; thus, the partially missing signal is not the most favourable hypothesis. Else, since the linear arrangement of these samples in both the $^{206}Pb/^{204}Pb$ vs $^{208}Pb/^{204}Pb$ and $^{206}Pb/^{204}Pb$ vs $^{207}Pb/^{204}Pb$ diagrams (dotted line) perfectly overlaps with the LBA Alpine slags, a mixing of the two extractive charges either during the smelting stage or at later stage is the most plausible hypotheses (Fig. 6.2). In fact, as stated by Stos (2009), if two pieces of copper are melted together, each representing a specific ore deposit, the resulting lead isotope composition of the final metal will lie along a straight line connecting these sources, and their relative position, more close to one deposit rather than the other, is controlled by the proportions of each mixing component, their lead content and the absolute isotopic composition. Furthermore, the compositional data support these observations, since all these ingots are made of pure or almost pure copper, primarily smelted from chalcopyrite associated to sphalerite. In this regard, it is interesting to note that even the Cervignano winged-axe (Cer-Ax) lies in a doubtful position remarked by an arrow in Fig. 6.2, very close to the Muscoli weapons in the Southalpine AATV field but not perfectly overlapped to them, as can be seen in $^{206}Pb/^{204}Pb$ vs $^{207}Pb/^{204}Pb$ diagram. Certainly, Southern Alpine copper has been employed, but it is not possible to surely discern if a mixing between copper from Trentino Alto Adige-Veneto (AATV) and a small quantity of copper from Valsugana VMS has been performed, as happened for the Cervignano ingots.

The chemical analyses revealed that only one of the Cervignano ingots differs in composition (Cer-PS-64, 2% Sb), even if the isotopic signal is markedly Southalpine (Fig. 6.2); indeed, this sample can be defined as a possible mixing between chalcopyrite from Calceranica/Vetriolo, having low levels of impurity, and fahlore copper with high levels of

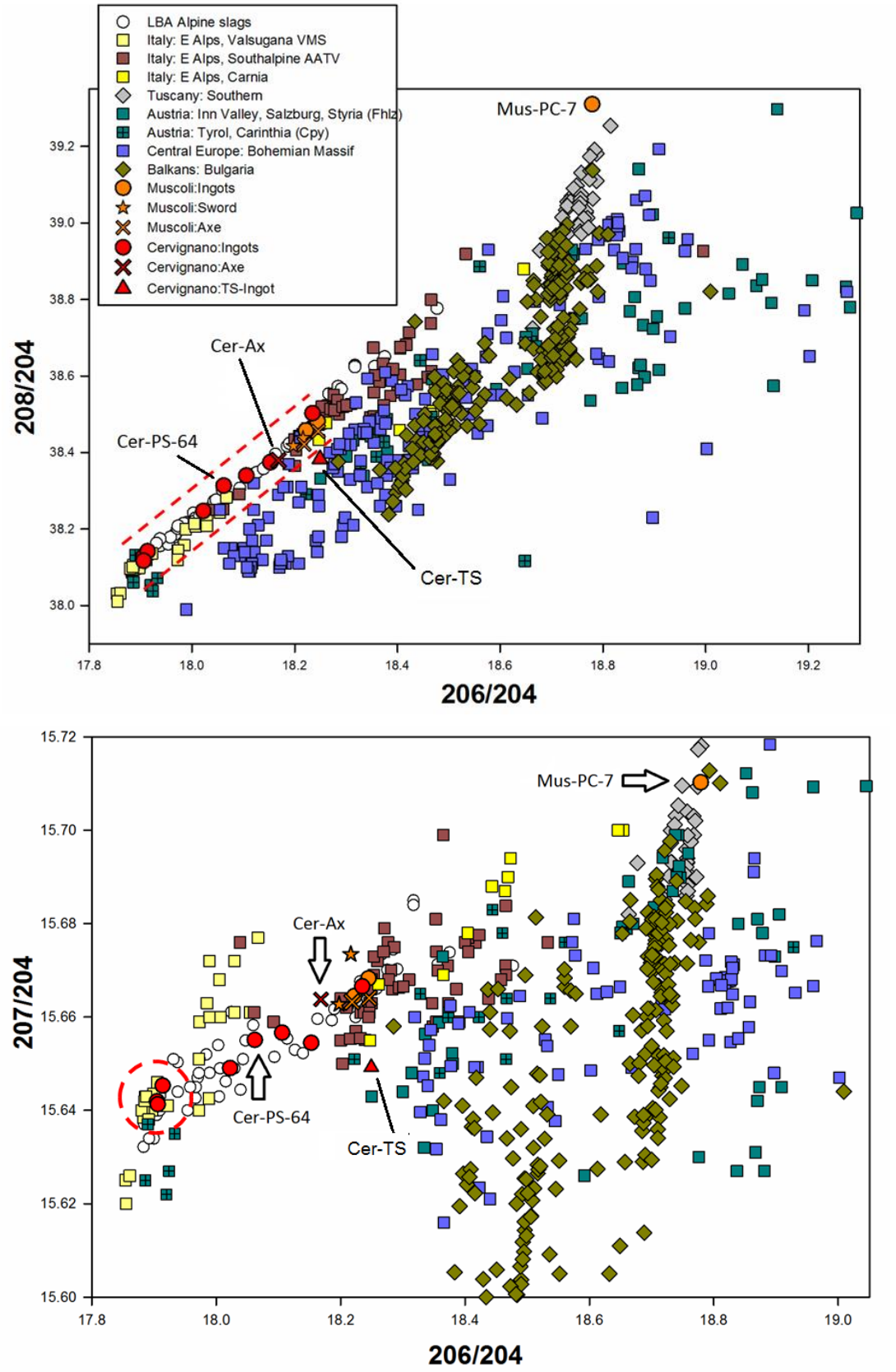

Fig. 6.2 – Lead isotope ratios diagrams of the ingots and the artefacts from the hoards of Cervignano and Muscoli compared with the possible ore-sources. The analytical uncertainty is equivalent or smaller than the size of the symbols.

Sb, such as tetrahedrite from the Carnia or from Northern Tyrol regions. From a technological point of view, the addition of As and Sb could be done intentionally, in order to improve the forgeability of the alloy, but this thesis is not supported by the presence of objects having the same composition. Moreover, one ingot from Muscoli (Mus-PC7) shows a distinct radiogenic signal (enriched in $^{208}Pb/^{204}Pb$), close to the field of Southern Tuscany deposits; however, as partially suggested by the Euclidean test (Appendix 4), in this latter case it is not possible to make an effective attribution, since the chemical pattern shows a copper having a low impurity content (only 0.2% Ni), but the idea of the use of Tuscan copper to smelt this ingot can also be a further proof of the cultural link between these two regions.

Differently, the Tongue-Shape ingot (TS) slightly falls out from the previously mentioned linear arrangement (red triangle in Fig. 6.2), showing a lower lead isotope signal both in $^{207}Pb/^{204}Pb$ and in $^{208}Pb/^{204}Pb$. In this specific case, the Euclidean test suggested different origins, and Glockner Nappe, Central Wales and Sardinia appear in the top ten. However, also taking into considerations the results obtained for the other ingots, it is not possible to exclude the Glockner Nappe area (Eastern Alps, Trentino), even if the perfect overlapping with one single deposit could distort the interpretation. In fact, observing the $^{206}Pb/^{204}Pb$ vs $^{208}Pb/^{204}Pb$ diagram (Fig. 6.2), it is not possible to exclude a metal mixing that involves copper from the main areas of the Italian Eastern Alps, from Austria and/or Central Europe. Indeed, an effective option could concern the use of copper from the Erzgebirge region, on the borders of Saxony and Czech Republic. This latter area is one of the possible tin sources of the Mediterranean world, although the actual exploitation with ancient mining technologies is still under debate (Bouzek *et al*. 1989; Niederschlag *et al.* 2003; Haustein *et al.* 2010). In this regard, further interesting considerations must be based taking into account that the TS-ingot exhibits high levels of Sn and, microstructurally, it does not appear as an ingot recycled from a “pool” of bronze scraps, but rather as a primary raw ingot (see Chapter 4). In the future, it might be fascinating to move the attention to the tin isotopes ratios for the cassiterite tracing.

Actually, there are remarkably little archaeometric studies of the provenance of tin; Rapp and colleagues (Rapp 1978; Rothe and Rapp 1995; Rapp *et al*. 1999) attempted to use trace elements to characterize deposits of cassiterite and tin metal produced from cassiterite, but no archaeological application has followed. Moreover, an initial interest in the use of tin isotopes for provenance of archaeological tin has been slowed because, even with the highest precision attainable, the observed variations in the isotopic ratios of tin metal, cassiterite ore and archaeological bronzes in these studies were barely greater than the analytical errors (Gale 1997; Begemann *et al.*, 1999; Clayton *et al.* 2002). Lately,

Haustein *et al.* (2010) were able to laid promising basis for ancient Sn provenance; in fact, their researches on a large number of ore samples have demonstrated that ores exhibited a homogeneous Sn isotope composition within the same deposit, whereas the isotopic signal deriving from different deposits outlined distinct fields. Thus, it is possible that the application of this new method of "tin isotope" might be a powerful tool with which the old question of the sources of ancient tin can be solved, giving a more precise definition of the metal trade network connecting tin mining areas and metalworking centres. This topic represents a major challenge for future archaeometallurgical researches and the TS-ingot could be a proper sample.

6.2 FBA1: The Castions di Strada hoard

As presented in Chapter 4, few ingots belonging to the Castions di Strada hoard were found to be chemically and microstructurally similar to those of Muscoli and Cervignano, while the others were characterized by a typical fahlerz-ore charge impurity pattern. Consistently, the lead isotope analysis suggests a diversification in terms of raw materials and exploited resources; indeed, Fig. 6.3 shows that six out of the seven analysed ingots fall in a region of the diagrams out from the Eastern Southern Alps field (dotted circle), suggesting a derivation from far sources. In particular, three ingots exhibiting a fahlerz composition (CdSA-P-17, CdSB-P-74 and CdSB-P-60, marked in the plot as *Fhlz ingot*) appear cluster together, whereas a fourth ingot (CdSA-PnB, another *Fhlz ingot*), is slightly shifted. All the fahlerz ingots are isotopically fully consistent with the ores from the Austrian Tyrol and, therefore, it is possible that they derive from the same ore-charge and perhaps even from the same ore source or mine. Conversely, two samples (CdSA-P-18 and CdSB-P-50 yellow circle in Fig. 6.3) are characterized by a quite pure copper with only small traces of As, Sb, Ni and Co and, therefore, it is not possible to make a certain attribution, and Bulgaria, Austria and Central Europe are the all equally probable source areas.

Finally, the last ingot (CdSB-P81), obtained by the smelting of chalcopyrite, shows a lead isotope composition that could match with both the Valsugana VMS and Carinthia (Austria) regions and, because of the quite similar lead isotope ratios of these two fields, it is impossible at the moment to clearly distinguish its provenance. On this basis, two hypotheses can be equally pointed out: it is possible that fahlerz- and chalcopyrite-ores could be mined in Austria, from Tyrol and Carinthia regions, respectively; on the other hand, it is even possible that the Valsugana has continued to be exploited in FBA1 for the

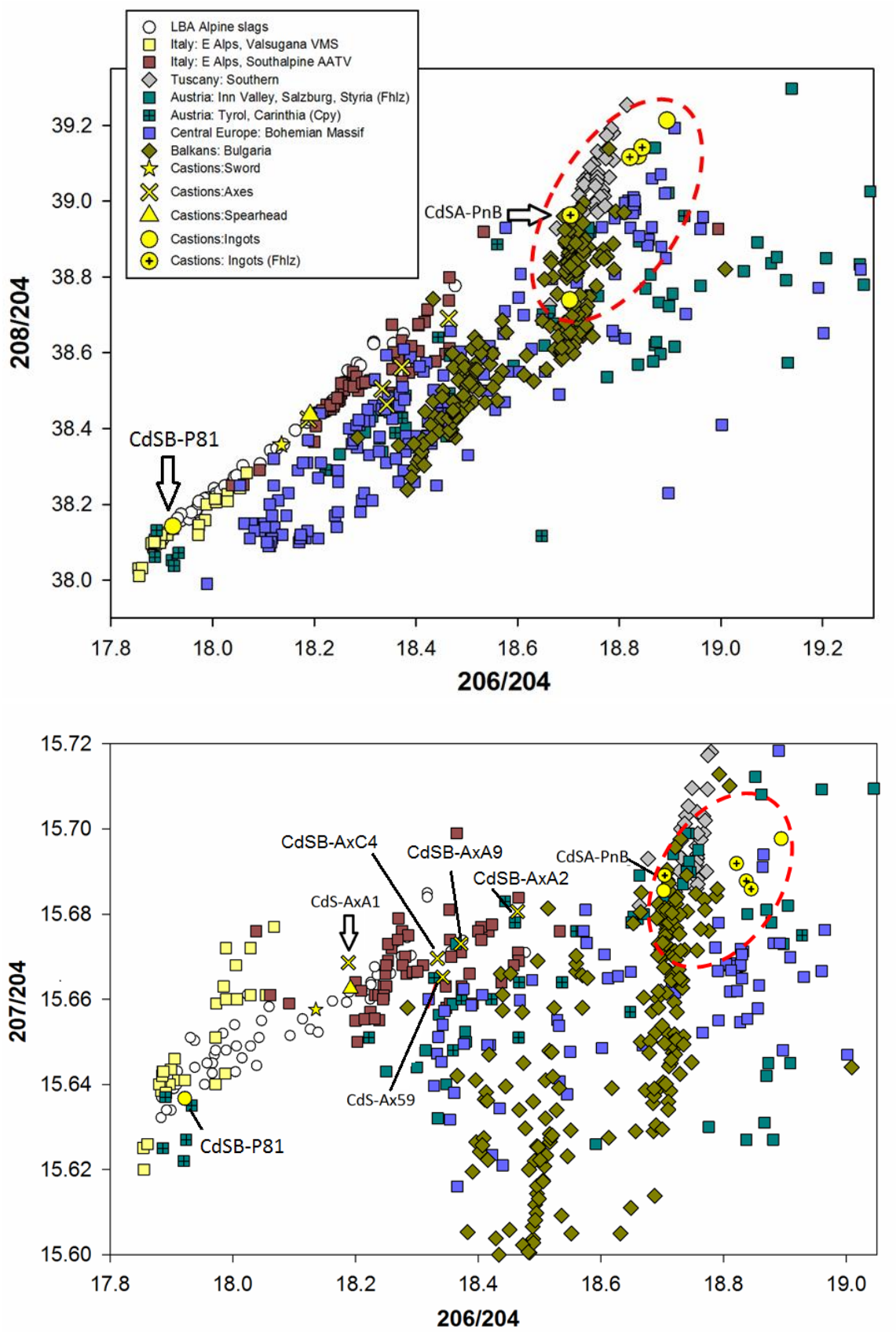

Fig. 6.3 – Lead isotope ratios diagrams of the ingots and the artefacts from the hoard of Castions di Strada compared with the possible ore-sources. The analytical uncertainty is equivalent or smaller than the size of the symbols.

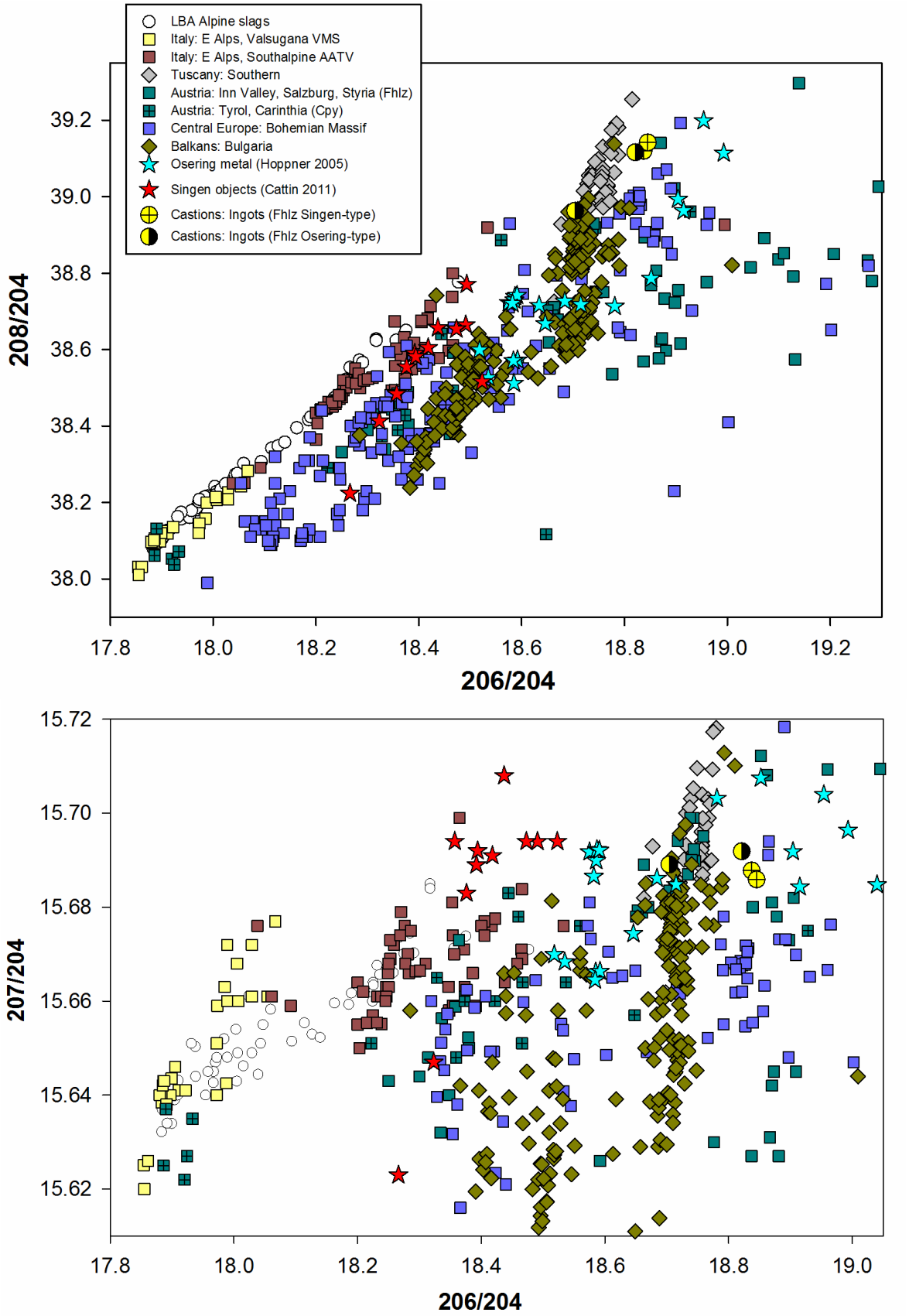

Fig. 6.4 – Lead isotope ratios diagrams of the fahlerz ingots from the hoard of Castions di Strada compared with the isotopic signal of the Osering metal (blue stars) and the Singen metal (red stars). The analytical uncertainty is equivalent or smaller than the size of the symbols. Note that the symbols used for the Castions di Strada ingots are referred to their fahlerz composition, with or without Ni.

chalcopyrite supplying. In any case, the presence of copper ingots of different origin found in the same site testifies the movement of the metal from the Alps toward the Central Europe and the Balkans. It is interesting that different types of ores were smelted. These observations are in agreement with what happened in Central Europe in the Late Bronze Age. As stated by in Lutz and Pernicka (2013), a resumption of the fahlore employment has been recorded in this period, possibly for the rising demand for copper that could not be covered by the chalcopyrite mines alone.

Furthermore, as discussed in Chapter 5, the samples from Castions di Strada can be chemically associated to the *Singen*-type metal or to the *Osering* copper, depending on the amount of Ni in the alloy and, besides the chemical classification, a more appropriate comparison between these materials can be performed thanks to the available isotopic data. Although these copper types had a widespread distribution in the Early Bronze Age in central Europe, it is evenly interesting to note the relationship with the Castions di Strada ingots. Indeed, the $^{206}Pb/^{204}Pb$ vs $^{208}Pb/^{204}Pb$ diagram highlights that the two Castions ingots with a fahlerz-type signal, characterized by the absence of Ni (remarked as yellow semicircle in Fig. 6.4), lie in a upper area respect the *Osering* metal objects studied by Hoppner *et al.* (2005); on the other hand, even the Castions ingots with a fahlerz-type signal having Ni (crossed circle in Fig. 6.4) do not show any affinity with the copper finds discovered in the Singen Cemetery (Cattin *et al.* 2011b). Although, this comparison does not lead to any additional information or new hypothesis on the origin of *Singen* and *Osering* metal, it clearly excludes the existence of a relationship between these classes of materials and the fahlerz-type objects. In fact, the comparison based only on the chemical similarities could lead to a misleading interpretation of the data.

For what concerns the weapons, the lead isotope signals of the investigated objects seem to be much more uniform, and these evidences allow for the observation of a more homogeneous picture. In fact, the sword, the spearhead and one of the axes (CdSA-AxA1) mostly lie in between the two major field of the Eastern Southalpine region, more close to the Southalpine AATV mines. The lowering in $^{206}Pb/^{204}Pb$ and $^{207}Pb/^{204}Pb$ ratios is especially evident for the sword and can be explained by a contribution of copper from Calceranica and Vetriolo mines. The results of the Euclidean test performed on the other axes revealed a sure attribution to the Southalpine AATV mines for one sample (CdSB-AxA9), whereas an ambiguous situation for two sample is manifested (CdSB-AxA2 and CdSB-C4), which does not allow for a safe geographical attribution. However, their chemical composition and their context argue in favour of the exploitation of the Eastern Alps, even if at the moment it is not possible to do a better discrimination. In addition, another doubt arises for CdSA-Ax59, since this axe exhibits a low $^{207}Pb/^{204}Pb$ ratio and it

falls in an area equally distant from some Slovakian deposits and the Trentino Alto Adige mines; however, this latter sample shows the same composition of the other axes (tin-bronzes with Ni and low traces of As and Ag). Therefore, it is plausible to suppose that the copper employed for the axes, the sword and the spearhead also derives from the South Eastern Alps.

6.3 FBA 1/2: The Celò-Cicigolis and Verzegnis hoards

Even in the case of the Celò deposit, ingots possess a low impurity level, mostly constituted by As, Sb, Ni and Co. Two out from four samples were isotopically analyzed and the corresponding $^{206}Pb/^{204}Pb$ vs $^{208}Pb/^{204}Pb$ and $^{206}Pb/^{204}Pb$ vs $^{207}Pb/^{204}Pb$ diagrams are reported in Fig. 6.5. The purest ingot (Cel-P-38), containing only traces of Ag, can be safely associated to the Southalpine AATV area, whereas for the other sample (Cel-P-41, labelled as *Fhlz ingot* in Fig. 6.5), exhibiting low amounts of As, Ni and Co, the interpretation is problematic; in fact, the Euclidean test suggested different locations including Les Valais area (Swiss), Inn Valley (Austria), Bohemian Massif (Slovakia) and the Carnia area, in Friuli (Italy). Thus, in order to shed light on this question, the attention was given to the deposits containing Co and, in this particular case, both Inn Valley (Austria) and Les Valais (Swiss) cannot be excluded as potential copper sources. In the latter hypothesis, it would have attested a long-distance economic and cultural interaction. From the same hoards, three axes, the sword, and the socketed-shovel were analysed. In $^{206}Pb/^{204}Pb$ vs $^{208}Pb/^{204}Pb$ diagram, it is possible to observe the linear arrangement of the lead isotope signals of all the objects (dotted line in the plot in Fig. 6.5) and this evidence distinctly encourages the hypothesis of manufacturing using copper from the Southalpine AATV field. However, the attribution for Cel-AxA8 is still under debate; in fact, both the combination of the different locations suggested by the Euclidean test and its position in the diagrams do not exclude the use of copper from the Carinthia region (Austria), since these deposits are characterised by chalcopyrite ores.

In the Verzegnis hoard, only two ingots were available for sampling, Ver-P-0 and Ver-P-9. The first was found to be clearly smelted from chalcopyrite ores, although low amounts of As and Sb were detected (0.2% and 0.6% respectively), whereas the second ingot exhibited high amounts of Fe, Co, Zn, As, Ag, Sn, Sb and Pb. Even the isotopic signals underline a difference among these two ingots and they fall into a region between Calceranica/Vetriolo and Mount Avanza, a strata-bound type of deposit containing mixed ores such as tetrahedrite, galena, pyrites, chalcopyrite and bournonite. Thus, by keeping in mind their particular composition, it is plausible to suppose a mixing between

chalcopyrite associated to sphalerite – which can justify the presence of zinc – and tetrahedrite – which would bring all other fahlerz elements. Moreover, their position along the ideal mixing line can be interpreted as proportional to the quantity of the ore-type used; indeed, the most “pure” ingot (Ver-P-0) matches with the Valsugana VMS mines, while Ver-P-9 is displaced closer to the Carnia region, hypothetically in a mid-position on the line connecting the Valsugana field and the Mount Avanza mine. Furthermore, in Ver-P-9, the amount of Pb reaches 2.4%, value which is higher than the average respect to the other analysed ingots; this evidence could indicate a greater contribution of Pb, being responsible of the shift towards the Carnia deposits.

Geographically, Verzegnis is located in the Carnian Prealps, in a crossroad of rivers; thus, it is not bizarre to think that a mixing with Carnian copper mined 50 km away has taken place. However, there is yet no evidence of prehistoric exploitation of these mines, and although in the past some galleries have tentatively been dated to Roman times, Mount Avanza was apparently first exploited in the late Middle Ages. In fact, the most recent studies have shown that the earliest traces discovered up to now are certain to be dated to the late Middle Ages; that is, to the period around the 13th century AD (Giumlia-Mair, 2009).

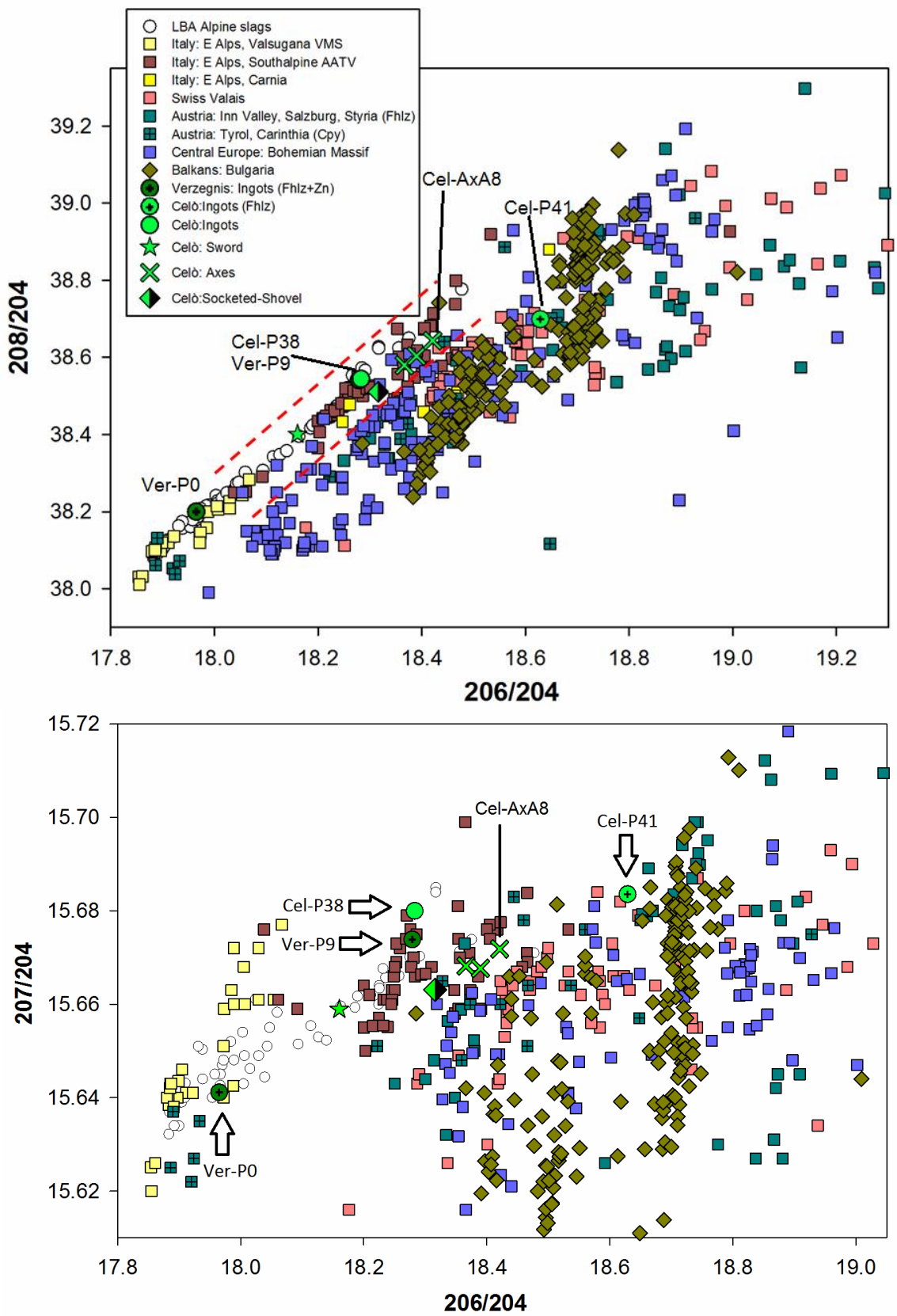

Fig. 6.5 – Lead isotope ratios diagrams of the ingots and the artefacts from the hoards of Celò and the ingots from Verzegnis compared with the possible ore-sources. The analytical uncertainty is equivalent or smaller than the size of the symbols.

6.4 FBA 2: The Galleriano and Porpetto hoards

Although the Galleriano and Porpetto hoards belong to the same chronological phase, the results of each hoard will be commented separately because of the great number of samples involved in the discussion.

Galleriano

From the Galleriano hoard, the bronze pick-ingots, the possible axe blade reinterpreted as an ingot fragment and the winged-axe were isotopically characterized. As observed in Chapter 4, pick-ingots are compatible with chalcopyrite as mineral charge for copper extraction, whereas the presence of antimony and traces of arsenic and silver in Gal-PI-3 could be recognized as a possible addiction of low amount of tetrahedrite during the smelting process. In Fig. 6.6, it is evident that the chemical differences recognized in these samples are accompanied by a difference in the isotopic composition. The pick-ingots (Gal-PI-4 and Gal-PI-5) are clustered together and they clearly overlap the Valsugana VMS deposits signature, supported by the lack of impurity in the bronze. On the other hand, the ingot fragment (Gal-PI-3), owing to its composition, could be interpreted as lying in a mid position between Calceranica/Vetriolo mines and the Carnia deposits, exactly as it has been previously suggested for the Verzegnis ingot and easily remarked in the $^{206}Pb/^{204}Pb$ vs $^{207}Pb/^{204}Pb$ diagram (Fig. 6.6). Although the lead isotopic ratios of the winged-axe (Gal-Ax) might appear closer to that of the ingot, the chemical composition reveals that this weapon has been made of Southern Alpine copper, probably with a contribution of chalcopyrite from Valsugana VMS and the Southalpine AATV area. A further comparison can be done using the data available for two pick-ingots discovered in Frattesina (Zaghis 2005) and for which the isotopic ratios are shown as magenta hexagons in Fig.6.6. In the diagrams, the substantial overlap with the Valsugana field does not leave doubts about the isotopic similarities among the pick-ingots, and is also supported by the chemical and microstructural analogies observed in Chapter 5.

In addition to this, according to Borgna (2000), the archaeological studies already indicate a connection with the Veneto area. In fact, in the Galleriano hoard, the presence of the bronze bangle decorated with V-shaped weaving pattern (*herringbone*) is the expression of a Western-style that could be interpreted as the witness of a long-distance trade network, rather than the expression of a social *status*. Therefore, in this specific case, it is important to stress that the chemical and isotopic analyses can confirm the existence of a commercial road from Galleriano towards the Po Valley, in particular with

Frattesina; however, the exploitation of the same copper supplying area for the weapon making cannot be ruled out.

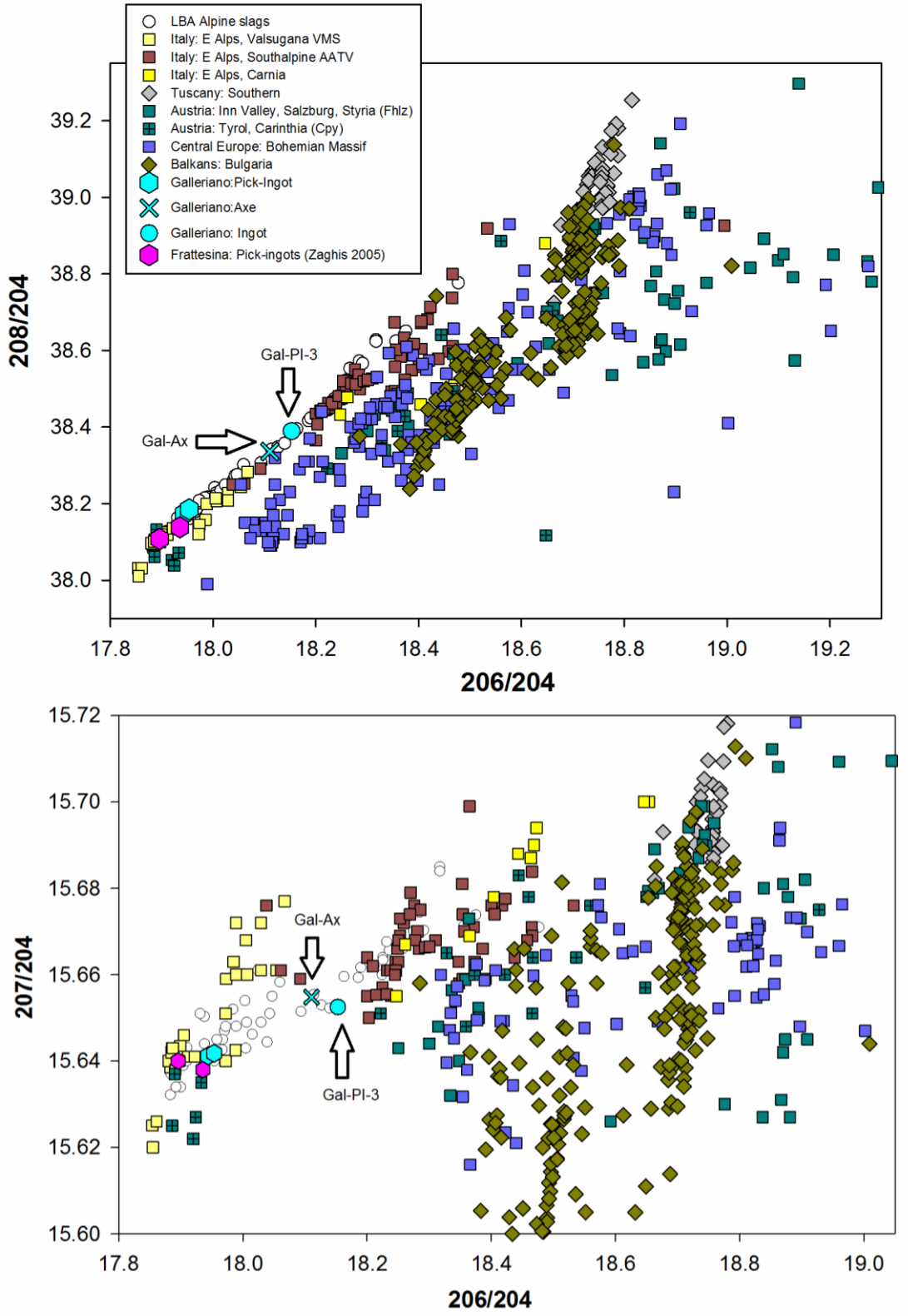

Fig. 6.6 – Lead isotope ratios diagrams of the ingots and the winged-exes from the hoard of Galleriano compared with the possible ore-sources and with the isotope composition of two pick-ingots discovered in Frattesina site. The analytical uncertainty is equivalent or smaller than the size of the symbols.

Porpetto

In the Porpetto hoard, five pick-ingots, ten ingots of different typologies, the socketed-shovels and the spearhead were taken into account for the lead isotope analysis. Apart from the distinction of the pick-ingots, the other typologies are here treated together. In order to cover the chemical variability observed in Chapters 4 and 5, the selected samples were divided in two main compositional classes on the basis of the trace element pattern remarked by PCA. Although the element concentrations change remarkably, the samples having As and Sb were divided from the samples exhibiting As, Sb, Ni and Co, as reported in the diagrams in Fig. 6.7. Only one sample out of the 29 of Porpetto differs from this scenario and exhibits exclusively Fe and Zn as major impurities (Por9-Pn-25); consistently with its composition, it should be noted that this particular sample fits the Calceranica/Vetriolo region, as shown in the $^{206}Pb/^{204}Pb$ vs $^{207}Pb/^{204}Pb$ diagram (Fig. 6.7).

Apart from this singularity, the isotopic signals of the Porpetto objects and ingots are in general spread out enough to cover an isotopic area characterized by the overlapping of the Trentino-Alto Adige, Central Europe and Austria fields (dotted circle). This situation is showed very clearly by the $^{206}Pb/^{204}Pb$ vs $^{208}Pb/^{204}Pb$ diagram, even if by the observation of the $^{206}Pb/^{204}Pb$ vs $^{207}Pb/^{204}Pb$ diagram it is possible to note that the signal of these samples could be apparently consistent with the Southalpine AATV area. Nevertheless, their chemical compositions are not compatible with the Southern Alpine mineralisations and, therefore, it must be recognized that this chemical-isotopic variance could be indicative of a substantial metal mixing, a common problem in the Late Bronze Age. Indeed, the distinctive amounts of Co and Ni detected in several samples should be employed as indicative tracers and, therefore, a closer look to the mines characterized by the presence of Co- and Ni-mineralizations might help to provide some plausible explanations.

In Fig. 6.8, the lead isotopic composition of those Porpetto samples characterized by Ni and Co is compared to that of the mineral deposits in which important mineralizations of Ni and Co, as well as Sb and As, are known to be present. These particular mines are located in Italy, Switzerland, Austria, Germany and Slovakia; for comparison, the signal of the field of Southeastern Alpine region is reported, even if there are not any known Co and Ni-rich mineralisations in this area. In the following, the alternatives that could be provided in order to explain this chemical and isotopic situation are suggested.

i. The Porpetto samples exhibit lead isotope ratios that almost overlay a famous cobalt locality in the Western Alps, in Piedmont. Actually, the Cruvino mine, near Usseglio, shows an assemblage of Ni-pentlandite and skutterudite, besides other Co and As species such as lollingite and safflorite are recognised (Fenoglio and Fornasieri,

1940; Piccoli, 2007); however, only two data are available for this mine and, therefore, it is not possible to give a sure attribution basing on such few data. Anyway, it is interesting to note that other investigations on FBA findings discovered in Piedmont lead to suggest the exploitation of this mine already in this period (Artioli *et al.* 2009; Angelini *et al.* 2008). If the hypothesis of Cruvino mine can be considered reliable, the isotopic signal and the chemical composition of Co- and Ni-enriched samples would not derive from a copper mixing, but from the exploitation of such deposit. Moreover, this could be a plausible evidence of either direct or indirect trade between Porpetto and the Western Italy, although at the moment the chemical analyses argue in favour of a more probable relationship of this settlement with the Slovenian region.

ii. The second hypothesis foresees the employment of Southernalpine copper, with the contribution of copper from a particular deposit in the Schladming district (Austria). According to Koppel (1997), the Vöttern Unterbaustollen mine is characterized by polymetallic deposits accompanied by the presence of Ni, Co, As and Bi. Following this argumentation, even the lowering of the $^{208/204}$Pb ratios in Fig. 6.7 could be explained by mixing characterized by a non-negligible contribution of the lead signal due to Austrian copper addition.

iii. In terms of copper mixing, the last alternative is the most extreme. In the Porpetto hoard, owing to both the presence of an ingot from Calceranica/Vetriolo (Por9-Pn25) and the evidence of a pronounced linear arrangement towards the Valsugana field (Fig. 6.7), it is possible to assume a substantial mixing with the copper from Valley Inn (Schwaz). In this mining district, the identification of prehistoric mining is now ascertained from at least the late second millennium BC onwards (Gustrein 1981; Goldenberg, 1998; Rieser and Schrattenthaler, 1998). The mineralisations in the Schwaz–Brixlegg area occur in three geological complexes. Economically, by far the most important deposits are located within the Schwazer dolomite, which is of lower Devonian age (the so-called Grauwacken zone, northern Alps); in these mines, the fahlore composition of the Schwazer dolomite is predominantly arsenical tetrahedrite. As stated by Hoppner *et al* (2005), chemical analyses have revealed Cu, S, As and Sb as major components, with significant concentrations of Zn, Hg, Fe and Ag, as well as traces of Bi; decomposed fahlores are enriched in Ag and Hg, and Co and Ni are often present. In this case of mixing, therefore, the lead isotopic signal would fall over the Southalpine AATV field because of the proportions of copper-ore used during the smelting.

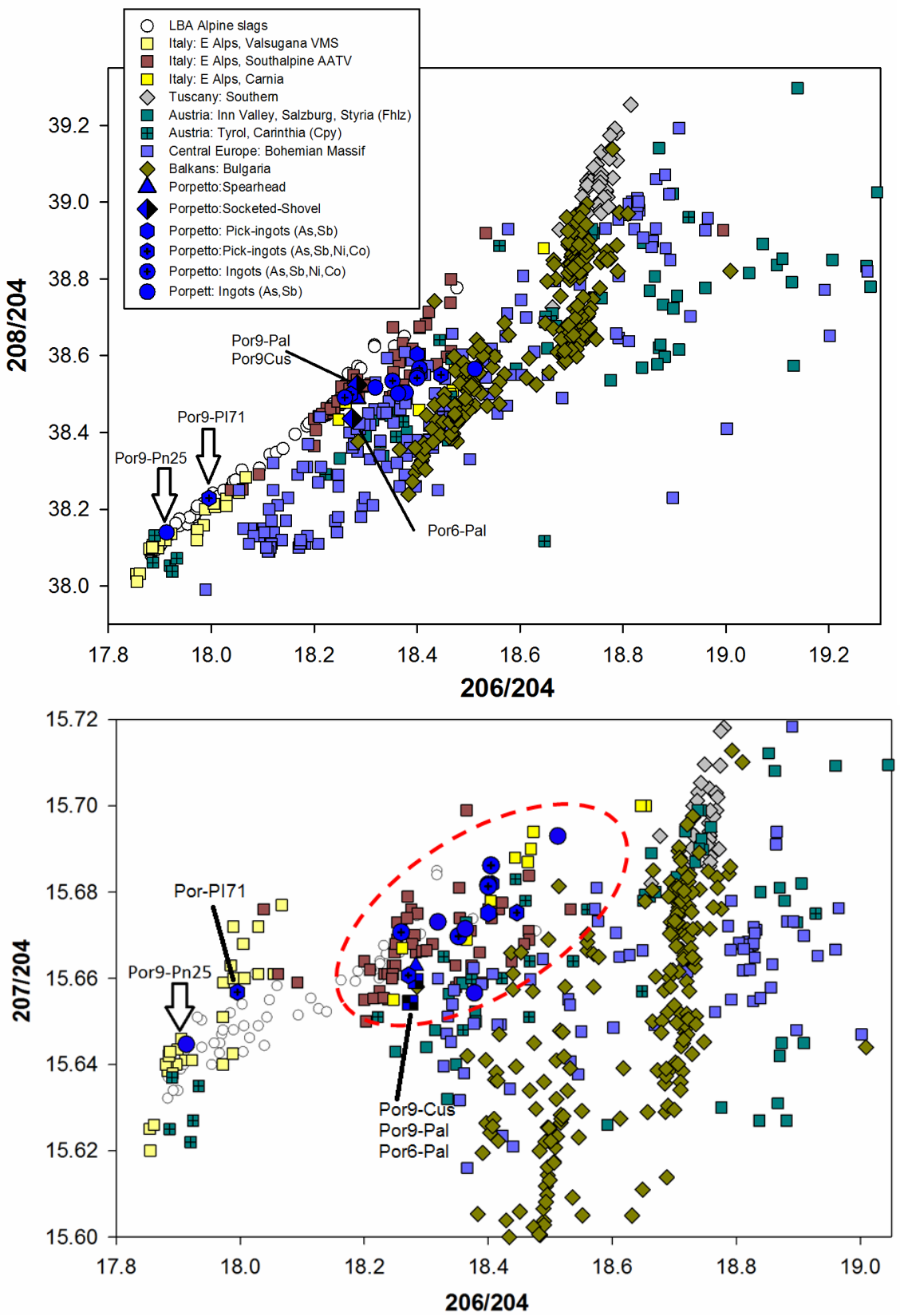

Fig. 6.7 – Lead isotope ratios diagrams of the ingots and the artefacts from the hoard of Porpetto compared with the possible ore-sources. The analytical uncertainty is equivalent or smaller than the size of the symbols.

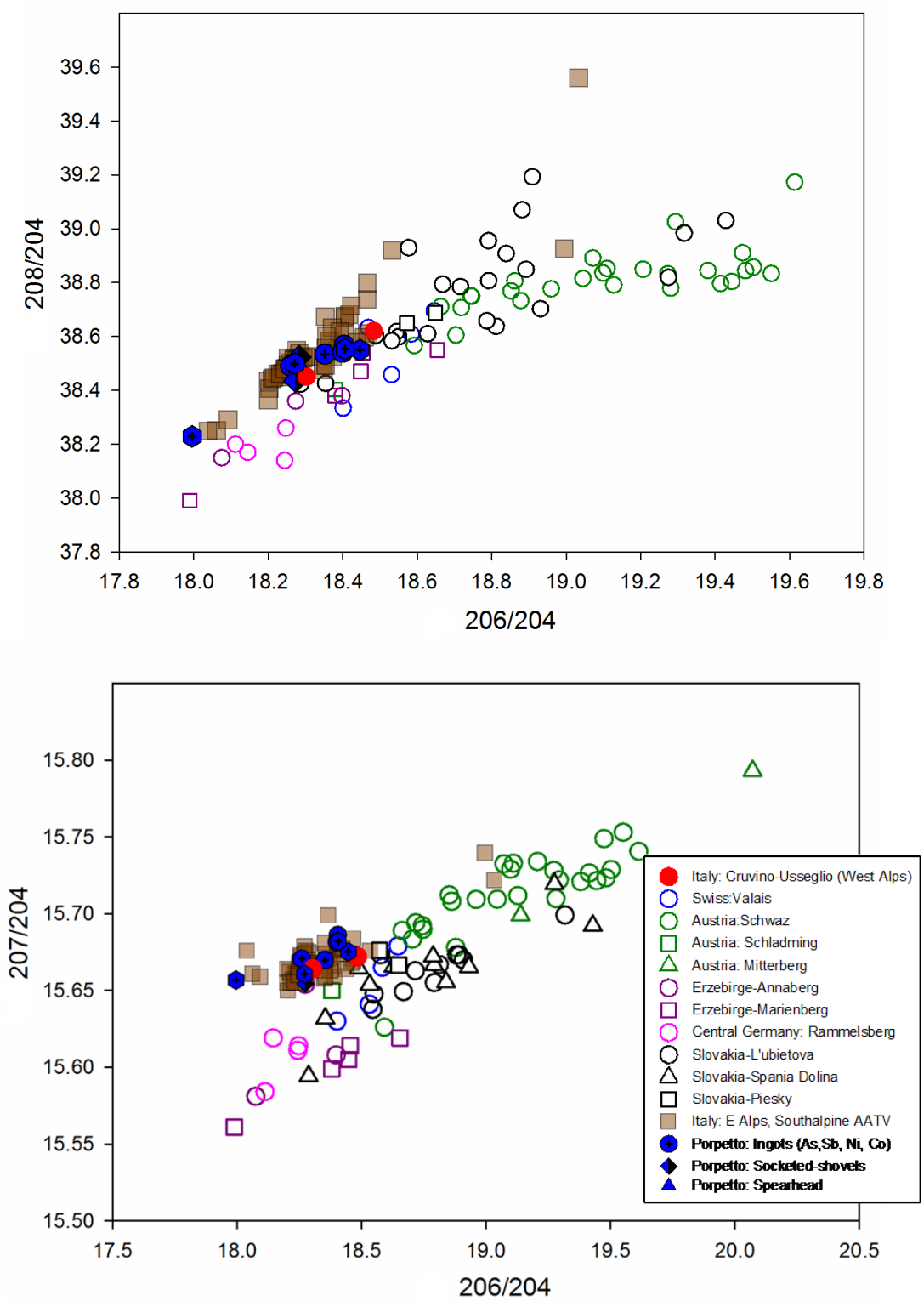

Fig. 6.8 – Lead isotope ratios diagrams of the fahlerz-ingots rich in Co and Ni from the hoard of Porpetto compared with the mines characterized by the presence of Co- and Ni-mineralizations. The analytical uncertainty is equivalent or smaller than the size of the symbols.

The last two options can be seriously taken into account, even if it is not possible to discern what actually has happened during the smelting process. In addition, another observation must be brought to the attention of the readers. In fact, as suggested by Paulin *et al.* (2003) for the Kanalski Vhr case study, it is possible that speiss ingots were employed as alloying additions in making melts for casting. Unfortunately, in literature there is a lack of isotopic data related to Slovenian copper-ores and, at the moment, a proper comparison is not possible.

The context of Porpetto is an eloquent witness of a site where raw metal processing have taken place, not as secondary and occasional activity, but as major activity in a settlement area (Borgna 2000). In this regard, since the shovels and the spearhead exhibit the same isotopic ratios and a quite similar fahlerz composition with Ni and Co, one might assert that the craftsman in this site provided to the creation of artefacts using the available raw materials. In the previous chapters, the quality of this alloy has been extensively discussed and, furthermore, it is important to underline that weapons for the hand-to-hand combat, such as a bladed weapon, have not been discovered in Porpetto; in fact, the scarce performance of the alloy could mean the death of the fighter.

6.5 Swords and axes

In order to define a clear picture on their provenance, the obtained isotopic data on swords and axes are here integrated with those deriving from two stray findings discovered in Canale Anfora[14] and Belvedere, thus embracing an undefined chronological period ranging from the Middle Bronze Age to the Final Bronze Age. In this regard, a close look to these distinctive objects might help to define any supply changes or trends linked to their dating. Therefore, in Fig. 6.9, the objects were arbitrary divided in two chronological ranges: the oldest axes and swords are reported in red (MBA-RBA), whereas the axes dated to a subsequent period are marked in green (RBA-FBA). All the chronological details are listed in Appendix 1, accompanied by their references.

The lead isotope analysis outlines a fairly homogenous picture. For the majority of weapons, Southeastern Alpine deposits are the most probable sources, reinforced also by the chemical compatibility with these mineralisation; however, as mentioned in Section 6.2, some doubts arise for one of the axes of Castions di Strada (CdSA-Ax59) that have a doubtful signal, possibly related to the Central Europe area (Slovakia). As can be seen in Fig. 6.9, no significant trend related either to a chronological/typological classification or to

[14] In Chapter 4, this sample was reinterpreted as an ingot rather than an refined object, however this item is here discussed owing to its typological features.

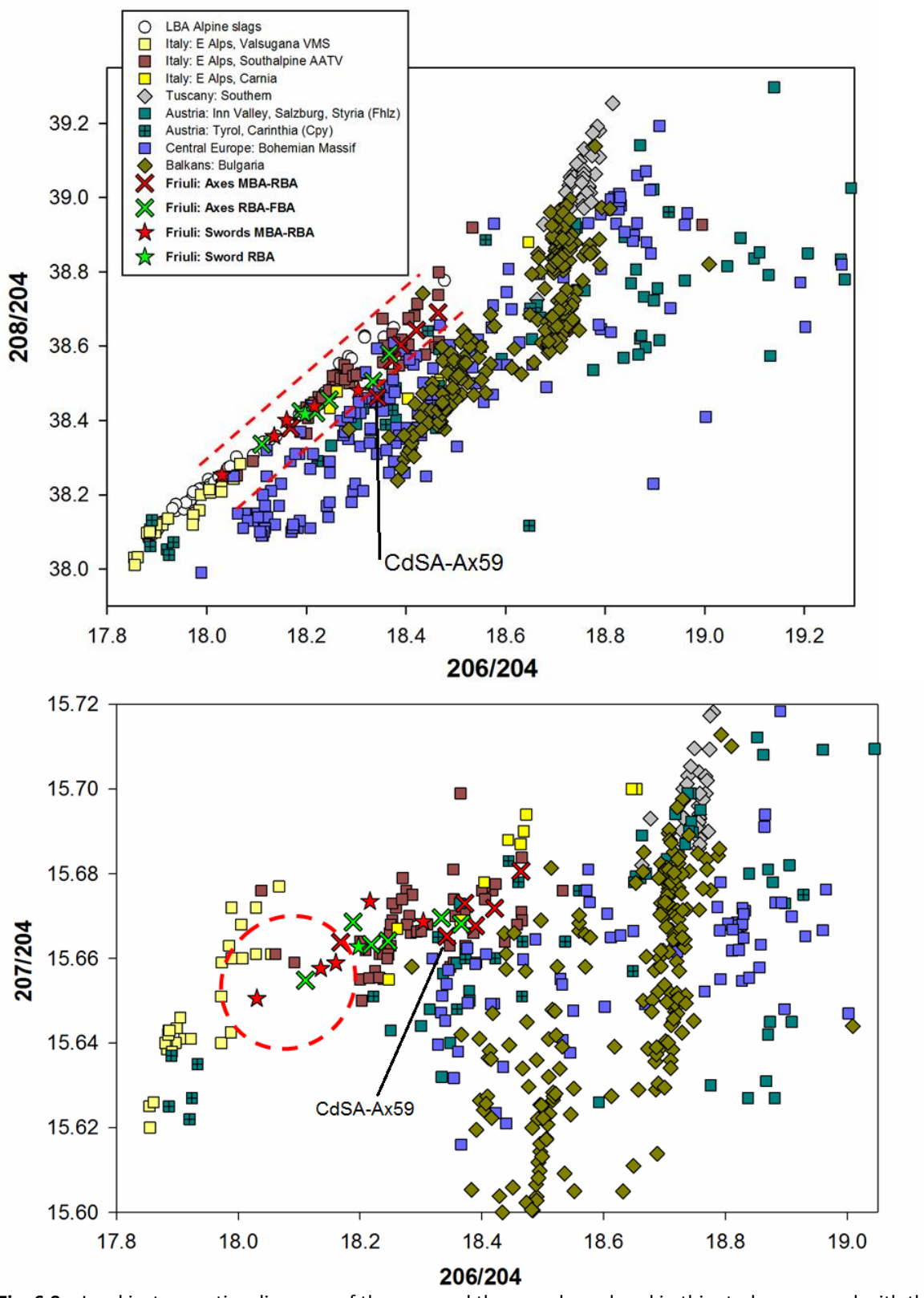

Fig. 6.9 – Lead isotope ratios diagrams of the axes and the swords analysed in this study compared with the possible ore-sources. The analytical uncertainty is equivalent or smaller than the size of the symbols.

previously examined context of discovery is evident. However, besides a linear displacement, some samples (dotted circle in Fig. 6.9) show a position more close to the Valsugana VMS field and these evidences can be ascribed to a probable employment of copper from the Valsugana VMS mines together with the Southalpine copper. In fact, it should be admitted that ores or ingots from several sources of this district could have been mixed during the time that inevitably passed between the mining of ore and the production of the artefact. Due to the low contents of nickel and the traces of arsenic, it was assumed that this metal is a product of fahlore addition with secondary copper containing Ni, as was already hypothesized by Hoppner *et al.* (2005) for the prehistoric copper production in the Inn Valley. However, this possible addition of fahlerz copper has probably occurred in such low quantities that the isotopic signal has not been altered. Moreover, it should be reminded that the chemical comparison between ingots and objects of a same hoard has revealed that these latter contain As and Ni in higher concentrations respect to the semi-products, thus leaving the question open on the introduction of Ni in the alloy.

In summary, the lead isotope data reveal that, during the entire Late Bronze Age, the weapons were mostly manufactured by the smelting of copper from South Eastern Alps and, moreover, this evidence indicates the continuous mining exploitation of this ore-district and the continuous trade towards Friuli Venezia Giulia.

6.6 Pick-ingots and socketed-shovels

A last comment is reserved to the pick-ingot and socketed-shovel circulation, since they are considered FBA2 markers and because they have been often found together in the same archaeological context. Traditionally, pick-ingots are treated as evidence of the metal trade between the mineral rich area of Southern Tuscany (the Colline Metallifere) and the North East of Italy (Bietti Sestieri 1981), whereas the lead isotopic ratios diagrams (Fig. 6.10) highlight a different and more complex picture.

In this work, the chemical analyses allowed for a compositional distinction between the pick-ingots from Galleriano, made of bronze, and those from Porpetto, characterized by a fahlerz composition, with or without Co and Ni. Generally, not many chemical studies have been conducted on pick-ingots (see Chapter 5), and even fewer lead isotope analyses. Recently, in their extended research involving LBA materials from Northern and Southern Italy, Jung *et al*. (2011) had isotopically analysed four pick-ingots, together with two socketed-shovels from Frattesina. Unfortunately, the specific data for each sample are not reported and direct comparisons are not possible, but the authors suggested that the raw

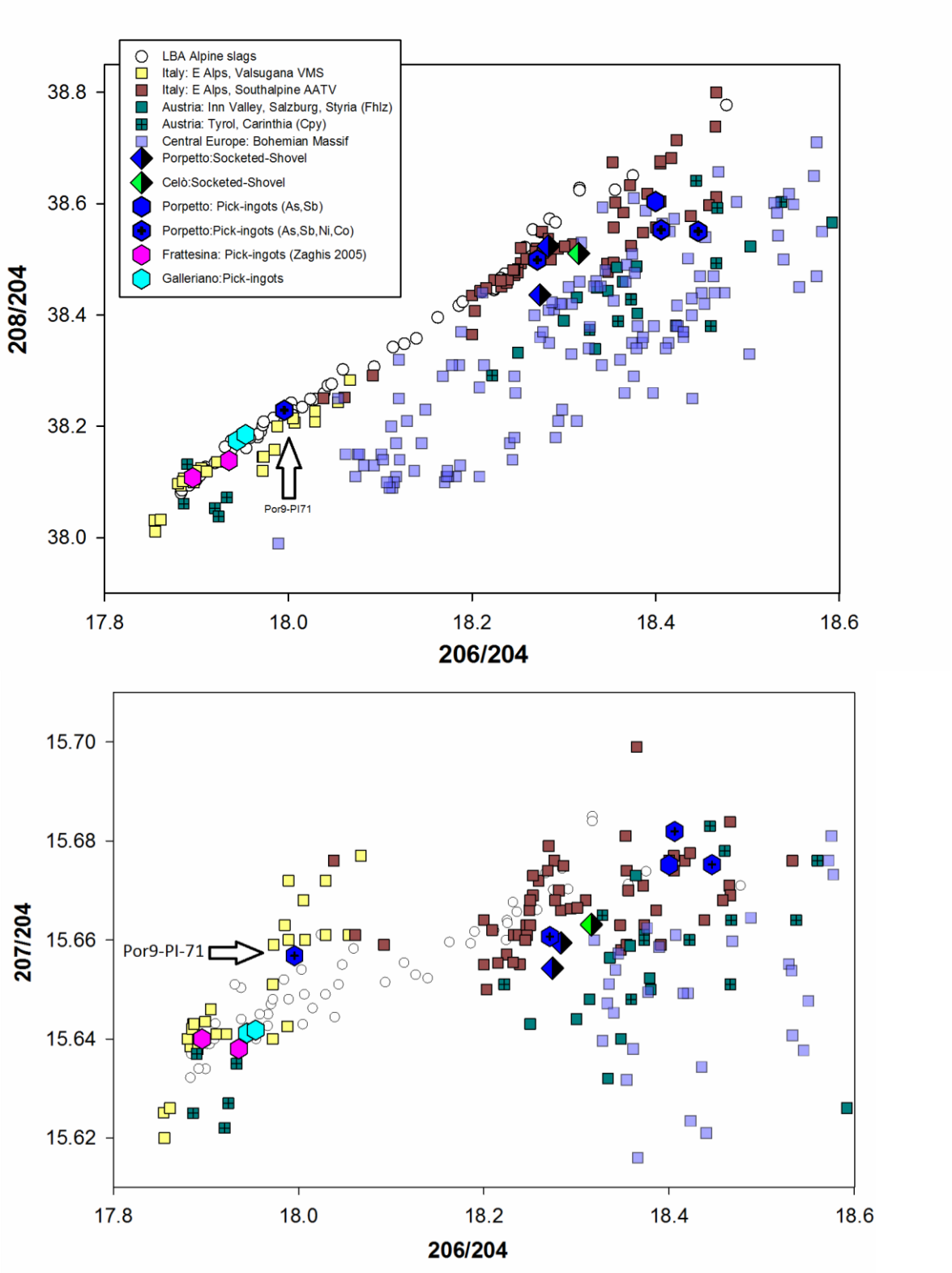

Fig. 6.10 – Lead isotope ratios diagrams of the pick-ingots and the socketed-shovels analysed in this study compared with the possible ore-sources. The samples from Frattesina are reported for comparison. The analytical uncertainty is equivalent or smaller than the size of the symbols.

the raw metal is to be sought in the Southern Alpine copper ore deposits. However, a comparison with Frattesina pick-ingots is possible thanks to the analyses conducted by Zaghis (2005). For the Galleriano samples, the isotopic analysis allows a safe attribution to the use of copper from the Valsugana VMS mines, exactly as for the Frattesina samples (Zaghis 2005). On the other hand, the provenance of the raw metal used for the smelting of the pick-ingots from Porpetto is still an unsolved question, but a clear chemical similarity with the Slovenian hoards was highlighted. Therefore, it is possible to define two different trade spheres: one of refined Sn-bronze, which includes the hoards of Frattesina, Redipuglia, Madriolo and Galleriano, and the other in which no tin have been detected, as in the case “tra Manciano e Samprugnano” and the Slovenian hoards of Veliki Otok, Kanalski Vrh I and II (Trampuž-Orel 1996).

The question thus arising at this stage is related to the pick-ingot function (Jankovits 1999; Santi and Leonardi 2007; Bellintani and Stefan 2008). In fact, as previously stated, these objects seem to be inspired to the shape of a mining tool but, actually, they were not conceived for working activities. Therefore, according to Borgna (1992), a connection to the concept of a pre-monetary system is suggested, in which ingots acquired a value depending on their shape that guarantees the quality and amount of the metal. In this regard, the doubt that Porpetto could be intended as a factory of "fake" ingots is considerable. Up to now, no discovery of fahlerz and bronze pick-ingots in the same hoard has been observed, highlighting a strong separation of the trade spheres. However, the sample Por9-PI-71 (remarked by the arrow in Fig. 6.10) suggests a possible mixing of the Valsugana signal with Porpetto-type Alpine copper, thus admitting a partial overlap among the commercial roads. In the future, it would be interesting to broaden the chemical and isotopic research on these ingots in order to deeply investigate this aspect.

Concerning the socketed-shovels, the available samples are limited, making it difficult to provide statistically solid considerations; however, it can be stressed that their chemical and isotopic characteristics are perfectly in agreement with the previously delineated scenario. On one side, the oldest socketed-shovel from Celò exhibits chemical and isotopic compositions that are compatible with the Southalpine district as a possible mining source, whereas, on the other side, the Porpetto specimens present the same issues of the ingots. Moreover, by taking into account that the socketed-shovels could be characterized by an economic value, as well as for the pick-ingots (Borgna, 1992), the considerations about the fahlerz metal circulation are further reinforced.

Conclusions

In the present work, a multi-analytical approach, involving chemical, metallographic and isotopic analyses was employed in the study of copper and bronze artifacts from well-dated protohistoric contexts in Friuli Venezia Giulia. The research was aimed to investigate the origin of the metal constituting such artifacts, with the scope to identify the exploitation areas and reconstruct the trade circuits in North-Eastern Italy during the Middle-Late Bronze Age. Indeed, the chemical and isotopic characterization of the copper-based artifacts was proved to be a powerful tool for identifying the provenance of the mineral charge. For the purpose of this *Ph.D* research, various types of artifacts were taken into account, subdivided in two main categories. On one hand, 66 ingots were selected, since they represent a manufacturing product that is closely related to the charge of extraction used in the smelting process; on the other, the choice was also extended to weapons with the aim to outline the commercial trade patterns and better understand the manufacturing techniques of the different types of objects, such as swords, axes and spearheads.

Concerning the ingots, the results showed that these semi-products are generally made of copper and only in few cases of bronze, which contain impurities whose concentrations depend on the technological knowledge of ancient smiths as well as upon the various sources of raw material. In the **RBA-FBA**, the study of the hoards of Cervignano and Muscoli revealed a quite homogeneous composition of ingots, almost exclusively characterized by the employment of chalcopyrite ore-charge, probably associated to sphalerite. In fact, all but one of the ingots belonging to these ancient deposits were found to be made of pure or almost pure copper, exhibiting Fe and Zn as major impurities and in which the presence of copper sulphide residues not completely roasted was observed. In particular, in the Cervignano hoard, the microstructural observations have permitted to relate the peculiar metallurgical features to the two ingot shapes that coexist in this hoard, thus revealing two different refining steps associated to each shape. In this case, parallel surface ingots can be interpreted as less refined than plano-convex ingots because of either the lack of the last refining step or the use of a less evolved process.

Concerning the Cervignano ingots provenance, the majority of the samples exhibited a lead isotope signal and a composition perfectly compatible with Eastern Southalpine field

(Veneto and Trentino-Alto-Adige), whereas other three samples agree rather well with the Valsugana field (Calceranica and/or Vetriolo mines). Only one of the Cervignano's ingots differed in composition (2% Sb) and it can be defined as a possible mixing between chalcopyrite from Calceranica/Vetriolo and tetrahedrite from Carnia or from Northern Tyrol. Moreover, an ingot from Muscoli showed a distinct radiogenic signal close to the field of Southern Tuscany deposits, which would strengthen the hypothesis of a cultural connection between these two regions; however, it was not possible to make an effective attribution, due to the low impurity content.

During the passage through the **FBA-FBA1/2**, the hoards became more heterogeneous, and various type of copper coexisted, such as chalcopyrite and fahlore with or without nickel. In the Castions di Strada hoard, several of the analyzed ingots were chemically and microstructurally similar to those of Muscoli and Cervignano, but the majority of them were characterized by different amounts of As, Sb, Ni and traces of Fe and Co that constitutes the typical impurity pattern of a fahlerz ore-charge. Furthermore, in the case of lack of pure copper and/or tin necessary for the bronze making, it is plausible to suppose that the smiths carefully selected the mineral charge and processed it consciously of their technological properties. Besides the chemical composition, even the lead isotope analysis suggested a diversification in terms of raw materials and exploited sources: for fahlerz-type ingots, Bulgaria, Austria and Central Europe are the all probable source areas, whereas for one ingot obtained by the smelting of chalcopyrite it is impossible at the moment to distinguish the provenance between the Valsugana and Carinthia regions, because of the quite similar Pb-isotope ratios.

Even in the case of the Celò deposit, three out of the four analyzed ingots possessed an impurity pattern associated to low levels of As, Sb, Ni and Co, whereas the fourth exhibited only traces of Ag. For the provenance purpose, two samples have been isotopically analyzed, from which the most pure can be safely associated to the Trentino area, whereas for the other (Co-rich) the interpretation is doubtful. In order to shed light on this question, the attention was given to those mineral deposits containing Co and, in this particular case, both Inn Valley (Austria) and Les Valais (Switzerland) cannot be excluded. In the latter hypothesis, it would have attested a long-distance economic and cultural interaction.

In the Verzegnis hoard, the employment of different ore-charges and their mixing was still more evident. One of the two investigated ingots was revealed to be clearly smelted from chalcopyrite ores, since only low amounts of As and Sb were detected, whereas high amounts of Fe, Co, Zn, As, Ag, Sn, Sb and Pb were recorded in the other. Since for the two samples the isotopic signals fell into a region between Calceranica/Vetriolo and

Carnia, it was possible to suggest an ore-mixing for both of them, although of varying extent. To our knowledge, the charge mined from the Mount Avanza could be chemically and isotopically compatible; however, this mine was apparently first exploited in the late Middle Ages.

In **FBA2**, besides the plano-convex or bar ingots, even the so-called pick-ingots were commonly in circulation. Traditionally, these particular semi-products have been identified as indicators of the bronze circulation in the final phase of the Late Bronze Age and the analyses on the samples belonging to the Galleriano and the Porpetto hoards lead to suggest the employment of chalcopyrite and fahlerz ore-charges, but in different and separate trade spheres. As expected, the pick-ingots of Galleriano were Sn-alloyed, while the ingot was made of quite pure copper. In any case, all ingots are compatible with chalcopyrite as mineral charge for copper extraction. The recorded difference in composition is also confirmed by Pb-isotope analyses; in fact, pick-ingots manifested the same signal that matches the specific area of Calceranica/Vetriolo, whereas it was possible to suppose the use of copper from Veneto-Trentino Alto Adige region for the other ingot. Moreover, a proper comparison among similar samples allowed to suppose a trade connection between Galleriano and Frattesina rather than a similar production.

Differently, in the Porpetto hoard, the pick-ingots were found in association to other ingot shapes and, even if the elements concentration was different from sample to sample, for all ingots the same trace element pattern was recorded: copper with variable amounts of Co, Ni, As, Ag, Sb, and Fe only in some samples. From PCA analysis it was possible to distinguish two groups, identified by the presence/absence of Co and Ni, whereas Sb and As were always present even if in different amounts. Arsenic and antimony harden copper and they generally would be considered as desirable elements when added in few percentages; however, an alloy containing the detected amounts is not workable and very brittle. Therefore, this metal is not technologically apt to tools and weapons making. The presence of such antimonial copper ingots has been attested in Velem in Hungary and in some Slovenian deposits.

From an isotopic point of view, all these samples fell in an area characterized by the overlapping of the Trentino-Alto Adige, Central Europe and Austria fields, but they were not chemically compatible with the indicated isotopic sources. This chemical-isotopic variance is a common problem for LBA metals, and could be indicative of metal mixing; however, the distinctive amounts of Co and Ni should be indicative tracers, and three main hypotheses arose. First, the exploitation of the Cruvino mine (Western Alps) can be considered reliable because of the isotopic signal and the Co- and Ni-mineralizations available in this deposit; another possibility is represented by the employment of

Southernalpine copper with the contribution of copper from a particular deposit in the Schladming district (Austria); and finally, owing to the evidence of a pronounced linear arrangement of the samples towards the Valsugana field, it is possible to assume a substantial mixing with the copper from Valley Inn (Schwaz). Indeed, it is important to admit the possibility of a substantial mixing or the use of *speiss* ingots as alloying additions in making melts for casting, thus showing an apparent connection to the trade sphere of the Carpathian Basin. Unfortunately, in literature there is a lack of isotopic data related to Slovenian copper-ores and, at the moment, a comparison is not possible. Interestingly, only one sample out of the 29 taken into account for Porpetto has Fe and Zn as major impurities and, isotopically, it fitted the Calceranica/Vetriolo region.

Other intriguing observations were deduced from the analysis of the weapons and tools. All the analyzed swords and axes were tin bronzes exhibiting the higher Sn content, ensuring a good castability and the workability of the alloy. Moreover, low amounts of Fe and Zn denoted a further purification of the metal and, generally, the rare presence of δ-phase suggested well-controlled manufacturing processes characterized by low cooling rate. The same picture can be enlarged to Celò shovel and Castions di Strada arrowhead that showed the same technological features.

As verified by the metallographic investigations, all the axes and swords underwent extensive plastic deformation followed by annealing cycles. Most of the samples, taken from the blade's edge, were in a strain-hardened state, since several slip lines were observed within the metal grains, according to the functional use of the weapons that needs hard cutting edges. One exception was represented by a sword from Muscoli, which showed exclusively twinned grains; however, this structure is compatible with the sampled area in the central part of the blade, since the analyses suggested that only the outer part of the blade was finished/hardened by hammering. Another exception was the Canale Anfora sword, whose matrix exhibited a dendritic structure, with a large number of solidification porosity and globular sulphides, and, although it looks like a sword, these microstructural features led to its reinterpretation as more close to a bronze bar-ingot. For the majority of weapons, lead isotope analysis outlined a fairly homogenous picture indicating the South-East Alpine deposits as the most probable sources; however, some doubts arose for two axes of Castions di Strada that have a signal consistent with several Tyrol mines rich in chalcopyrite.

The situation discovered for the Porpetto shovels and arrowhead was different, since these objects were characterized by a low or negligible Sn content, offset by the addition of As, Sb, Ni and Co. This chemical pattern is similar to those of the Porpetto ingots and, therefore, it is natural to think that, given the low melting point, the ingots have been

simply cast into a mould in order to create the object, as supported by the presence of dendritic segregations. Consistently, the lead signal of these objects fell in the same area of the Porpetto. In this regard, since the shovels and the spearhead exhibited the same isotopic ratios and a quite similar chemical composition, one might assert that the craftsman in this site provided to the creation of artefacts using the available raw materials. Observing the quality of the employed alloy, especially for pick-ingots creation, two hypotheses can be made on the role of Porpetto in the commercial scene of the Late Bronze Age. If, in general, pick-ingots may be connected to a pre-monetary system and their shape would be a guarantee of high quality bronze, the doubt that Porpetto could be intended as a factory of "fake" ingots is considerable. Otherwise, since no information about the discovery of fahlerz and bronze pick-ingots in the same hoard has been remarked, it is possible that the trade spheres were strongly separated.

Nevertheless, there are still many aspects that should be investigated in order to complete the picture. Trace elements analyses, which are a powerful tool in the provenance issues, are currently in progress and will be applied both to metals and minerals in order to reduce the number of the possible copper sources in the doubtful cases, making the attribution as accurate as possible. Moreover, it would be useful to sample some Slovenian mines to fill this isotopic gap and, at the same way, it might be interesting to isotopically characterize the Slovenian ingots, especially pick-ingots. Finally, in the future, it might be fascinating to move the attention to the tin isotopes ratios for the cassiterite tracing, whereby the TS-ingot could be a proper sample.

Appendix 1

Appendix 1. Information about the find circumstances, category of items, typology and chronology of all the analyzed Bronze Age objects within this study. The materials are presently preserved to the National Archaeological Museums of Aquileia, to the National Archaeological Museums of Cividale and to the Soprintendenza of Udine. L=Lengh, W=Width, H=Height, Ø= Hole diameter, Fr=Fragment, U.D.=Unpublished data, "-"=impossible to date.

Sample	Typology	Description	Dimensions (cm)	Weight (g)	Context	Chronology	References
Bel-S	Sword, Sprockoff Ia - IIa	Broken	L 51.3 - W 3.2	486	Stray finds, S. Marco di Belvedere	MBA III	Foltiny 1964
Can-S	Sword	Fragment	L 22.4 - W 2.3	145	Stray finds, Canale Anfora	MBA III	U.D.
Cer-Ax	Winged-axe	Complete	L 14.2 - W blade 4.4 - H 2.3	208	Cervignano hoard	MBA-RBA	Borgna 2001; Vitri 1991
Cer-PC-56	Plano-convex ingot	Fragment	L 9.5 - W 6.8- H 2.6	447	Cervignano hoard	RBA	U.D.
Cer-PC-57	Plano-convex ingot	Fragment	Ø 6.8 - H 2.3	336	Cervignano hoard	RBA	U.D.
Cer-PC-66	Plano-convex ingot	Fragment	Ø 5.6 - H 3.2	441	Cervignano hoard	RBA	U.D.
Cer-PC-70	Plano-convex ingot	Fragment	L 6.5 -W 3.5 - H 3.8	315	Cervignano hoard	RBA	U.D.
Cer-PC-72	Plano-convex ingot	Fragment	Ø 4.6 - H 2.9	244	Cervignano hoard	RBA	U.D.
Cer-PC-79	Plano-convex ingot	Fragment	L 5.1 - W 3.5 - H 1.7	109	Cervignano hoard	RBA	U.D.
Cer-PS-61	Parallel-surface ingot	Fragment	L 7.1 - W 6.5 -H 2.6	556	Cervignano hoard	RBA	U.D.
Cer-PS-62	Parallel-surface ingot	Fragment	L 7.8 -W 5.1 - H 3.4	539	Cervignano hoard	RBA	U.D.
Cer-PS-64	Parallel-surface ingot	Fragment	L 4.6 - W 3.5 - H 2.4	216	Cervignano hoard	RBA	U.D.
Cer-PS-77	Parallel-surface ingot	Fragment	L 3.6 - W 2.5 - H 1.6	66	Cervignano hoard	RBA	U.D.
Cer-PS-82	Parallel-surface ingot	Fragment	L 2.7 - W 1.9 - H 1.0	26	Cervignano hoard	RBA	U.D.
Cer-TS	Tongue-shaped ingot	Fragment	L 5.3 - W 4.1 - H 0.8	91	Cervignano hoard	RBA	U.D.
Mus-S2	Flange-hilted sword, Cetona-type	Broken	L 15.0 - W blade 2.8	117	Muscoli hoard	RBA	Anelli 1949; Bianco Peroni 1970; Borgna 2001
Mus-S3	Flange-hilted sword, Sacile-type	Broken	L 11.8 - W blade 3.4	189	Muscoli hoard	MBA	Anelli 1949; Bianco Peroni 1970; Borgna 2001
Mus-Ax6	Socketed axe, "V" decoration	Complete	L 14.4 - W blade 5.1 Ø handle hole 4.7 x 6.2	547	Muscoli hoard	RBA-FBA	Anelli 1949; Borgna 2001 Carancini 1984; Marchesetti 1903; Vitri 1983
Mus-Ax7	Socketed axe, pseudo-wings decoration	Complete	L 9.2 - W blade 3.3 Ø handle hole 3.5 x 3.2	139	Muscoli hoard	FBA	Anelli 1949; Borgna 2001 Carancini 1984; Marchesetti 1903; Vitri 1983
Mus-PC-1	Plano-convex ingot	Fragment	L 17.7 - W 12.7 - H 7.2	3013	Muscoli hoard	RBA-FBA	U.D.
Mus-PC-2	Plano-convex ingot	Fragment	L 10.5 - W 5.1 - H 4.3	1453	Muscoli hoard	RBA-FBA	U.D.
Mus-PC-3	Plano-convex ingot	Fragment	L 12.6 - W9.0 - H 5.2	1415	Muscoli hoard	RBA-FBA	U.D.

Appendix 1 *(Continued)*

Sample	Typology	Description	Dimensions (cm)	Weight (g)	Context	Chronology	References
Mus-PC-6	Plano-convex ingot	Fragment	L 6.8 - W 3.8 - H 2.7	405	Muscoli hoard	RBA-FBA	U.D.
Mus-PC-7	Plano-convex ingot	Fragment	L 7.0 - W 3.6 - H 2.5	256	Muscoli hoard	RBA-FBA	U.D.
Mus-PC-8	Plano-convex ingot	2 Fragments	Fr.A: L 3.1 -W 2.6 - H 0.9; Fr.B: L 3.7 - W 4.1 - H 2.9	Fr.A: 41 Fr.B: 164	Muscoli hoard	RBA-FBA	U.D.
CdsA-S	Flange-hilted sword, Boiu-Keszethely type	Broken	L 5.9 - W 3.6 - H 0.6	65	Castions di Strada hoard	MBA II-III	Foltiny 1964; Borgna 2001
CdSA-Ax-59	Winged-axe	Broken	L 13.5 - W blade 4.6 - H 3.6	528	Castions di Strada hoard	MBA-RBA	Pellegrini 1911; Borgna 2001
CdSA-AxC-4	Socketed axe	Broken	L 8.6 - W 2.8 Ø handle hole 4x2.8	126	Castions di Strada hoard	FBA	Pellegrini 1911; Borgna 2001
CdSB-AxA1	Winged-axe	Complete	L 13.7 - W blade 3.6 - H 2.8	214	Castions di Strada hoard	RBA-FBA1	Borgna 2001
CdSB-AxA2	Winged-axe	Broken	L 11.1 - W blade 5.0 - H 1.8	260	Castions di Strada hoard	MBA-RBA	Borgna 2001
CdSB-AxA9	Winged-axe	Broken	L 12.8 - W blade 4.9 - H 3.9	550	Castions di Strada hoard	MBA-RBA	Borgna 2002
CdSB-Cp	Spearhead	Broken	L 3.8 -W 2.6 Ø handle hole 1.3	17	Castions di Strada hoard	-	Pellegrini 1911; Borgna 2001
CdSA-PnB	Bar-ingot	Fragment	L 4.8 - W 5.3 - H 1.0	121	Castions di Strada hoard	FBA1	Pellegrini 1911; Borgna 2001
CdSA-P-17	Plano-convex ingot	Complete	L 19.5 - W 14.5 H 4.0	2466	Castions di Strada hoard	FBA1	Pellegrini 1911
CdSA-P-19	Plano-convex ingot	2 Fragments	Fr.A: L 6.5 - W 4.0 - H 1.3 Fr.B: L 6.5 - W 4.3 - H 1.3	Fr. A: 126 Fr. B: 131	Castions di Strada hoard	FBA1	U.D.
CdSA-P-20	Plano-convex ingot	2 Fragments	Fr.A: L 18.5 - W 11 - H 7.5 Fr.B: L 18.5 - W 10.5 - H 7.5	Fr.A: 3084 Fr.B: 2621	Castions di Strada hoard	FBA1	U.D.
CdSB-P-50	Plano-convex ingot	Fragment	L 9.0 - W 3.8 - H 2.1	268	Castions di Strada hoard	FBA1	U.D.
CdSB-P-60	Plano-convex ingot	Fragment	L 10 - W 9.8 - H 2.0	573	Castions di Strada hoard	FBA1	U.D.
CdSB-P-61	Plano-convex ingot	Fragment	L 12.5 - W 13.2 - H 2.7	1088	Castions di Strada hoard	FBA1	U.D.
CdSB-P-81	Plano-convex ingot	Fragment	L 6.4 - W 7.7 - H 3.8	648	Castions di Strada hoard	FBA1	U.D.
CdSA-P-18	Truncated ingot	Complete	Ø 21.2 - H 7.5	8650	Castions di Strada hoard	FBA1	U.D.

Appendix 1 *(Continued)*

Sample	Typology	Description	Dimensions (cm)	Weight (g)	Context	Chronology	References
CdSA-P-22	Ingot	2 Fragments	Fr.A: L 9.0 - W 5.1. Fr.B: L 14.0 - W 7.0	Fr.A: 893 Fr.B: 430	Castions di Strada hoard	FBA1	U.D.
CdSB-P-71	Ingot	Fragment	L 8.2 - W 7.5 - H 7.5	1191	Castions di Strada hoard	FBA1	U.D.
CdSB-P-74	Ingot	Fragment	L 14.5 - W 6.0 - H 2.8	690	Castions di Strada hoard	FBA1	U.D.
Cel-S	Flange-hilted sword	Broken	L 13.3 - W blade 2.3	78	Celò hoard	MBA-RBA	Borgna 2007
Cel-AxA-2	Winged-axe	Complete	L 17.0 - W blade 4.8 - H 3.9	634	Celò hoard	MBA	Borgna 2007
Cel-AxA-3	Winged-axe	Complete	L 13.4 - W blade 2.7 - H 2.9	193	Celò hoard	MBA-RBA	Borgna 2007
Cel-AxA-8	Winged-axe	Broken	L 9.6 - W blade 4.9	115	Celò hoard	RBA	Borgna 2007
Cel-AxC-1	Socketed axe	Broken	L 15.5 - W blade 5.1 Ø hand hole 5.7x4.9	309	Celò hoard	RBA-FBA	U.D.
Cel-AxC-8	Socketed axe, "V" decoration	Complete	L 9.4 - W blade 6.1. Ø hand hole 4.1x2.6	487	Celò hoard	RBA-FBA	Borgna 2007
Cel-Pal	Socketed-shovel, *Fondo Paviani*-type	Broken	L 6.7 - W shoulders 3.4 Ø hand hole 3.1x2.1	71	Celò hoard	FBA	Borgna 2007; Bellintani and Stefan 2008
Cel-P37	Plano-convex ingot	Complete	Ø 17.9 - H 2.5	2822	Celò hoard	FBA1-2	Borgna 2007
Cel-P39	Plano-convex ingot	Complete	Ø 13.3 - H 5.0	3169	Celò hoard	FBA1-2	Borgna 2007
Cel-P41	Truncated ingot	Complete	Ø 13.1 - H 3.8	2309	Celò hoard	FBA1-2	Borgna 2007
Cel-P38	Truncated ingot	Complete	Ø 17.5 -H 5.2	6560	Celò hoard	FBA1-2	Borgna 2007
Ver-P0	Plano-convex ingot	Fragment	L 9.4 - W 4.4 - H 3.8	581	Verzegnis hoard	FBA1-2	U.D.
Ver-P9	Plano-convex ingot	Fragment	L 4.1 - W 2.9 - H 1.5	73	Verzegnis hoard	FBA1-2	U.D.
Gal-Ax	Winged-axe	Complete	L 18.2 - W blade 5.2 - H 4.0	470	Galleriano hoard	FBA2	Vitri 1999; Cividini 2000; Borgna 2001
Gal-PI-4	Pick-ingot	Arm fragment	L 6.9 - W 3.7 -H 2.7	405	Galleriano hoard	FBA1	Borgna 2001
Gal-PI-5	Pick-ingot	Arm fragment	L 5.9 - W 3.3 - H 3.5	426	Galleriano hoard	FBA2	Borgna 2001
Gal-PI-3	Blade/Ingot	Fragment	L 2.7. W 2.5	19	Galleriano hoard	FBA2	Borgna 2001
Por6-Pal	Socketed-shovel, Tra Manciano e Semprugnano-type	Handle-hole fragment	L 4.0 - W 3.0 - H 1.1 Ø handle hole 0.9	38	Porpetto hoard	FBA2	Borgna and Turk 1998; Bellintani and Stefan 2008
Por9-Pal	Socketed-shovel, Tra Manciano e Semprugnano-type	Shoulder/blade fragment	L 4.0 - W 1.5 - H 0.4	6	Porpetto hoard	FBA2	Borgna and Turk 1998; Bellintani and Stefan 2008
Por9-Cus-46	Spearhead	Fragment	L 2 - W 1.7 - H 0.6	6	Porpetto hoard	FBA2	U.D.

Appendix 1 *(Continued)*

Sample	Typology	Description	Dimensions (cm)	Weight (g)	Context	Chronology	References
Por-9-PI-60	Pick-ingot	Complete	L 14.7 - W 4.5 - H 2.6 Ø hole 2.6	963	Porpetto hoard	FBA2	Borgna and Turk 1998
Por-9-PI-64	Pick-ingot	Arm fragment	L 7.0 - W 3.5 - H 2.5	440	Porpetto hoard	FBA2	Borgna and Turk 1998
Por-9-PI-71	Pick-ingot	Arm fragment	L 11.3 - W 4.2 - H 2.8	124	Porpetto hoard	FBA2	Borgna and Turk 1998
Por-9-PI-73	Pick-ingot, without hole	Arm fragment	L 23.0 - W 8.2 - H 4.1	2856	Porpetto hoard	FBA2	Borgna and Turk 1998
Por-9-PI-77	Pick-ingot	Arm fragment	L 6.8 - W 4.1 - H 2.2 Ø hole 2.8	307	Porpetto hoard	FBA2	Borgna and Turk 1998
Por-9-PI-93	Pick-ingot	Arm fragment	L 9.2 - W 2.2 - H 2.4	485	Porpetto hoard	FBA2	Borgna and Turk 1998
Por-6-PI-9	Pick-ingot	Arm fragment	L 16.3 - W 6.3 - H 4.0 Ø hole 3.4	1035	Porpetto hoard	FBA2	Borgna and Turk 1998
Por-6-PC-5	Plano-convex ingot	Complete	Ø 24 - H 4.5	5500	Porpetto hoard	FBA2	U.D.
Por-6-PC-6	Plano-convex ingot	Fragment	L 11.2 - W 8.7 - H 4.1	962	Porpetto hoard	FBA2	U.D.
Por-9-Pn-25	Plano-convex ingot	Complete	L 10.0 - W 11.0 - H 5.0	1248	Porpetto hoard	FBA2	U.D.
Por-9-PC-24	Plano-convex ingot	Complete	L 17.3 - W 15.9 - H 3.2	1580	Porpetto hoard	FBA2	U.D.
Por-9-PC-30	Plano-convex ingot	Fragment	L 9.6 - W 15.6 - H 2.4	1175	Porpetto hoard	FBA2	U.D.
Por-9-PC-49	Plano-convex ingot	Fragment	L 3.8 - W 4.7 - H 0.9	60	Porpetto hoard	FBA2	U.D.
Por-9-Boz	Plano-convex ingot	Fragment	L 6.4 - W 4.1 - H 0.8	108	Porpetto hoard	FBA2	U.D.
Por-9-Tub	Plano-convex ingot	Fragment	L 6.7 - W 5.2 - H 2.4	314	Porpetto hoard	FBA2	U.D.
Por-6-TC-6	Truncated ingot	Complete	Ø 14.4 - H 4.5	2311	Porpetto hoard	FBA2	U.D.
Por-6-TC-8	Truncated ingot	Complete	Ø 25.0 - H 8.0	11250	Porpetto hoard	FBA2	U.D.
Por-9-TC-29	Truncated ingot	Fragment	L 21.0 - W 12.3 - H 4.3	3800	Porpetto hoard	FBA2	U.D.
Por-9-LAP	Bar-ingot	Fragment	L 10.4 - W 4.2 - H 0.8	214	Porpetto hoard	FBA2	U.D.
Por-9-Bar-2	Bar-ingot	Complete	L 16.4 - W 3.2 - H 0.6	250	Porpetto hoard	FBA2	U.D.
Por-9-Bar-5	Bar-ingot	Fragment	L 10.3 - W 8.1 - H 0.6	663	Porpetto hoard	FBA2	U.D.
Por-6-SN-1	flat/blade's axe-ingot	Fragment	L 6.2 - W 4.6 - H 0.4	54	Porpetto hoard	FBA2	U.D.
Por-6-SN-2	flat/blade's axe-ingot	Fragment	L 5.2 - W 4.1 - H 0.4	39	Porpetto hoard	FBA2	U.D.
Por-6-SN-7	flat/blade's axe-ingot	Fragment	L 3.2 - W 2.3 - H 0.9	46	Porpetto hoard	FBA2	U.D.
Por-6-SN-8	flat/blade's axe-ingot	Fragment	L 7.0 - W 4.3 - H 0.8	155	Porpetto hoard	FBA2	U.D.
Por-6-PP-7	Ingot	Fragment	Ø 14.2 - H 2.5	1131	Porpetto hoard	FBA2	U.D.

Appendix 2

Appendix 2: Table 1. Mean chemical analyses of all the objects and ingots obtained by SEM-EDS area analyses (wt%). Data are calculated as a mean of 3÷5 area analyses. For each sample the main features observed by SEM-EDS are reported. SD = standard deviation of the measures; tr= detected in traces; N.D.=Not Detected.

Sample	Cu	Sn	Fe	Zn	S	Pb	As	Sb	Ni	Co	Ag	Sulphides	Sulphide zoning	Other inclusions
CAN-S	85.4	12.3			1.0	1.3						$(Cu,Fe)_2S$	Fe+Zn	(Pb,Bi)-particles; (α+δ)-phase (traces of Co, Ni, Ag and Pb).
SD	*0.6*	*0.3*			*0.1*	*0.4*								
BEL-S	85.6	11.0			0.8	1.3			1.4			Cu_2S; $(Cu,Fe)_2S$	Fe	(Pb,Bi)-particles; (α+δ)-phase (traces of Co, Ni, Ag and Pb).
SD	*0.9*	*0.5*			*0.2*	*0.5*			*0.2*					
CER-Ax	89.3	8.9			0.4	0.8			0.5			Cu_2S; $(Cu,Fe)_2S$	Fe; Fe+Zn.	(Pb,Bi)-particles.
SD	*0.4*	*0.3*			*0.0*	*0.2*			0.2					
Cer-TS	76.3	20.2	1.1		0.5	0.6			1.2			Cu_2S; $(Cu,Fe)_2S$	Fe; Zn+Fe	Cu prills; Fe-rich segregations (74%Fe)
SD	*1.7*	*1.6*	*0.1*		*0.2*	*0.6*			*0.0*					
Cer-PS-61	94.4		1.0		1.9	2.6						$(Cu,Fe)_2S$	Zn+Fe	(Pb,Ag, Sb)-particles.
SD	*1.6*		*0.2*		*0.3*	*1.3*								
Cer-PS-62	96.5		0.5		1.4	1.5						Cu_2S; $(Cu,Fe)_2S$	Fe; Fe+Zn; FeOx	(Pb,Ag, Sb)-particles; Ag and As in sulphides.
SD	*1.4*		*0.2*		0.9	*0.9*								
Cer-PS-64	92.4		2.6		1.7	1.3		1.9				$(Cu,Fe)_2S$	Zn+Fe; Fe+Zn+Sb	(Pb,Bi)-particles. Sb-rich segregations; Sb in sulphides.
SD	*1.1*		*0.5*		*0.5*	*0.4*		0.1						
Cer-PS-77	95.6		1.9		1.1	1.4						$(Cu,Fe)_2S$	Zn+Fe	(Pb,Bi)-particles; (Pb,Ag)-particles; Fe-Co segregations.
SD	*0.5*		*0.2*		*0.1*	*0.8*								
Cer-PS-82	93.6		3.5		1.4	1.5						$(Cu,Fe)_2S$; $(Cu,Fe,Zn)_2S$	N.D.	(Pb,Bi,Ag)-particles. Fe-rich segregations; Fe inclusions; Cu prill.
SD	*0.6*		*0.3*		*0.5*	*0.8*								
Cer-PC-56	95.0		1.4		1.7	1.9						$(Cu,Fe)_2S$	Zn+Fe; Co tr	(Pb,Bi)-particles; (Pb,Bi,Ag)-particles.
SD	*0.4*		*0.1*		*0.5*	*0.5*								
Cer-PC-57	94.3		1.6		1.6	2.6						Cu_2S; $(Cu,Fe)_2S$	Zn+Fe	(Pb,Bi)-particles.
SD	*0.2*		*0.2*		*0.2*	*0.2*								
Cer-PC-66	95.2		1.5		1.5	1.8						(Cu,Fe)2S; $(Cu,Fe,Zn)_2S$	Zn+Fe	(Pb,Bi)-particles; (Pb,Bi,Ag)-particles.
SD	*0.6*		*0.1*		*0.2*	*0.9*								
Cer-PC-70	98.1				1.9	tr.						Cu_2S; $(Cu,Fe)_2S$	Zn+Fe	(Pb,Bi)-particles.
SD	*0.5*				*0.5*									
Cer-PC-72	96.7				1.4	1.9						Cu_2S; $(Cu,Fe)_2S$	N.D.	(Pb,Bi)-particles; (Pb,Bi,Ag)-particles.
SD	*0.7*				*0.3*	*0.9*								
Cer-PC-79	98.2				1.8	tr.						$(Cu,Fe)_2S$	Zn+Fe	(Pb,Bi)-particles; (Pb,Bi,Ag)-particles.
SD	*0.1*				*0.1*									
Mus-S2	84.6	12.1			0.8	0.7			1.6			$(Cu,Fe)_2S$	Fe; FeOx; Fe+Sn	(Pb,Bi)-particles.
SD	*0.7*	*0.2*			*0.2*	*0.6*			*0.2*					
Mus-S3	85.1	12.1			0.9	0.4			1.3			$(Cu,Fe)_2S$	Fe	(Pb,Bi)-particles.
SD	*1.3*	*1.1*			*0.2*	*0.6*			*0.4*					
Mus-Ax 6	90.2	8.2			0.7	0.9			1.2			Cu_2S; $(Cu,Fe)_2S$	Fe, FeOx	(Pb,Bi)-particles; δ-phase (traces of Pb, Ni, Sb and Ag)
SD	*0.9*	*0.7*			*0.5*	*0.7*			*0.3*					
Mus-Ax 7	84.5	12.2			0.4	1.4			1.4			$(Cu,Fe)_2S$	Fe, FeOx	(Pb,Bi)-particles.
SD	*0.3*	*0.3*			*0.3*	*0.6*			*0.3*					
Mus-PC-1	96.2				1.5	2.4						$(Cu,Fe)_2S$	Fe	(Pb,Bi)-particles; (Pb,Bi,Ag)-particles.
SD	*0.9*				*0.5*	*1.2*								
Mus-PC-2	97.3				1.4	1.3						Cu_2S	Fe,Co,Sn,Zn	(Pb,Bi,As)-particles; Sn-rich inclusions (86-93%Sn)
SD	*0.6*				*0.4*	*0.7*								
Mus-PC-3	96.9				1.5	1.6						Cu_2S; $(Cu,Fe)_2S$	N.D.	(Pb,Ag)-particles, (Pb,Bi)-particles; Pb, Ag, As in sulphides.
SD	*0.6*				*0.2*	*0.5*								
Mus-PC-6	95.2		3.0		1.8							Cu_2S	Fe	N.D.
SD	*0.3*		*0.0*		*1.8*									
Mus-PC-7	97.3		1.0		1.7							$(Cu,Fe)_2S$	FeOx	N.D.
SD	*0.7*		*0.2*		*0.7*									
Mus-PC-8	95.9				1.8	2.2						$(Cu,Fe)_2S$	Zn	(Pb,Ag)-particles, (Pb,Bi)-particles.
SD	*1.0*				*0.1*	*0.9*								

Appendix 2: Table 1 *(Continued)*

Sample	Cu	Sn	Fe	Zn	S	Pb	As	Sb	Ni	Co	Ag	Sulphides	Sulphide zoning	Other inclusions
CdSA-S	86.2	10.3	0.9		0.8	0.8			1.0			$(Cu,Fe)_2S$	Fe+Zn; Fe	(Pb,Bi)-particles; No (α+δ)-phase; Pb in sulphides.
SD	*0.3*	*0.3*	*0.1*		*0.1*	*0.5*			*0.1*					
CdSA-Ax-59	84.2	12.9			0.5	1.4			1.0			Cu_2S; $(Cu,Fe)_2S$	(Fe-Co)Ox FeOx	(Pb,Bi)-particles; (α+δ)-phase (with traces of Ni, Co, Ag and Pb); Pb in sulphides.
SD	*0.6*	*0.3*			*0.3*	*0.7*			*0.4*					
CdSA-AxC-4	86.7	11.1			1.0	0.2			1.0			Cu_2S; $(Cu,Fe)_2S$	N.D.	(Pb,Bi)-particles; (α+δ)-phase (with traces of Ni, Co and Pb); Pb in sulphides.
SD	*1.0*	*1.0*			*0.1*	*0.2*			*0.3*					
CdSB-AxA-1	86.1	13.1			0.4	0.4						Cu_2S; $(Cu,Fe)_2S$	FeOx, Fe+Zn, Fe	(Pb,Bi)-particles; (α+δ)-phase (with traces of Ni, Co and Ag); Fe oxides; Pb,Co and Zn in sulphides.
SD	*0.3*	*0.3*			*0.1*	*0.3*								
CdSB-AxA-2	88.8	5.6			0.6	1.6	2.0		1.4			Cu_2S	(Fe-Co)Ox (Fe,Co,Zn)Ox	(Pb,Bi)-particles; No δ-phase; Pb and Ag in sulphides.
SD	*1.6*	*0.7*			*0.3*	*1.1*	*0.4*		*0.1*					
CdSB-AxA-9	91.0	8.3			0.3	0.4						Cu_2S; $(Cu,Fe)_2S$	Fe, FeOx	(Pb,Bi)-particles. No δ-phase.
SD	*0.2*	*0.1*			*0.1*	*0.3*								
CdSB-Cp	85.0	12.1			1.0	0.5			1.4			(CuFe)2S	Fe, Fe+Zn, FeOx	(Pb,Bi)-particles. No δ-phase.
SD	*1.0*	*0.6*			*0.2*	*0.4*			*0.2*					
CdSA-PnB	91.0		1.0		1.4	tr	3.6	2.1	1.0			Cu_2S; $(Cu,Fe)_2S$	N.D.	As-rich segregations; Ag, Sn, Ni and Co in sulphides.
SD	*0.4*		*0.2*		*0.3*		*1.7*	*0.2*	*0.2*					
CdSA-P-17	92.3		1.0		1.5	1.3	2.2	1.0				$(Cu,Fe)_2S$	Fe, FeOx	Pb particles; As-rich segregations; Co and As in sulphides.
SD	*1.1*		*0.2*		*0.5*	*0.6*	*0.5*	*0.6*						
CdSA-P-18	96.2		0.7		1.8	1.3						$(Cu,Fe)_2S$	N.D.	(Pb,Bi)-particles; Pb, Ag and Co in sulphides.
SD	*0.5*		*0.2*		*0.7*	*0.4*								
CdSA-P-19	94.5		2.3		1.6	1.6						$(Cu,Fe)_2S$	Fe	(Pb,Bi)-particles, (Pb,Ag)-particles; Pb, Ag and Zn in sulphides.
SD	*1.0*		*0.1*		*0.7*	*0.5*								
CdSA-P-20	89.5		0.7		3.8	1.6	1.2	1.6	1.5			Cu_2S; $(Cu,Fe)_2S$	Fe	Sb-rich segregations
SD	*0.6*		*0.1*		*0.5*	*0.3*	*0.3*	*0.4*	*0.1*					
CdSA-P-22	92.3						4.4	3.3				Cu_2S	N.D.	(Pb,As,Sb)-particles; (As,Sb)- rich segregations; mineral remains.
SD	*1.3*						*0.4*	*1.0*						
CdSB-P-50	96.5		1.3		2.2	tr						$(Cu,Fe)_2S$	N.D.	(Pb,As)-particles; As-rich segregations; Co, As and Pb in sulphides.
SD	*0.5*		*0.2*		*0.3*									
CdSB-P-60	82.5		9.5		2.3		3.2	1.3	1.1			$(Cu,Fe)_2S$	Fe	(Pb,As,Sb)-particles; As-rich segregations;Fe-rich phases (89%Fe); As and Ni-Co in sulphides.
SD	*6.6*		*5.6*		*0.5*		*0.2*	*0.6*	*0.2*					
CdSB-P-61	93.8				1.9		1.9	1.5	1.8			Cu_2S	(Fe, Co, Ni, Zn)Ox	Ag-particles; Sb-rich segregations.
SD	*1.3*				*0.6*		*0.5*	*0.4*	*0.2*					
CdSB-P-71	96.9		0.7		2.4							$(Cu,Fe)_2S$	Fe-Co	(Pb,Ag)-particles; As in sulphides.
SD	*1.8*		*0.5*		*1.6*									
CdSB-P-74	91.7		1.0		1.5	tr	3.4	2.4				Cu_2S; $(Cu,Fe)_2S$	N.D.	(Pb,As,Sb)-particles;Sb-rich segregations; Fe-Co phases.
SD	*0.3*		*0.2*		*0.6*		*0.7*	*0.6*						
CdSB-P-81	96.5				1.5	2.5						$(Cu,Fe)_2S$	N.D.	(Pb,Bi)-particles; Pb and Zn in sulphides.
SD	*0.5*				*0.2*	*0.7*								
Cel-Pal	92.5	5.7			0.4	0.6			0.6			$(Cu,Fe)_2S$	Fe	Pb-particles; (α+δ)-phase with Ni (1%).
SD	*0.4*	*0.3*			*0.0*	*0.1*			*0.1*					
Cel-AxC1	91.3	6.9			0.2	0.6			0.9			Cu_2S	FeOx	Pb-particles; (α+δ)-phase with Ni (3%).
SD	*0.8*	*0.5*			*0.1*	*0.3*			*0.4*					

Appendix 2. Table 1 *(Continued)*

Sample	Cu	Sn	Fe	Zn	S	Pb	As	Sb	Ni	Co	Ag	Sulphides	Sulphide zoning	Other inclusions
Cel-AxC8	91.0	8.0			0.2	0.4			0.3			Cu_2S	Fe	Pb-particles; (Pb,Bi)-particles; (α+δ)-phase with Ni (3%).
SD	*0.2*	*0.7*			*0.1*	*0.4*			*0.1*					
Cel-AxA2	92.4	6.7			0.3	0.7						Cu_2S	FeOx	(Pb,Bi)-particles; No δ-phase.
SD	*0.2*	*0.2*			*0.1*	*0.1*								
Cel-AxA3	90.9	8.1			0.2	0.8						$(Cu,Fe)_2S$	Fe	(Pb,Bi)-particles; No δ-phase.
SD	*0.2*	*0.2*			*0.2*	*0.0*								
Cel-AxA8	91.0	7.7			0.4	0.4			0.5			$(Cu,Fe)_2S$	Fe; FeOx	(Pb,Bi)-particles; No δ-phase.
SD	*0.1*	*0.2*			*0.0*	*0.1*			*0.1*					
Cel-S	90.2	8.8			0.3	0.7						Cu_2S; $(Cu,Fe)_2S$	(Fe,Zn)Ox Co tr	(Pb,Bi)-particles; (α+δ)-phase (with traces of Pb, Ag and Ni).
SD	*0.4*	*0.3*			*0.0*	*0.2*								
Cel-P37	97.0		0.8		1.3	0.9			tr			$(Cu,Fe)_2S$	Fe	Pb-particles.
SD	*0.8*		*0.0*		*0.2*	*0.8*								
Cel-P38	97.8				0.8	1.4						Cu_2S	(Fe,Zn)Ox Sn tr	(Pb,Bi)-particles.
SD	*0.6*				*0.1*	*0.7*								
Cel-P39	98.5		0.6		0.9							$(Cu,Fe)_2S$	Fe	Pb-particles; (Pb,As,Sb)-particles.
SD	*0.2*		*0.1*		*0.2*									
Cel-P41	97.2		0.8		0.9	1.2						Cu_2S; $(Cu,Fe)_2S$	N.D.	Pb particles.
SD	*0.6*		*0.0*		*0.4*	*0.5*								
Ver-P0	94.5		3.2		1.0	1.3						$(Cu,Fe)_2S$	Zn	Pb particles; Fe-rich phases (90%Fe); Sb-rich segregations.
SD	*0.5*		*0.3*		*0.1*	*0.1*								
Ver-P9	90.9		1.8	1.7	0.8	2.4	2.4					$(CuFe)_2S$; $(CuFeZn)_2S$	Zn	(Pb,Ag)-particles; Sb-rich segregations; Fe-rich phases (83%Fe).
SD	*0.6*		*0.0*	*0.1*	*0.2*	*0.3*	*0.4*							
Gal-Ax	88.9	9.9			0.1	1.1						$(Cu,Fe)_2S$	Fe	Pb particles.
SD	*0.4*	*0.2*			*0.1*	*0.2*								
Gal-PI3	93.4		1.5	1.3	0.5	2.4		0.8				$(Cu,Fe)_2S$	Fe-Zn	(Pb,Bi)-particles; Sb-rich segregations.
SD	*0.6*		*0.1*	*0.7*	*0.1*	*0.6*		*0.1*						
Gal-PI4	88.1	12.0	0.9		1.0	tr						$(Cu,Fe)_2S$	Fe-Zn	Pb particles; (Pb,Ag)-particles; δ-phase.
SD	*0.6*	*0.6*	*0.0*		*0.1*									
Gal-PI5	81.0	15.0	1.3		1.3	tr						Cu_2S	Fe; Fe-Zn	Pb particles; (α+δ)-phase.
SD	*1.3*	*0.6*	*0.1*		*0.9*									
Por6-Pal	55.1				0.6	23.0	10.5	6.8	3.4	0.7		Cu_2S	N.D.	(Pb,Sb)-particles; Sb-rich segregations.
SD	*6.7*				*0.1*	*5.3*	*1.5*	*0.6*	*0.2*	*0.0*				
Por6-PI-9	73.7		1.9		0.7	12.3	5.1	2.2	3.0	1.0		Cu_2S	N.D.	(Pb,Ag)-particles; Sb-rich segregations; (Fe,Co,Ni) phases
SD	*1.5*		*0.5*		*0.1*	*1.9*	*0.2*	*0.1*	*0.2*	*0.2*				
Por6-TC-6	89.1				0.3	0.2	2.9	5.9			1.6	$(Cu,Fe)_2S$	(Fe,Co,Zn,Sn) Ox	(Pb,Sb,Ag)-particles;Sb-rich segregations; Ag, As and Sb in sulphides.
SD	*0.5*				*0.1*	*0.1*	*0.2*	*1.2*			*0.8*			
Por6-TC-8	91.7				1.1	1.2	tr	1.6	3.1	0.5	0.7	Cu_2S	N.D.	(Pb,Ag)-particles;Sb-rich segregations.
SD														
Por6-PC-5	94.3				0.1	0.2	2.1	2.2			1.0	Cu_2S	N.D.	Sb-rich segregations; cuprite.
SD	*0.4*				*0.1*	*0.2*	*0.3*	*0.7*			*0.2*			
Por6-PC-6	90.7		0.3		1.7	1.4	tr	1.2	3.4	0.8	0.7	$(Cu,Fe)_2S$	Zn	(Pb,Ag)-particles.Sb-rich segregations.
SD	*0.3*		*0.0*		*0.1*	*0.3*		*0.3*	*0.2*	*0.1*	*0.1*			
Por6-PP-7	93.8						3.3	2.1			0.9	Cu_2S	N.D.	(As,Sb)-rich segregations; mineral remains.
SD	*0.5*						*0.5*	*0.2*			*0.2*			
Por6-SN-1	73.0		2.2		1.6	1.5	3.6	6.9	8.3	3.0		Cu_2S	Fe	(Pb,Ag)-particles. Sb-rich segregations; (Fe,Co,Ni)-phases.
SD	*0.2*		*0.1*		*0.1*	*0.3*	*0.2*	*0.1*	*0.2*	*0.1*				
Por6-SN-2	74.0		3.1		1.1	1.2	5.5	4.6	7.0	2.7		$(Cu,Fe)_2S$	Fe	(Pb,As,Sb)-particles; As-rich segregations; (Fe,Co,Ni)-phases.
SD	*0.6*		*0.3*		*0.1*	*0.2*	*0.1*	*0.3*	*0.1*	*0.3*				

Appendix 2. Table 1 *(Continued)*

Sample	Cu	Sn	Fe	Zn	S	Pb	As	Sb	Ni	Co	Ag	Sulphides	Sulphide zoning	Other inclusions
Por6-SN-2	74.0		3.1		1.1	1.2	5.5	4.6	7.0	2.7		$(Cu,Fe)_2S$	Fe	(Pb,As,Sb)-particles; As-rich segregations; (Fe,Co,Ni)-phases.
SD	*0.6*		*0.3*		*0.1*	*0.2*	*0.1*	*0.3*	*0.1*	*0.3*				
Por6-SN-7	85.9	3.8	0.6		0.5	tr	1.2	7.4	0.6			$(Cu,Fe)_2S$	Fe, Zn	(Pb,Bi)-particles; Sb-rich segregations.
SD	*0.4*	*0.2*	*0.2*		*0.1*		*0.1*	*0.1*	*0.1*					
Por6-SN-8	88.1				0.6	1.1	3.5	5.7			1.0	Cu_2S	N.D.	(Pb,Bi,Sb)-particles; Sb-rich segregations.
SD	*0.5*				*0.1*	*0.1*	*0.4*	*0.1*			*0.1*			
Por9-Cus-46	82.5	6.0			0.5	0.9	2.6	3.8	3.1	0.7		$(Cu,Fe)_2S$	N.D.	(Pb,Bi,Ag)-particles; (Sb,Sn,As)-rich segregations.
SD	*1.4*	*0.5*			*0.0*	*0.4*	*0.2*	*0.7*	*0.1*	*0.0*				
Por9-Pal	82.6	7.2	0.8		1.1	1.1	1.6	1.7	3.1	1.0		$(Cu,Fe)_2S$	Fe	Pb particles; (α+δ)-phase with Ni (6%), Sb (4%) and As (2%).
SD	*1.4*	*0.6*	*0.0*		*0.0*	*0.2*	*0.2*	*0.3*	*0.1*	*0.0*				
Por9-Pn-25	84.8		13.5		1.1	1.0						Cu_2S; $(Cu,Fe)_2S$	N.D.	Pb particles;Fe-rich phases; Fe oxides; Zn in sulphides.
SD	*4.7*		*4.2*		*0.2*	*0.0*								
Por9-TC-29	90.5		0.6		1.6	1.6	1.1	1.2	1.8	0.9		$(Cu,Fe)_2S$	N.D.	(Pb,Bi,Ag)-particles; Ag-rich phase; Sb-rich segregations; Pb, Co, Ni, Zn, As and Ag in sulphides.
SD	*0.2*		*0.0*		*0.1*	*0.2*	*0.0*	*0.0*	*0.1*	*0.0*				
Por9-PC-24	84.9				0.6		4.6	7.2	1.5		1.3	Cu_2S	N.D.	Ag particles; Sb-rich segregations; mineral remains; Pb, Sb and Ag in sulphides.
SD	*1.4*				*0.5*		*0.3*	*0.4*	*0.4*		*0.7*			
Por9-PC-30	84.5				tr		6.1	7.9			1.5	N.D.	N.D.	(As,Sb)-rich segregations.
SD	*0.7*						*0.1*	*0.4*			*0.3*			
Por9-PC-49	89.5		0.2		tr		4.1	4.8			1.3	N.D.	N.D.	(Pb,As,Sb)-particles; (As,Sb)-rich segregations; mineral remains.
SD	*0.5*		*0.1*				*0.2*	*0.5*			*0.4*			
Por9-Boz	90.1		0.4		4.7		0.8	4.1				Cu_2S; $(Cu,Fe)_2S$	Fe	Sb-rich segregations
SD	*0.7*		*0.0*		*0.7*		*0.1*	*0.0*						
Por9-Tub	88.7				0.3		3.5	6.0			1.6	Cu_2S	N.D.	(Pb,Bi,Ag)-particles; As-rich phases; Sb-rich segregations; Pb in sulphides.
SD	*0.6*				*0.1*		*0.2*	*0.2*			*0.2*			
Por9-LAP	83.9				0.9	1.0	4.7	9.4				Cu_2S	N.D.	Sb-rich phases (80% Sb); Sb-rich phases; Pb in sulphides.
SD	*1.3*				*0.1*	*0.3*	*0.3*	*1.1*						
Por9-Bar-2	84.5				0.5	0.6	5.8	5.1	2.6		1.1	Cu_2S	(Co-Ni)Ox	(Pb,Ag)-particles; Sb-rich phases; Co, Ni, As and Ag in sulphides.
SD	*0.5*				*0.2*	*0.3*	*0.4*	*0.5*	*0.2*		*0.1*			
Por9-Bar-5	77.3		3.3		1.8	1.4	7.0	2.4	4.3	2.5		Cu_2S; $(Cu,Fe)_2S$	Fe	Sb-rich phases; (Fe,Co,Ni)-rich phases;mineral remains; Co, Ni, As and Sb in sulphides.
SD	*0.4*		*0.2*		*0.8*	*0.4*	*0.4*	*0.4*	*0.3*	*0.2*				
Por9-PI-60	86.3				0.4	0.6	5.0	6.1			1.6	Cu_2S	N.D.	Ag particles; Sb-rich phases; Sb, As, Ag in sulphides.
SD	*1.9*				*0.1*	*0.1*	*0.2*	*1.8*			*0.1*			
Por9-PI-64	89.3		1.0		1.6	tr	2.6	2.4	2.7	0.6		Cu_2S; $(CuFeCoNi)_2S$	Fe	Ag particles; Pb particles; Sb-rich phases; Sb, As, Ag and Pb in sulphides.
SD	*0.2*		*0.2*		*0.1*		*0.3*	*0.2*	*0.1*	*0.1*				
Por9-PI-71	83.0		1.7		1.5	1.0	4.8	2.5	4.0	1.5		$(Cu,Fe)_2S$	N.D.	(Pb,Ag)-particles; As-rich phases; Co, Zn, Sb, As, Ag and Pb in sulphides.
SD	*0.3*		*0.1*		*0.2*	*0.1*	*0.2*	*0.2*	*0.1*	*0.1*				

Appendix 2. Table 1 *(Continued)*

Sample	Cu	Sn	Fe	Zn	S	Pb	As	Sb	Ni	Co	Ag	Sulphides	Sulphide zoning	Other inclusions
Por9-PI-73	81.3		2.9		1.4	0.9	4.7	2.8	4.1	2.0		Cu_2S; $(Cu,Fe)_2S$	Fe	(As,Sb)-rich phases; (Fe,Co,Ni)-rich segregations; Co, Ni, Sb, As and Ag in sulphides.
SD	*1.1*		*0.3*		*0.1*	*0.1*	*0.2*	*0.4*	*0.4*	*0.1*				
Por9-PI-77	79.2		3.6		1.7	1.0	5.3	0.9	6.6	1.9		Cu_2S; $(Cu,Fe)_2S$	N.D.	As-rich phases; (Fe,Co,Ni)-rich segregations.
SD	*0.5*		*0.1*		*0.1*	*0.4*	*0.0*	*0.1*	*0.1*	*0.1*				
Por9-PI-93	80.6		2.4		1.9	1.1	2.8	3.2	5.9	2.2		$(Cu,Fe)_2S$	Fe	Sb-rich phases;(Fe,Co,Ni)-rich segregations.
SD	*1.2*		*0.2*		*0.7*	*0.2*	*0.2*	*0.4*	*0.3*	*0.2*				

Appendix 2: Table 2. Quantitative EPMA chemical analyses (wt%) of the α- phase of the metal of all the samples. Data are calculated as a mean of 7÷10 points analysis. d.l. = detection limit; SD = standard deviation of the measures; "*" = arithmetic mean between Cu-rich and Cu-poor phases.

Sample	S	Cl	Mn	Fe	Co	Ni	Cu	Zn	As	Ag	Sn	Sb	Pb	Bi
d.l. (%)	**0.03**	**0.02**	**0.03**	**0.02**	**0.02**	**0.03**	**0.1**	**0.05**	**0.06**	**0.06**	**0.05**	**0.05**	**0.12**	**0.45**
CAN-S*	0.01	0.00	0.01	0.05	0.03	0.02	89.88	0.03	0.00	0.05	10.95	0.00	0.09	0.00
SD	*0.01*	*0.00*	*0.01*	*0.01*	*0.01*	*0.01*	*1.71*	*0.04*	*0.00*	*0.03*	*2.11*	*0.00*	*0.11*	*0.00*
BEL-S*	0.00	0.00	0.01	0.05	0.03	0.55	89.79	0.02	0.23	0.04	9.58	0.00	0.04	0.08
SD	*0.01*	*0.00*	*0.01*	*0.01*	*0.01*	*0.05*	*1.49*	*0.02*	*0.05*	*0.02*	*0.99*	*0.00*	*0.04*	*0.16*
CER-Ax	0.01	0.00	0.00	0.07	0.02	0.28	88.45	0.01	0.13	0.14	10.56	0.00	0.04	0.00
SD	*0.02*	*0.01*	*0.00*	*0.02*	*0.02*	*0.02*	*0.60*	*0.01*	*0.05*	*0.03*	*0.82*	*0.00*	*0.03*	*0.00*
Cer-TS	0.00	0.00	0.01	0.79	0.06	0.55	85.88	0.01	0.27	0.02	13.48	0.00	0.05	0.00
SD	*0.00*	*0.01*	*0.01*	*0.08*	*0.01*	*0.04*	*0.86*	*0.01*	*0.09*	*0.03*	*0.59*	*0.00*	*0.07*	*0.00*
Cer-PS-61	0.01	0.00	0.01	0.44	0.06	0.03	98.86	0.64	0.04	0.07	0.05	0.15	0.07	0.00
SD	*0.01*	*0.00*	*0.02*	*0.05*	*0.02*	*0.02*	*0.16*	*0.06*	*0.05*	*0.03*	*0.04*	*0.10*	*0.08*	*0.01*
Cer-PS-62	0.01	0.00	0.00	0.07	0.01	0.01	99.79	0.08	0.17	0.06	0.01	0.00	0.11	0.00
SD	*0.01*	*0.00*	*0.01*	*0.01*	*0.02*	*0.01*	*0.41*	*0.06*	*0.06*	*0.03*	*0.02*	*0.01*	*0.10*	*0.00*
Cer-PS-64	0.01	0.00	0.00	2.52	0.07	0.01	96.37	0.38	0.09	0.03	0.18	0.09	0.04	0.02
SD	*0.01*	*0.00*	*0.00*	*0.21*	*0.02*	*0.01*	*0.88*	*0.06*	*0.06*	*0.03*	*0.11*	*0.09*	*0.09*	*0.04*
Cer-PS-77	0.01	0.00	0.00	1.73	0.10	0.04	98.22	0.30	0.01	0.05	0.03	0.05	0.06	0.00
SD	*0.01*	*0.01*	*0.01*	*0.23*	*0.02*	*0.02*	*0.89*	*0.03*	*0.01*	*0.02*	*0.03*	*0.05*	*0.06*	*0.00*
Cer-PS-82	0.01	0.01	0.01	2.22	0.08	0.03	97.76	0.27	0.15	0.10	0.07	0.16	0.01	0.00
SD	*0.01*	*0.01*	*0.01*	*0.45*	*0.03*	*0.03*	*1.03*	*0.06*	*0.06*	*0.05*	*0.04*	*0.05*	*0.03*	*0.00*
Cer-PC-56	0.01	0.01	0.01	0.76	0.05	0.02	99.43	0.56	0.04	0.06	0.02	0.07	0.09	0.00
SD	*0.01*	*0.01*	*0.01*	*0.05*	*0.01*	*0.02*	*0.54*	*0.06*	*0.04*	*0.04*	*0.03*	*0.04*	*0.07*	*0.00*
Cer-PC-57	0.01	0.01	0.00	0.81	0.05	0.03	99.41	0.22	0.28	0.08	0.05	0.06	0.05	0.00
SD	*0.01*	*0.01*	*0.00*	*0.10*	*0.01*	*0.03*	*0.34*	*0.03*	*0.20*	*0.05*	*0.05*	*0.05*	*0.05*	*0.00*
Cer-PC-66	0.01	0.00	0.01	0.90	0.04	0.02	99.34	0.23	0.04	0.04	0.04	0.05	0.00	0.06
SD	*0.01*	*0.00*	*0.01*	*0.05*	*0.02*	*0.02*	*0.56*	*0.05*	*0.02*	*0.05*	*0.02*	*0.03*	*0.00*	*0.13*
Cer-PC-70	0.02	0.01	0.00	0.27	0.07	0.04	99.94	0.04	0.31	0.09	0.09	0.05	0.05	0.00
SD	*0.04*	*0.01*	*0.00*	*0.04*	*0.01*	*0.03*	*0.68*	*0.03*	*0.12*	*0.05*	*0.06*	*0.02*	*0.05*	*0.00*
Cer-PC-72	0.00	0.00	0.01	0.12	0.02	0.03	99.85	0.07	0.03	0.07	0.03	0.14	0.16	0.00
SD	*0.01*	*0.00*	*0.01*	*0.03*	*0.01*	*0.02*	*0.21*	*0.05*	*0.04*	*0.04*	*0.04*	*0.05*	*0.14*	*0.00*
Cer-PC-79	0.01	0.01	0.00	0.37	0.02	0.03	99.16	0.11	0.10	0.08	0.04	0.16	0.07	0.00
SD	*0.01*	*0.01*	*0.00*	*0.03*	*0.01*	*0.02*	*0.29*	*0.03*	*0.04*	*0.04*	*0.01*	*0.07*	*0.08*	*0.00*
Mus-S2	0.11	0.01	0.01	0.01	0.04	0.65	86.69	0.02	0.35	0.05	11.97	0.00	0.06	0.00
SD	*0.20*	*0.01*	*0.01*	*0.01*	*0.01*	*0.07*	*0.32*	*0.03*	*0.07*	*0.03*	*0.26*	*0.00*	*0.10*	*0.00*
Mus-S3	0.02	0.01	0.01	0.05	0.04	0.38	86.76	0.01	0.21	0.04	12.66	0.00	0.05	0.02
SD	*0.02*	*0.01*	*0.01*	*0.02*	*0.02*	*0.05*	*0.49*	*0.03*	*0.04*	*0.05*	*0.41*	*0.00*	*0.07*	*0.05*
Mus-Ax 6*	0.00	0.01	0.01	0.03	0.03	0.36	92.87	0.01	0.25	0.05	7.12	0.09	0.13	0.00
SD	*0.01*	*0.01*	*0.01*	*0.02*	*0.01*	*0.03*	*0.99*	*0.01*	*0.08*	*0.03*	*0.82*	*0.05*	*0.23*	*0.00*
Mus-Ax 7	0.01	0.01	0.01	0.08	0.03	0.52	86.60	0.00	0.38	0.03	12.25	0.00	0.08	0.04
SD	*0.01*	*0.01*	*0.01*	*0.02*	*0.02*	*0.03*	*0.43*	*0.00*	*0.05*	*0.02*	*0.49*	*0.00*	*0.13*	*0.10*
Mus-PC-1	0.01	0.01	0.01	0.25	0.02	0.01	99.67	0.04	0.06	0.11	0.06	0.02	0.05	0.00
SD	*0.01*	*0.01*	*0.01*	*0.03*	*0.02*	*0.01*	*0.30*	*0.04*	*0.04*	*0.03*	*0.03*	*0.03*	*0.04*	*0.00*
Mus-PC-2	0.02	0.01	0.01	0.01	0.01	0.01	99.55	0.01	0.54	0.10	0.03	0.03	0.01	0.00
SD	*0.01*	*0.01*	*0.01*	*0.01*	*0.01*	*0.01*	*0.44*	*0.01*	*0.12*	*0.10*	*0.02*	*0.02*	*0.01*	*0.00*
Mus-PC-3	0.02	0.01	0.01	0.01	0.01	0.00	99.96	0.00	0.09	0.31	0.00	0.01	0.04	0.00
SD	*0.02*	*0.01*	*0.01*	*0.01*	*0.01*	*0.01*	*0.76*	*0.00*	*0.05*	*0.13*	*0.01*	*0.01*	*0.05*	*0.00*
Mus-PC-6	0.00	0.01	0.01	2.34	0.01	0.03	98.26	0.01	0.04	0.03	0.02	0.00	0.03	0.00
SD	*0.01*	*0.01*	*0.01*	*0.47*	*0.01*	*0.02*	*0.50*	*0.03*	*0.04*	*0.03*	*0.02*	*0.01*	*0.03*	*0.00*
Mus-PC-7	0.00	0.00	0.01	0.45	0.02	0.21	99.19	0.01	0.04	0.01	0.01	0.00	0.05	0.00
SD	*0.01*	*0.01*	*0.01*	*0.04*	*0.01*	*0.03*	*0.34*	*0.02*	*0.04*	*0.01*	*0.01*	*0.00*	*0.07*	*0.00*
Mus-PC-8	0.01	0.00	0.01	0.16	0.01	0.03	99.29	0.28	0.02	0.06	0.03	0.02	0.09	0.00
SD	*0.01*	*0.00*	*0.01*	*0.03*	*0.01*	*0.02*	*0.41*	*0.05*	*0.03*	*0.05*	*0.02*	*0.02*	*0.06*	*0.00*

Appendix 2: Table 2 *(Continued)*

Sample	S	Cl	Mn	Fe	Co	Ni	Cu	Zn	As	Ag	Sn	Sb	Pb	Bi
d.l. (%)	**0.03**	**0.02**	**0.03**	**0.02**	**0.02**	**0.03**	**0.1**	**0.05**	**0.06**	**0.06**	**0.05**	**0.05**	**0.12**	**0.45**
CdSA-S*	0.01	0.00	0.01	0.24	0.04	0.23	90.27	0.01	0.13	0.05	10.06	0.00	0.04	0.02
SD	*0.01*	*0.01*	*0.02*	*0.03*	*0.01*	*0.02*	*0.77*	*0.01*	*0.06*	*0.04*	*0.45*	*0.00*	*0.06*	*0.05*
CdSA-Ax-59*	0.02	0.00	0.00	0.01	0.03	0.32	87.70	0.01	0.23	0.02	12.62	0.00	0.08	0.06
SD	*0.01*	*0.01*	*0.01*	*0.01*	*0.02*	*0.03*	*0.73*	*0.02*	*0.08*	*0.02*	*0.32*	*0.00*	*0.09*	*0.13*
CdSA-AxC-4*	0.01	0.00	0.00	0.02	0.03	0.37	91.94	0.00	0.31	0.06	8.64	0.00	0.02	0.00
SD	*0.01*	*0.01*	*0.00*	*0.01*	*0.01*	*0.01*	*0.95*	*0.00*	*0.06*	*0.04*	*0.82*	*0.00*	*0.03*	*0.00*
CdSB-AxA-1	0.02	0.01	0.00	0.03	0.11	0.06	86.01	0.01	0.05	0.12	14.34	0.00	0.00	0.00
SD	*0.01*	*0.01*	*0.00*	*0.01*	*0.02*	*0.02*	*0.36*	*0.01*	*0.06*	*0.03*	*0.24*	*0.00*	*0.00*	*0.00*
CdSB-AxA-2	0.02	0.01	0.01	0.01	0.04	0.30	94.97	0.01	0.63	0.09	5.32	0.07	0.03	0.02
SD	*0.01*	*0.01*	*0.01*	*0.01*	*0.02*	*0.03*	*0.24*	*0.02*	*0.08*	*0.05*	*0.34*	*0.04*	*0.02*	*0.05*
CdSB-AxA-9*	0.00	0.00	0.00	0.01	0.02	0.26	91.00	0.01	0.47	0.04	8.99	0.00	0.06	0.00
SD	*0.00*	*0.01*	*0.00*	*0.02*	*0.02*	*0.04*	*0.83*	*0.03*	*0.06*	*0.02*	*0.71*	*0.00*	*0.08*	*0.00*
CdSB-Cp	0.00	0.00	0.01	0.06	0.05	0.15	88.34	0.02	0.08	0.08	11.58	0.00	0.07	0.02
SD	*0.00*	*0.01*	*0.01*	*0.01*	*0.02*	*0.04*	*0.59*	*0.02*	*0.04*	*0.04*	*0.34*	*0.00*	*0.09*	*0.05*
CdSA-PnB*	0.01	0.00	0.00	0.44	0.11	0.32	95.87	0.01	2.58	0.03	0.09	1.56	0.03	0.01
SD	*0.02*	*0.01*	*0.01*	*0.11*	*0.02*	*0.06*	*1.23*	*0.02*	*0.46*	*0.02*	*0.04*	*0.45*	*0.07*	*0.03*
CdSA-P-17	0.02	0.01	0.01	0.33	0.03	0.07	98.98	0.00	1.13	0.02	0.00	0.05	0.02	0.00
SD	*0.02*	*0.00*	*0.01*	*0.09*	*0.01*	*0.01*	*0.11*	*0.01*	*0.17*	*0.02*	*0.01*	*0.04*	*0.04*	*0.00*
CdSA-P-18	0.02	0.01	0.01	0.17	0.18	0.13	99.77	0.00	0.14	0.04	0.03	0.03	0.00	0.00
SD	*0.02*	*0.00*	*0.01*	*0.09*	*0.01*	*0.01*	*0.11*	*0.01*	*0.17*	*0.02*	*0.01*	*0.04*	*0.04*	*0.00*
CdSA-P-19	0.01	0.01	0.01	1.94	0.04	0.03	98.75	0.05	0.04	0.06	0.06	0.02	0.00	0.00
SD	*0.01*	*0.02*	*0.01*	*0.27*	*0.02*	*0.01*	*0.52*	*0.03*	*0.08*	*0.05*	*0.05*	*0.03*	*0.00*	*0.00*
CdSA-P-20	0.00	0.01	0.00	0.17	0.01	0.87	99.21	0.01	0.48	0.01	0.02	0.43	0.02	0.00
SD	*0.00*	*0.01*	*0.00*	*0.01*	*0.01*	*0.05*	*0.73*	*0.01*	*0.17*	*0.01*	*0.01*	*0.16*	*0.03*	*0.00*
CdSA-P-22*	0.01	0.01	0.01	0.01	0.01	0.16	95.68	0.00	3.00	0.02	0.01	0.70	0.01	0.00
SD	*0.01*	*0.01*	*0.01*	*0.01*	*0.01*	*0.02*	*0.81*	*0.00*	*0.59*	*0.02*	*0.02*	*0.26*	*0.03*	*0.00*
CdSB-P-50	0.02	0.01	0.01	0.76	0.33	0.19	98.85	0.02	0.29	0.04	0.03	0.00	0.05	0.00
SD	*0.01*	*0.01*	*0.01*	*0.09*	*0.05*	*0.05*	*0.47*	*0.03*	*0.11*	*0.04*	*0.04*	*0.00*	*0.07*	*0.00*
CdSB-P-60	0.02	0.01	0.00	2.61	0.03	0.10	97.18	0.01	1.05	0.02	0.01	0.18	0.05	0.00
SD	*0.01*	*0.01*	*0.00*	*0.45*	*0.02*	*0.02*	*0.48*	*0.02*	*0.69*	*0.02*	*0.02*	*0.14*	*0.07*	*0.00*
CdSB-P-61	0.01	0.01	0.00	0.00	0.00	0.42	98.92	0.01	0.68	0.01	0.02	0.34	0.02	0.00
SD	*0.02*	*0.01*	*0.00*	*0.00*	*0.01*	*0.08*	*0.19*	*0.02*	*0.15*	*0.03*	*0.02*	*0.12*	*0.05*	*0.01*
CdSB-P-71	0.01	0.00	0.01	0.42	0.37	0.05	99.43	0.01	0.11	0.02	0.03	0.01	0.02	0.02
SD	*0.01*	*0.00*	*0.01*	*0.08*	*0.07*	*0.02*	*0.27*	*0.01*	*0.04*	*0.03*	*0.03*	*0.02*	*0.05*	*0.04*
CdSB-P-74	0.01	0.01	0.01	0.71	0.14	0.17	96.76	0.00	2.03	0.03	0.03	0.49	0.01	0.03
SD	*0.01*	*0.01*	*0.01*	*0.02*	*0.02*	*0.02*	*0.28*	*0.00*	*0.22*	*0.03*	*0.02*	*0.06*	*0.01*	*0.08*
CdSB-P-81	0.02	0.01	0.00	0.14	0.02	0.02	99.95	0.09	0.03	0.06	0.01	0.03	0.00	0.00
SD	*0.02*	*0.01*	*0.01*	*0.01*	*0.01*	*0.01*	*0.19*	*0.07*	*0.03*	*0.07*	*0.01*	*0.02*	*0.01*	*0.00*
Cel-Pal*	0.01	0.01	0.01	0.07	0.08	0.27	94.27	0.01	0.48	0.03	5.62	0.00	0.01	0.01
SD	*0.01*	*0.01*	*0.01*	*0.02*	*0.01*	*0.03*	*1.55*	*0.01*	*0.07*	*0.02*	*1.30*	*0.01*	*0.02*	*0.02*
Cel-AxC1*	0.01	0.01	0.01	0.01	0.02	0.38	93.33	0.00	0.67	0.05	6.35	0.04	0.03	0.03
SD	*0.00*	*0.01*	*0.01*	*0.01*	*0.02*	*0.03*	*1.05*	*0.00*	*0.18*	*0.05*	*0.97*	*0.07*	*0.05*	*0.06*
Cel-AxC8*	0.01	0.01	0.01	0.01	0.04	0.33	91.93	0.01	0.41	0.06	7.39	0.00	0.03	0.00
SD	*0.01*	*0.01*	*0.02*	*0.01*	*0.01*	*0.04*	*0.88*	*0.02*	*0.10*	*0.03*	*0.58*	*0.01*	*0.05*	*0.00*
Cel-AxA2	0.02	0.01	0.02	0.01	0.04	0.39	92.18	0.01	0.37	0.04	7.15	0.00	0.05	0.04
SD	*0.02*	*0.01*	*0.02*	*0.02*	*0.02*	*0.02*	*0.64*	*0.03*	*0.07*	*0.03*	*0.30*	*0.00*	*0.05*	*0.09*
Cel-AxA3	0.00	0.00	0.01	0.07	0.04	0.33	89.74	0.01	0.49	0.05	9.25	0.00	0.05	0.00
SD	*0.00*	*0.00*	*0.00*	*0.02*	*0.02*	*0.02*	*0.54*	*0.02*	*0.06*	*0.03*	*0.08*	*0.00*	*0.06*	*0.00*
Cel-AxA8	0.01	0.01	0.01	0.06	0.05	0.51	90.00	0.01	0.72	0.07	8.62	0.00	0.05	0.02
SD	*0.00*	*0.01*	*0.01*	*0.03*	*0.00*	*0.03*	*0.51*	*0.02*	*0.09*	*0.04*	*0.25*	*0.01*	*0.06*	*0.04*
Cel-S*	0.04	0.01	0.01	0.01	0.03	0.10	89.50	0.01	0.07	0.10	10.61	0.00	0.06	0.02
SD	*0.09*	*0.01*	*0.00*	*0.40*	*0.02*	*0.04*	*0.94*	*0.02*	*0.06*	*0.03*	*0.79*	*0.00*	*0.08*	*0.03*

Appendix 2: Table 2 *(Continued)*

Sample	S	Cl	Mn	Fe	Co	Ni	Cu	Zn	As	Ag	Sn	Sb	Pb	Bi
d.l. (%)	**0.03**	**0.02**	**0.03**	**0.02**	**0.02**	**0.03**	**0.1**	**0.05**	**0.06**	**0.06**	**0.05**	**0.05**	**0.12**	**0.45**
Cel-P37	0.01	0.01	0.00	0.40	0.22	0.14	99.68	0.01	0.27	0.06	0.04	0.00	0.05	0.01
SD	*0.01*	*0.01*	*0.01*	*0.03*	*0.02*	*0.03*	*0.69*	*0.02*	*0.04*	*0.03*	*0.03*	*0.00*	*0.07*	*0.01*
Cel-P38	0.01	0.01	0.01	0.01	0.01	0.00	99.97	0.00	0.08	0.10	0.01	0.02	0.02	0.02
SD	*0.01*	*0.01*	*0.01*	*0.01*	*0.01*	*0.00*	*0.38*	*0.01*	*0.03*	*0.05*	*0.01*	*0.02*	*0.03*	*0.04*
Cel-P39	0.02	0.01	0.00	0.30	0.25	0.10	99.84	0.00	0.36	0.03	0.08	0.01	0.01	0.01
SD	*0.02*	*0.01*	*0.00*	*0.03*	*0.03*	*0.02*	*0.50*	*0.00*	*0.11*	*0.03*	*0.06*	*0.02*	*0.01*	*0.02*
Cel-P41	0.01	0.00	0.01	0.39	0.36	0.19	99.04	0.02	0.49	0.07	0.08	0.01	0.05	0.00
SD	*0.01*	*0.00*	*0.01*	*0.03*	*0.03*	*0.03*	*0.57*	*0.02*	*0.16*	*0.04*	*0.03*	*0.02*	*0.09*	*0.00*
Ver-P0	0.01	0.00	0.00	1.98	0.06	0.07	97.15	0.38	0.22	0.07	0.03	0.62	0.04	0.00
SD	*0.01*	*0.00*	*0.00*	*0.70*	*0.03*	*0.02*	*0.83*	*0.05*	*0.07*	*0.04*	*0.03*	*0.28*	*0.08*	*0.00*
Ver-P9*	0.02	0.01	0.01	1.18	0.10	0.04	95.52	1.01	1.76	0.31	0.46	0.39	0.16	0.00
SD	*0.02*	*0.01*	*0.01*	*0.09*	*0.02*	*0.01*	*0.67*	*0.07*	*0.23*	*0.05*	*0.06*	*0.08*	*0.17*	*0.00*
Gal-Ax	0.01	0.00	0.01	0.10	0.04	0.12	90.15	0.03	0.13	0.10	9.93	0.00	0.17	0.00
SD	*0.01*	*0.01*	*0.02*	*0.03*	*0.01*	*0.02*	*2.06*	*0.04*	*0.02*	*0.05*	*1.84*	*0.00*	*0.32*	*0.00*
Gal-PI3	0.01	0.01	0.00	1.52	0.11	0.07	97.54	0.99	0.16	0.07	0.05	0.08	0.02	0.04
SD	*0.01*	*0.01*	*0.00*	*0.07*	*0.02*	*0.02*	*0.17*	*0.10*	*0.02*	*0.03*	*0.04*	*0.05*	*0.05*	*0.09*
Gal-PI4*	0.01	0.00	0.01	0.35	0.02	0.03	91.20	0.12	0.04	0.05	9.13	0.00	0.05	0.01
SD	*0.00*	*0.00*	*0.01*	*0.05*	*0.01*	*0.01*	*0.83*	*0.04*	*0.02*	*0.03*	*0.93*	*0.00*	*0.05*	*0.02*
Gal-PI5*	0.00	0.02	0.00	0.80	0.05	0.02	88.43	0.26	0.03	0.06	11.09	0.00	0.02	0.04
SD	*0.01*	*0.03*	*0.00*	*0.09*	*0.02*	*0.01*	*1.16*	*0.05*	*0.02*	*0.02*	*1.04*	*0.00*	*0.04*	*0.09*
Por6-Pal*	0.01	0.01	0.01	0.07	0.56	2.76	92.40	0.00	2.05	0.08	0.19	2.57	0.09	0.00
SD	*0.01*	*0.01*	*0.01*	*0.04*	*0.07*	*0.20*	*1.13*	*0.00*	*0.25*	*0.02*	*0.03*	*0.60*	*0.10*	*0.00*
Por6-PI-9*	0.01	0.01	0.00	1.49	0.93	3.25	91.66	0.18	1.62	0.05	0.07	1.73	0.09	0.00
SD	*0.02*	*0.01*	*0.01*	*0.22*	*0.10*	*0.12*	*0.67*	*0.03*	*0.11*	*0.02*	*0.03*	*0.17*	*0.07*	*0.00*
Por6-TC-6*	0.02	0.01	0.01	0.01	0.01	0.09	92.61	0.01	2.67	1.00	0.02	4.05	0.03	0.01
SD	*0.01*	*0.01*	*0.01*	*0.01*	*0.01*	*0.04*	*0.98*	*0.02*	*0.21*	*0.13*	*0.02*	*0.61*	*0.05*	*0.03*
Por6-TC-8	0.00	0.01	0.01	0.08	0.54	2.98	94.31	0.01	1.23	0.54	0.05	1.54	0.05	0.00
SD	*0.01*	*0.01*	*0.01*	*0.02*	*0.03*	*0.13*	*0.56*	*0.03*	*0.24*	*0.07*	*0.02*	*0.36*	*0.07*	*0.00*
Por6-PC-5	0.01	0.01	0.01	0.01	0.00	0.02	97.87	0.00	1.17	0.75	0.00	0.48	0.00	0.00
SD	*0.01*	*0.01*	*0.01*	*0.01*	*0.00*	*0.03*	*0.72*	*0.00*	*0.30*	*0.26*	*0.01*	*0.14*	*0.00*	*0.00*
Por6-PC-6*	0.01	0.00	0.01	0.10	0.78	3.15	92.18	0.06	1.18	0.80	0.03	2.20	0.02	0.01
SD	*0.01*	*0.01*	*0.01*	*0.03*	*0.15*	*0.38*	*0.46*	*0.04*	*0.23*	*0.19*	*0.03*	*0.29*	*0.04*	*0.04*
Por6-PP-7	0.01	0.00	0.00	0.00	0.01	0.01	96.34	0.01	1.50	0.66	0.01	0.56	0.01	0.00
SD	*0.01*	*0.01*	*0.01*	*0.00*	*0.01*	*0.01*	*1.00*	*0.01*	*0.32*	*0.18*	*0.02*	*0.13*	*0.02*	*0.00*
Por6-SN-1	0.03	0.01	0.01	1.43	2.45	6.42	85.16	0.08	1.76	0.46	0.52	2.54	0.03	0.00
SD	*0.01*	*0.01*	*0.01*	*0.35*	*0.50*	*0.65*	*0.93*	*0.04*	*0.31*	*0.21*	*0.08*	*0.47*	*0.05*	*0.00*
Por6-SN-2	0.02	0.00	0.01	2.00	1.94	5.07	88.18	0.00	2.08	0.11	0.54	1.34	0.08	0.04
SD	*0.01*	*0.00*	*0.01*	*0.73*	*0.62*	*0.80*	*1.23*	*0.01*	*0.51*	*0.08*	*0.32*	*0.76*	*0.09*	*0.09*
Por6-SN-7*	0.01	0.01	0.01	0.10	0.01	0.32	92.00	0.02	0.83	0.27	3.36	3.86	0.02	0.04
SD	*0.01*	*0.01*	*0.01*	*0.02*	*0.01*	*0.03*	*1.20*	*0.02*	*0.09*	*0.04*	*0.33*	*0.49*	*0.02*	*0.10*
Por6-SN-8	0.01	0.01	0.01	0.00	0.01	0.01	91.35	0.01	3.71	0.73	0.04	5.46	0.04	0.00
SD	*0.01*	*0.01*	*0.01*	*0.00*	*0.01*	*0.01*	*0.49*	*0.01*	*0.15*	*0.10*	*0.02*	*0.42*	*0.07*	*0.00*
Por9-Cus-46*	0.01	0.00	0.01	0.02	0.40	1.92	90.55	0.00	1.64	0.22	4.72	1.48	0.02	0.00
SD	*0.01*	*0.01*	*0.01*	*0.01*	*0.03*	*0.12*	*0.61*	*0.01*	*0.22*	*0.04*	*0.48*	*0.14*	*0.03*	*0.00*
Por9-Pal*	0.01	0.01	0.01	0.41	0.93	2.58	89.39	0.01	0.72	0.15	6.37	0.29	0.03	0.05
SD	*0.01*	*0.01*	*0.01*	*0.03*	*0.05*	*0.10*	*0.77*	*0.02*	*0.16*	*0.06*	*0.66*	*0.12*	*0.06*	*0.12*
Por9-Pn-25	0.03	0.01	0.00	3.17	0.04	0.05	97.01	0.25	0.05	0.03	0.06	0.05	0.09	0.01
SD	*0.02*	*0.01*	*0.01*	*0.13*	*0.02*	*0.03*	*0.58*	*0.05*	*0.05*	*0.03*	*0.03*	*0.05*	*0.09*	*0.02*
Por9-TC-29*	0.02	0.01	0.01	0.25	0.81	1.78	94.26	0.08	1.11	0.77	0.02	1.51	0.10	0.03
SD	*0.01*	*0.01*	*0.01*	*0.02*	*0.02*	*0.10*	*0.46*	*0.04*	*0.10*	*0.12*	*0.01*	*0.24*	*0.12*	*0.06*
Por9-PC-24	0.00	0.01	0.02	0.01	0.01	0.73	92.49	0.00	3.85	0.46	0.02	3.69	0.02	0.00
SD	*0.01*	*0.01*	*0.01*	*0.01*	*0.01*	*0.12*	*1.59*	*0.01*	*1.12*	*0.21*	*0.02*	*0.69*	*0.02*	*0.00*
Por9-PC-30*	0.01	0.00	0.01	0.00	0.00	0.02	93.60	0.00	3.84	0.54	0.02	2.49	0.04	0.00
SD	*0.01*	*0.01*	*0.01*	*0.00*	*0.01*	*0.01*	*0.71*	*0.01*	*0.36*	*0.09*	*0.02*	*0.22*	*0.06*	*0.00*

Appendix 2: Table 2 *(Continued)*

Sample	S	Cl	Mn	Fe	Co	Ni	Cu	Zn	As	Ag	Sn	Sb	Pb	Bi
d.l. (%)	**0.03**	**0.02**	**0.03**	**0.02**	**0.02**	**0.03**	**0.1**	**0.05**	**0.06**	**0.06**	**0.05**	**0.05**	**0.12**	**0.45**
Por9-PC-49*	0.02	0.01	0.01	0.02	0.01	0.07	93.55	0.00	3.15	1.22	0.02	2.16	0.02	0.03
SD	*0.01*	*0.01*	*0.01*	*0.02*	*0.01*	*0.02*	*2.93*	*0.00*	*0.89*	*0.57*	*0.02*	*1.40*	*0.03*	*0.02*
Por9-Boz*	0.01	0.01	0.01	0.07	0.01	0.17	94.01	0.00	0.90	0.05	0.05	5.05	0.02	0.01
SD	*0.01*	*0.01*	*0.02*	*0.02*	*0.01*	*0.01*	*0.62*	*0.00*	*0.09*	*0.04*	*0.03*	*0.36*	*0.06*	*0.01*
Por9-Tub*	0.01	0.01	0.01	0.01	0.01	0.02	96.07	0.01	2.15	0.50	0.01	2.13	0.02	0.09
SD	*0.01*	*0.01*	*0.01*	*0.01*	*0.01*	*0.02*	*1.29*	*0.02*	*0.58*	*0.02*	*0.02*	*0.64*	*0.03*	*0.18*
Por9-LAP*	0.01	0.01	0.01	0.01	0.00	0.07	94.55	0.00	2.82	0.50	0.02	2.93	0.02	0.00
SD	*0.01*	*0.01*	*0.01*	*0.01*	*0.01*	*0.03*	*0.77*	*0.01*	*0.20*	*0.06*	*0.03*	*0.29*	*0.02*	*0.01*
Por9-Bar-2*	0.01	0.00	0.00	0.01	0.05	2.19	92.60	0.00	3.36	0.58	0.09	1.88	0.02	0.03
SD	*0.01*	*0.00*	*0.01*	*0.01*	*0.02*	*0.31*	*0.70*	*0.00*	*0.55*	*0.20*	*0.03*	*0.19*	*0.02*	*0.07*
Por9-Bar-5*	0.02	0.00	0.01	1.39	1.18	2.60	90.52	0.00	2.84	0.05	0.03	1.76	0.03	0.08
SD	*0.02*	*0.01*	*0.01*	*0.29*	*0.23*	*0.19*	*0.64*	*0.00*	*0.26*	*0.03*	*0.03*	*0.46*	*0.05*	*0.13*
Por9-PI-60*	0.01	0.01	0.01	0.01	0.01	0.01	93.23	0.02	3.67	0.65	0.01	2.76	0.04	0.00
SD	*0.01*	*0.01*	*0.01*	*0.01*	*0.01*	*0.01*	*0.77*	*0.03*	*0.23*	*0.14*	*0.02*	*0.47*	*0.05*	*0.00*
Por9-PI-64	0.02	0.01	0.00	0.71	0.97	3.33	90.87	0.05	2.25	0.38	0.07	1.73	0.08	0.09
SD	*0.01*	*0.01*	*0.01*	*0.02*	*0.03*	*0.15*	*0.82*	*0.03*	*0.23*	*0.10*	*0.05*	*0.44*	*0.18*	*0.25*
Por9-PI-71*	0.01	0.01	0.01	0.64	0.93	3.18	91.90	0.05	2.80	0.09	0.07	1.58	0.10	0.00
SD	*0.01*	*0.01*	*0.01*	*0.19*	*0.15*	*0.35*	*1.00*	*0.05*	*0.39*	*0.05*	*0.04*	*0.49*	*0.15*	*0.00*
Por9-PI-73*	0.03	0.00	0.01	1.24	1.07	2.79	90.93	0.01	2.54	0.05	0.04	2.30	0.05	0.00
SD	*0.02*	*0.00*	*0.01*	*0.43*	*0.29*	*0.17*	*0.72*	*0.02*	*0.23*	*0.03*	*0.02*	*0.46*	*0.08*	*0.00*
Por9-PI-77	0.01	0.00	0.01	1.86	1.35	5.52	87.68	0.00	3.20	0.02	0.01	0.65	0.06	0.15
SD	*0.01*	*0.01*	*0.02*	*0.59*	*0.33*	*0.28*	*1.53*	*0.01*	*0.18*	*0.03*	*0.03*	*0.15*	*0.06*	*0.23*
Por9-PI-93*	0.02	0.01	0.01	2.01	2.12	5.28	86.80	0.05	1.59	0.34	0.40	1.66	0.04	0.02
SD	*0.01*	*0.01*	*0.01*	*0.40*	*0.35*	*0.47*	*0.75*	*0.04*	*0.16*	*0.13*	*0.09*	*0.31*	*0.06*	*0.06*

Appendix 3

Appendix 3. Samples analysed and Pb isotope values divided by typology. 2SE is analytical uncertainties calculated as twice the individual in-run precision on the samples. "-"= undefined typology.

Cu ingots							
Sample	**Typology**	**206/204**	**±2SE**	**207/204**	**±2SE**	**208/204**	**±2SE**
CER-PC-56	Plano-convex	15.649	0.001	15.649	0.001	38.247	0.004
CER-PC-70	Plano-convex	18.235	0.001	15.667	0.001	38.503	0.003
CER-PC-72	Plano-convex	17.905	0.001	15.642	0.001	38.126	0.004
CER-PC-79	Plano-convex	18.062	0.001	15.655	0.002	38.314	0.005
CER-PS-64	Parallel- surface	18.106	0.001	15.657	0.002	38.340	0.005
CER-PS-82	Parallel- surface	17.914	0.002	15.645	0.002	38.142	0.005
CER-PS-62	Parallel- surface	18.153	0.001	15.655	0.002	38.375	0.005
CER-PS-77	Parallel- surface	17.906	0.002	15.641	0.002	38.117	0.006
MUS-PC-2	Plano-convex	18.245	0.002	15.668	0.003	38.482	0.008
MUS-PC-3	Plano-convex	18.222	0.001	15.664	0.001	38.458	0.005
MUS-PC-7	Plano-convex	18.779	0.006	15.710	0.005	39.310	0.012
CdS A-P-17	Plano-convex	18.837	0.004	15.688	0.004	39.120	0.009
CdS A-P-18	Truncated ingot	18.894	0.004	15.698	0.003	39.213	0.008
CdS B-P-50	Plano-convex	18.703	0.003	15.686	0.003	38.739	0.007
CdS B-P-74	Ingot	18.845	0.002	15.686	0.002	39.142	0.006
CdS B-P-81	Plano-convex	17.922	0.002	15.637	0.002	38.143	0.005
CdSA-PnB	Bar-ingot	18.704	0.003	15.689	0.003	38.963	0.007
CdSB-P60	Plano-convex ingot	18.821	0.002	15.692	0.002	39.116	0.008
Cel-P-38	Truncated ingot	18.283	0.003	15.680	0.003	38.544	0.008
Cel-P-41	Truncated ingot	18.629	0.003	15.684	0.002	38.699	0.006
Ver-P-0	Plano-convex ingot	17.965	0.002	15.641	0.002	38.200	0.007
Ver-P-9	Plano-convex ingot	18.279	0.003	15.674	0.002	38.541	0.007
Gal-PI-3	Blade/Ingot	18.153	0.002	15.652	0.002	38.389	0.006
Por6-TC8	Truncated ingot	18.404	0.003	15.686	0.003	38.567	0.007
Por9-TC29	Truncated ingot	18.400	0.003	15.681	0.002	38.542	0.006
Por6-PC6	Plano-convex ingot	18.400	0.003	15.682	0.003	38.547	0.007
Por9-PC24	Plano-convex ingot	18.363	0.005	15.671	0.004	38.501	0.012
Por9-PC49	Plano-convex ingot	18.319	0.003	15.673	0.003	38.517	0.010
Por6-SN2	Flat/blade's axe-ingot	18.352	0.003	15.670	0.002	38.534	0.007
Por6-SN8	Flat /blade's axe-ingot	18.378	0.003	15.657	0.003	38.504	0.007
Por6-PP7	Ingot	18.512	0.022	15.693	0.019	38.565	0.068
Por9-Bar5	Bar-ingot	18.259	0.002	15.671	0.003	38.491	0.008
Por9-Pn25	Plano-convex ingot	17.913	0.002	15.645	0.002	38.139	0.010
Por-6-PI-9	Pick Ingot	18.271	0.003	15.661	0.002	38.499	0.007
Por9-PI71	Pick Ingot	17.995	0.003	15.657	0.003	38.229	0.012
Por9-PI60	Pick Ingot	18.400	0.005	15.675	0.005	38.604	0.012
Por9-PI73	Pick Ingot	18.446	0.008	15.675	0.007	38.550	0.017
Por9-PI93	Pick Ingot	18.406	0.003	15.682	0.003	38.553	0.007

Appendix 3 *(Continued)*

Bronze ingots

Sample	Typology	206/204	±2SE	207/204	±2SE	208/204	±2SE
Can-S	Sword/ingot	18.031	0.002	15.651	0.002	38.253	0.005
Cer-TS	Tongue-shaped ingot	18.249	0.002	15.649	0.002	38.383	0.005
Gal-PI-4	Pick Ingot	17.944	0.002	15.641	0.002	38.174	0.006
Gal-PI-5	Pick Ingot	17.954	0.002	15.642	0.002	38.185	0.007

Swords

Sample	Typology	206/204	±2SE	207/204	±2SE	208/204	±2SE
BEL-S	Sprockoff Ia - IIa	18.304	0.002	15.669	0.002	38.481	0.005
MUS-S2	Flange-hilted sword, Cetona-type	18.197	0.001	15.663	0.002	38.417	0.005
MUS-S3	Flange-hilted sword, Sacile-type	18.216	0.002	15.673	0.002	38.438	0.006
CdS A-S	Flange-hilted sword, Boiu-Keszethely type	18.135	0.002	15.658	0.002	38.357	0.006
Cel-S	Flange-hilted sword	18.160	0.002	15.659	0.002	38.401	0.006

Axes

Sample	Typology	206/204	±2SE	207/204	±2SE	208/204	±2SE
Cer-Ax	Winged-axe	18.168	0.002	15.664	0.002	38.380	0.005
CdS B-AxA-1	Winged-axe	18.189	0.002	15.669	0.002	38.424	0.007
CdS B-AxA-2	Winged-axe	18.464	0.002	15.681	0.002	38.690	0.007
CdS B-AxA-9	Winged-axe	18.372	0.002	15.673	0.002	38.562	0.007
CdS A-Ax-59	Winged-axe	18.342	0.002	15.665	0.002	38.463	0.006
Gal-Ax	Winged-axe	18.110	0.002	15.655	0.002	38.336	0.006
Cel-AxA3	Winged-axe	18.390	0.003	15.668	0.002	38.603	0.007
Cel-AxA8	Winged-axe	18.421	0.003	15.672	0.002	38.643	0.007
Mus-Ax6	Socketed axe	18.246	0.002	15.664	0.002	38.455	0.006
Mus-Ax7	Socketed axe	18.218	0.002	15.663	0.002	38.421	0.005
CdS A-AxC-4	Socketed axe	18.334	0.002	15.670	0.002	38.505	0.008
Cel-AxC8	Socketed axe	18.366	0.002	15.668	0.002	38.580	0.006

Socketed shovels

Sample	Typology	206/204	±2SE	207/204	±2SE	208/204	±2SE
Cel-Pal-1	*Fondo Paviani*-type	18.316	0.002	15.663	0.002	38.511	0.005
Por-6-Pal	*Tra Manciano e Semprugnano*-type	18.283	0.002	15.659	0.002	38.524	0.007
Por-9-Pal	*Tra Manciano e Semprugnano*-type	18.274	0.003	15.654	0.002	38.436	0.006

Spearheads

Sample	Typology	206/204	±2SE	207/204	±2SE	208/204	±2SE
CdS B-Cp	-	18.192	0.003	15.663	0.003	38.436	0.008
Por9-Cus-46	-	18.283	0.002	15.663	0.002	38.489	0.006

Appendix 4

Appendix 4. "Euclidean Test" procedure for all the ingots and objects selected for the Lead Isotope Analysis. For each sample, the top part of the result table is reported and the ores and slags listed here are the ones with the closest Euclidean distance to the ratio of the artefacts (Rank). The entire table has over 3500 entries for published/unpublished lead isotope ratios of copper ores from all of Europe, Near and Middle East and North Africa.

Artefact	Ore/Slag Sample n.	Data base field	Region	Site/Mine	Rank
CER-PC-56	LU-PS45	LBA Alpine slags	Trentino	Luserna	**0.0070**
	VAL-SC2	LBA Alpine slags	Trentino	Vallarsa	**0.0123**
	860-1	Iberia: Center, Alcudia valley	Iberia Center	San Bartolome	**0.0141**
	SEG-G4 bis	LBA Alpine slags	Trentino	Segonzano	**0.0151**
	duplicate	Iberia: Center, Alcudia valley	Iberia Center	Pontones	**0.0152**
	LU-GM57	LBA Alpine slags	Trentino	Luserna	**0.0206**
	LU-G56 M	LBA Alpine slags	Trentino	Luserna	**0.0210**
	LU-P6	LBA Alpine slags	Trentino	Luserna	**0.0253**
	PAT-BOR	E Alps, Southalpine AATV	Veneto	Pian della Stua	**0.0313**
	VI-05	E Alps, Valsugana VMS	Veneto	Valle Imperina	**0.0315**
CER-PC-70	GRUA_Ep1	E Alps, Southalpine AATV	Trentino	Maso Erdemolo	**0.0209**
		Maghreb	Morocco	Merouane, Jebel Sarhro	**0.0236**
	CD-a-11	E Alps, Southalpine AATV	Trentino	Montefondoli	**0.0250**
	F	E Alps, Southalpine AATV	Veneto	Val Livergon	**0.0251**
	MT2	E Alps, Southalpine AATV	Veneto	Monte Trisa	**0.0259**
	MFO_Ap1	E Alps, Southalpine AATV	Trentino	Montefondoli	**0.0260**
	GRUA_Gs1	E Alps, Southalpine AATV	Trentino	Maso Erdemolo	**0.0261**
	GRUA_Dsxp1	E Alps, Southalpine AATV	Trentino	Maso Erdemolo	**0.0278**
	SEG-M2	LBA Alpine slags	Trentino	Segonzano	**0.0288**
	398	Iberia: SW, Ossa Morena	Iberia SW	La Dehesa	**0.0291**
CER-PC-72	CALC-1	E Alps, Valsugana VMS	Trentino	Calceranica	**0.0041**
	LU-G59 M	LBA Alpine slags	Trentino	Luserna	**0.0054**
	LU-G59	LBA Alpine slags	Trentino	Luserna	**0.0061**
	CALC7	E Alps, Valsugana VMS	Trentino	Calceranica	**0.0082**
	CALC-2	E Alps, Valsugana VMS	Trentino	Calceranica	**0.0094**
	LU-G59 He	LBA Alpine slags	Trentino	Luserna	**0.0141**
	23114R T24	Levant: Timna, Faynan	Egypt		**0.0164**
		Austria: Tyrol, Carinthia (cpy)	Salzburg	Rettenbach	**0.0166**
	LU-GM57	LBA Alpine slags	Trentino	Luserna	**0.0174**
	LU-G59	LBA Alpine slags	Trentino	Luserna	**0.0194**
CER-PC-79	LU-G56 Cp	LBA Alpine slags	Trentino	Luserna	**0.0123**
	861-43	Iberia: Center, Alcudia valley	Iberia Center	Mina Atilana	**0.0163**
	861-7	Iberia: Center, Alcudia valley	Iberia Center	Los Diegos	**0.0208**
	duplicate	Iberia: Center, Alcudia valley	Iberia Center	San Justo	**0.0209**
	861-5	Iberia: Center, Alcudia valley	Iberia Center	San Justo	**0.0211**
	861-13	Iberia: Center, Alcudia valley	Iberia Center	San Benito	**0.0215**
	861-12	Iberia: Center, Alcudia valley	Iberia Center	Pontones/Santa Isabel	**0.0255**
	861-7	Iberia: Center, Alcudia valley	Iberia Center	Los Diegos	**0.0319**
	SEG-P14	LBA Alpine slags	Trentino	Segonzano	**0.0325**
	PAM-1	E Alps, Southalpine AATV	Trentino	Pamera	**0.0379**

Appendix 4 *(Continued)*

Artefact	Ore/Slag Sample n.	Data base field	Region	Site/Mine	Rank
CER-PS-64	LU-GM57 M	LBA Alpine slags	Trentino	Luserna	**0.0084**
	LU-PR34	LBA Alpine slags	Trentino	Luserna	**0.0223**
	23118U C3	Levant: Timna, Faynan	Egypt	Timna, area S/T	**0.0287**
	AP 92.6		Shropshire	Shelve Grit mine	**0.0305**
	SEG-P14	LBA Alpine slags	Trentino	Segonzano	**0.0356**
	LU-P61	LBA Alpine slags	Trentino	Luserna	**0.0383**
	861-7	Iberia: Center, Alcudia valley	Iberia Center	Los Diegos	**0.0442**
	861-43	Iberia: Center, Alcudia valley	Iberia Center	Mina Atilana	**0.0451**
	861-5	Iberia: Center, Alcudia valley	Iberia Center	San Justo	**0.0466**
	861-13	Iberia: Center, Alcudia valley	Iberia Center	San Benito	**0.0478**
CER-PS-82	LU-GM57	LBA Alpine slags	Trentino	Luserna	**0.0111**
	CALC-3	E Alps, Valsugana VMS	Trentino	Calceranica	**0.0111**
	LU-G59 M	LBA Alpine slags	Trentino	Luserna	**0.0160**
	CALC-1	E Alps, Valsugana VMS	Trentino	Calceranica	**0.0193**
	23078V U6	Levant: Timna, Faynan	Egypt		**0.0204**
	LU-G59	LBA Alpine slags	Trentino	Luserna	**0.0214**
	CALC-2	E Alps, Valsugana VMS	Trentino	Calceranica	**0.0237**
	CALC7	E Alps, Valsugana VMS	Trentino	Calceranica	**0.0267**
	SD 1006C	Sardinia: SW Iglesiente	SW Sardinia	Sa Duchessa	**0.0271**
		Austria: Tyrol, Carinthia (cpy)	Salzburg	Rettenbach	**0.0272**
CER-PS-62	LU-P61	LBA Alpine slags	Trentino	Luserna	**0.0216**
	RED1P	LBA Alpine slags	Trentino	Redebus	**0.0236**
	23070P P1	Levant: Timna, Faynan	Egypt	Timna, area P	**0.0290**
	809-037	Iberia: Center, Alcudia valley	Iberia Center	Villazaide	**0.0364**
	LU-PR34	LBA Alpine slags	Trentino	Luserna	**0.0375**
	862-001	Iberia: Center, Alcudia valley	Iberia Center	Mina Rica Nueva	**0.0391**
	396	Iberia: SW, Ossa Morena	Iberia SW	La Dehesa	**0.0424**
	MOR41-122	W Alps 1, Falda Pemontese	Piemonte	Chialamberto	**0.0431**
	23083Q ARB64	Levant: Timna, Faynan	Egypt		**0.0459**
	104 P	Central Europe: Germany, Erzgebirge	Central Germany	Kamsdorf	**0.0483**
CER-PS-77	CALC-2	E Alps, Valsugana VMS	Trentino	Calceranica	**0.0053**
	LU-G59 Qz>90	LBA Alpine slags	Trentino	Luserna	**0.0056**
	LU-G59 He	LBA Alpine slags	Trentino	Luserna	**0.0063**
	CALC7	E Alps, Valsugana VMS	Trentino	Calceranica	**0.0075**
	CALC-1	E Alps, Valsugana VMS	Trentino	Calceranica	**0.0089**
	LU-G59 M	LBA Alpine slags	Trentino	Luserna	**0.0102**
	23114R T24	Levant: Timna, Faynan	Egypt		**0.0103**
	LU-G59	LBA Alpine slags	Trentino	Luserna	**0.0118**
	LU-G59 Cp	LBA Alpine slags	Trentino	Luserna	**0.0175**
	M1200	E Alps, Valsugana VMS	Trentino	Calceranica	**0.0206**

Appendix *(Continued)*

Artefact	Ore/Slag Sample n.	Data base field	Region	Site/Mine	Rank
Cer-TS	PRE_IIIAs1	E Alps, Predoi	Trentino	Glockner Nappe	**0.0081**
	PD8a		Central Wales	Llanerch-yr-aur mine	**0.0092**
	Pb 32		Central Wales	Dylife	**0.0121**
	SARD 121b	Sardinia: NW Sassarese	NW Sardinia	Calabona	**0.0135**
	CWM92-2a	UK: Wales, Great Orme, Copa Hill	Wales	Cwmystwyth, Copa Hill	**0.0147**
	CWM92-la	UK: Wales, Great Orme, Copa Hill	Wales	Cwmystwyth, Copa Hill	**0.0151**
	835-015	Iberia: Center, Alcudia valley	Iberia Center	Nuestra Senora de la Paz	**0.0155**
	R 1000B	Sardinia: Center-Sulcis	Sulcis	Rosas, Nuxis, (CA)	**0.0162**
	CWM92-2b	UK: Wales, Great Orme, Copa Hill	Wales	Galena	**0.0174**
	PD8b		Central Wales	Llanerch-yr-aur mine	**0.0178**
MUS-PC-2	GRUA_Dsxp1	E Alps, Southalpine AATV	Trentino	Maso Erdemolo	**0.0056**
	GRUA_Gs1	E Alps, Southalpine AATV	Trentino	Maso Erdemolo	**0.0076**
	MT2	E Alps, Southalpine AATV	Veneto	Monte Trisa	**0.0076**
	REG-2	E Alps, Southalpine AATV	Trentino	Val Reganel	**0.0078**
	F	E Alps, Southalpine AATV	Veneto	Val Livergon	**0.0083**
	GRUA_Ddxp1	E Alps, Southalpine AATV	Trentino	Maso Erdemolo	**0.0111**
	SEG-M2	LBA Alpine slags	Trentino	Segonzano	**0.0121**
	GRUA_Ep1	E Alps, Southalpine AATV	Trentino	Maso Erdemolo	**0.0142**
	Cu-NT	Liguria, Apennines-Cu nativo	Toscana	Impruneta	**0.0146**
	MA-5pBIS	E Alps, Carnia	Friuli	Monte Avanza	**0.0168**
MUS-PC-3	LU-SC1 bis	LBA Alpine slags	Trentino	Luserna	**0.0033**
	MT1-360	E Alps, Southalpine AATV	Veneto	Monte Trisa	**0.0094**
	SEG-G9	LBA Alpine slags	Trentino	Segonzano	**0.0104**
	GRUA_As1	E Alps, Southalpine AATV	Trentino	Maso Erdemolo	**0.0126**
	RED-1G-Fa	LBA Alpine slags	Trentino	Redebus	**0.0134**
	LU-SC1	LBA Alpine slags	Trentino	Luserna	**0.0136**
	MT4	E Alps, Southalpine AATV	Veneto	Monte Trisa	**0.0138**
	MT3	E Alps, Southalpine AATV	Veneto	Monte Trisa	**0.0149**
	GRUA_Cp1	E Alps, Southalpine AATV	Trentino	Maso Erdemolo	**0.0163**
	PA6	E Alps, Southalpine AATV	Trentino	Pamera	**0.0196**
MUS-PC-7	LP 1A	Tuscany: Southern	Tuscany	La Pesta	**0.0821**
	AGAB29Pb	Maghreb	Tunisia	Chaambi-Agab	**0.1158**
	AON1001	Turkey: Taurus Mountains	Turchia		**0.1160**
	LP 10 A	Tuscany: Southern	Tuscany	La Pesta	**0.1215**
	GD2	Maghreb	Tunisia	Sekarna	**0.1225**
	SL867	Maghreb	Tunisia	Slata	**0.1225**
	HALLIDAY1	Iberia: SE Murcia Cartagena	Iberia SE	S. Valentin l'Unione mine	**0.1274**
	CAPN 4A	Tuscany: Southern	Tuscany	Fenice Capanne	**0.1313**
	LP 11A	Tuscany: Southern	Tuscany	La Pesta	**0.1378**
	PA13661	NE Catalunya, Baleares, Cord Iberica	Iberia NE	Sa Argentera	**0.1401**

Appendix 4 *(Continued)*

Artefact	Ore/Slag Sample n.	Data base field	Region	Site/Mine	Rank
CdSA-P-17		Austria: Inn valley, Salzburg, Styria (Fhz)	Tyrol	Rö	**0.0396**
	TEM 1A	Tuscany: Southern	Tuscany	Temperino	**0.0608**
	BaS-21	Slovakia, Bohemian Massif	Slovakia	Banska Stiavnica	**0.0663**
	LP 4A	Tuscany: Southern	Tuscany	La Pesta	**0.0671**
	AON411	Turkey: Taurus Mountains	Turchia		**0.0677**
	AON243	Turkey: Taurus Mountains	Turchia	Akcakisla Ozge Mine	**0.0680**
	Lub-01	Slovakia, Bohemian Massif	Slovakia	L'ubietova	**0.0682**
	LP 2A	Tuscany: Southern	Tuscany	La Pesta	**0.0708**
	PA13527B	Iberia: SE Andalusia-Jaen	Iberia SE	Pinar de Bedar	**0.0718**
	JLT2	Maghreb	Tunisia	Jalta	**0.0732**
CdSA-P-18	Lub-04	Slovakia, Bohemian Massif	Slovakia	L'ubietova	**0.0377**
	AON457	Turkey: Taurus Mountains	Turchia	Karamadazi	**0.0713**
		Austria: Inn valley, Salzburg, Styria (Fhz)	Tyrol	Rö	**0.0780**
	AAN907	Levant: Timna, Faynan	Palestine		**0.0830**
	B50108	Maghreb	Tunisia	Djebba	**0.0870**
	CAB 7	Iberia: SE Murcia Cartagena	Iberia SE	Near Corbija Grande	**0.0899**
	AON1001	Turkey: Taurus Mountains	Turchia		**0.0950**
	LP 1A	Tuscany: Southern	Tuscany	La Pesta	**0.1073**
	AON411	Turkey: Taurus Mountains	Turchia		**0.1085**
	GD2	Maghreb	Tunisia	Sekarna	**0.1133**
CdSB-P-50	CSG2	Sardinia: NW Sassarese	NW Sardinia	Calabona	**0.0149**
	36-M28	Swiss Valais	Valais area	Tsirouc	**0.0173**
	BUL56/95	Balkans: Bulgaria	Central Bulgaria	Bakadijk	**0.0195**
	ZID 3c	Balkans: Bulgaria	Central Bulgaria	Zidarovo	**0.0208**
	BUL57/95	Balkans: Bulgaria	Central Bulgaria	Bakadijk	**0.0259**
	CFS12rock	Sardinia: NW Sassarese	NW Sardinia	Calabona	**0.0271**
	Reo-A11	Iberia: NE, Euskadi	Iberia Euskadi	Santander	**0.0273**
	Gal-1	Iberia: NE, Euskadi	Iberia Euskadi	Santander	**0.0279**
	NIK 1	Greece: Trakia	Grecia	Nikisiani	**0.0294**
	BUl49/95	Balkans: Bulgaria	Central Bulgaria	Bakadijk	**0.0321**
	?	Iberia: NE, Euskadi	Iberia Euskadi	Santander	**0.0328**
CdSB-P-74		Austria: Inn valley, Salzburg, Styria (Fhz)	Tyrol	Rö	**0.0252**
	AON411	Turkey: Taurus Mountains	Turchia		**0.0639**
	TEM 1A	Tuscany: Southern	Tuscany	Temperino	**0.0750**
	LP 2A	Tuscany: Southern	Tuscany	La Pesta	**0.0772**
	LP 4A	Tuscany: Southern	Tuscany	La Pesta	**0.0801**
	CAPN 4A	Tuscany: Southern	Tuscany	Fenice Capanne	**0.0806**
	Lub-01	Slovakia, Bohemian Massif	Slovakia	L'ubietova	**0.0809**
	Lub-04	Slovakia, Bohemian Massif	Slovakia	L'ubietova	**0.0832**
	AON1001	Turkey: Taurus Mountains	Turchia		**0.0838**
	BaS-21	Slovakia, Bohemian Massif	Slovakia	Banska Stiavnica	**0.0843**

Appendix 4 *(Continued)*

Artefact	Ore/Slag Sample n.	Data base field	Region	Site/Mine	Rank
CdSB-P-81	CALC-3	E Alps, Valsugana VMS	Trentino	Calceranica	**0.0079**
	LU-GM57	LBA Alpine slags	Trentino	Luserna	**0.0098**
	23078V U6	Levant: Timna, Faynan	Egypt	Timna, area U	**0.0191**
	LU-G59 M	LBA Alpine slags	Trentino	Luserna	**0.0208**
	LU-G56	LBA Alpine slags	Trentino	Luserna	**0.0229**
	LU-G59	LBA Alpine slags	Trentino	Luserna	**0.0244**
	CALC-1	E Alps, Valsugana VMS	Trentino	Calceranica	**0.0260**
	CALC-2	E Alps, Valsugana VMS	Trentino	Calceranica	**0.0263**
	VAL-SC1	LBA Alpine slags	Trentino	Vallarsa	**0.0266**
	CALC7	E Alps, Valsugana VMS	Trentino	Calceranica	**0.0327**
CdSA-PnB	56	Balkans: Bulgaria	South Bulgaria	Madan	**0.0063**
	Madan	Balkans: Bulgaria	South Bulgaria	Madan	**0.0118**
	59	Balkans: Bulgaria	South Bulgaria	Luki	**0.0152**
	57	Balkans: Bulgaria	South Bulgaria	Madan	**0.0169**
	PA13786	NE Catalunya, Baleares, Cord Iberica	Iberia NE	Sa Argentera	**0.0170**
	107	Balkans: Bulgaria	South Bulgaria	Madan	**0.0177**
	Spn12	Iberia: SE Murcia Cartagena	Iberia SE	Cartagena	**0.0198**
	TG 59c	Greece: Euboea	Grecia	Kallianou	**0.0228**
	65	Balkans: Bulgaria	South Bulgaria	Luki	**0.0235**
	106	Balkans: Bulgaria	South Bulgaria	Madan	**0.0241**
CdSB-P60	TEM 1A	Tuscany: Southern	Tuscany	Temperino	**0.0454**
	LP 4A	Tuscany: Southern	Tuscany	La Pesta	**0.0505**
		Austria: Inn valley, Salzburg, Styria (Fhz)	Tyrol	Rö	**0.0557**
	LP 2A	Tuscany: Southern	Tuscany	La Pesta	**0.0566**
	R16A	Iberia: SE Murcia Cartagena	Iberia SE	Mazarron	**0.0589**
	AON411	Turkey: Taurus Mountains	Turchia		**0.0619**
	AON243	Turkey: Taurus Mountains	Turchia	Akcakisla Ozge Mine	**0.0625**
	PA13527B	Iberia: SE Andalusia-Jaen	Iberia SE	Pinar de Bedar	**0.0671**
	PA 13530A	Iberia: SE Murcia Cartagena	Iberia SE	Sierra Cantar	**0.0702**
	BaS-21	Slovakia, Bohemian Massif	Slovakia	Banska Stiavnica	**0.0712**
Cel-P38	MFO_Ap2	E Alps, Southalpine AATV	Trentino	Montefondoli	**0.0097**
	TR-M2	LBA Alpine slags	Trentino	Transacqua	**0.0135**
	P067-b-hv	Iberia: SW, Portugal	Iberia SW	FG-060570	**0.0136**
	P3	E Alps, Southalpine AATV	Trentino	Pamera	**0.0158**
	TR-M11	LBA Alpine slags	Trentino	Transacqua	**0.0200**
	TR-P14	LBA Alpine slags	Trentino	Transacqua	**0.0253**
	MFO-KW	E Alps, Southalpine AATV	Trentino	Montefondoli	**0.0282**
	50411-	E Alps, Southalpine AATV	Trentino	Cinque Valli	**0.0284**
	TR-G3	LBA Alpine slags	Trentino	Transacqua	**0.0289**
	PN11-14	E Alps, Southalpine AATV	Veneto	Pian della Stua	**0.0302**

Appendix 4 *(Continued)*

Artefact	Ore/Slag Sample n.	Data base field	Region	Site/Mine	Rank
Cel-P41	4-M30	Swiss Valais	Valais area	Biolec	**0.0182**
	36-M27	Swiss Valais	Valais area	Tsirouc	**0.0190**
		Austria: Inn valley, Salzburg, Styria (Fhz)	Inn Valley	Groskogel	**0.0221**
	19	France: Central Massif, Mont Lozere	France	Le Bleymard	**0.0237**
	Kre-05	Slovakia, Bohemian Massif	Slovakia	Kremnica	**0.0251**
	Pie-02	Slovakia, Bohemian Massif	Slovakia	Piesky	**0.0289**
	35	France: Central Massif, Mont Lozere	France	Montmirat	**0.0304**
	MA-1p	E Alps, Carnia	Friuli	Monte Avanza	**0.0324**
	FG-011192	Austria: Inn valley, Salzburg, Styria (Fhz)	Inn Valley	Mockleiten	**0.0329**
	PEV 100A	Cyprus	Cyprus	Pevkos	**0.0344**
Ver-P0	LU-SC1a	LBA Alpine slags	Trentino	Luserna	**0.0100**
	LU-G56	LBA Alpine slags	Trentino	Luserna	**0.0120**
	LU-M4	LBA Alpine slags	Trentino	Luserna	**0.0148**
	LU-SC1a bis	LBA Alpine slags	Trentino	Luserna	**0.0150**
	LU-PS65	LBA Alpine slags	Trentino	Luserna	**0.0199**
	LU-M47	LBA Alpine slags	Trentino	Luserna	**0.0225**
	CAL 5	E Alps, Valsugana VMS	Trentino	Calceranica	**0.0230**
	LU-GM57	LBA Alpine slags	Trentino	Luserna	**0.0265**
	LU-GM57	LBA Alpine slags	Trentino	Luserna	**0.0302**
	809-004	Iberia: Center, Alcudia valley	Iberia Center	Navalcuerno	**0.0354**
Ver-P9	TR-M2	LBA Alpine slags	Trentino	Transacqua	**0.0093**
	MFO_Ap2	E Alps, Southalpine AATV	Trentino	Montefondoli	**0.0094**
	P3	E Alps, Southalpine AATV	Trentino	Pamera	**0.0099**
	P067-b-hv	Iberia: SW, Portugal	Iberia SW	Mannheim	**0.0121**
	TR-M11	LBA Alpine slags	Trentino	Transacqua	**0.0174**
	MFO-KW	E Alps, Southalpine AATV	Trentino	Montefondoli	**0.0237**
	50411-	E Alps, Southalpine AATV	Trentino	Cinque Valli	**0.0245**
	JDLL	Iberia: Center, Linares-La Carolina	Iberia Center	La Carolina	**0.0263**
	PN11-14	E Alps, Southalpine AATV	Veneto	Pian della Stua	**0.0273**
	TR-P14	LBA Alpine slags	Trentino	Transacqua	**0.0280**
Por6-TC8	LAV-1	E Alps, Southalpine AATV	Trentino	Furli di Lavis	**0.0149**
	MA 5/26	Tuscany: Alpi Apuane	Toscana	M. Arsiccio	**0.0177**
	VBA 5	Tuscany: Alpi Apuane	Toscana	Pollone	**0.0224**
	34-0000	W Alps 2, Argentera Ivrea	Piemonte	Fej di Doccia	**0.0237**
	VyB-02	Slovakia, Bohemian Massif	Slovakia	Vysna Boca	**0.0254**
	AA 93.13		Cumbria		**0.0286**
	T-15	France: Massif Central, Cevennes	France	Les Malines	**0.0309**
	B-21	France: Massif Central, Cevennes	France	Les Malines	**0.0311**
	33b	W Alps 2, Argentera Ivrea	Piemonte	Sella Bassa	**0.0317**
	8N3 6253		North. Pennines		**0.0321**

Appendix 4 *(Continued)*

Artefact	Ore/Slag Sample n.	Data base field	Region	Site/Mine	Rank
Por6-PC6	LAV-1	E Alps, Southalpine AATV	Trentino	Furli di Lavis	**0.0115**
	MOR41-119	W Alps 2, Argentera Ivrea	Piemonte	Bars de l'Ors	**0.0138**
	AA 93.13		Cumbria		**0.0152**
	OUM 18537		Cornwall and Devon	Bere Alston	**0.0159**
	T-26	France: Massif Central, Cevennes	France	Les Malines	**0.0177**
	MA 5/26	Tuscany: Alpi Apuane	Toscana	M. Arsiccio	**0.0204**
	COB20d	Sardinia: NW Sassarese	NW Sardinia	Calabona (SS)	**0.0209**
	VBO2p1	E Alps, Southalpine AATV	Veneto	Valbona - Sasso Negro	**0.0211**
	BO-CuNt	Liguria, Apennines-Cu nativo	Emilia Romagna	Ca' de' Vanni Sopra	**0.0213**
	VBA 5	Tuscany: Alpi Apuane	Toscana	Pollone	**0.0218**
Por6-SN2	PA13567C	Iberia: SE Andalusia-Jaen	Iberia SE	Fondon 1	**0.0109**
	PA11658	NE Catalunya, Baleares, Cord Iberica	Iberia NE	Falset	**0.0125**
	15	France: Central Massif, Mont Lozere	France	Vialas	**0.0130**
	BM.1927,103	Iberia: SE Andalusia-Jaen	Iberia SE	Los Belgas Mine	**0.0138**
	PA13792B	Iberia: SE Andalusia-Jaen	Iberia SE	Mina Almagrera	**0.0177**
	16	France: Central Massif, Mont Lozere	France	Vialas	**0.0200**
	14	France: Central Massif, Mont Lozere	France	Vialas	**0.0202**
	PA12378	NE Catalunya, Baleares, Cord Iberica	Iberia NE	Sant Julia (Gerona)	**0.0207**
	BED-2	E Alps, Southalpine AATV	Trentino	Stol de Pecè	**0.0231**
	VBA 5	Tuscany: Alpi Apuane	Toscana	Pollone	**0.0233**
Por6-SN8	TG 268F	Balkans: Serbia	Serbia	Cadinje	**0.0069**
	AG/j	Iberia: SW, IPB	Iberia SW	Los Molares	**0.0093**
	PA11996	NE Catalunya, Baleares, Cord Iberica	Iberia NE	Linda Mariquita	**0.0100**
	T-27	France: Massif Central, Cevennes	France	Les Malines	**0.0158**
	FG-011190	Austria: Inn valley, Salzburg, Styria (Fhz)	Inn Valley	Innsbruck,	**0.0169**
	TG10	Turkey: Pontic Mnts.	Turchia	Kurudere	**0.0180**
	MAV 34	Tuscany: Alpi Apuane	Toscana	M. Arsiccio	**0.0205**
	BED-MM1 (1)	E Alps, Southalpine AATV	Trentino	Vecchia Bedovina	**0.0217**
	PA11657	NE Catalunya, Baleares, Cord Iberica	Iberia NE	Falset	**0.0238**
	T-18	France: Massif Central, Cevennes	France	Les Malines	**0.0253**
Por9-TC29	MOR41-119	W Alps 2, Argentera Ivrea	Piemonte	Bars de l'Ors	**0.0099**
	OUM 18537 OUM	Cornwall and Devon			**0.0126**
	T-26	France: Massif Central, Cevennes	France	Les Malines	**0.0145**
	AA 93.13		Cumbria		**0.0162**
	BO-CuNt	Liguria, Apennines-Cu nativo	Emilia Romagna	Ca' de' Vanni Sopra	**0.0164**
	LAV-1	E Alps, Southalpine AATV	Trentino	Furli di Lavis	**0.0164**
	COB20d	Sardinia: NW Sassarese	NW Sardinia	Calabona (SS)	**0.0167**
	B-4	France: Massif Central, Cevennes	France	Les Malines	**0.0213**
	BN3 6254		Nort. Pennines		**0.0214**
	VBO2p1	E Alps, Southalpine AATV	Veneto	Valbona - Sasso Negro	**0.0217**

Appendix 4 *(Continued)*

Artefact	Ore/Slag Sample n.	Data base field	Region	Site/Mine	Rank
Por6-PP7	Da 7739 Bristol		Mendips/Bristol	Hobbs Quarry	**0.0205**
	Da 10375 Bristol		Mendips/Bristol	Hobbs Quarry	**0.0218**
	Da 10371 Bristol		Mendips/Bristol	Hobbs Quarry	**0.0291**
	Da 6736 Bristol		Mendips/Bristol	Brentry Hospital grounds	**0.0313**
	BN10 20919		Northern Pennines	Frazers Hush	**0.0345**
	F-1/006aa	France: Cabriere	Languedoc	La Roussignole	**0.0345**
	BM 1930.344		Southern Pennines	Millclose mine	**0.0349**
	AEM 10	UK: Wales, Great Orme, Copa Hill	Cheshire	Malachite	**0.0355**
	43b	Balkans: Bulgaria	Central Bulgaria	Gramatikovo	**0.0373**
	AE92-20	UK: Wales, Great Orme, Copa Hill	Cheshire	Galena	**0.0375**
Por9-Pn25	LU-GM57	LBA Alpine slags	Trentino	Luserna	**0.0095**
	CALC-3	E Alps, Valsugana VMS	Trentino	Calceranica	**0.0103**
	LU-G59 M	LBA Alpine slags	Trentino	Luserna	**0.0130**
	CALC-1	E Alps, Valsugana VMS	Trentino	Calceranica	**0.0164**
	LU-G59	LBA Alpine slags	Trentino	Luserna	**0.0184**
	CALC-2	E Alps, Valsugana VMS	Trentino	Calceranica	**0.0207**
	23078V U6	Levant: Timna, Faynan	Egypt	Timna, area U	**0.0218**
	CALC7	E Alps, Valsugana VMS	Trentino	Calceranica	**0.0239**
		Austria: Tyrol, Carinthia (cpy)	Salzburg	Rettenbach	**0.0253**
	23114R T24	Levant: Timna, Faynan	Egypt	Timna, area S/T	**0.0278**
Por9-Bar5	GRUA_Ep1	E Alps, Southalpine AATV	Trentino	Maso Erdemolo	**0.0070**
	CD-a-11	E Alps, Southalpine AATV	Trentino	Montefondoli	**0.0105**
	DRO 89-1		Central Wales	Drosgol	**0.0118**
	MA-5pBIS	E Alps, Carnia	Friuli	Monte Avanza	**0.0132**
	GRUA_Gs1	E Alps, Southalpine AATV	Trentino	Maso Erdemolo	**0.0149**
	GRUA_Dsxp1	E Alps, Southalpine AATV	Trentino	Maso Erdemolo	**0.0163**
	REG-2	E Alps, Southalpine AATV	Trentino	Val Reganel	**0.0176**
	MT2	E Alps, Southalpine AATV	Veneto	Monte Trisa	**0.0192**
	F	E Alps, Southalpine AATV	Veneto	Val Livergon	**0.0206**
	GRUA_Ddxp1	E Alps, Southalpine AATV	Trentino	Maso Erdemolo	**0.0242**
Por9-PC24	PA11657	NE Catalunya, Baleares, Cord Iberica	Iberia NE	Falset	**0.0052**
	T-27	France: Massif Central, Cevennes	France	Les Malines	**0.0063**
	MOR41-123	W Alps 1, Falda Pemontese	Piemonte	Chialamberto	**0.0120**
	PA11996	NE Catalunya, Baleares, Cord Iberica	Iberia NE	Linda Mariquita	**0.0153**
	BED-MM1 ter (3)	E Alps, Southalpine AATV	Trentino	Vecchia Bedovina	**0.0168**
	PAS-2	W Alps 2, Argentera Ivrea	Liguria	Murialdo-Pastori	**0.0185**
	BED-MM1 bis (2)	E Alps, Southalpine AATV	Trentino	Vecchia Bedovina	**0.0201**
	FG-011165 PP005	Austria: Inn valley, Salzburg, Styria (Fhz)	Inn Valley	Silberberg	**0.0205**
	16	France: Central Massif, Mont Lozere	France	Vialas	**0.0238**
	PAS-1	W Alps 2, Argentera Ivrea	Liguria	Murialdo-Pastori	**0.0240**

Appendix 4 *(Continued)*

Artefact	Ore/Slag Sample n.	Data base field	Region	Site/Mine	Rank
Por9-PC49	BM.40788	Iberia: SE Andalusia-Jaen	Iberia SE	Almeria	**0.0117**
	PAT-SID	E Alps, Southalpine AATV	Veneto	Pian della Stua	**0.0143**
	PA11993	NE Catalunya, Baleares, Cord Iberica	Iberia NE	Mina Regia	**0.0149**
	?	NE Catalunya, Baleares, Cord Iberica	Iberia NE	Mineralogia	**0.0153**
	PA11954	NE Catalunya, Baleares, Cord Iberica	Iberia NE	Linda Mariquita	**0.0160**
	?	NE Catalunya, Baleares, Cord Iberica	Iberia NE	Mineralogia	**0.0165**
	PA12008	NE Catalunya, Baleares, Cord Iberica	Iberia NE	Linda Mariquita	**0.0169**
	VBA 5	Tuscany: Alpi Apuane	Toscana	Pollone	**0.0179**
	C-25-B	NE Catalunya, Baleares, Cord Iberica	Iberia NE	Martorell	**0.0179**
	Bre-03	Slovakia, Bohemian Massif	Slovakia	Brezno	**0.0189**
Por6-PI-9	LAV-2	E Alps, Southalpine AATV	Trentino	Furli di Lavis	**0.0152**
	CD-a-11	E Alps, Southalpine AATV	Trentino	Montefondoli	**0.0167**
	MFO-MU	E Alps, Southalpine AATV	Trentino	Montefondoli	**0.0202**
	MFO_Ap3	E Alps, Southalpine AATV	Trentino	Montefondoli	**0.0206**
	GRUA_Ep1	E Alps, Southalpine AATV	Trentino	Maso Erdemolo	**0.0209**
	MFO-KW	E Alps, Southalpine AATV	Trentino	Montefondoli	**0.0233**
	MA-5pBIS	E Alps, Carnia	Friuli	Monte Avanza	**0.0242**
	DRO 89-1		Central Wales	Drosgol	**0.0260**
	50411-	E Alps, Southalpine AATV	Trentino	Cinque Valli	**0.0271**
	GRUA_Gs1	E Alps, Southalpine AATV	Trentino	Maso Erdemolo	**0.0273**
Por9-PI60	MN2	E Alps, Southalpine AATV	Veneto	Monte Naro	**0.0055**
	1-	Greece: Euboea	Grecia	Ano Valsamonero	**0.0179**
	MA 5/17	Tuscany: Alpi Apuane	Toscana	M. Arsiccio	**0.0188**
	BED-1 bis	E Alps, Southalpine AATV	Trentino	Min. Bedovina	**0.0234**
	SKO - HpI - 1	Cyprus	Cipro	Skouriotissa	**0.0242**
	Dve-01	Slovakia, Bohemian Massif	Slovakia	Dolna Lehota	**0.0255**
	8N3 6253		Northern Pennines		**0.0274**
	Sok-01	Slovakia, Bohemian Massif	Slovakia	Sokolova Dolina	**0.0278**
	87.47G.M72		Central Wales	Loveden	**0.0288**
	6	France: Central Massif, Mont Lozere	France	Ramponeche	**0.0302**
Por9-PI73	12 S	Swiss Valais	Valais area	La Barma	**0.0088**
	S 10	France: Massif Central, Cevennes	France	Les Malines	**0.0117**
	18 S	Swiss Valais	Valais area	La Barma	**0.0139**
	BN7 6214		Northern Pennines		**0.0204**
	T-28	France: Massif Central, Cevennes	France	Les Malines	**0.0233**
	B-21	France: Massif Central, Cevennes	France	Les Malines	**0.0244**
	15 S	Swiss Valais	Valais area	La Barma	**0.0264**
	33b	W Alps 2, Argentera Ivrea	Piemonte	Sella Bassa	**0.0265**
	L-2	France: Massif Central, Cevennes	France	Les Malines	**0.0276**
	14-M10	Swiss Valais	Valais area	Grand Alou	**0.0290**

Appendix 4 *(Continued)*

Artefact	Ore/Slag Sample n.	Data base field	Region	Site/Mine	Rank
Por9-PI93	LAV-1	E Alps, Southalpine AATV	Trentino	Furli di Lavis	**0.0094**
	MOR41-119	W Alps 2, Argentera Ivrea	Piemonte	Bars de l'Ors	**0.0179**
	34-0000	W Alps 2, Argentera Ivrea	Piemonte	Fej di Doccia	**0.0190**
	33b	W Alps 2, Argentera Ivrea	Piemonte	Sella Bassa	**0.0195**
	VBA 5	Tuscany: Alpi Apuane	Toscana	Pollone	**0.0197**
	MA 5/26	Tuscany: Alpi Apuane	Toscana	M. Arsiccio	**0.0199**
	AA 93.13		Cumbria		**0.0215**
	OUM 18537 OUM		Cornwall and Devon	Bere Alston	**0.0220**
	VyB-02	Slovakia, Bohemian Massif	Slovakia	Vysna Boca	**0.0240**
	BN3 6254		North. Pennines	Nentsberry mine	**0.0245**
Por9-PI71	LU-P6	LBA Alpine slags	Trentino	Luserna	**0.0131**
	LU-GM57	LBA Alpine slags	Trentino	Luserna	**0.0154**
	LU-GM57	LBA Alpine slags	Trentino	Luserna	**0.0161**
	SEG-G4	LBA Alpine slags	Trentino	Segonzano	**0.0184**
	LU-GM57	LBA Alpine slags	Trentino	Luserna	**0.0186**
	VET-s1	E Alps, Valsugana VMS	Trentino	Vetriolo	**0.0187**
	809-004	Iberia: Center, Alcudia valley	Iberia Center	Navalcuerno	**0.0191**
	VI GAL	E Alps, Valsugana VMS	Veneto	Valle Imperina	**0.0209**
	SEG-G4 bis	LBA Alpine slags	Trentino	Segonzano	**0.0230**
	VI FIG15	E Alps, Valsugana VMS	Veneto	Valle Imperina	**0.0253**
Gal-PI-3	RED1P	LBA Alpine slags	Trentino	Redebus	**0.0136**
	LU-P61	LBA Alpine slags	Trentino	Luserna	**0.0342**
	23070P P1	Levant: Timna, Faynan	Egypt	Timna, area P	**0.0379**
	809-037	Iberia: Center, Alcudia valley	Iberia Center	Villazaide	**0.0413**
	SEG-P5	LBA Alpine slags	Trentino	Segonzano	**0.0433**
	862-001	Iberia: Center, Alcudia valley	Iberia Center	Mina Rica Nueva	**0.0455**
	213)62	Iberia: SW, Ossa Morena	Iberia SW	Afortunada	**0.0455**
	213)610	Iberia: SW, Ossa Morena	Iberia SW	Afortunada	**0.0461**
	BA-18	Iberia: SW, Ossa Morena	Iberia SW	Azuaga S	**0.0469**
	BA-9	Iberia: SW, Ossa Morena	Iberia SW	Azuaga N	**0.0475**
Gal-PI-4	VAL-SC2	LBA Alpine slags	Trentino	Vallarsa	**0.0110**
	LU-M47	LBA Alpine slags	Trentino	Luserna	**0.0153**
	LU-GM57	LBA Alpine slags	Trentino	Luserna	**0.0165**
	LU-G56	LBA Alpine slags	Trentino	Luserna	**0.0183**
	VAL-SC1	LBA Alpine slags	Trentino	Vallarsa	**0.0197**
	LU-PS65	LBA Alpine slags	Trentino	Luserna	**0.0235**
	LU-M4	LBA Alpine slags	Trentino	Luserna	**0.0262**
	LU-G56 Qz	LBA Alpine slags	Trentino	Luserna	**0.0315**
	23078V U6	Levant: Timna, Faynan	Egypt		**0.0338**
	LU-SC1a	LBA Alpine slags	Trentino	Luserna	**0.0401**

Appendix 4 *(Continued)*

Artefact	Ore/Slag Sample n.	Data base field	Region	Site/Mine	Rank
Gal-PI-5	LU-M47	LBA Alpine slags	Trentino	Luserna	**0.0084**
	LU-M4	LBA Alpine slags	Trentino	Luserna	**0.0139**
	LU-PS65	LBA Alpine slags	Trentino	Luserna	**0.0141**
	LU-G56 Qz	LBA Alpine slags	Trentino	Luserna	**0.0182**
	VAL-SC2	LBA Alpine slags	Trentino	Vallarsa	**0.0209**
	LU-GM57 Cu	LBA Alpine slags	Trentino	Luserna	**0.0244**
	LU-SC1a	LBA Alpine slags	Trentino	Luserna	**0.0257**
	LU-SC1a bis	LBA Alpine slags	Trentino	Luserna	**0.0313**
	LU-G56	LBA Alpine slags	Trentino	Luserna	**0.0323**
	VAL-SC1	LBA Alpine slags	Trentino	Vallarsa	**0.0330**
Can-S	LU-PS45	LBA Alpine slags	Trentino	Luserna	**0.0045**
	LU-G56 M	LBA Alpine slags	Trentino	Luserna	**0.0121**
	duplicate	Iberia: Center, Alcudia valley	Iberia Center	Pontones	**0.0125**
	VAL-SC2	LBA Alpine slags	Trentino	Vallarsa	**0.0130**
	860-1	Iberia: Center, Alcudia valley	Iberia Center	San Bartolome	**0.0222**
	LU-G70	LBA Alpine slags	Trentino	Luserna	**0.0237**
	SEG-G4 bis	LBA Alpine slags	Trentino	Segonzano	**0.0245**
	861-48	Iberia: Center, Alcudia valley	Iberia Center	Pozo Rico	**0.0253**
	PAT-BOR	E Alps, Southalpine AATV	Veneto	Pian della Stua	**0.0267**
	VI-08	E Alps, Valsugana VMS	Veneto	Valle Imperina	**0.0275**
BEL-S	PA11987	NE Catalunya, Baleares, Cord Iberica	Iberia NE	Mineralogia	**0.0092**
	Pb 813		Central Wales	Llwynmalus	**0.0117**
	PA11995	NE Catalunya, Baleares, Cord Iberica	Iberia NE	Raimunda	**0.0137**
	PA11998	NE Catalunya, Baleares, Cord Iberica	Iberia NE	Barranco Hondo	**0.0137**
	PA12288	NE Catalunya, Baleares, Cord Iberica	Iberia NE	Jalapa	**0.0180**
	PA12274	NE Catalunya, Baleares, Cord Iberica	Iberia NE	Barranco Hondo	**0.0190**
	BLRBR-5A	Tuscany: Alpi Apuane	Toscana	Bottino	**0.0205**
	Clai-2	Iberia: SE Andalusia-Jaen	Iberia SE	Alhamilla	**0.0210**
	PA11992	NE Catalunya, Baleares, Cord Iberica	Iberia NE	Mina Regia	**0.0213**
	LIN-2	Iberia: Center, Linares-La Carolina	Iberia Center	Grupo Matacabras	**0.0215**
Mus-S2	SEG-P13	LBA Alpine slags	Trentino	Segonzano	**0.0102**
	SEG-P5	LBA Alpine slags	Trentino	Segonzano	**0.0123**
	MIE-107	E Alps, Southalpine AATV	Trentino	Viarago	**0.0172**
	MIE-113	E Alps, Southalpine AATV	Trentino	Viarago	**0.0182**
	PC 92.3		Central Wales	Nantyreira	**0.0235**
	SEG-M10	LBA Alpine slags	Trentino	Segonzano	**0.0278**
	PA6	E Alps, Southalpine AATV	Trentino	Pamera	**0.0284**
	MT3	E Alps, Southalpine AATV	Veneto	Monte Trisa	**0.0364**
	LU-SC1	LBA Alpine slags	Trentino	Luserna	**0.0387**
	RED1P	LBA Alpine slags	Trentino	Redebus	**0.0410**

Appendix 4 *(Continued)*

Artefact	Ore/Slag Sample n.	Data base field	Region	Site/Mine	Rank
Mus-S3	SEG-M10	LBA Alpine slags	Trentino	Segonzano	**0.0131**
	PA6	E Alps, Southalpine AATV	Trentino	Pamera	**0.0145**
	SEG-G9	LBA Alpine slags	Trentino	Segonzano	**0.0170**
	LU-SC1	LBA Alpine slags	Trentino	Luserna	**0.0172**
	MIE-113	E Alps, Southalpine AATV	Trentino	Viarago	**0.0190**
	MT3	E Alps, Southalpine AATV	Veneto	Monte Trisa	**0.0208**
	LU-SC1 bis	LBA Alpine slags	Trentino	Luserna	**0.0240**
	GRUA_As1	E Alps, Southalpine AATV	Trentino	Maso Erdemolo	**0.0241**
	MT1-360	E Alps, Southalpine AATV	Veneto	Monte Trisa	**0.0310**
	GRUA_Cp1	E Alps, Southalpine AATV	Trentino	Maso Erdemolo	**0.0321**
CdSA-S	LU-PR34	LBA Alpine slags	Trentino	Luserna	**0.0139**
	LU-GM57 M	LBA Alpine slags	Trentino	Luserna	**0.0266**
	23118U C3	Levant: Timna, Faynan	Egypt	Timna, area S/T	**0.0387**
	23070P P1	Levant: Timna, Faynan	Egypt	Timna, area P	**0.0420**
	RED1P	LBA Alpine slags	Trentino	Redebus	**0.0469**
	AP 92.6		Shropshire	Shelve Grit mine	**0.0490**
	396	Iberia: SW, Ossa Morena	Iberia SW	La Dehesa	**0.0510**
	862-001	Iberia: Center, Alcudia valley	Iberia Center	Mina Rica Nueva	**0.0524**
	809-037	Iberia: Center, Alcudia valley	Iberia Center	Villazaide	**0.0531**
Cel-S	RED1P	LBA Alpine slags	Trentino	Redebus	**0.0058**
	SEG-P5	LBA Alpine slags	Trentino	Segonzano	**0.0300**
	SEG-P13	LBA Alpine slags	Trentino	Segonzano	**0.0376**
	23070P P1	Levant: Timna, Faynan	Egypt	Timna, area P	**0.0418**
	MIE-107	E Alps, Southalpine AATV	Trentino	Viarago	**0.0442**
	809-037	Iberia: Center, Alcudia valley	Iberia Center	Villazaide	**0.0467**
	LU-P61	LBA Alpine slags	Trentino	Luserna	**0.0482**
	213)62	Iberia: SW, Ossa Morena	Iberia SW	Afortunada	**0.0483**
	MOR41-122	W Alps 1, Falda Pemontese	Piemonte	Chialamberto	**0.0507**
	213)610	Iberia: SW, Ossa Morena	Iberia SW	Afortunada	**0.0523**
Cer-Ax	RED1P	LBA Alpine slags	Trentino	Redebus	**0.0171**
	23070P P1	Levant: Timna, Faynan	Egypt	Timna, area P	**0.0190**
	MOR41-122	W Alps 1, Falda Pemontese	Piemonte	Chialamberto	**0.0317**
	809-037	Iberia: Center, Alcudia valley	Iberia Center	Villazaide	**0.0330**
	P28	E Alps, Southalpine AATV	Trentino	Pamera	**0.0363**
	23083Q ARB64	Levant: Timna, Faynan	Egypt	Beer Ora, site 64	**0.0375**
	LU-P61	LBA Alpine slags	Trentino	Luserna	**0.0381**
	BMR8.92 DAR Al		Central Wales	Daren	**0.0390**
	862-001	Iberia: Center, Alcudia valley	Iberia Center	Mina Rica Nueva	**0.0396**
	SEG-P5	LBA Alpine slags	Trentino	Segonzano	**0.0410**

Appendix 4 *(Continued)*

Artefact	Ore/Slag Sample n.	Data base field	Region	Site/Mine	Rank
Mus-Ax6	GRUA_Cp1	E Alps, Southalpine AATV	Trentino	Maso Erdemolo	**0.0090**
	MN3	E Alps, Southalpine AATV	Veneto	Monte Naro	**0.0140**
	GRUA_As1	E Alps, Southalpine AATV	Trentino	Maso Erdemolo	**0.0148**
	GRUA_Ddxp1	E Alps, Southalpine AATV	Trentino	Maso Erdemolo	**0.0166**
	Cu-NT	Liguria, Apennines-Cu nativo	Toscana	Impruneta	**0.0174**
	MT4	E Alps, Southalpine AATV	Veneto	Monte Trisa	**0.0179**
	RED-1G-Fa	LBA Alpine slags	Trentino	Redebus	**0.0186**
	REP_As1	Liguria, Apennines-secondari	Liguria	Reppia secodari	**0.0204**
	LU-SC1 bis	LBA Alpine slags	Trentino	Luserna	**0.0209**
	SEG-M2	LBA Alpine slags	Trentino	Segonzano	**0.0212**
Mus-Ax7	SEG-M10	LBA Alpine slags	Trentino	Segonzano	**0.0213**
	PC 92.3		Central Wales	Nantyreira	**0.0225**
	MIE-113	E Alps, Southalpine AATV	Trentino	Viarago	**0.0229**
	PA6	E Alps, Southalpine AATV	Trentino	Pamera	**0.0236**
	LU-SC1	LBA Alpine slags	Trentino	Luserna	**0.0245**
	MIE-107	E Alps, Southalpine AATV	Trentino	Viarago	**0.0249**
	BMR8.92 YSB 2		Central Wales	Ysbyty Ystwyth	**0.0254**
	SEG-G9	LBA Alpine slags	Trentino	Segonzano	**0.0275**
	MT3	E Alps, Southalpine AATV	Veneto	Monte Trisa	**0.0279**
	SEG-P13	LBA Alpine slags	Trentino	Segonzano	**0.0288**
CdSB-AxA1	SEG-P13	LBA Alpine slags	Trentino	Segonzano	**0.0070**
	SEG-P5	LBA Alpine slags	Trentino	Segonzano	**0.0120**
	MIE-113	E Alps, Southalpine AATV	Trentino	Viarago	**0.0166**
	PA6	E Alps, Southalpine AATV	Trentino	Pamera	**0.0288**
	MIE-107	E Alps, Southalpine AATV	Trentino	Viarago	**0.0289**
	SEG-M10	LBA Alpine slags	Trentino	Segonzano	**0.0292**
	PC 92.3		Central Wales	Nantyreira	**0.0318**
	MT3	E Alps, Southalpine AATV	Veneto	Monte Trisa	**0.0383**
	RED1P	LBA Alpine slags	Trentino	Redebus	**0.0394**
	LU-SC1	LBA Alpine slags	Trentino	Luserna	**0.0421**
CdSB-AxA2	AA 93.7		Cumbria		**0.0160**
	25	France: Central Massif, Mont Lozere	France	Les Bondons	**0.0163**
	33	France: Central Massif, Mont Lozere	France	Montmirat	**0.0195**
	12380	NE Catalunya, Baleares, Cord Iberica	Iberia NE	Mina Leonor	**0.0210**
	SARD 118	Sardinia: NW Sassarese	NW Sardinia	Nulvi	**0.0219**
	29	France: Central Massif, Mont Lozere	France	Montmirat	**0.0222**
	?	Iberia: NE, Euskadi	Iberia Euskadi	Sta. Barbara	**0.0247**
	11	France: Central Massif, Mont Lozere	France	Bedoues-Cocures	**0.0264**
	24	France: Central Massif, Mont Lozere	France	Les Bondons	**0.0273**
	?	Iberia: NE, Euskadi	Iberia Euskadi	Otxamentegi	**0.0286**

Appendix 4 *(Continued)*

Artefact	Ore/Slag Sample n.	Data base field	Region	Site/Mine	Rank
CdSB-AxA9	BED-2	E Alps, Southalpine AATV	Trentino	Stol de Pecè	**0.0186**
	MA 5/26	Tuscany: Alpi Apuane	Toscana	M. Arsiccio	**0.0193**
	AA 93.13		Cumbria		**0.0202**
	PA11956	NE Catalunya, Baleares, Cord Iberica	Iberia NE	Linda Mariquita	**0.0206**
	VBO2p1	E Alps, Southalpine AATV	Veneto	Valbona	**0.0210**
	15	France: Central Massif, Mont Lozere	France	Vialas	**0.0213**
	BM 1947.4		Cumbria		**0.0249**
	14	France: Central Massif, Mont Lozere	France	Vialas	**0.0259**
	87.47G.M39		Central Wales	Pandy mine	**0.0277**
	LAV-1	E Alps, Southalpine AATV	Trentino	Furli di Lavis	**0.0287**
CdSA-AxC4	PA12289	NE Catalunya, Baleares, Cord Iberica	Iberia NE	Jalapa	**0.0069**
	12379	NE Catalunya, Baleares, Cord Iberica	Iberia NE	Sant Julia	**0.0086**
	Ptno-1	Iberia: SE Andalusia-Jaen	Iberia SE	Alhamilla	**0.0117**
	RB 23	Tuscany: Alpi Apuane	Toscana	Pollone	**0.0139**
	PA11954	NE Catalunya, Baleares, Cord Iberica	Iberia NE	Linda Mariquita	**0.0149**
	PA13567B	Iberia: SE Andalusia-Jaen	Iberia SE	Fondon 1	**0.0153**
	VBA 5	Tuscany: Alpi Apuane	Toscana	Pollone	**0.0160**
	?	NE Catalunya, Baleares, Cord Iberica	Iberia NE	Linda Mariquita	**0.0169**
	BM.40788	Iberia: SE Andalusia-Jaen	Iberia SE	Almeria	**0.0170**
	MOR41-123	W Alps 1, Falda Pemontese	Piemonte	Chialamberto	**0.0177**
CdSA-Ax59	Pon-03	Slovakia, Bohemian Massif	Slovakia	Poniky	**0.0160**
	BED-1	E Alps, Southalpine AATV	Trentino	Min. Bedovina	**0.0170**
	FG-011177	Austria: Inn valley, Salzburg, Styria (Fhz)	Inn Valley	Maukenotz	**0.0177**
	PT-6/4	Iberia: SW, IPB	Iberia SW	Norte Paterna	**0.0177**
	Pon-02	Slovakia, Bohemian Massif	Slovakia	Poniky	**0.0196**
	Pon-05	Slovakia, Bohemian Massif	Slovakia	Poniky	**0.0229**
		Austria: Inn valley, Salzburg, Styria (Fhz)	Inn Valley	Brixlegg 339	**0.0231**
	Pon-04	Slovakia, Bohemian Massif	Slovakia	Poniky	**0.0231**
	PA13792C	Iberia: SE Andalusia-Jaen	Iberia SE	Mina Almagrera	**0.0254**
	TG 268D	Balkans: Serbia	Serbia	Cadinje	**0.0256**
Gal-Ax	LU-GM57 M	LBA Alpine slags	Trentino	Luserna	**0.0068**
	LU-PR34	LBA Alpine slags	Trentino	Luserna	**0.0199**
	23118U C3	Levant: Timna, Faynan	Egypt	Timna, area S/T	**0.0250**
	AP 92.6		Shropshire		**0.0327**
	SEG-P14	LBA Alpine slags	Trentino	Segonzano	**0.0341**
	LU-P61	LBA Alpine slags	Trentino	Luserna	**0.0362**
	861-7	Iberia: Center, Alcudia valley	Iberia Center	Los Diegos	**0.0464**
	861-43	Iberia: Center, Alcudia valley	Iberia Center	Mina Atilana	**0.0479**
	861-5	Iberia: Center, Alcudia valley	Iberia Center	San Justo	**0.0486**
	PAM-1	E Alps, Southalpine AATV	Trentino	Pamera	**0.0491**

Appendix 4 *(Continued)*

Artefact	Ore/Slag Sample n.	Data base field	Region	Site/Mine	Rank
Cel-AxC8	87.47G.M39		Central Wales	Pandy mine	**0.0164**
	Min	Iberia: SE Andalusia-Jaen	Iberia SE	Sierra de Gador	**0.0241**
	D-7	E Alps, Southalpine AATV	LOMBARDIA	Duadello	**0.0246**
	Dve-01	Slovakia, Bohemian Massif	Slovakia	Dolna Lehota	**0.0259**
	BED-2	E Alps, Southalpine AATV	Trentino	Stol de Pecè	**0.0264**
	MA 5/26	Tuscany: Alpi Apuane	Toscana	M. Arsiccio	**0.0301**
	Tolv-1	Iberia: SE Andalusia-Jaen	Iberia SE	Tolva	**0.0303**
	REG-1	E Alps, Southalpine AATV	Trentino	Val Reganel	**0.0312**
	PA11956	NE Catalunya, Baleares, Cord Iberica	Iberia NE	Linda Mariquita	**0.0312**
	Sov-01	Slovakia, Bohemian Massif	Slovakia	Jasenie-Soviansko	**0.0312**
Cel-AxA3	1-	Greece: Euboea	Grecia	Ano Valsamonero	**0.0147**
	Sok-01	Slovakia, Bohemian Massif	Slovakia	Sokolova Dolina	**0.0161**
	MN2	E Alps, Southalpine AATV	Veneto	Monte Naro	**0.0168**
	BED-1 bis	E Alps, Southalpine AATV	Trentino	Min. Bedovina	**0.0172**
	Dve-01	Slovakia, Bohemian Massif	Slovakia	Dolna Lehota	**0.0182**
	MA 5/17	Tuscany: Alpi Apuane	Toscana	M. Arsiccio	**0.0235**
	6	France: Central Massif, Mont Lozere	France	Ramponeche	**0.0261**
	87.47G.M72		Central Wales	Loveden	**0.0285**
	?	Iberia: NE, Euskadi	Iberia Euskadi	Otxamentegi	**0.0323**
	6	France: Central Massif, Montaigne Noire	France	Millau	**0.0324**
Cel-AxA8	?	Iberia: NE, Euskadi	Iberia Euskadi	Modesta	**0.0210**
	30	France: Central Massif, Mont Lozere	France	Montmirat	**0.0212**
	PA12007	NE Catalunya, Baleares, Cord Iberica	Iberia NE	Linda Mariquita	**0.0223**
	16 S	Swiss Valais	Valais area	La Barma	**0.0255**
		Austria: Tyrol, Carinthia (cpy)	Tyrol	St. Cristoph	**0.0257**
	?	Iberia: NE, Euskadi	Iberia Euskadi	Otxamentegi	**0.0266**
	?	Iberia: NE, Euskadi	Iberia Euskadi	Oportuna	**0.0267**
	87.47G.M72		Central Wales	Loveden	**0.0273**
	ATT-3	NE Catalunya, Baleares, Cord Iberica	Iberia NE	Atrevida	**0.0278**
	31-0000	W Alps 2, Argentera Ivrea	Piemonte	lsola di Vocca	**0.0284**
Cel-Pal	BM.40788	Iberia: SE Andalusia-Jaen	Iberia SE	Almeria	**0.0074**
	RB 23	Tuscany: Alpi Apuane	Toscana	Pollone	**0.0142**
	?	Iberia: Center, Linares-La Carolina	Iberia Center	Linares	**0.0156**
	Ptno-1	Iberia: SE Andalusia-Jaen	Iberia SE	Alhamilla	**0.0167**
	PAT-SID	E Alps, Southalpine AATV	Veneto	Pattine	**0.0182**
	CWB 89-1		Central Wales	Cwmbach	**0.0186**
	BTM-1	Tuscany: Alpi Apuane	Toscana	Bottino	**0.0195**
	PA11954	NE Catalunya, Baleares, Cord Iberica	Iberia NE	Linda Mariquita	**0.0198**
	PN11-17	E Alps, Southalpine AATV	Veneto	Pian della Stua	**0.0199**
	12379	NE Catalunya, Baleares, Cord Iberica	Iberia NE	Sant Julia	**0.0202**

Appendix 4 *(Continued)*

Artefact	Ore/Slag Sample n.	Data base field	Region	Site/Mine	Rank
Por6-Pal	MFO-KW	E Alps, Southalpine AATV	Trentino	Montefondoli	**0.0123**
	PN11-14	E Alps, Southalpine AATV	Veneto	Pian della Stua	**0.0133**
	P3	E Alps, Southalpine AATV	Trentino	Pamera	**0.0148**
	LAV-2	E Alps, Southalpine AATV	Trentino	Furli di Lavis	**0.0166**
	PN11-17	E Alps, Southalpine AATV	Veneto	Pian della Stua	**0.0191**
	P067-b-hv	Iberia: SW, Portugal	Iberia SW	FG-060570	**0.0215**
	MFO-MU	E Alps, Southalpine AATV	Trentino	Montefondoli	**0.0225**
	50411-	E Alps, Southalpine AATV	Trentino	Cinque Valli	**0.0241**
	BDC-L1	Tuscany: Alpi Apuane	Toscana	Bottino	**0.0257**
	TR-PS17	LBA Alpine slags	Trentino	Transacqua	**0.0265**
Por9-Pal	LIN-5	Iberia: Center, Linares-La Carolina	Iberia Center	Filon el Cobre	**0.0103**
	GEO2	Sardinia: Center-Sulcis	East Sardinia	Genna Olidoni	**0.0109**
	SARD 125	Sardinia: Center-Sulcis	Central Sardinia	Baunei	**0.0140**
	REP_As1	Liguria, Apennines-secondari	Liguria	Reppia secodari	**0.0163**
	SARD 126	Sardinia: Center-Sulcis	Central Sardinia	Funtana Raminosa	**0.0210**
	16	France: Central Massif, Montaigne Noire	France	La Rabasse	**0.0232**
	23057U A1	Levant: Timna, Faynan	Egypt	Timna, area A	**0.0236**
	58.464GR102		Northeast Wales		**0.0243**
	87.47G.M292		Central Wales	Bleanceulan mine	**0.0257**
	GEO1	Sardinia: Center-Sulcis	East Sardinia	Genna Olidoni	**0.0271**
CdSB-Cp	MIE-113	E Alps, Southalpine AATV	Trentino	Viarago	**0.0084**
	SEG-P13	LBA Alpine slags	Trentino	Segonzano	**0.0120**
	PA6	E Alps, Southalpine AATV	Trentino	Pamera	**0.0187**
	SEG-M10	LBA Alpine slags	Trentino	Segonzano	**0.0200**
	SEG-P5	LBA Alpine slags	Trentino	Segonzano	**0.0201**
	MT3	E Alps, Southalpine AATV	Veneto	Monte Trisa	**0.0275**
	MIE-107	E Alps, Southalpine AATV	Trentino	Viarago	**0.0332**
	LU-SC1	LBA Alpine slags	Trentino	Luserna	**0.0336**
	SEG-G9	LBA Alpine slags	Trentino	Segonzano	**0.0358**
	LU-SC1 bis	LBA Alpine slags	Trentino	Luserna	**0.0401**
Por9-Cus	MFO_Ap3	E Alps, Southalpine AATV	Trentino	Montefondoli	**0.0164**
	Pb 813		Central Wales	Llwynmalus	**0.0183**
	LAV-2	E Alps, Southalpine AATV	Trentino	Furli di Lavis	**0.0231**
	BLRBR-5A	Tuscany: Alpi Apuane	Toscana	Bottino	**0.0235**
	MA-5pBIS	E Alps, Carnia	Friuli	Monte Avanza	**0.0251**
	BDC-L1	Tuscany: Alpi Apuane	Toscana	Bottino	**0.0253**
	DRO 89-1		Central Wales	Drosgol	**0.0281**
	CD-a-11	E Alps, Southalpine AATV	Trentino	Montefondoli	**0.0282**
	LIN-2	Iberia: Center, Linares-La Carolina	Iberia Center	Grupo Matacabras	**0.0282**
	?	Iberia: Center, Linares-La Carolina	Iberia Center	Linares	**0.0294**

References

AAcP: http://www.geoscienze.unipd.it/aacp/welcome.html

AA.VV., Ed. by Bernabò Brea M., Cardarelli A., Cremaschi M. (1997) Le Terramare. La più antica civiltà padana, Catalogo della Mostra.

Addis A., Angelini I., Nimis P., Artioli G. (2015) Late Bronze Age Copper Smelting Slags from Luserna (Trentino, Italy): Interpretation of the Metallurgical Proce. Archaeometry, DOI: 10.1111/arcm.12160

Addis A., Angelini I., Artioli, G. (2012). Final Bronze Age copper slags from Luserna (Trentino, Italy). Atti VII Congresso Nazionale di Archeometria, Conference Proceeding on CD.

Addis A. (2013). Late Bronze age metallurgy in the Italian Eastern Alps: copper smelting slags and mine exploitation, Ph.D. *dissertation*, University of Padua.

Amov B. G. 1999. Lead isotope data for ore deposits from Bulgaria and the possibility for their use in archaeometry. Berliner Beitrage zur Archaometrie, 16, pp. 5-19.

Amov B., Kolkovski B., Dimitrov R. 1993. Hydrothermal ore mineralisation in the Rhodope metallogenetic zone on the basis of the isotopic composition of lead in galena, Annuaire de l'Universte de Sofia “St. Kliment Ochridski”, Faculte de Geologie et Geographie, Livre 1-Geologie, Tome 85, pp. 73-98.

Anelli F. (1949). Vestigia protostoriche dell'agro aquileiese, Aquileia Nostra, nr. 20, pp. 1-24

Angelini I., Artioli G., Bellintani P., Diella V., Gemmi M, Polla A., Rossi A. (2004). Chemical analyses of Bronze Age glasses from Frattesina di Rovigo, Northern Italy. Journal of Archaeological Science 31, pp. 175-184.

Angelini I., Molin G., Artioli G. (2009). L'atelier metallurgico di Monte Cavanero: indagini chimiche e metallografiche. In: Il ripostiglio del Monte Cavanero di Chiusa di Pesio (Cuneo), a cura di M. Venturino Gambari, Soprintendenza per i Beni Archeologici del Piemonte e del Museo Antichità Egizie, Comune di Chiusa di Pesio, LineaLab.edizioni, Alessandria, pp. 107-166.

Angelini I., Polla A., Molin G. (2010). Studio analitico dei vaghi in vetro provenienti dalla necropoli di Narde. In: Catalogo della mostra "la Fragilità dell'Urna. I recenti scavi a Narde Necropoli di Frattesina (XII-IX) sec. a. C.)" Ed. by Luciano Salzani and Cecilia Colonna, Rovigo 5 October 2007 - 30 March 2008, pp. 105-134

Angelini I. (2005), Le armi della necropoli di Olmo di Nogara: analisi chimiche, metallografiche e microstrutturali. In "La Necropoli dell'Età del Bronzo all'Olmo di Nogara (Verona)". Collana Memorie del Museo Civico di Storia Naturale di Verona, Sezione Scienze dell'Uomo, N° 8, Verona, pp. 515-527.

Angelini I. (In press), Archaeometric investigation of swords from Olmo di Nogara (North, Italy) compared with the available data for coeval weapons. In: Warfare and Aristocracy in Bronze Age Italy, BAR International Series, Archaeopress.

Angelini I. (2009). Evidenze Metallurgiche nell'areale padano del bronzo medio-bronzo finale: studi archeometrici, Ph.D. *dissertation*, University of Padua.

Antonacci Sanpaolo E. (1992). Archeometallurgia. Ricerche e prospettive, Atti del colloquio internazionale, Dozza Imolese (BO), Bologna.

Artioli G., Angelini I., Nimis P., Addis A., Villa I.M. (2014): Prehistoric copper metallurgy in the Italian Eastern Alps: recent results. Historical metallurgy 47, pp. 51-59.

Artioli G., Angelini I., Tecchiati U., Pedrotti A. (2015). Eneolithic copper smelting slags in the Eastern Alps: local patterns of metallurgical exploitation in the Copper Age. J. Arch. Sci. 63, pp. 78-83, DOI: 10.1016/j.jas.2015.08.013

Artioli G., Baumgarten B., Marelli M., Giussani B., Recchia S., Nimis P., Giunti I., Angelini I., Omenetto P. 2008. Chemical and isotopic tracers in alpine copper deposits: geochemical links between mines and metal. Geo Alp. 5, pp. 139-148

Artioli G., Angelini I., Giunti I., Omentetto P., Villa I. (2009). La provenienza del metallo degli oggetti di Monte Cavanero: considerazioni basate sugli isotopi del Pb e sulla geochimica delle mineralizzazioni cuprifere limitrofe. In: Venturino Gambari M. (ed.) Il ripostiglio del Monte Cavanero di Chiusa di Pesio (Cuneo). LineLab.Edizioni, Alessandria. pp. 167-178.

Artioli G. (2010). Scientific Methods and Cultural Heritage: An Introduction to the Application of Materials Science to Archaeometry and Conservation Science. Ed. by OUP Oxford..

Bachmann, H.-G., 1982. The Identification of Slags from Archaeological Sites. Institute of Archaeology, London. Occasional Publication No. 6, pp. 29-30

Bagolan M. and Leonardi G. (2000). Il Bronzo finale nel Veneto. In: Il Protovillanoviano al di qua e al di là dell'Appennino, Atti della giornata di studio (Pavia, Collegio Ghislieri, 17 giugno 1995), 17 giugno 1995, 2000. Ed. by M. Harari and M. Pearce, New Press, pp. 15-46.

Barker G. (1971). The first metallurgy in Italy in the light of the metal analyses from the Pigorini Museum. Bullettino di Paletnologia Italiana, 80, pp. 183-212.

Barker G. (1981). Landscape and society: Prehistoric central Italy. London: Academic Press

Baron S., Tămaş C.G., Le Carlier C. (2013). How Mineralogy and Geochemistry Can Improve the Significance of Pb Isotopes in Metal Provenance Studies, Archaeometry DOI: 10.1111/arcm.12037

Barzero A., Caramella Crespi V., Genova N., Meloni S., Oddone M., Pearce M. (1991).Indagine chimica sul ripostiglio di Pieve Albignola (Pavia), In Pearce M.: materiali Preistorici. Cataloghi dei Civici Musei di Pavia, Ennerre, Milano, pp. 163-169

Baxter M.J. (2003). Statistics in Archaeology, London, Arnold.

Begemann F., Kallas K., Schmitt-Strecker S., Pernicka E. (1999). Tracing ancient tin via isotope analysis, in The Beginnings of metallurgy, eds. A. Hauptmann, E. Pernicka, Th. Rehren and Ü. Yalç.n, Der Anschnitt, Beiheft 8. Deutsches Bergbau-Museum, Bochum, pp. 277-84

Bellintani P., Stefan L. (2008). Sulla tipologia delle palette con immanicatura a cannone dell'età del Bronzo finale, Rivista di scienze preistoriche, vol. 58, pp. 301-320

Belshaw N.S., Freedman P.A., O'Nions R.K., Frank M., Guo Y. (1998). A new variable dispersion double-focussing plasma mass spectrometer with performance illustrated for Pb isotopes. Int. J. Mass Spec. Ion Proc. 181, pp. 51-58

Benvenuti M., ChiarantiniI L., Norfini L. , Casini A., Guideri S., Tanelli G. (2003). The "Etruscan tin": a preliminary contribution from researches at Monte Valerio and Baratti-Populonia (southern Tuscany, Italy), XIVth Congress of the International Union of Prehistoric and Protohistoric Sciences, Vol. 1199, XIVth Congress of the International Union of Prehistoric and Protohistoric Sciences - Liege, Belgio, pp. 55-65, 2-8 Settembre 2001

Bianco Peroni V. (1970). Le spade nell'Italia Continentale, PBF IV, 1, Munchen.

Bietti Sestieri A.M. (1981). Produzione e Scambio nell'Italia Protostorica: alcune ipotesi sul ruolo dell'industria metallurgica nell'etruria mineraria alla fine dell'età del Bronzo, in Etruria mineraria, Atti del XII Convegno di Studi Etruschi e Italici, 16-20 giugno, Firenze, pp. 223-264.

Bietti Sestieri A.M. (1996). Protostoria. Teoria e pratica. Roma: La Nuova Italia Scientifica.

Bietti Sestieri A. M. (1997). Italy in Europe in the Early Iron Age, Proc.Prehist.Soc. 63, pp.371-402

Bogucki P. (2008). Europe, Northern and Western: Bronze Age, in Encyclopedia of Archaeology, edited by Deborah M. Pearsall, volume 2, New York: Academic Press, pp. 1216-1226.

Borgna E. (1996-1997). Porpetto, il ripostiglio del fonditore, in Prima dei Romani, pp.16-17

Borgna E. and Girelli D. (2011). I bronzi di Galleriano tra Friuli ed Europa, in Simeoni G. and Corazza S. (Ed.), Di terra e di ghiaia, Tumuli e Castellieri del Medio Friuli tra Europa ed Adriatico, La Grame.

Borgna E. and Turk P. (1998). Metal Exchange and Circulation of Bronze Objects between Central Italy and theCaput Adriae (XI-VIII B.C.): Implications for the Community Organisation, in The Bronze Age in Europe and the Mediterranean, Proceedings XIII International Congress of Prehistoric and Protohistoric Sciences

Borgna E. (1992). Il ripostiglio di Madriolo presso Cividale e i pani a piccone del Friuli-Venezia Giulia, ed. Quasar, Roma, pp. 147

Borgna E. (2000). I ripostigli del Friuli, in L'età del Bronzo Recente in Italia. Atti del Congresso nazionale di Lido di Camaiore, 26-29 ott. 2000, a c. di D. Cocchi Genick, Viareggio 2004, pp. 90-100.

Borgna E. (2001). I ripostigli del Friuli: proposta di seriazione cronologica e di interpretazione funzionale, Rivista di Scienze Preistoriche, nr. 51, pp. 289-335.

Borgna E. (2006). Patterns of Bronze Circulation and Deposition in the northern Adriatic at the Close of the Late Bronze Age. In: From the aegean to the Adriatic: Social organisations, modes of exchange and interaction in postpalatial times (12th-11th B.C.), Quasar, pp. 289-310.

Borgna E. (2007), I ripostiglio di Celò e altri bronzi: osservazioni sui contesti di circolazione e deposizione del metallo nel comprensorio Natisone-Isonzo durante l'età del bronzo, in Le Valli del Natisone tra centroeuropa e Adriatico. Atti del Convegno internazionale di studi. San Pietro al Natisone, Udine, 15-16 settembre 2006, Trieste 2007, pp. 209-223.

Bosi C., Garagnani G. L., Imbeni V. , Martini C., Mazzeo R., Poli G. (2002). Unalloyed copper inclusions in ancient bronze artefacts, Journal of Materials Science, Vol. 37, Issue 20, pp. 4285-4298

Bouzek J., Koutecky D., Simon K. (1989). Tin and Prehistoric mining in the Erzgebirge (ore Mountains): some new evidence, Oxford Journal of Archaeology, 8, pp. 203-212. doi: 10.1111/j.1468-0092.1989.tb00200.x

Bradley R. (1988). Hoarding, recycling and the consumption of prehistoric metalwork: Technological change in western Europe, World Archaeology,Vol. 20, Iss. 2, pp. 249-260.

Bradley R. (2005) Ritual and Domestic Life in Prehistoric Europe, New York.

Brettscaife Mediterranean database: http://www.brettscaife.net

Brigo L., Colbertaldo D. (1972). Proc. II Int. Symp Min Dep Alps. Ljubiana, pp.109-124.

Bulat M. (1967). Broncanodobni depo iz Kalpelna kod Mjhalica, Osjecki Zbornik 11, pp. 9-22

Bunnefeld J. and Schwenzer S. (2011). Traditionen, Innovationen und Technologietransfer - zur Herstellungstechnik und Funktion älterbronzezeitlicher Schwerter in Niedersachsen. Praehistorische Zeitschrift, 86(2), pp. 207-253. doi:10.1515/pz.2011.012

Carancini G. and Peroni R. (1999). L'età del bronzo in Italia: per una cronologia della produzione metallurgica, Perugia.

Carancini G.L. (1984). Le asce dell'Italia Continentale, II, PBF IX, 12, Munchen.

Casagrande A., Garagnani G.L., Landi E., Pellegrini E., Spinedi P. (1993). Indagini analitico strutturali su reperti metallici di Età Protostorica dell'Italia continentale:dati e considerazioni preliminari su un programma di ricerca pilota. Studi Etruschi, Vol LXIII, serie III, pp. 255-277

Casagrande A., Garagnani G.L., Spinedi P., Pellegrini E. (1994). Microstructural and Analytical Characterization of Bronze Age Copper Ingots and some Metallic Artifacts, PACT, 45, II, 7.

Cassola P. and Vitri S. (1997). Gli insediamenti arginati della pianura friulana nell'età del bronzo. In: Le Terramare: La più antica civiltà padana. Modena, Foro Boario, 15 marzo-1 giugno 1997.Milano: Electa.

Cassola Guida P. and Vitri S. (1997). Gli insediamenti arginati della pianura friulana nell'età del bronzo, in Terramare, pp. 257-262.

Cattin F., Merkl M., Strahm Chr., Villa I.M. (2011). Elemental and lead isotopic data of copper finds from the Singen cemetery, Germany - a methodological approach of investigating Early Bronze Age networks. In : Hauptmann, Andreas and Modarressi-Tehrani, Diana, Proceedings Archaeometallurgy in Europe III, p.29

Cattin F., Villa I.M., Besse M. (2009). Copper supply during the Final Neolithic at the Saint-Blaise/Bains des Dames site (Neuchâtel, Switzerland), Archaeological and Anthropological Sciences, 1 (3), pp. 161-176.

Cattin F., Guénette-Beck B., Curdy P., Meisser N., Ansermet S., Hofmann B., Kündig R., Hubert V., Wörle M., Hametner K., Günther D., Wichser A., Ulrich A., Villa I.M., Besse M. (2011). Provenance of Early Bronze Age metal artefacts in Western Switzerland using elemental and lead isotopic compositions and their possible relation with copper minerals of the nearby Valais. Journal of Archaeological Science, 38 (6), pp. 1221-1233.

Chapman J. (2000). Fragmentation in Archaeology: People, Places and Broken Objects in the Prehistory of South Eastern Europe. London: Routledge.

Cierny J., Weisgerber G., Perini R. (1992). Ein spätbronzezeitlicher Hüttenplatz in Bedollo/Trentino, Universitätsforschungen Prähistorische Archäologie, Bonn, 8, pp.75-82.

Cierny J., Hauptmann A., Hohlmann B., Marzatico F., Schröder B., and Weisgerber G. (1995). Endbronzezeitliche Kupferproduktion im Trentino. Ein Vorbericht, Der Anschnitt, 47/3, Deutsches Bergbau-Museum, Bochum, pp. 82-91.

Cierny J. (1997). Rame, stagno e bronzo, in Ori delle Alpi, Catalogo della mostra (eds. L. Endrizzi and F. Marzatico), Castello del Buonconsiglio, Trento, pp. 61-70.

Cierny J., Marzatico F. (2002). Note sulla cronologia relativa dei siti fusori e sulla circolazione del metallo, in I Bronzi Antichi: produzione e tecnologia, Atti del XV Congresso Internazionale sui Bronzi Antichi, Grado-Aquileia 22-26 maggio 2001 (ed. A. Giumlia-Mair), éditions Monique Mergoil, Montagnac, pp. 258-268.

Cierny, J.; Weisgerber, G. (2003), "The "Bronze Age tin mines in Central Asia", in Giumlia-Mair, A.; Lo Schiavo, F., The Problem of Early Tin, Oxford: Archaeopress, pp. 23-31

Cividini T. (2000). Presenze romane nel territorio del Medio Friuli, Vol. 7 Lestizza, Progetto Integrato Cultura del Medio Friuli.

Clayton R., Andersson P., Gale N.H., Gillis C., Whitehouse M.J. (2002). Precise determination of the isotopic composition of tin by ICP-MS, Journal of Analytical Atomic Spectrometry, 17, pp. 1248-1256.

Coghlan H.H. (1975). Notes on the Metallurgy of Copper and Bronze in the Old World, The University Press, Oxford.

Coghlan H. H. (1960). Prehistorical Working of Bronze and Arsenical Copper, Simbrium, 5, pp.145-152

Coles J., Harding A. (1979). The Bronze Age in Europe. London: Methuen.

Concina E. (1997). I bronzi protostorici del ripostiglio di Čelò (Pulfero), Forum Iulii XXI.

Cowen J. D. (1956). Einführung in die Geschichte der bronzenen GriffzungeNSchwerter in Süddeutschland, 36, RGKomm 1955, Berlin, pp. 52-155

Craddock P.T., Meeks N.D. (1987). Iron in ancient copper, Archaeometry, nr. 29 (2), pp.187-204

Craddock P.T. (1995). Early metal mining and production, Edinburgh University Press, Edinburgh.

Craddock P. T. (2000). From hearth to furnace : evidences for the earliest metal smelting technologies in the Eastern Mediterranean. In: Paléorient,, vol. 26, n°2, La pyrotechnologie à ses débuts. Evolution des premières industries faisant usage du feu, sous la direction de Andreas Hauptmann, pp. 151-165. DOI : 10.3406/paleo.2000.4716

Cui J., Wu X. (2011). An Experimental Investigation on Lead Isotopic Fractionation during Metallurgical processes.Archaeometry, 53, pp. 205-214. doi: 10.1111/j.1475-4754.2010.00548.x

Cupitò M., (2006). Tipocronologia del Bronzo medio e recente tra l'Adige e il Mincio sulla base delle evidenze funerarie, Saltuarie dal Laboratorio del Piovego, 7, Padova

Curti E. (1987). Lead and oxygen isotope evidence for the origin of the Monte Rosa gold lode deposits (Western Alps, Italy): a comparison with Archean lode deposits. Economic geology, 82, pp. 2115-2140.

Czajlik Z. and Sólymos K. G. (2002). Analyses of ingots from Transdanubia and adjacent areas. In: Jerem E., Bíró K. T., Rudner E., Archaeometry 98. Proceedings of the 31st Symposium Budapest, April 26 - May 3 1998, Volume II, BAR International Series 1043 (II), pp. 317-325

Davis,J. R. (2001). Copper and copper alloys, ASM specialty handbook, Materials Park, Ohio ASM International.

Dayton J.E., Dayton A. (1986). Uses and limitations of lead isotopes in archaeology. Proceedings of the 24th International Archaeometry Symposium, eds. J.S. Olin & M.J. Blackman. Smithsonian Institution Press, Washington D.C. pp. 13-41

De Marinis R.C. (1999). Towards a Relative and Absolute Chronology of the Bronze Age in Northern Italy. Notizie Archeologiche Bergomensi, 7, pp. 23-100.

De Marinis R.C. (2006) Aspetti della metallurgia dell'età del Rame e dell'antica età del Bronzo nella penisola italiana. Riv. Sc. Preist. Vol. LVI, pp.211-272.

De Marinis R.C. (2011). La Metallurgia a sud delle Alpi, in Marzatico F., Gebhard R., Gleirscher P.: Le Grandi vie delle civiltà. Relazioni fra il Mediterraneo e il Centro Europa dalla Preistoria alla Romanità. Trento, pp.127-135.

Dietrich O. (2014). Learning from 'Scrap' about Late Bronze Age Hoarding Practices: A Biographical Approach to Individual Acts of Dedication in Large Metal Hoards of the Carpathian Basin. European Journal of Archaeology, 17 (3), pp. 468-486. DOI: 10.1179/1461957114Y.0000000061

Duberow E., Pernicka E., Krenn-Leeb A. (2009). Eastern Alps or Western Carpathians: Early Bronze Age Metal within the Wieselburg Culture. In: T.L. Kienlin, B.W. Roberts (eds.): Metals and Societies, Studies in honour of Barbara S. Ottaway.Universitätsforschungen zur prähistorischen Archäologie Bd. 169, Habelt, Bonn, pp. 336-349

Eckel F. (1992). Studien zur Form-und Materialtypologie von Spagenbarren und Osenringbarren. Eckel F.: Studien zur Form- und Materialtypologie von Spangen- und Ösenringbarren. Zugleich ein Beitrag zur Frage der Relation zwischen Kupferlagerstätten, Halbzeugprodukten und Fertigwarenhande. N. 54 in Saarbrucker Beitrage zur Alterumskunde. Dr. Rudolf Habelt, Bonn.

Fasani L., Salzani L. (1975). Nuovo insediamento dell'età del bronzo in località "Fondo Paviani" presso Legnago (VR), Bollettino del Museo Civico di Storia Naturale di Verona, II, 259-281.

Faure G., Mensing T.M. (2005). Isotopes: Principles and Applications. John Wiley& Sons. 897, pp. 214-250

Faure G. (1986). Principles of Isotope Geology. John Wiley, New York (2nd edn.).

Fenoglio M., Fornaseri M. (1940). Il giacimento di nichelio e cobalto del Cruvino in Val di Susa, Periodico di Mineralogia XI, pp. 23-43.

Foltiny S. (1964). Flange-Hilted Cutting Swords of Bronze in Central Europe, Northeast Italy and Greece, American Journal of Archaeology Vol. 68, No. 3, pp. 247-257.

Gale N.H., Stos-Gale Z.A., Radouncheva A., Ivanov I.,Lilov P., Todorov T., Panayotov I. (2000). Early metallurgy in Bulgaria. In: Annuary of department archaeology, volume 4-5. New Bulgarian University, Institute of Archaeology with Museum, Bulgarian Academy of Sciences, Sofia, pp. 102-168.

Gale N.H., Stos-Gale Z.A. (1981). Cycladic lead and silver metallurgy, Annual of the British School at Athens, 76, pp.169-224.

Gale N.H., Woodhead A. P., Stos-Gale Z. A. , Walder A., Bowen I. (1999). Natural variation detected in the isotopic composition of copper: possible applications to archaeology and geochemistry, International Journal of Mass Spectrometry, 184 (1), pp.1-9

Gale N.H. and Stos-Gale Z. A. (1982). Bronze Age Copper Sources in the Mediterranean: A New Approach, Science, 216 (4541), pp.11-19

Gale N. H. (1996). A new method for extracting and purifying lead from difficult matrices for isotopic analysis. Anal Chim Acta, 332, pp. 15-21

Gale N.H. (1997). The isotopic composition of tin in some ancient metals and the recycling problem in metal provenancing, Archaeometry, 39(1), pp. 71-82

Gale N.H. (2009). A response to the paper by A.M. Pollard: What a long, strange trip it's been: lead isotopes in archaeology. In: 'From Mine to Microscope - Advances in the Study of Ancient technology'. Eds. A.J Shortland, I.C. Freestone and T. Rehren. Oxbow Books, Oxford, pp.191-196

Garagnani G.L., Imbeni V. Martini C. (1997). Analisi chimiche microstrutturali di manufatti in rame e bronzo dalle terramare, in Bernabò Brea, Cardarelli A., Cremaschi M (Ed.), Le terramare la più antici civiltà Padana, Milano, Electa, pp. 554-566

Giumlia-Mair A. (2009). Ancient metallurgical traditions and connections around the Caput Adriae, Journal of Mining and Metallurgy 45 B (2), pp. 141-222.

Giumlia-Mair A. (1998). La metallurgia dei bronzi di S.Lucia/Most na Soci, Aquileia Nostra, LXIX, pp. 30 - 135

Giumlia-Mair A. (2000), Bronze Technology in the Eastern Alpine Regions between the Final Bronze Age and the Early Iron Age. Proceedings of the “Workshop on Ancient Metallurgy between Oriental Alps and Pannonian Plain”, (Giumlia-Mair ed.), 29-30 Ottobre, Dipartimento di Ingegneria dei Materiali e Chimica Applicata, Università di Trieste. Quaderni di Aquileia Nostra, 8, pp. 77-91

Giumlia-Mair A. (2003). Iron Age tin in the Oriental Alps. Proceedings of the Colloquium The problems of Early Tin, Giumlia-Mair A. and Lo Schiavo F. ed., XIV International Congress of Prehistoric and Protohistoric Sciences, Liège, September 2001, Le problème de l’ètain à l’origine de la mètallurgie/ The Problem of Early Tin, BAR International Series 1199, Oxford, pp. 93-108

Giumlia-Mair A. (2005). Copper and Copper alloys in the Southeastern Alps: An overview. Archaeometry, 47, 2, pp. 275-292

Gnesotto F. (1980). Terzo d’Aquileia, Aquileia Nostra, LI, p. 393

Gnesotto F. (1981). L’insediamento preistorico di Canale Anfora, Aquileia Nostra, LII, pp. 6-36

Goldenberg G. (1998). L’exploitation du cuivre dans les Alpes autrichiennes à l’Âge du Bronze, in L’Atelier du bronzier en Europe du XXe au VIIIe siècle avant notre ère. Actes du colloque international Bronze ’96 Neuchâtel et Dijon II: Du minerai au métal, du métal à l’objet (eds. C. Mordant, M. Pernot and V. Rychner), Comité des traveaux historiques et scientifiques, Paris, pp. 9-24

Gori M. (2014), Metal Hoards as Ritual Gifts. Circulation, Collection and Alienation of Bronze Artefacts in Late Bronze Age Europe, in: F. Carlà, F. and M. Gori (Eds.), Gift giving and the “embedded” economy in the ancient world, Heidelberg: Universitätsverlag Winter, pp. 269-288.

Guénette-Beck B., Meisser N., Curdy P. (2005).New insights into the ancient silver production of the Wallis area, Switzerland,Archaeological and Anthropological Sciences, 1, pp. 215-229

Gustrein P. (1981). Prähistorischer Bergbau am Burgstall bei Schwaz (Tirol), Veröffentlichungen des Museums Ferdinandeum, 61, pp. 25-46.

Harari M., Pearce M. (2000). Il Protovillanoviano al di qua e al di là dell’Appennino. Atti della giornata di Studio (Pavia 17 Giugno 1995). Como.

Harding A. F. (2000). European Societies in the Bronze Age, Cambridge University Press, Cambridge.

Hauptmann A., Maddin R., Prange M. (2002). On the Structure and Composition of Copper and Tin Ingots Excavated from the shipwreck of Uluburun. Bulletin of the American Schools of Oriental Research 328, pp. 1-30.

Haustein M., Gillis C., Pernicka E. (2010). Tin Isotopy - a new method for solving old questions Archaeometry, 52 (5), pp. 816-832

Hirata T. (1996). Lead isotopic analysis of NIST standard reference materials using multiple collector-inductively coupled plasma mass spectrometry coupled with modified external correction method for mass discrimination effect, The Analyst 121, pp. 1407-1411

Höppner B., Bartelheim M., Huijsmans M., Krauss R., Martinek K.-P., Pernicka E., Schwab R. (2005). Prehistoric copper production in the Inn Valley (Austria), and the earliest copper in central Europe, Archaeometry, 47 (2), pp. 293-315

Horner J., Neubauer F., Paar W.H., Hansmann W., Koeppel V., Robl K. 1997. Structure, mineralogy, and Pb isotopic composition of the As-Au-Ag deposit Rotgulden, Eastern Alps (Austria): signicance for formation of epigenetic ore deposits within metamorphic domes.Mineralium Deposita, 32. Pp. 555-568.

Horwitz E.P., Chiarizia R., Dietz M. L. (1992). A novel strontium-selective extraction chromatographic resin. Solv Extr Ion Exch 10. pp. 313-336

Howe H.M. (1885). Copper Smelting ,U.S. Government Printing Office, 1885, p. 107.

Huska A., Powell W., Mitrovic S., Bankoff H. A., Bulatovic A., Filipovic V., Boger R. (2014). Placer Tin Ores from Mt. Cer, West Serbia, and Their PotentialExploitation during the Bronze Age, Geoarchaeology: An International Journal, 29, pp. 477-49

Jankovits K. 1998-99 (1999), La presenza di palette con immanicatura a cannone in Ungheria nell'età del bronzo finale. Padusa XXXIV/XXXV, 109-118.

Jung R., Mehofer M., Pernicka E. (2011). Metal Exchange in Italy from the Middle to the Final Bronze Age (14th-11th Century B.C.E.). Metallurgy: Understanding How Learning WhY. Studies in Honor of James D. Muhly edited by Philip P. Betancourt and Susan C. Ferrence. Prehistory Monographs 29. INSTAP Academic Press. pp. 231-248

Junghans S., Sangmeister E., Schröder M. (1960). Metallanalysen kupferzeitlicher undfrühbronzezeitlicher Bodenfunde aus Europa, Gebr. Mann Verlag, Berlin

Junghans S., Sangmeister E., Schröder, M. (1968). Kupfer und Bronze in der frühen MetallzeitEuropas 1-3, Berlin

Junghans S., Sangmeister E., Schröder M. (1974). Kupfer und Bronze in der frühen MetallzeitEuropas 4, Gebr. Mann Verlag, Berlin.

Junghans S., Sangmeister E., Schröder M. (1968). Studien zu den Anfängen der Metallurgie. Berlin: Gebr. Mann.

Junk M. (2003). Material properties of copper alloys containing arsenic, antimony, and bismuth, Ph.D. dissertation.

Keesmann I. (1999). Eisen in antiken Schlacken des sudwestiberischen Sulphiderz-Gurtels. Pallas 50, 339-360.

Klemenc S., Budic B., Zupan, J. (1999). Statistical evaluation of data obtained by inductively coupled plasma atomic emission spectrometry (ICP-AES) for archaeological copper ingots, Analytica Chimica Acta, nr. 389, p. 141-150. doi:10.1016/S0003-2670(98)00841-1

Knapp A. B. (1988). Hoards d'oeuvres: of metals and men on Bronze Age Cyprus, Oxford Journal of Archaeology, 7(2), pp.147-175.

Koppel V., Schroll E. 1983. Lead isotopes of paleozoic, stratabound to stratiform galena bearing sulfide deposits of eastern alps (Austria): implications for their geotectonic setting: Schweiz. Mineral. Petrogr. Mitt. v. 63, pp. 347-360.

Koppel V. (1997). Weber, L., Handbuch der Lagerstätten der Erze, Industrieminerale und Energierohstoffe Österreichs - Erläuterungen zur Metallogenetischen Karte v. Österreich 1 : 500.000 unter Einbeziehung der Industrieminerale u. Energierohstoffe. Arch. f. Lagerst. forsch. Geol. B.-A., 19, Wien, pp. 1-607

Krause R. (2003). Studien zur kupfer- und frühbronzezeitlichen Metallurgie zwischen Karpatenbecken und Ostsee. Vorge-schichtliche Forschungen 24. Rahden/Westf.: VML 2003

Krause R., Pernicka E. (1996). SMAP-The Stuttgart Metal Analysis Project. Archaologisches Nachrichtenblatt 1, pp. 274-291.

Lattanzi P., Hansmann W., Koeppel V., Costagliola P. (1992). Source of metals in Metamorphic Ore-forming Processes in the Apuane Alps (NW Tuscany, Italy): constraints by Pb-isotope Data. Mineralogy and petrology, 45, pp. 217-229.

Leonardi G. (1979). Il Bronzo finale nell'Italia nord-orientale, proposta per una suddivisione in fasi, Atti XXI Riunione Scientifica dell'Istituto Italiano di Preistoria e Protostoria, Firenze 21-23 ottobre 1977, 21-23 ottobre 1977 1979, pp. 155-188.

Leoni M., Diana M., Guidi G., Perdominici F. (1991). La Metallurgia Italiana, n. 83, Vol. 11, p. 1033.

Levy J.E. (1982). Social and religious organization in Bronze Age Danmark. An Analysis of Ritual hoard Finds, Oxford.

Ling J., Stos-Gale Z., Grandin L., Billström K. , Hjärthner-Holdar E. and Persson P. O. (2014). Moving metals II: Provenancing Scandinavian Bronze Age artefacts by lead isotope and elemental analyses, Journal of Archaeological Science, vol. 41, pp.106-132.

Liversage D. (1994). Interpreting composition patterns in ancient bronze: The Carpathian Basin. Acta Archaeologica, 65, pp. 57-134

Liversage D. (2000). Interpreting Impurity Patterns in Ancient Bronze. Denmark. In: Nordiske Fortidsminder Ser. C, vol. 1. Kongelige Nordiske Oldskriftselskab, Copenhagen.

Lutz J., Pernicka E. (2013). Prehistoric copper from the Eastern Alps, Open Journal of Archaeometry 1:e25, pp. 122-126.

Maddin R., Wheeler T. S., Muhly J. D. (1980). Distinguishing artifacts made of native Copper, Journal of Archaeological Science, 7, pp. 211-225.

Mangou H., Ioannou P.V. (2000). Studies of the Late Bronze Age copper-based ingots found in Greece, The Annual of the British School at Athens, 95, pp. 207-17. doi:10.1017/S0068245400004640

Marchesetti C. (1903). Castellieri preistorici di Trieste e della regione Giulia, Museo civico di Storia naturale, Trieste.

Merkel J.F. (1983). Summary of experimental results for LBA copper smelting and refining, MASCA. J., 2, pp.173-178

Merkl M. B. (2011). Bell Beaker copper use in central Europe: a distinctive traditions? BAR international Series 2267, Oxford, Archaeopress.

Moedlinger M. (2011). Ritual object or powerful weapon - the usage of Central Europe Bronze Age swords in: Uckelmann, M. and Mödlinger, M. (eds), Warfare in Bronze Age Europe: Manufacture and Use of Weaponry. British Archaeological Reports International Series 2255. Oxbow books

Muhly J. D. (1985). Sources of tin and the beginnings of bronze metallurgy. American Journal of Archaeology, 89, pp. 275-291.

Newton J., Wilson C. (1942). Metallurgy of copper, John Wiley And Sons Inc., p. 70.

Niederschlag E., Pernicka E., Seifert T., Bartelheim M. (2003). The determination of lead isotopes ratios by multiple collector ICP-MS: a case of study of early bronze age artefacts and their possible relation with ore deposits of the Erzgebirge. Archaeometry 45, 1, pp. 61-100.

Nimis P. (2010). Some remarks on the use of geochemical tracres for metal provenancing, in: Magrini C. and Sbarra F. (eds), Late Roman Glazed pottery in Carlino and in Central-East Europe (Oxford: BAR International Series 2068), pp. 3-9.

Nimis P., Omenetto P., Giunti I., Artioli G., Angelini I. (2012). Lead isotope systematics in hydrothermal sulphide deposits from the central-eastern Southalpine (northern Italy). Eur. J. Mineral., 24, pp. 23-37.

Nimis P., Omenetto P., Giunti I., Artioli G., Angelini I. (2012). Lead isotope systematics in hydrothermal sulphide deposits from the central-eastern Southalpine (northern Italy). Eur.J.Miner.24, p.23.

Northover J. P. (1989). Properties and use of arsenic-copper alloys. In E. Pernicka & G. Wagner (Eds.), Old world archaeometallurgy, andreas hauptmann (pp. 111-118). Der Anschnitt Beiheft 7. Bochum: Deutsches Bergbau Museum.

Ottaway B. (1994). Prähistorische Archäometallurgie, Marie Leidorf, Espelkamp

Otto H., Witter W. (1952). Handbuch der ältesten vorgeschichtlichen Metallurgie in Mitteleuropa. Leipzig: Barth Verlag.

OXALID database: http://oxalid.arch.ox.ac.uk

Pare C.F.E. (2000). Bronze and the Bronze Age. In C.F.E. Pare, Metals Make the World Go Round, Oxbow Books, Oxford, pp. 1-38

Paulin A., Spaic S., Zalar A., Trampuž-Orel N. (2003). Metallographic analysis of a 3000-year-old Kanalski Vrh hoard pendant. Mat. Charact., 51, pp. 205-218.

Paulin A., Spaic S., Spruk S., Heath D.J., Trampuž-Orel N. (1999). Speiss from Late Bronze Age, Erzmetall 52 (11), pp. 615-622

Pearce M. (1993). The origins of metallurgy and ore sources: a north Italian case study, The Journal of the Accordia Research Centre Volume 4, pp. 49-62.

Pearce M.J. (2004). The Italian Bronze Age. In: Ancient Europe 8000 B.C.-A.D 1000: encyclopedia of the Barbarian world Volume 1: The Mesolithic to Copper Age (c.8000-2000 B.C.). Ed. by Bogucki P., Crabtree P. New York: Charles Scribner's Sons, pp. 34-42.

Pellegrini G., (1911). Ripostiglio di oggetti cupro-enei e spada antichissima di bronzo scoperti presso Castions di Strada (Udine). Bullettino di Paletnologia Italiana, 37, Parma, pp. 231-236.

Pellegrini E. (1992), Aspetti regionali e relazioni interregionali nella produzione metallurgica del Bronzo finale nell'Italia continentale: i ripostigli con pani a piccone, in Antonacci Sanpaolo E., Archeometria.Ricerche e Prospettive, Atti del Colloquio Internazionale di Archeometallurgia, Clueb, Bologna, pp. 589-603.

Pellegrini E. (1995). Aspetti della metallurgia nell'Italia continentale tra XVI e XI secolo a.C.: produzione e relazioni interregionali tra area centrale tirrenica e area settentrionale. In: Settlement and economy in Italy 1500 BC to AD 1500. Papers of the fi fth Conference of Italian Archaeology, Ed. Christie N., JSTOR, Oxford, pp. 511-519

Pernicka E., Salzani P. (2011). Remarks on the analyses and future prospects. In: A. Aspes (Hrsg.): I bronzi del Garda - Valorizzazione dell collezioni di bronzi preistorici di uno dei più importante centri metallurgici dell'Europa del II° millennio a.C. Memorie del Museo Civico di Storia Naturale di Verona - 2. serie, Sezione delle Scienze dell'Uomo 11, pp. 89-98.

Pernicka E., Begamen F., Schmitt-Streckers S., Torodova H., Kuleff I. (1997). Prehistoric copper in Bulgaria, Eurasia Antiqua, Zeitschrift fur archaologie Eurasiens, Deutcsches Archaologischens Institut 3, pp. 41-180.

Pernicka E. (1984). Instrumentelle Multi-elementanalyse archäologischer Kupfer- und Bronzeartefakte: ein Methodenvergleich. Jarhb. Röm.-Germ, Zentralmus, Mainz 31, pp. 517-531.

Pernicka E., Begemann F., Schmitt-Strecker S., WagnerG. A. (1993). Eneolithic and Early Bronze Age Copper Artefacts from the Balkans and their Relation to Serbian Copper Ores. Praehistorische Zeitschrift 68, pp. 1-54.

Pernicka E. (1987). Erzlagerstätten in der Ägäis und ihre Ausbeutung im Altertum: Geochemische Untersuchungen zur Herkunftsbestimmung archäologischer Metallobjekte. Jahrb. Röm.-Germ. Zentralmus. 34, pp. 607-714.

Pernicka, E. (1990). Entstehung und Ausbreitung der Metallurgie in prähistorischer Zeit. Jahrb. Röm.-Germ. Zentralmus, 37, pp. 21-129.

Pernicka E. (1999). Trace element fingerprinting of ancient copper: a guide to technology of provenance?. In: Metals in antiquity. BAR International Series 792. Ed. by Young SMM, Pollard AM, Budd P, Ixter RA. Hadrian Books, Oxford, pp. 163-171.

Pernicka E. (2011). Provenance determination of archaeological metal objects. In: A. Aspes (Hrsg.): I bronzi del Garda - Valorizzazione dell collezioni di bronzi preistorici di uno dei più importante centri metallurgici dell'Europa del II° millennio a.C. Memorie del Museo Civico di Storia Naturale di Verona - 2. serie, Sezione delle Scienze dell'Uomo 11, pp. 27-37.

Pernicka E. (2014). Provenance determination of archaeological metal objects, Archaeometallurgy in Global Perspective: Methods and Syntheses, pp. 239-268

Peroni R., Carancini G. (1997). La Koinè metallurgica, in Bernabo Brea M., Cardarelli A., Cremaschi M. (Eds): Terramare la più antica civiltà padana, Modena, pp. 595-601.

Peroni R. (2004). L'Italia alle soglie della storia. Roma-Bari, cap. I: pp. 52-62; cap. II: pp. 137-151, 157-163; cap. III: pp. 238-244, 248-252, 260-265.

Pettke T., Frei R. 1996. Isotope systematics in vein gold from brusson, Val d'Ayas (NW Italy). 1. Pb/Pb evidence for a Piemonte metaophiolote Au source. Chemical Geology, 127, pp. 111-124.

Piccoli G.C. (2007). Minerali del Piemonte e della Valle d'Aosta (Alba).

Pigorini L. (1895). Antichi pani di rame e di bronzo da fondere rinvenuti in Italia, Bullettino di Paletnologia italiana, 21, pp. 5-38.

Pigorini L. (1904). Ripostigli di bronzi arcaici nell'Italia austriaca, Bullettino di Paletnologia Italiana, nr. 3, pp. 138-142

Pigorini L. (1895). Antichi pani di rame e di bronzo da fondere rinvenuti in Italia, Bullettino di Paletnologia italiana, 21, pp. 5-38.

Pollard A. M., Thomas R. G., Ware D. P., Williams P. A. (1991). Experimental smelting of secondary copper minerals: Implications for Early Bronze Age metallurgy in Britain, in E. Pernicka, G. A. Wagner (Eds.), Archaeometry '90, Basel, Birkhäuser Verlag, pp. 127-136.

Pollard A.M. (2009). What a Long Strange Trip It's Been: lead isotopes in archaeology, in "From Mine to Microscope - Advances in the Study of Ancient Technology; Shortland A J., Freestone, I. C., and. Rehren, T., (eds.)", pp. 181-189, Oxbow Books, Oxford.

Rapp G., R. Rothe, Jing Z. (1999). Using neutron activation analysis to source ancient tin (cassiterite), in Metals in antiquity, eds. Young S. M. M., Pollard A.M., Budd P., Ixer R., BAR International Series 792, Archaeopress, Oxford, pp. 153-162

Rapp G. (1978). Trace elements as a guide to the geographical source of tin ore: smelting experiments, in The search for ancient tin (eds. A.D. Franklin, J. Olin, and T. Wertime), Smithsonian Institution Press, Washington, pp. 59-63

Rapp G. R. (2013). Archaeomineralogy, Springer Science & Business Media.

Rehkamper M., Halliday A.M. (1998). Accuracy and long-term reproducibility of lead isotopic measurements by MC-ICP-MS using an external method for correction of mass discrimination. Int. J. Mass Spec. Ion Proc. 58, pp.123-133

Rehkämper M., Mezger K. (2000). Investigation of matrix effects for Pb isotope ratio measurements by multiple collector ICP-MS: Verification and application of optimized analytical protocols, Journal of analytical atomic spectrometry, 15 (11), pp. 1451-1460. DOI: 10.1039/b005262k

Rehren Th., Schneider J., Bartels Ch. (1999). Medieval lead-silver smelting in the Siegerland, West Germany. Historical Metallurgy 33, pp. 73-84

Rezi B. (2010). Voluntary Destruction and Fragmentation in Late Bronze Age Hoards from Central Transylvania, in Berecki S., Nemeth R.E., Rezi B.: Bronze Age rites and rituals in the Carpathian Basin, Proceedings of the international colloquium from Targu Mures, 8-10 October 2010.

Ribbe P.H. (1974). Short Course Notes-Sulfide Mineralogy, Mineralogical Society of America (Ed.), Washington.

Rieser B., Schrattenthaler H. (1998), Urgeschichtlicher Kupferbergbau im Raum Schwaz-Brixlegg, Tirol, Archaeologia Austriaca, 82-3, pp. 135-79.

Rothe R., Rapp G. (1995). Trace-element analyses of Egyptian Eastern Desert tin and its importance to Egyptian archaeology, in Proceedings of the Egyptian-Italian seminar on the geosciences and archaeology in the Mediterranean countries, eds. A.A.A. Hussein, M. Miele, and S. Riad, Special Publication #70 of the Geological Survey of Egypt, Cairo, pp. 229-244.

Sabatini B.J. (2015). The As-Cu-Ni System: A Chemical Thermodynamic Model for Ancient Recycling, JOM, Volume 67, Issue 12, pp. 2984-2992

Santi E., Leonardi G. (2007). Le palette a cannone nel contesto Europeo. Tesi di Laurea di Santi E. con relatore G. Leonardi, Università degli Studi di Padova, A.A. 2006/2007.

Schauer P. (1971) Die Schwerter in Suddeutschland, Osterreich und der Schweiz I. Prahistorische Bronzefunde Abteilung IV. Band 2. Munchen.

Schroll E., Koppel V., Cerny I. (2006). Pb and Sr isotope and geochemical data from the Pb-Zn deposit Bleiberg (Austria): constraints on the age of mineralization. Mineralogy and Petrology, 86, p. 129-156.

Scott D.A. (2012). Ancient Metals: Microstructure and Metallurgy Volume 1. Copper and copper alloys. CSP: Conservation Science Press.

Simeoni G., Corazza S. (2011). Di terra e di ghiaia, Tumuli e Castellieri del Medio Friuli tra Europa ed Adriatico, La Grame.

Smodic A. (1956). Bronasti depo iz Miljane, AArchSlov 7, pp. 43-50.

Sommerfeld C. (1994). Gerätegeld Sichel. Studien zur monetären Struktur bronzezeitlicher Horte im nördlichen Mitteleuropa, Berlin.

Stos Z.A. (2009). Across the wine dark seas. Sailor tinkers and royal cargoes in the Late Bronze Age eastern Mediterranean. In: Shortland, A.J., Freestone, I.C., Rehren, T. (Eds.), From Mine to Microscope e Advances in the Study of Ancient Technology. Oxbow Books, Oxford, pp. 163-180.

Stos-Gale Z.A. and Gale N.H. (2009). Metal provenancing using isotopes and the Oxford archaeological lead isotope database (OXALID). Archaeological and Anthropological Sciences 1, pp. 195-213.

Stos-Gale Z.A., Gale N.H., Annetts N., Todorov T., Lilov P., Raduncheva A., Panayotov I. (1998). Lead isotope data from the Isotrace Laboratory, Oxford: Archaeometry Database 5, Ores from Bulgaria. Archaeometry 40 (1), pp. 217-226.

Tasca G. (2011). Tipologia e cronologia della produzione ceramica del Bronzo medio-recente nella Bassa Pianura Friulana, PhD dissertation, University of Padua.

Thornton, C.P.; Rehren, T.; Piggot, V.C. (2009). "The production of speiss (iron arsenide) during the Early Bronze Age in Iran. Journal of Archaeological Science 36 (36): 308-316. doi:10.1016/j.jas.2008.09.017

Tite M. S. (1996). In defence of lead isotope analysis. Antiquity, 70, pp. 959-962. doi:10.1017/S0003598X00084246.

Towle A., Henderson J., Bellintani P., Gambacurta G. (2001). Frattesina and Adria: report of scientific analysis of early glass from the Veneto. Padusa XXXVII, pp. 7-68.

Trampuž-Orel N., Milic Z., Hudnik V., Orel B. (1991). Inductively coupled plasma-atomic emission spectroscopy analysis of metals from Late Bronze Age hoards in Slovenia, Archaeometry 33, pp. 267-277. doi:10.1111/j.1475-4754.1991.tb00704.x

Trampuž-Orel N., Heath D.J., Hudnik V. (1998). Chemical analysis of Slovenian bronzes from the Late Bronze Age, In L'atelier du bronzier en Europe du XXe au VIIIe siècle avant notre ère, Vol. I, Proceedings of the International Conference Bronze ´96, C. Mordant, M. Pernot, V. Rychner ed., Neuchatel et Dijon, I, Dijon, pp. 223-237.

Trampuž-Orel N., Heath D.J. (2001). The Kanalski Vrh hoard: a case study of the metallurgical knowledge and metals at the beginning of the 1st millennium BC.ARHEOLOŠKI VESTNIK 52, pp. 143-171

Trampuž-Orel N. (1996). Spectrometric research of the Late Bronze Age Hoard Finds, In Depojske in posamezne kovinske najdbe bakrene in bronaste dobe na Slovenskem/Hoards and Individual Metal Finds from the Eneolithic and Bronze Ages in Slovenia II, B.Teržan ed., Katalogi in Monografije 30, Ljubljana, pp. 165-242

Tuniz C., ConfalonieriL., Milazzo M., Monichino M., Katsanos A. (1986-87). Uso di tecniche atomiche e nucleari per lo studio archeologico di antichi oggetti metallici, Bollettino della Società Adriatica di Scienze 69, pp. 17-27.

Turk, P. (1997). Das Depot eines Bronzegiessers aus Slowenien: Opfer oder Materiallager? Berlin: Staatliche Museen Preussischer Kulturbesitz, Museum für Vor- u. Frühgeschichte.

Turk P. (1996). The Dating of Late Bronze Age Hoards, in Terzan B., Hoards and Individual Metal Finds from the Eneolithic and Bronze Ages in Slovenia II, Ljubljana.

Tylecote R.F. and Boydell P.J. (1978). Chalcolithic Copper Smelting, IAMS, London.

Tylecote R.F., Ghaznavi H.A., Boydell P.J. (1977). Partitioning of trace elements between the ores, fluxes, slags and metal during the smelting of copper. Journal of Archaeological Science 1997, 4, pp. 305-333

Tylecote R.F. (1981). International Archaeological Symposium: Early Metallurgy in Cyprus 4000-500 BC, Cyprus, p. 81

Tylecote R.F. (1992). A history of metallurgy (2nd Edition), The Metals Society, London

Tylecote R.F. (1970). The composition of metal artifacts: A guide to provenance? Antiquity, 44, pp.19-25

Vander Voort G. F. (1984). Metallography, Principles and Practice, ASM International.

Venturino Gambari M. (2009). Il ripostigio di Monte Cavanero di Chiusa di Pesio, Alessandria LineLab.edizioni, pp. 27-54

Villa I.M. (2009). Lead isotopic measurements in archeological objects. Archaeological and Anthropological Sciences, 1(3), pp. 149-153.

Vinski-Gasparini K. (1973). Kultura polja sa žarama u sjevernoj Hrvatskoj, Zadar.

Vitri S. (1983). La raccolta preistorica del Museo di Aquileia, In: I Musei di Aquileia 1, pp. 117-126

Vitri S. (1984). Cervignano (Udine), Aquileia Nostra, nr. 55, pp. 268-269

Vitri S. (1990). Carte archeologiche e schede di sito, in Desinan C.C., Toponomastica e archeologia del Friuli prelatino con note di aggiornamento di protostoria friulana, Pordenone, pp. 158-174

Vitri S. (1991). Cervignano (via Lazzaro), Relazioni della Soprintendenza per i beni AAAAS del Friuli Venezia Giulia 8, pp. 130-133.

Vitri S. (1999). Nuovi ritrovamenti di Bronzi protostorici in Friuli. Contributo alla definizione del ruolo del Caput Adriae nell'età del Bronzo Finale, AN LXX, pp. 289-296.

Von Bibra E. (1869). Die Bronzen und Kupferlegierungen der alten und ältesten Völker, mit Rücksichtnahme auf jene der Neuzeit. Erlangen.

Von Fellenberg L. R. (1860-1867). Analysen von antiken Bronzen. Mitt. D. naturf. Ges. Bern.

Wang Q. and Merkel J. F. (2001). Studies on the redeposition of copper in Jin bronzes from Tianma-Qucun, Shanxi, China. Studies in Conservation, 46(4), pp. 242-250.

Weisgerber G., Goldenberg G. (2004). Alpenkupfer - Rame delle Alpi (Bochum: Der Anschnitt 17).

White W.M., Albarède F., Télouk P. (2000) .High-precision analysis of Pb isotope ratios by multi-collector ICP-MS, Chemical Geology, 167 (3-4), pp. 257-270. DOI: 10.1016/S0009-2541(99)00182-5

Witter W. (1953). Neues zu den Barrenring-Hortfunden im Vorlande der Ostalpen. Prahistorische Zeitschrift, 34/35. pp 179-190

Zaghis F. (2005). Metallic artefacts and slags: Etnoarchaeology of Bronze and Iron Production, PhD dissertation, University of Padua.

Zucchini R. (1998). Miniere e mineralizzazioni nella provincia di Udine. Aspetti storici e mineralogici, Edizioni del Museo Friulano di Storia Naturale, Udine.

Acknowledgements

It is a great pleasure to thank Prof.Gilberto Artioli and Dr. Ivana Angelini for their scientific and thoughtful guidance during the doctoral years. I wish to thank the *Soprintendenza per i Beni Archeologici del Friuli Venezia Giulia* in the persons of Dr. Luigi Fozzati and Dr. Roberto Micheli for their permission to study and analyze these materials. In particular, I would like to express my gratitude to Dr. Fabio Pagano and Mrs. Iole Zurco (Museo Archeologico Nazionale of Cividale, Udine), Dr. Paola Ventura and Mr. Daniele Pasini (Museo Archeologico Nazionale of Aquileia), and Mr. Giorgio Procaccioli for their helpfulness and support in the sampling stage. I am particularly grateful to Prof. Elisabetta Borgna for her collaboration in the selection of the deposits and, especially, for her deep interest in the discussion of the results.

Next, I need to thank all the people who create such a good atmosphere in the lab; I wish to thank Leonardo Tauro, Elena Masiero, Lorenzo Raccagni and Raul Carampin of the Department of Geosciences of the Padova University for their help and support during the preparation of the samples and the analyses. Thanks also to Giancarlo Cavazzini for the patience to teach me with precision and dedication.

I am grateful to Michele e Anna, above all, for their support in my difficult moments and for their encouragement, love and precious suggestions during these Ph.D. years. Thanks also to Lisa, Sara, Gregorio, Elisa because a silent smile is better than a thousand of *"How are you?"*.

I need to further thank all my friends, particularly Marta, who always took the time to listen, even when I was complaining on myself.

I would like to thank my parents, Mauro and Rosetta, for allowing me to realize my own potential. All the silent support they have provided me over the years was the greatest gift anyone has ever given me. Also, I need to thank Patrizia and Ezio, who taught me that the curiosity is an additional value, but also the *otium* is an art that should not be underestimated.

Finally, I am grateful to Marco for his patience, for his support, for his shoulder..for his love!